UNIVERSITY OF LIVERPOOL

Institute of Ageing

and Chronic Disease

An *in vitro* investigation of human ocular surface epithelial stem cell homeostasis

Thesis submitted in accordance with the requirements of the University of Liverpool for the degree of Doctor in Philosophy by Tiago Andre da Silva Ramos

Supervisors: Dr Sajjad Ahmad MB BS, FRCOphth, PhD

Dr Rosalind Stewart BSc (Hons) MB BCh (Hons), FRCOphth PhD

Professor Stephen Kaye

Dr Kevin Hamill

January 2018

Abstract

The anterior surface of the eye is composed of the clear cornea centrally and the conjunctival and white sclera peripherally. The clarity of the cornea is of crucial importance for the transmission and focusing of light to the retina for visual perception. The limbus harbours the stem cells for corneal regeneration, the so-called limbal stem cells, and acts as a physical barrier preventing the conjunctiva and its blood vessels from encroaching onto the corneal surface. Upon injury or other inherited causes, the ocular surface homeostasis is impaired resulting in a migration of conjunctival epithelium onto the corneal surface, in a process called conjunctivalisation. Upon conjunctivalisation, which results in loss of corneal clarity and visual impairment, the conjunctival migrating cells can undergo a process of transdifferentiation towards cornea epithelial-like cells. This process of transdifferentiation seems to be incomplete, with the differentiated cells showing differences in glycogen metabolism, keratin profiling and tensile strength when compared to the native corneal epithelial cells. Limbal epithelial transplantation forms the mainstay of treatment in severe cases of such deficiency. However, two main hurdles stand for this treatment, including the requirement of large amounts of healthy tissue and the need of immunosuppression therapies in the case of allografts. Therefore, the emergence of cell-based therapies that potentially promote the complete transdifferentiation of conjunctival cells into corneal epithelial cells would overcome these two hurdles. This study aims to understand ocular surface and epithelial cell differentiation in response to the composition and morphogenic properties of the extracellular matrix (ECM). Cell cultures were treated with strong alkali solutions, by a process called “de-roofing”, resulting in systems devoid of any cell and cell debris with only the respective ECM proteins attached to the cultureware. For the first-time, cells were driven to differentiate towards the lineage of the ECM depositing-cell. This process of differentiation required an intermediate step of cell dedifferentiation as suggested by the increased expression of early progenitor epithelial cell markers ΔNp63 and ABCB5. The ECM composition and protein deposition profiles were extensively characterized to narrow the possible cues involved in the process of cell differentiation. Laminin-511 coated surface was shown to be a potential candidate to promote epithelial cell differentiation, with cell response shown to be concentration and time-dependent. Furthermore, the phosphorylation or cleavage levels of 18 different proteins, mainly involved in cell growth and differentiation, were assessed to understand the mechanisms behind this process. Additionally, and for the first-time, microvesicles were extracted from epithelial cells derived from human ocular epithelial cells. These microvesicles showed cargo containing several mRNA and miRNA molecules. Furthermore, the microvesicles were used to drive cell differentiation towards the lineage of the exosome-originating cells. Lastly, by replicating factors within the conjunctival and corneal epithelium environment, human embryonic stem cells were partially differentiated into conjunctival and corneal epithelial-like cells, respectively.

Acknowledgements

The successful completion of this thesis must not be attributed to me alone. It is result of a collaboration with my supervisors, my work colleagues, those who have provided financial support for this work, my family and friends.

To those who kindly donated their tissue and to their families, thank you.

I would like to start by thanking my supervisory team Dr Sajjad Ahmad, Dr Kevin Hamill, Professor Stephen Kaye, and Dr Rosalind Stewart for their support and encouragement. Dr Ahmad has provided me with constant guidance and support throughout my whole journey. Dr Hamill has always been there with his endless expertise in cellular biology and sense of humour, therefore I will always be truly grateful to him. Professor Kaye and Dr Stewart held the clinical point of view of my work. They, above all, taught me the basics of Eye and Vision Science.

Everything I have achieved is down to my parents, Mr Edmundo Ramos and Mrs Cilia Silva. They have always been tremendously supportive since the day I moved to the UK, through the ups and downs of my journey. I will always carry with me their willingness for education, their lessons and example that hard work never goes unrewarded.

I also express my deepest sense of gratitude to my friends, who, being away, have always found the time to give the support one seeks and encourage of my work. I will always carry all the cherished moments we had the pleasure to share. That being said, I would like to thank Miss Sofia Miranda and my friends Mr Andre Martins, Mr Celso Silvestre, Mr Diogo Santos, Mr Joao Ribeirinho, and Miss Rita Pinho. You truly are beautiful people, I adore you. Thank you all.

I am also very grateful to all those at the Institute of Ageing and Chronic Disease (University of Liverpool) for their support, help, and guidance with so many techniques. I would like to include here all the people from the Research Eye Bank from Liverpool who provide access to human corneal and conjunctival tissue.

Finally, I want to thanks to Crossley Barnes Foundation for their financial support this research.

A massive thanks to you all.

Tiago Ramos

Table of Contents

Table of Figures

Table of Tables

Declaration and statement of copyright

I confirm that no part of the material offered has previously been submitted by me for a degree in this or any other University. Material here generated has been acknowledged and the appropriate publications cited. In all other cases, material from others' work has been acknowledged and quotations suitably indicated.

Publications and abstracts

Abstracts

"The extracellular environment plays a role in human ocular surface epithelial plasticity *in vitro*" Roy Mapstone Prize (University of Liverpool, UK, December 2014).

"An in vitro investigation of human ocular surface epithelial stem cell homeostasis" Antibody Resource (May 2015).

Publications

T. Ramos, D. Scott, S. Ahmad, An Update on Ocular Surface Epithelial Stem Cells: Cornea and Conjunctiva. Stem cells international 2015, 601731 (2015).

A copy of the manuscript can be found at the end of this document, see Appendix C.

Awards

Onassis Foundation award for the 2015 Lectures in Biology devoted to "Stem Cells: From basic biology to translational research" (Crete, Greece; July 2015).

Talks

"The extracellular environment plays a role in human ocular surface epithelial plasticity *in vitro*", Roy Mapstone Prize (University of Liverpool, United Kingdom, December 2014).

"The role of the extracellular matrix on human corneal and conjunctival epithelial plasticity". Presentation at the Association for Research in Vision and Ophthalmology Annual Meeting (Washington State Convention Centre, Washington, USA; May 2016).

"The role of the extracellular matrix on human corneal and conjunctival epithelial plasticity". Presentation at Venice Eye Bank (Venice, Italy; September 2016).

Abbreviations

A

A.U. arbitrary units

ABC ATP-binding cassette

AM amniotic membrane

AMP adenosine monophosphate

AMPK adenosine monophosphate kinase

Asp aspartate

B

BM basement membrane

BMP bone morphogenetic protein

Bp base pair

BPE bovine pituitary extract

BrdU bromodeoxyuridine

BSA bovine serum albumin

C

CALT conjunctiva-associated lymphoid tissue

CD cluster of differentiation

CFE colony forming efficiency

COL collagen

Ct cycle threshold

D

DC dendritic cell

DMEM Dulbecco's Modified Eagle's Medium

DMSO dimethyl sulfoxide

DNA deoxyribonucleic acid

DPBS Dulbecco's phosphate-buffered saline

DTT dithiothreitol

E

EC epithelial cell

ECM extracellular matrix

EDTA ethylenediaminetetraacetic acid

EGF epithelial growth factor

EGFR epidermal growth factor receptor

ERK extracellular signal-regulated kinase

ESC embryonic stem cell

ESCRT endosomal sorting complexes required for transport

EV extracellular vesicle

F

FA formic acid

FCS foetal calf serum

FDR false discovery rate

FGF fibroblast growth factor

FGFR fibroblast growth factor receptor

FITC fluorescein isothiocyanate

G

GAPDH gene-to-glyceraldehydes-3-phosphate dehydrogenase

GFP green fluorescent protein

GRP glucose-regulated protein

GSK-3β glycogen synthase kinase-3β

H

HaCaT human adult low calcium Temperature keratinocyte

HCjE-Gi immortalized conjunctival epithelial cell

HD hemidesmosome

hESC human embryonic stem cell

HGF hepatocyte growth factor

HMG high motility group

HRP horseradish peroxidase

HSP heat shock protein

hTCEpi telomerase-immortalized human corneal epithelial cell

I

ICC immunocytochemistry

ICM inner cell mass

IL interleukin

ILV intraluminal vesicles

iPS induced pluripotent cell

J

JAK Janus kinase

K

KGF keratinocyte growth factor

KRT keratin

KSFM keratinocyte serum free medium

L

LAM laminin

LC-MS liquid chromatography–mass spectrometry

LSC limbal stem cell

LSCD limbal stem cell deficiency

M

MALT mucosa-associated lymphoid tissue

MAPK mitogen-activated protein kinase

MEK mitogen-activated protein kinase kinase

MHC major histocompatibility complex

miRNA microRNA

MSC mesenchymal stem cell

mTOR mammalian target of rapamycin

MUC mucin

MV microvesicle

MVB multivesicular body

N

NGS next generation sequencing

NSS not statistically significant

O

OCT4 octamer-binding transcription factor 4

P

P/S penicillin/streptomycin

PARP poly (ADP-ribose) polymerase

PAS periodic acid Schiff

PBS phosphate buffered saline

PCR polymerase chain reaction

PD proteome discoverer

PDK1 3-phosphoinositide-dependent protein kinase-1

POU5F1 POU domain class 5 transcription factor 1

PRAS40 proline-rich Akt substrate 40

R

RNA ribonucleic acid

RPE retinal pigmented cells

RPL5 ribosomal protein L5

Rpm revolutions per minute

RT room temperature

S

SC stem cell

SDS sodium dodecyl sulphate

Ser serine

SHEM supplemented hormonal epithelial medium

SP side population

SSEA specific embryonic antigens

STAT signal transducers and activators of transcription

T

TAC transient amplifying cells

TCPS tissue culture polystyrene

TDC terminally differentiated cell

TEM tetraspanin-enriched microdomain

TFA trifluoroacetic acid

TGF transforming growth factor

Thr threonine

TRA tumour rejection antigens

TSG Tumour susceptible gene

Tyr tyrosine

U

UTR untranslated region

Chapter 1 - Introduction

1.1. Structure and functions of the cornea, limbus, and conjunctiva

The anterior surface of the eye is composed of the clear cornea centrally and the conjunctiva and white sclera peripherally. The limbus forms the transition zone between the cornea and the sclera and conjunctiva, Figure 1.

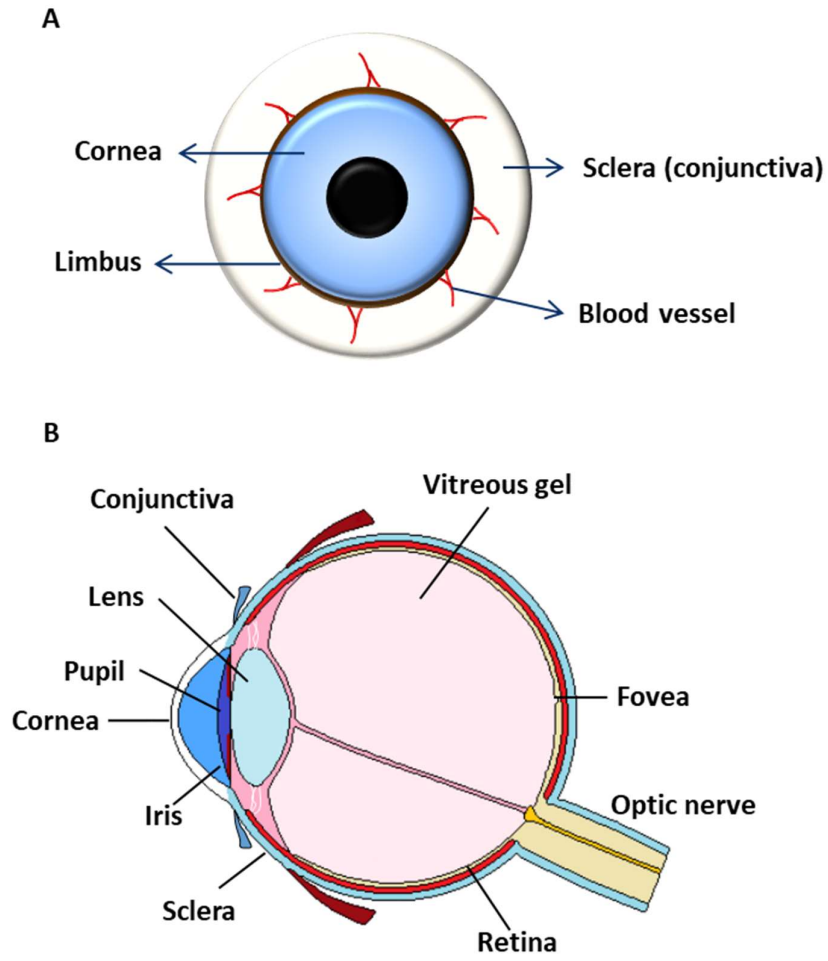

Figure 1 – Schematic anterior view and sagittal cross-section of the human eye (not to scale). (A) The limbus forms the transition zone between the cornea located centrally and the sclera and conjunctiva located peripherally. (B) Sagittal cross-section of the human eye.

The cornea is a specialized transparent avascular structure, composed of five main layers, Figure 2. The first layer, which forms the outer surface, is made up of approximately five to seven cell layers of non-keratinized, stratified, and squamous epithelium. The second layer, called the Bowman's layer, is formed by a thin acellular collagenous layer and serves as a

basement membrane (BM) for the epithelial layer. The third layer is the avascular stroma and comprises about 90% of the corneal thickness. The corneal stroma is composed of aligned arrays of collagen fibrils interspersed with specialised fibroblasts, called keratocytes. The fourth layer, called the Descemet's membrane, serves as the BM of the fifth layer - the corneal endothelium. The endothelial cells transport nutrients and water to and from the stroma preventing corneal oedema and therefore maintaining optimal hydration [8]. The main function of the cornea is to enable the transmission and focusing of the light into the retina by providing two-thirds of the eye's refractive power. It also acts as a first line of defence against injury, infection and desiccation [8].

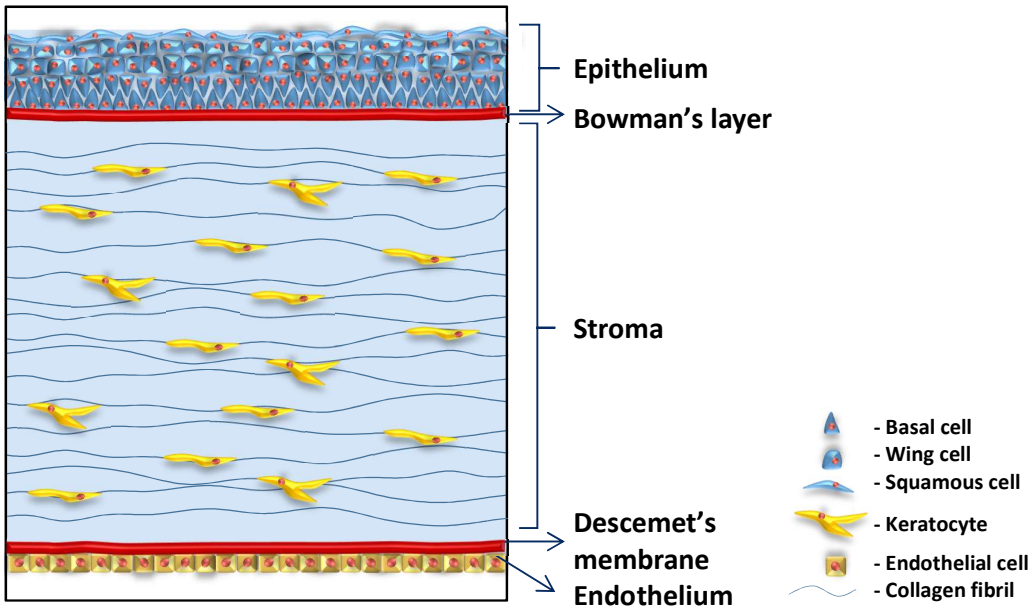

Figure 2 – Cross section of the human cornea (not to scale). The cornea is composed of five main layers: the epithelium on the outer surface, the Bowman's layer, the collagenous stroma, the Descemet's membrane and the endothelium on the inner surface. Adapted from [9].

The superficial layers of the cornea (the stratified epithelium and the Bowman's layer) are continuous with the peripheral conjunctiva. The conjunctiva is a thin loose mucous membrane that covers and bridges the anterior surface of the globe and the posterior surface of the eyelids [8]. The conjunctiva is composed of two to ten cell layers of non-keratinized, stratified squamous and columnar epithelium with scattered mucin (MUC)-producing goblet cells and an underlying highly vascularised substantia propria, Figure 3. The conjunctiva is of crucial importance to: (i) support the structure of the corneal epithelial tear film, (ii) enable the independent motion of the eyeball and eyelids, and (iii) protection of the cornea and the interior of the eye from the external environment by secreting mucins,

antibacterial proteins, and water to form the inner mucous layer of the tear film [10]. Besides its nonspecific defence mechanisms, the conjunctiva provides with a system of specific immune response in the form of mucosa-associated lymphoid tissue (MALT) [11, 12]. This tissue consists of an arrangement of lymphatic cells situated underneath the epithelium [13]. MALT detects antigens and induces an immune response through direct action of the lymphatic cells or secretion of soluble antibodies [14]. In human conjunctiva the presence of an associated lymphoid tissue has been shown elsewhere [15], suggesting the term conjunctiva-associated lymphoid tissue (CALT).

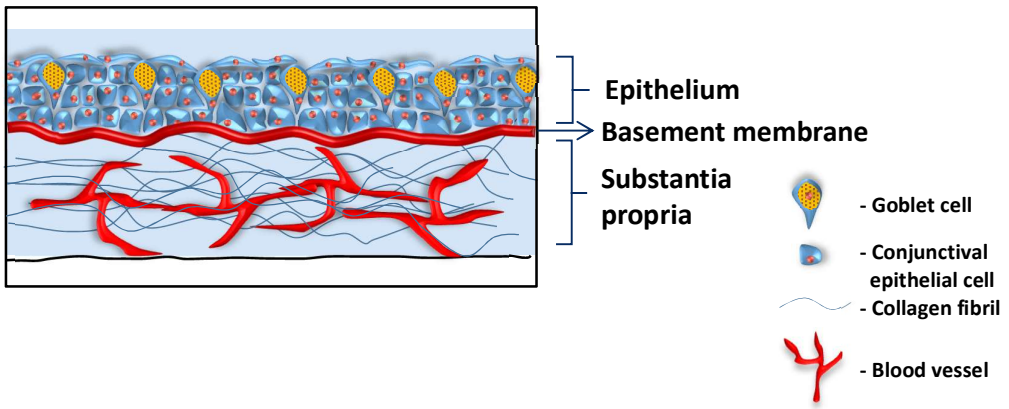

Figure 3 - Cross-section of the human conjunctiva (not to scale). The conjunctiva is composed of three main layers: the outer epithelium containing scattered goblet cells, the basement membrane, and a substantia propria containing blood vessels.

The conjunctiva is divided into three main regions, as follows:

i. **Palpebral conjunctiva**. The palpebral conjunctiva lines the posterior surface of the eyelid and is divided into marginal, tarsal, and orbital regions. The marginal region starts at the intermarginal strips of the eyelid as a continuation of the skin and continues into the posterior surface of the eyelid up to a shallow groove, named sub tarsal sulcus, where it merges with the orbital region. The tarsal region is a highly vascular structure and very adherent to the tarsal plates. The orbital region is a looser entity covering between the tarsal plate and the fornix [16].

ii. **Forniceal conjunctiva.** The forniceal conjunctiva covers the posterior surface of the eyelids up to the anterior surface of the globe. This structure is thicker and loosely attached to allow free movement of the eye globe. It is divided into superior, inferior, lateral, and medial fornix regions [16, 17].

iii. **Bulbar conjunctiva**. The bulbar conjunctiva is the thinnest and the clearest of all parts of the conjunctiva, allowing the white sclera and its blood vessels to be seen easily. It is loosely attached, exception made for the zone near the limbus. Belonging to the bulbar conjunctiva is the limbus conjunctiva that covers the limbal region and fuses with the corneal epithelium [16, 18].

Table 1 – Characteristics of conjunctival epithelium. Adapted from [19].

Conjunctival regions	Number of layers	Cells in layers
Marginal	5 layers of non-keratinized stratified squamous epithelium	Superficial layer: squamous cells Middle three layers: polyhedral cells Deepest layer: cylindrical cells
Tarsal	2 layers of stratified cuboidal epithelium	Superficial layer: cylindrical cells Deepest layer: cuboidal cells
Fornix and bulbar	3 layers of stratified squamous epithelium	Superficial layer: cylindrical cells Middle three layers: polyhedral cells Deepest layer: cuboidal cells
Limbal	10 layers of stratified squamous epithelium	Superficial layer: squamous cells Middle three layers: polygonal cells Basal layer: cuboidal cells

Physically separating the cornea and the conjunctiva is a narrow band known as limbus that encircles the cornea. It starts at the termination of Bowman's layer and is approximately 1.5mm wide. The limbus' main function is twofold in maintaining the corneal clarity. Firstly, the limbal epithelium acts as a physical barrier, preventing the phenotypically different conjunctival epithelium and its stromal blood vessels from encroaching onto the cornea, thereby impairing its clarity [20]. Secondly, the limbal epithelium harbours the stem cells (SCs) that renew the corneal epithelium, the so called limbal stem cells (LSCs) [21, 22]. Unlike the transparent cornea, both the limbus and the conjunctiva are vascularised.

1.2. Embryology

The major development of the human eye occurs between the 3rd and 10th week of gestation and mainly involves the ectoderm, the neural crest cells, and the mesenchyme. The eye begins to develop as a pair of two small optic grooves on each side of the forebrain at the end of the 3rd week of gestation. These grooves will eventually close becoming the optic vesicles which will then invaginate to form a double-layered structure called the optic cup. The optic vesicles will contact the surface ectoderm triggering the necessary changes for further eye development, initiated by the master control gene *PAX6*. The *PAX6* gene product is a transcription factor playing a key role in the regulation of eye development. Further

differentiation and mechanical rearrangement of cells gives rise to the fully developed eye [23, 24].

Different germ layers form different areas of the eye: the neural tube ectoderm gives rise to the retina, iris, ciliary body epithelia, optic nerve, smooth muscles of the iris, and some of the vitreous humour. Surface ectoderm gives rise to the lens, the corneal and conjunctival epithelium, the eyelids, and the lacrimal apparatus. The remaining ocular structures are formed from the mesenchyme.

The developing corneal epithelium is first apparent at 6 weeks post-ovulation [25] when the mesenchyme that surrounds the external surface of the optic cup condenses into two different layers. The inner layer is pigmented and vascular, known as choroid. The outer layer is fibrous and is called the sclera. The mesenchyme, anterior to the developing lens, splits into two layers that surrounds the newly formed anterior chamber of the eye. The outer layer, continuous with the sclera, will form the corneal stroma. The corneal endothelium develops from the surface ectoderm and the inner endothelium from migrating neural crests cells from the optic cup. The primitive corneal epithelium is initially composed of two cell layers (as compared to the five to seven layers in the adult). This primitive epithelium is also responsible for forming a prominent primary acellular corneal stroma and the Bowman's layer. Sometime between the 8th week of gestation (when the eyelids fuse together) and the 26th week (when eyelids open), the corneal epithelium stratifies into a structure of four to five cell layers thick. Adhesion complexes only become detectable by 19 weeks of gestation. Further development in utero leads to an increase in the number of hemidesmosomes (HDs), increase in fibril penetration into the Bowman's layer, and an increase in the Bowman's layer thickness. Maturation of the corneal epithelium is therefore related to eyelid development [25].

The conjunctival epithelium is derived from the surface ectoderm and becomes distinguishable from the limbal-corneal epithelium at the 7th week of gestation [26]. At the 8th week of gestation the conjunctival epithelium develops within the lid folds from surface ectoderm along the posterior surface of the lids and around the developing cornea. Budding of the epithelium in the forniceal region at the 12th week leads to the formation of the lacrimal and accessory lacrimal glands [27]. Contrarily to corneal epithelium, the conjunctival epithelium does not stratify until the eyelids re-open (26th week of gestation) [28]. The normal eye development results therefore, from a sequential interaction of the various tissues, with some being the inducers for the development of other tissues.

Despite their closeness, the corneal epithelial cells (ECs) and the conjunctival ECs belong to distinct lineages [29, 30] arising from different cell populations [31]. *In vivo* studies in rabbit models have shown that limbal and corneal EC-derived cysts contained only stratified squamous-type cells. In contrast, conjunctival EC-derived cysts contained stratified columnar-type cells interspersed with periodic acid-Schiff (PAS) staining cells (PAS test is widely used as MUC staining method) with a goblet-like structure (the goblet cells) [31]. This supports the hypothesis that corneal and limbal ECs originate along a different embryonic lineage to conjunctival ECs, with the goblet cells originating from the conjunctival compartment.

1.3. Basic stem cell biology

The classical definition of a SC is 'an undifferentiated cell that is both capable of self-renewing and has the ability to generate one or more differentiated cell types (cell potency). Broadly, two main groups of SCs can be distinguished:

- **Embryonic SCs (ESCs).** ESCs are derived from the undifferentiated inner cell mass (ICM) of the blastocyst. They were firstly established from human in 1998 [32]. Like their counterparts in the inner cell mass, they are pluripotent, i.e. they can give rise to all derivatives of the three primary germ layers: ectoderm, endoderm, and mesoderm. ESCs are distinguished from other SCs by two distinctive properties: their pluripotency and by their indefinite ability to replicate.

- **Adult SCs**. Adult SCs are undifferentiated cells found among differentiated cells within a tissue or organ. These cells can renew themselves and can differentiate into the major specialized cell types of the tissue or organ of origin. They have, however, a more limited ability to generate differentiated cells compared to ESCs. Their main role is to maintain and repair the tissue where they reside [33].

The ability of ESCs to maintain the self-renewal and pluripotency is associated with their ability to remain in a proliferative state. ESCs cell divide rapidly [34] and undergo successive symmetrical cell divisions to generate new progeny structurally and functionally equivalent to the mother cells [35]. Their cell cycle progression is controlled by accurate mechanisms to ensure the rapid replication and accurate transmission of the genetic material to the daughter cells. The cell cycle is divided into four phases; the S phase (chromosome replication, M phase (chromosome transmission), and two gap phases (G1 and G2) that

temporally separates the S and M phase [35]. ESCs have an unusual cell cycle, consisting mainly of S phase and truncated G1 phase [36]. In human, ESCs reside 65% of the time in S phase and 15% of the time in G1 phase (on the other hand, somatic cells reside 40% of the time in G1 phase and 25 to 30% in S phase) [34]. Both tritiated thymidine and bromodeoxyuridine (BrdU), an analogue of thymidine, have been used in the detection of cells in S phase [37, 38] as it has been postulated that they can retain these markers for longer periods of time [39, 40]. More differentiated cells however, cycle much more rapidly therefore retaining these markers for shorter periods of time. This so-called 'label retaining property' has been used to distinguish SCs from other differentiated cells in the ocular surface [40-42].

1.4. Stem cell niche

Schofield suggested in the "Stem Cell Niche hypothesis" that SCs are located in a specialized microenvironment, known as a niche [43]. The niche varies depending on the tissue type, although it generally consists of a group of SCs and their transient amplifying cells (TACs), which are anchored together by specific junctions surrounded by a specialized extracellular matrix (ECM), Figure 4. The niche regulates cell cycle quiescence, maintenance, self-renewal, activation, and proliferation providing external signals [44, 45]. Besides their differences, all SCs niches share common features, such as an enriched blood supply and well protected areas with specialized ECM [46].

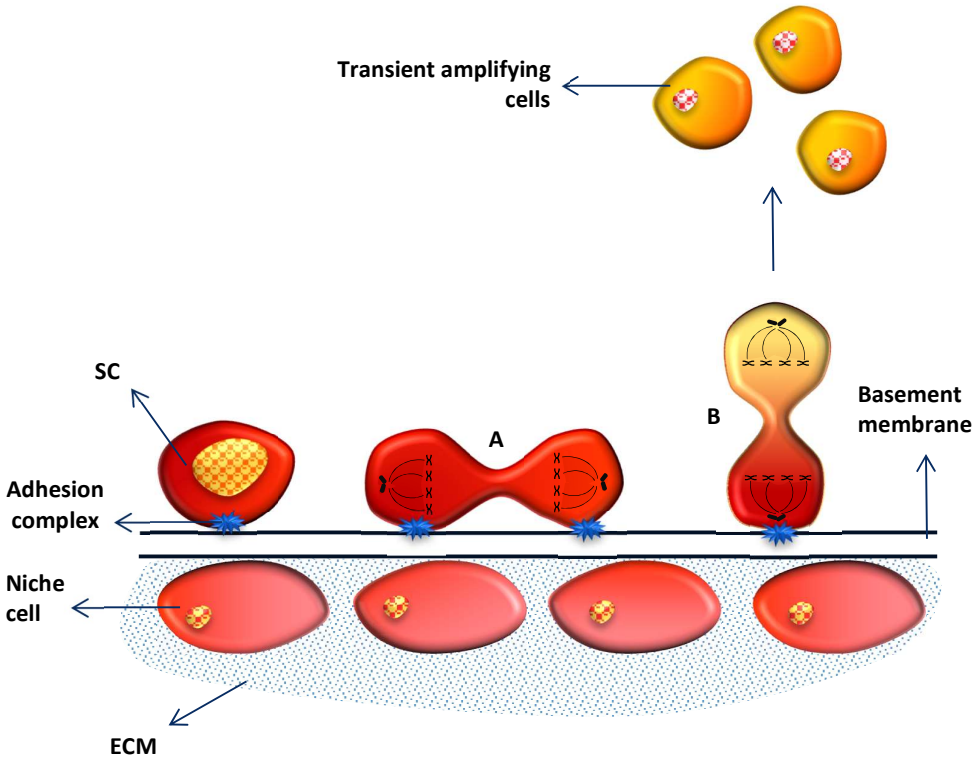

Figure 4 – Schematic illustration of a stem cell niche. The SC niche consists of a group of SCs and transient amplifying cells, anchored together by specific adhesion complexes. Surrounding these cells is a very specialized ECM which drives SCs to (A) self-renew or (B) to differentiate into its transient amplifying cell. Abbreviations used SC: stem cell, ECM: extracellular matrix. Adapted from [47].

1.5. Limbal stem cell niche

Differences in the microenvironments of limbus and cornea epithelium allow LSCs to maintain their relatively undifferentiated state in the limbus. These include the presence of palisades of Vogt [41, 48, 49], crypts [50, 51], and adhesion complexes [52, 53], as well as differences in the BM composition [46, 52].

1.5.1. Palisades of Vogt

Anatomically the LSCs reside within the palisades of Vogt, firstly proposed by Davanger and Evenson [48] and subsequently supported by *in vivo* evidence [49, 51]. This region is characterized by numerous undulations of richly vascularized stroma projected into the limbal epithelium. The function of these stromal projections is two-fold. Firstly, these invaginations allow basal limbal cells to interact with the underlying richly vascularized stroma, which provides nutrients and other soluble factors [41, 54]. Closeness to vascular networks has been postulated as being a prerequisite for the SC state [41, 52]. Secondly, these undulations also provide an increased surface area, allowing a higher concentration of

LSCs within a small area [41, 49, 52]. The deep limbal ridges also protect LSCs from trauma. Scattered amongst LSCs and ECs are melanocytes that offer additional protective mechanisms against ultraviolet radiation [55]. In addition, it has also been suggested that the LSC niche may be enriched in epithelial crypts associated with palisades of Vogt [50, 51]. These are formed by epithelial projections from the periphery of the palisade which extend either radially from the limbus into the conjunctival stroma or circumferentially within the limbus. These crypts are sparsely distributed, with only 6-7 per human eye [50, 51].

1.5.2. Basement membrane

The BM is a thin, fibrous layer that separates the epithelium and endothelium from the underlying connective tissue. Together with all other niche features, the BM plays a critical role in the maintenance of SC properties [43, 56]. Individual components of the BM regulate cell growth, proliferation, differentiation, and migration through interactions with cell surface receptors. BM provides structural support, and in addition stores and traps growth factors and cytokines, functioning as a reservoir of soluble factors that can be released in response to changes in physiological conditions [46]. It is mainly composed of collagen type IV, various types of laminin isoforms and fibronectin. A detailed comparison of limbus, cornea, and conjunctiva BM can be found in Section 3.1.2.

1.5.3. Fibroblasts

Fibroblasts are classically defined as fusiform mesenchymatous cells possessing an elongated nucleus parallel to the long axis of the cell, a cytoplasm rich in organelles, and a rough endoplasmic reticulum. Upon injury to the cornea, fibroblasts can transit into various phenotypes dependent on specific extracellular cues [57]. Stromal fibroblasts played an important role in the regulation of progenitor EC differentiation both *in vitro* and *in vivo*, providing cytokines and soluble factors that mediate their paracrine interactions [47]. Briefly, Li et al. found that:

i. **Type I cytokines,** such as interleukin (IL)-1β, are released by injured corneal ECs and their receptors expressed by fibroblasts. IL-1β results in type III cytokine production by both limbal and corneal fibroblasts [58, 59].

ii. **Type II cytokines,** such as transforming growth factor (TGF)-β1, are released by healing corneal ECs and their receptors are expressed by both ECs and fibroblasts [58, 59]. TGF-β1 inhibits type III cytokine production by both limbal and corneal fibroblasts [58].

iii. **Type III cytokines,** such as keratinocyte growth factor (KGF) and hepatocyte growth factor (HGF), are expressed by fibroblasts, but their receptors are predominantly expressed by ECs [58, 59]. KGF causes the proliferation of limbal ECs, and HGF causes the migration of ECs over the surface of the cornea [60].

1.5.4. Adhesion structures

Epithelial attachment to the underlying stroma is aided by three adhesion structures – hemidesmosome, anchoring fibrils, and adhesion plaques, Figure 5 [52].

i. **Hemidesmosomes.** HDs help the adhesion of basal cell membranes to the underlying BM [52].

ii. **Anchoring fibrils.** Anchoring fibrils, mainly composed of collagen type VII, link the BM to adhesion plaques in the underlying stroma [52].

iii. **Adhesion plaques**. Adhesion plaques are small patches of BM within the stroma itself, and are attached to the BM by anchoring fibrils [52].

The limbal area shows a smaller number of HDs, anchoring fibrils and adhesion plaques, a discontinuous basement membrane, and a more irregular surface when compared to the corneal BM [52, 53].

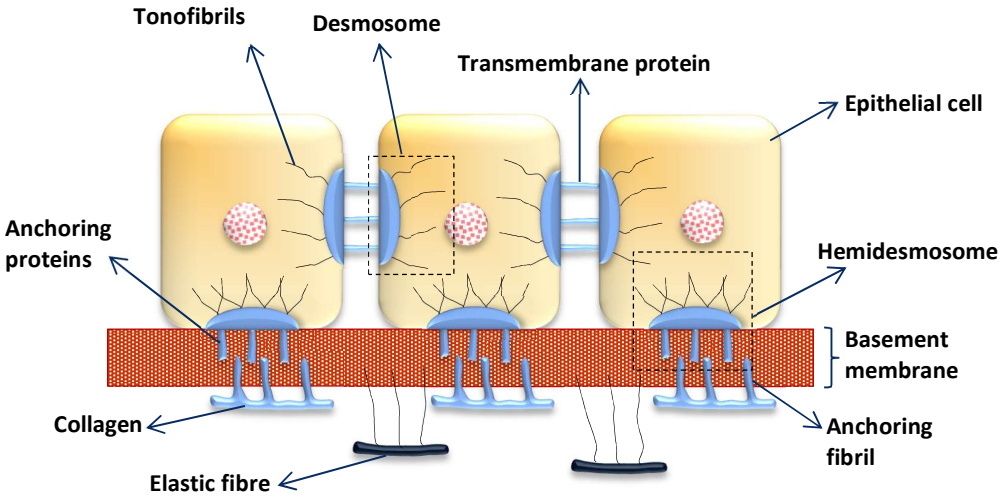

Figure 5 - The basement membrane of the limbal and corneal epithelia. The basement membrane zone ensures adherence of the overlying epithelium to the underlying stroma, through four main components: the hemidesmosomes, the basement membrane, the anchoring fibrils, and the elastic fibres. The cell-cell adhesion is mediated by desmosomes and transmembrane proteins. Adapted from [7].

1.6. Conjunctival stem cell niche

1.6.1. Common features

1.6.1.1. Fibroblasts

Fibroblasts are responsible for secreting fibres and other ECM proteins that form the conjunctival stroma. The fibroblasts play an important role in the regulation of progenitor EC differentiation both *in vitro* and *in vivo* providing cytokines and other soluble factors which mediate the paracrine interactions between themselves and ECs [58, 59].

1.6.1.2. Nutrients supply

The medial canthal and the inferior areas of the conjunctiva, two of the suggested areas for conjunctival SC location, are densely vascularized providing a plentiful supply of nutrients, blood-borne growth factors and other survival factors [61].

1.6.1.3. Protection

Solari et al. have suggested the presence of melanocytes interspaced in the plica semilunaris and caruncle [62]. These melanocytes offer protection against the carcinogenic insults from the ultraviolet light and subsequent formation of reactive oxygen species. The plica semilunaris is particularly enriched in both specific and non-specific immune cells. The intra-epithelial mucous crypts, abundant on the medial canthal and inferior forniceal regions, provide an increased surface area and protective locations allowing higher concentrations of conjunctival SCs within a small area.

1.7. The X, Y, Z model of the corneal epithelial renewal

Our understanding about the location and biological properties of the SCs has come primarily from investigations on the hematopoietic system [63] and intestinal epithelium [64]. In all these tissues three different cell populations can be distinguished: (i) the SCs, (ii) the TACs, and (iii) the terminally differentiated cells (TDCs), Figure 6 .Their main properties are explained below:

i. **SCs.** SCs are fewer in number and have a high capacity for self-renewal and high proliferative potential. In health they remain relatively quiescent. They give rise to TACs during normal tissue homeostasis and become more active during episodes of significant wound healing [65], although small wounds may be healed without upregulating SCs.

ii. **TACs.** TACs are larger in number and have limited proliferative potential capacity and limited capacity for self-renewal, and in healthy tissue they proliferate quickly. They give rise to TDCs.

iii. **TDCs.** TDCs are the main functioning cells in a given tissue. They have no capacity for self-renewal and no proliferative potential. In healthy tissue, they are continuously replaced due to their limited life-span.

The advantage of having a TAC population in a self-renewing tissue is considerable. The TACs amplify each SC division and therefore minimize the number of SC divisions. This conserves SCs energy and load, providing additional genetic protection by reducing the accumulations of mutations.

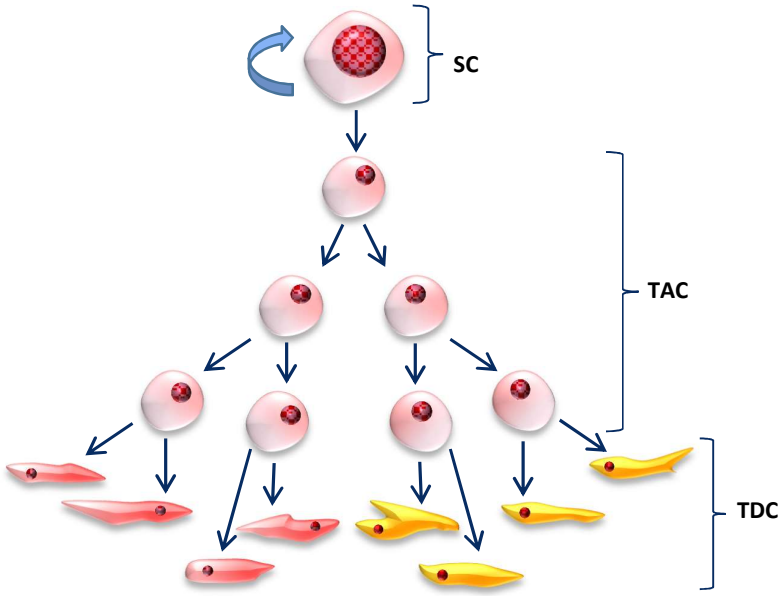

Figure 6 – The hierarchy of the cells in the adult stem cells system. The SCs have the greatest capability to self-renew. The TACs are larger in number and have reduced ability to self-renew. The TDCs form most cells in adult tissues and have no ability to self-renew. Abbreviations used SC: Stem cell, TAC: transient amplifying cells, TDC: terminally differentiated cell.

Besides the evidence for the preferred location of LSCs, others have also showed that TACs for the corneal epithelium are preferentially localized to the basal layers of the limbal and peripheral corneal epithelia. These include:

i. **Wound healing studies.** Matsuda et al. have shown in rabbits that corneal epithelial wounds that involved the peripheral cornea heal faster than those involving central corneal epithelial [66].

ii. **Cell culture studies.** *In vitro* studies have suggested that human peripheral corneal cultures grow better than central corneal epithelium cultures. Thus, these findings indicated that peripheral cornea contains cells with higher proliferative potential than the central cornea [65, 67].

iii. **Radio-labelling studies.** *in vivo* studies have identified cells actively dividing in the basal layers of the limbal and peripheral corneal epithelium in mice and rabbit [65, 68].

Collectively these studies show that certain cells in the basal layers of the limbal epithelium and the peripheral corneal epithelium exhibited properties of TACs, which are cells with high proliferative potential and actively proliferating in health. This contrasts with the LSCs at the limbus which have higher proliferative potential but remain relatively quiescent in healthy tissues.

LSCs can undergo asymmetric division whereby one daughter cell is retained in the SC niche, while the other detaches from its BM and loses its 'stemness' as it migrates centripetally towards the cornea. The differentiated cell is now termed a TAC. Following multiple rounds of replication, it becomes a post-mitotic TDC that is shed from the corneal surface. This homeostasis in which the corneal epithelium is renewed was summed up by Thoft and Friend in the "X, Y, Z hypothesis of corneal epithelial maintenance" [69]. This hypothesis predicts that the balance between cell proliferation and cell loss is directed by the following equation:

$$X + Y = Z$$

Equation 1 – X, Y, Z hypothesis of corneal epithelium maintenance.

The X component represents the proliferation of basal ECs [68, 70], the component Y represents the contribution to the cell mass by centripetal movement of peripheral cells [71, 72], and component Z represents the loss of ECs shed from the cornea surface [73, 74], Figure 7.

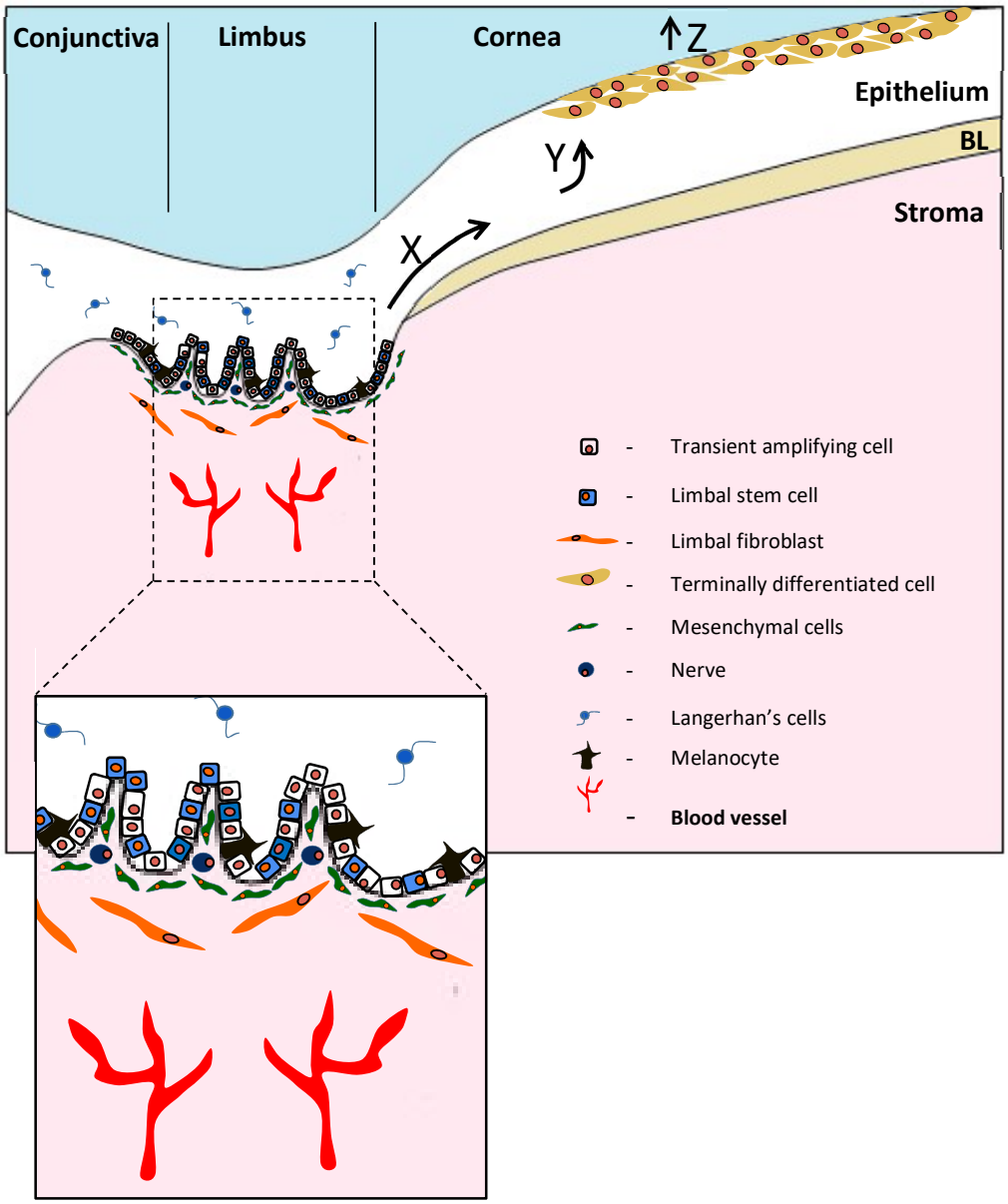

Figure 7 – The X, Y, Z hypothesis of corneal epithelium maintenance. X component is the migration of cells from the basal layers of the corneal epithelium to the epithelial surface. Y component is the migration of epithelial cells from the periphery of the cornea to the central cornea. Z component is the loss of corneal epithelial cells from shedding. Abbreviations used BL: Bowman's layer. Adapted from [75, 76].

1.7.1. Challenging the XYZ hypothesis

Recently, the XYZ hypothesis has been challenged by observations made in other mammals. These new evidences suggested that uninjured cells in the central cornea can generate holoclones (SC colonies with proliferative potential) with regenerative epithelial capabilities, which may also be responsible for the maintenance of the corneal epithelium [77, 78].

Supporting these controversial findings, central islands of normal corneal ECs have been described in patients with apparently complete clinical absence of LSCs [79].

1.8. Conjunctival epithelial stem cell location

Whilst it is commonly accepted that the SCs for the corneal epithelium, the LSCs, are located within the basal layers of the limbal epithelium, the location of SCs for the conjunctival epithelium is less well defined. In the human, conjunctival SCs have been identified throughout the whole tissue, especially in the bulbar and forniceal regions [61, 80-82]. Studies elucidating conjunctival stem cell location in various animal species are conflicting but may support this [83, 84].

Three main approaches have identified the bulbar and forniceal regions as the areas with highest concentrations of the SCs in the human conjunctiva:

i. **Stem cell markers expression.** Although there are no specific markers for conjunctival SCs, ATP-binding cassette subfamily G member 2 (ABCB2) and ΔNp63 have long been described as putative epithelial SC markers, described in detail in section 1.9. Stewart et al., using the expression of these two putative SCs markers, showed that SCs are distributed throughout the conjunctiva but with greatest concentration in the medial canthal and the inferior forniceal areas. Other studies also suggest the presence of conjunctival SCs on the bulbar conjunctival surface [81].

ii. **Clonogenic activity.** Another important property of the epithelial SCs is their ability to initiate clonal growth in vitro and form colonies consisting of small cells that have a long survival time, the holoclones. Stewart et al also performed in vitro clonogenic analysis of epithelial colonies from all the different regions of the conjunctiva confirming the findings found with SC marker expression [61]. Others have found similar observations, however only the bulbar and forniceal regions were assessed [80].

iii. **Circumstantial evidences.** Clinical observations also indicate that the conjunctival SCs are located in the fornix and/or in the bulbar conjunctiva [82].

The medial bulbar and inferior forniceal areas may provide greater physical protection, but more importantly are especially rich in goblet cells, intra-epithelial mucous crypts, blood vessels, melanocytes, and immune cells, common features shared with other SC niches [61].

In the other mammalian species, three approaches have identified different regions as the locations of SCs for conjunctival epithelium which would support the findings above:

i. **Label retention studies.** Similarly to what was performed on mouse corneas and limbus by Cotsarelis et al. [41]; Nagasaki et al. using BrdU retention (a property of quiescent SCs) in GFP-labelled mice cells, suggested that epithelial SCs are uniformly distributed throughout the whole conjunctiva [85].

ii. **Slow cell-cycling and proliferative potential.** Wei et al. showed, by analysing slow cell-cycling (by continuous administration of 3H-TdR to detect cells in S phase) and the proliferative potential (by single administration of 3H-TdR), that the forniceal region of the conjunctiva contains the largest proportions of cells with high proliferative potential [30] and a higher percentage of slow cycling cells (14% of ECs) when compared to the bulbar (5%) and palpebral conjunctiva (1%) [83].

iii. **Stem cell markers expression.** ABCG2-positive cells have been found in palpebral and forniceal conjunctiva regions of rabbits and these cells shared features consistent with the epithelial SC phenotype, including slow cycling [84].

Conjunctival SCs are thought to be bipotent in health giving rise not only to ECs, but also to mucin-producing goblet cells, which are scattered throughout the conjunctival epithelium [80, 86].

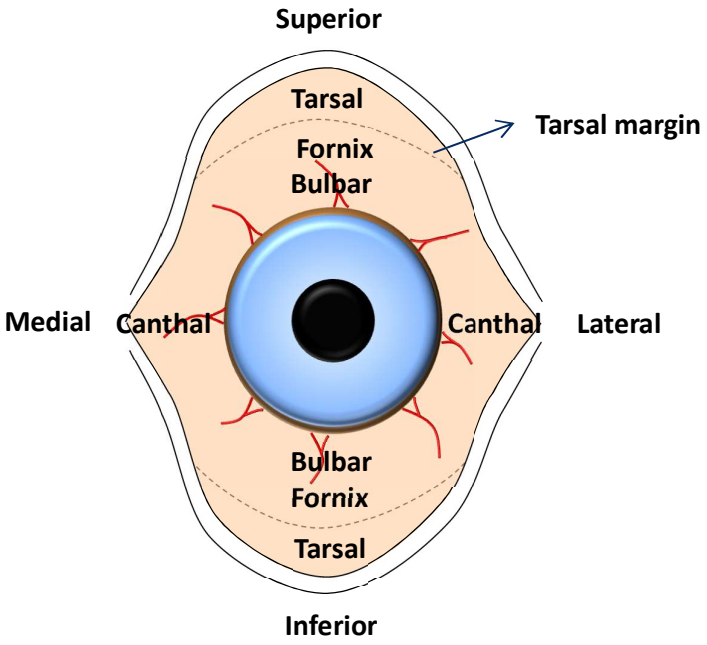

Figure 8 – Schematic anterior view of the human conjunctiva. Several regions have been proposed as possible regions for conjunctival stem cells, although the medial canthal and the inferior forniceal regions have been suggested as the preferred regions. These regions provide greater protection and share many features with other SCs niches. Adapted from [87].

1.9. Corneal epithelial stem cell location

Six main studies have identified the basal layer of the limbal epithelium as the preferred location of the SCs for the corneal epithelium:

i. **Pigment migration studies.** Davanger and Evensen were the first to propose the basal epithelial layer of the limbus as the "generative organ for corneal epithelial cells" [48]. Using guinea-pig eyes, where the basal layer of the limbal epithelium was pigmented, they demonstrated that the cornea healed with pigmented epithelium when the normally non-pigmented central cornea epithelium was removed [48]. These results suggested that cells located at limbal basal layer have proliferative potential for corneal regeneration.

ii. **High proliferative capacity of limbal epithelial culture.** Using in vitro cultures, Ebato et al. showed that human limbal epithelium has higher proliferative potential when compared to either corneal or conjunctival ECs [88]. Since the potential for proliferation is one of the hallmarks of SCs, this provides further evidence for the limbal location of SCs.

iii. **Radiolabelled thymidine studies.** Cotsarelis et al. used tritiated thymidine to radio-label cells in S phase of the cell cycle in mouse cornea and limbus models [41]. They showed that the basal cells of the limbal epithelium are slow cycling in nature (an important property of SCs), but in central corneal wounds they can be made to cycle much more rapidly [41]. Being this an important property of SCs, they concluded that the "corneal epithelial SCs are located preferentially, if not exclusively, in the limbal area".

iv. **Corneal epithelial regeneration with limbal grafts.** Kenyon and Tseng showed that, in patients who have a LSCs deficiency (LSCD), normal corneal epithelium can be restored by transplanting large healthy grafts of limbal epithelium [89].

v. **Corneal conjunctivalisation with limbal epithelial removal.** Several authors, using corneal wound healing studies in rabbits, showed that removal of the basal layers of the limbal epithelium prevents normal regeneration of the corneal epithelium. In such studies, the adjacent conjunctival epithelium and its blood vessels was seen to encroach over the corneal surface [20, 29, 90].

vi. **Circumstantial evidence.** Tumours of the ocular surface normally involve the limbus and it is well known for other tissue/organ systems that tumour cells may preferentially arise from SCs enriched systems [91, 92].

Collectively, the stated studies show that SCs for corneal epithelium exist in the basal layer of the limbus and have high proliferative potential, remaining relatively quiescent *in vivo* in health (important properties of SCs). Furthermore, studies have shown that LSCs are not evenly distributed throughout the limbus but are more abundant in the superior and inferior zones when compared to the nasal and temporal limbal zones [93, 94]. This uneven distribution may be explained by the higher protection offered by the upper and lower eyelids.

Recent studies in animal models however suggested that there is also a reservoir of SCs within the corneal epithelium itself in addition to the LSCs. A number of nonhuman studies have shown corneal epithelial maintenance without limbal input, and survival and self-maintenance of SCs outside the limbal SC niche [95]. Successful corneal epithelial regeneration by sequential corneal epithelial transplantation in a murine model was first proposed as evidence for this [96]. Recently, again in a murine model, lineage-tracing experiments have shown that although the limbus is the prime source for corneal epithelial

maintenance, there is also a reservoir of cells with colonies forming potential (properties of SCs) within the corneal epithelium itself [97]. In addition to these studies, 48-week follow-up rabbit studies have shown that although normal corneal epithelium cannot initially be maintained following the removal of limbal epithelium, there is evidence of corneal epithelial normalization at 48 weeks [98]. Further research is required particularly in human studies, to provide strength and consistency to this theory.

1.10. Epithelial stem cells markers

Despite decades of research, no definitive marker for ocular SCs has been identified. One of the reasons for this elusive task is the very few LSCs present, probably as few as 100 in the mouse limbus [99]. Comprehensive reviews of suggested putative LSC markers have been extensively published [56, 100]. These include transcription factors and ATP-binding cassette (ABC) family members as positive SC markers and keratins as negative markers.

1.10.1. Markers for corneal stem cells

In brief, putative positive markers include the transcription factor ΔNp63α [101-103], the ATP-binding cassette transporter ABCG2 [84, 104, 105], whilst negative markers include keratin (KRT)3 and KRT12, the structural proteins found in the corneal epithelium [106-108].

TP63. This gene encodes a transcription factor that belongs to a family of tumour suppressor proteins which includes p53 and p73 [109]. Alternative splicing of this gene results in transcript variants encoding different isoforms that vary in their functional properties, which include adult/SC progenitor cell regulation [109]. Pellegrini et al., using immunohistochemistry and *in vitro* studies, localised the ΔNp63α isoform (one of the six p63 isoforms) within the LSCs holoclones, which are thought to be generated by SCs, but not in the paraclones (comparable to more differentiated cells) [101]. More recently Di Iorio et al., using Western blotting, real time PCR, and quantitative fluorescence immunohistochemistry have shown that the ΔNp63α isoform is specific to LSCs [102, 103], challenging other studies where ΔNp63α was also expressed by early TACs [110-112].

ABC transporters. ABC transporters are a family of surface transmembrane proteins whose functions are related with the transport of potentially harmful metabolic products out of the cells [113]. Conceptually, ABC transporters may form a component of the molecular mechanisms by which long-lived cells reduce the potential for genomic damage over their

extended lives, and their expression has been associated with SC activity [114]. Two ABC transporters have been suggested as markers for LSCs:

- **ABCG2.** Using Fluorescence-Activated Cell Sorting ABCG2-positive limbal ECs were isolated as a side population (SP). This SP contained cells exhibiting properties associated with LSCs, including slow-cycling nature, higher clonogenic capacity and p63 expression [104]. It has recently been demonstrated that ABCG2 expression can be localized to basal cells of the human limbal epithelium [84, 105]. However, some of the ABCG2-positive cells with high nucleus:cytoplasma ratio (striking feature of progenitor cells) in the rat limbus have later been identified as Langerhans cells rather than epithelial SCs [115].
- **ABC sub family C member 5 (ABCB5).** More recently, murine and human studies have shown that cells expressing ABCB5 are required for corneal epithelial homeostasis and repair [116]. Those studies showed that ABCB5-positive cells were localized to the limbus and co-expressed ΔNp63α but not KRT12.

Integrins. Integrins belong to a family of cell membrane glycoproteins involved in cell-cell and cell-matrix adhesion, they are obligate heterodimers composed of a α and β subunit [117]. The α9β1 integrin has been localized to the basal cells of healthy adult limbal epithelium, similarly to LSCs [118]. The expression of tenascin-C, a ligand for the α9β1 integrin, is limited to the extracellular space in the limbal region [119] and its upregulation in wounded murine corneas has suggested that this integrin is associated with TACs [120].

Other proteins have too been used as positive markers to distinguish cells present in human basal limbal but not in basal corneal epithelium. These include the type III intermediate filament, vimentin [56], the mediator for cell-cell adhesion, N-cadherin [121], the proto-oncogene, Bmi1 [122], and the self-renewal regulator, C/EBPδ [122].

1.10.2. Markers for conjunctival epithelial stem cells

Similar to LSCs, no specific marker for conjunctival SCs has yet been reported. Positive putative markers ΔNp63α and ABCG2 are nevertheless the most widely used [61, 81, 110-112].

ΔNp63. p63 is a transcription factor known to be expressed by LSCs and early TACs [110-112]. Stewart et al. using cytochemistry analysis, showed a preferred location of this transcription factor in the inferior forniceal and medial canthal regions– the preferred

location for conjunctival SCs. The cells in those areas also exhibited properties associated with SCs, including higher clonogenic capacity [61].

ABCG2. In human beings, ABCG2-positive cells have been found in biopsies from basal [84], medial canthal and inferior forniceal areas of the conjunctiva [61]. Those cells display many features that are consistent with the epithelial SC phenotype including slow cycling, clonogenic capacity, and resistance to phorbol-induced differentiation [61].

Heat shock protein (Hsp) 70. The Hsp70 belongs to a protein family that assists a wide range of folding processes, including protein folding and assembly of newly synthesized proteins and refolding of misfolded and aggregated proteins [123]. Besides their important role in the cell's machinery for protein folding, Hsp70 is known to aid to protect cells from thermal and oxidative stress [124, 125]. Hsp70 also inhibits apoptosis [126]. Because of their role in protecting cell against harmful metabolites, Hsps have been used as markers for SCs (an extensive review can be found at Fan et al. [127]). Interestingly, its expression was found higher in the inferior forniceal and medial canthal areas of the conjunctiva [61], which are believed to be the preferred location for the human conjunctival SC [61, 82].

KRT15. Initially proposed as a marker for hair follicle progenitor cells [128], it was recently proposed as a potential marker for progenitor conjunctival ECs [129]. Two studies revealed that KRT15 is expressed in the basal layers of the limbal and conjunctival epithelia but absent in the corneal epithelium [108, 129]. One *in vitro* study has shown that KRT15 is not expressed only by conjunctival epithelial progenitor cells, but more differentiated conjunctival cells may also express this protein, limiting their usefulness as a marker for progenitor cells [10].

1.11. Differentiated epithelial cell markers

The identification of a distinguishable marker that is expressed in the conjunctival epithelium but not in the corneal epithelium and vice-versa has been a growing need and is of crucial importance for the herein studies. Thereafter, the degree of cell plasticity in response to the extracellular cues will be based on the expression of such markers. Currently the two main markers to distinguish these two epithelia are the KRTs and the MUCs, as follows:

1.11.1. Keratins

KRTs are a heterogeneous class of structurally related proteins that comprise the intermediate filament-forming system and, together with microfilaments and microtubules, are responsible for the structural integrity and function of ECs [130]. The KRT gene family consists of the highest number in humans with 54 distinct functional genes (37 encoding for epithelial KRTs and 17 for hair KRTs) [130]. Based on their isoelectric charge, they are divided into type I (acidic) and type two (basic or neutral) subfamilies [106]. The type I subfamily include KRT9 to KRT20 and the type II include KRT1 to KRT8. *In vivo*, the intermediate filament unit is made up of a type I KRT subunit that dimers with a type II KRT subunit to form specific pairs. Because of their different patterns of expression, KRTs have widely been used to distinguish the different populations of ECs from the ocular surface [131], Table 2.

Table 2 - The distribution of different keratins across the ocular surface epithelia adapted from [106-108, 131]. – negative, -/+ weak, + moderate, ++ strong labelling.

Keratin	Cornea	Limbus	Conjunctiva
1	-/+	-/+	-/+
2	-	-	-
3	+ (basal) ++ (suprabasal and superficial)	- (basal) -/+ (suprabasal and superficial)	-
4	-/+ (basal) + (suprabasal and superficial)	- (basal) + (suprabasal and superficial)	- (basal) + (suprabasal and superficial)
5	+	-/+ (basal) + (suprabasal and superficial)	-/+ (basal) + (suprabasal and superficial)
6	- (basal) -/+ (suprabasal and superficial)	- (basal) -/+ (suprabasal and superficial)	- (basal and suprabasal) -/+ (superficial)
7	-	-	- (basal and suprabasal) -/+ (superficial)
8	-/+ (basal) + (suprabasal and superficial)	++	-/+ (basal and suprabasal) + superficial
9	-	-	-
10	-	-	-
12	All layers	+ peripheral (superficial)	-
13	-	+ peripheral (suprabasal and superficial)	++ (suprabasal and superficial)
14	++ (basal and suprabasal) + (superficial)	++ (basal) + (suprabasal and superficial)	++ (basal) + (suprabasal and superficial)
15	-	+ (basal) -/+ (suprabasal) - (superficial)	+ (basal) -/+ (suprabasal and superficial)
16	-/+ (basal and superficial) ++ (suprabasal)	- (basal and superficial) -/+(suprabasal)	- (basal and superficial) -/+suprabasal
17	-	-	-
18	+	-/+	+ (basal and suprabasal) -/+ (superficial)
19	+ (central and peripheral)	+ (basal suprabasal) ++ (superficial)	++ (basal and superficial) + (suprabasal)
20	-	-	-

1.11.2. Mucins

MUCs are a heterogeneous group of highly glycosylated glycoproteins found in all mucous secretions on wet-surfaced epithelia. At the ocular surface they act as lubricants, stabilizers of the preocular tear film to prevent desiccation of the underlying epithelium, and as a barrier to pathogens [132]. 20 human MUC genes have been identified [133]. MUCs can be categorized into secreted or membrane-spanning. Secreted MUCs can be further sub-classified as gel-forming (responsible for the rheological properties of the mucous) or soluble

[134]. In the epithelia of the ocular surface, the gel-forming MUC5AC is expressed in conjunctival goblet cells, Figure 9, and the membrane-spanning mucins MUC1 and MUC4 are primarily expressed by the stratified cells [132]. The limbal and corneal epithelia express transmembrane-type MUC1. MUC4 is also present at the peripheral corneal and limbal epithelia (at lower levels when compared to conjunctival epithelium). MUC16 (another membrane-associated mucin) has also been shown to be present on human stratified cells of corneal and conjunctival epithelium [135]. Human lacrimal gland has also been suggested as other sources of soluble mucins (MUC7). In the healthy tear film, membrane-spanning mucins provide a negatively charged, hydrated EC surface, which supports the spreading of the hydrated tear film [132].

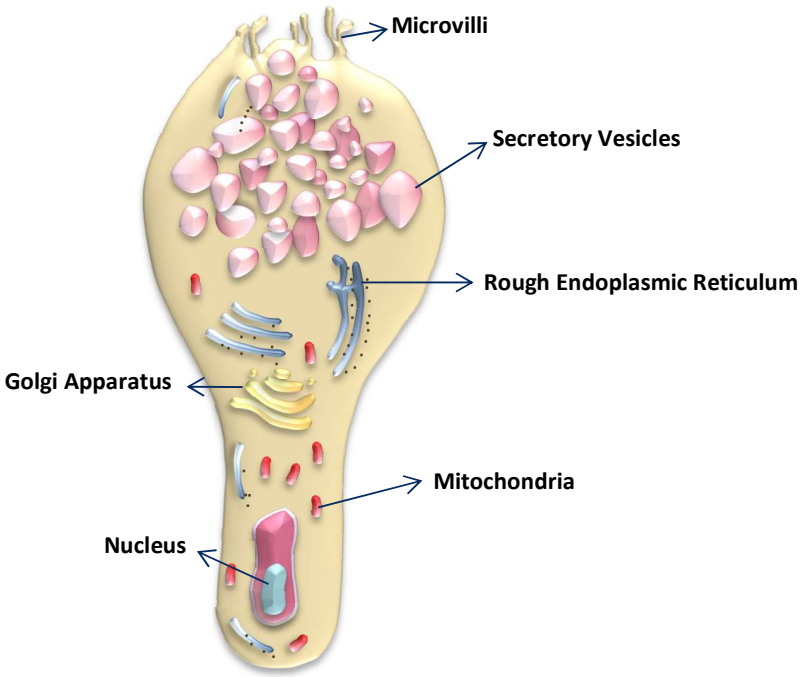

Figure 9 - Schematic illustration of a goblet cell. The goblet cells are highly polarized cells with organelles mainly located at the base of the cells. The remaining cytoplasm is occupied by secretory vesicles which contain the mucins. The microvilli increase the surface area for secretion. Adapted from [136].

1.11.3. Markers for differentiated corneal epithelial cells

KRT3/12. Schermer et al. were the first to propose that the "acidic 55KDa (KRT3) and basic 64KDa (KRT12) keratins represent markers for an advanced stage of corneal epithelial differentiation" [107]. KRT3/12 is the most widely accepted dimer marker for corneal ECs with countless studies showing its presence in all layers of the corneal epithelium and the

suprabasal layers of the limbus, but not in the conjunctival epithelium. These include microarrays, qRT-PCR and immunocytochemistry studies [106-108].

Missense mutations within KRT12 gene, one of the causes for Meesmann epithelial corneal dystrophy [137, 138], led to a significant increase in expression of KRT4 and KRT13 (amongst others) [139], two suggested markers for conjunctival ECs (see section below). These observations may be interpreted as a loss of corneal phenotype associated with the gain of other epithelial-like phenotypes, including conjunctival-like.

Besides the KRT3/12 dimer, other proteins have been used to identify cells present only in basal cornea but not in basal limbal epithelium. These include nerve growth factor receptor (p75NTR) [54], involucrin [54], the gap junction protein connexin 43 [54, 56], the cell-cell adhesion protein E-cadherin [54], and the type IV intermediate filament nestin [56]. Because of their expression pattern, these markers are commonly used as negative markers for the presence of limbal SCs [54, 56, 75, 140].

1.11.4. Markers for differentiated conjunctival epithelial cells

Whilst it is commonly regarded that KRT3/12 dimer is the most widely accepted marker for corneal ECs, a specific marker for conjunctival ECs is still not established with confounding results arising from different investigations. KRT19 was firstly proposed by Donisi et al. [141] as a specific marker for conjunctival ECs, however, others have found its expression also in corneal ECs [129, 142, 143]. Amongst all the candidates, KRT4/13 dimer has been shown to be the more specific for conjunctival ECs [10, 106, 144].

KRT4. KRT4 has been shown to be expressed in all the epithelial layers in conjunctival mice however, its expression in the basal layers is reported as weaker and more focal. Moreover, KRT4 expression has also been detected in the superficial layers of the mouse and rabbit corneal epithelium [145, 146]. *In vitro* studies have also shown that both human adult conjunctival and corneal ECs express KRT4 in the suprabasal and superficial cells, but few KRT4-positive cells are observed in the basal layer [108].

KRT7. KRT7 pairs with KRT19 and its expression is characteristic of glandular epithelia [147]. Its expression has been found in goblet cells from human conjunctiva and trachea, but not in the mucosa of the intestinal tract nor in the stratified epithelia of the skin [147]. This may suggest that goblet cells from conjunctival epithelium are related more closely to those present in the respiratory epithelium than those present in the intestine [148, 149]. Its

expression has been shown to be highly specific of conjunctival differentiation, being positive in all the tissues derived from 12 eyes evaluated in one study [150].

KRT13 and KRT19. Ramirez-Miranda et al. have shown that KRT13 and KRT19 transcript expression is significantly upregulated in the human conjunctiva in comparison to the human cornea [106]. Using immunostaining they found a complete absence of KRT13-positive cells in the cornea, with their expression being only detected in the suprabasal limbal epithelium and in all layers of the conjunctival epithelium [106]. KRT19 is reported to be present at substantial levels in the peripheral corneal epithelium, and in all layers of the conjunctiva epithelium and limbus (either at transcript and protein expression levels) [54, 106, 129, 142]. None of the KRT12-positive cells in the central cornea were found to express KRT13. Limbal ECs expressed either KRT12 or KRT13 with KRT12 and KRT19 positive cells co-located throughout the limbus and the peripheral cornea [106]. These results suggest a higher specificity of KRT13 for differentiated conjunctival ECs than KRT19. The same conclusions have been made more recently by Poli et. al [150].

MUC1 and MUC5AC. Both MUC1 and MUC5AC have been postulated as being markers for conjunctival ECs and/or goblet cells. The exclusivity of MUC1 to conjunctival ECs is debated with some proposing it as a conjunctival epithelial specific marker [143] and others showing its expression throughout the entire ocular surface [151, 152]. MUC5AC, on the other hand, has long been postulated as being specific to the conjunctival goblet cells [153]. Although not detected in the ECs of the conjunctiva, it is the best surrogate marker for the presence of conjunctival epithelium by identifying its interspaced goblet cells.

1.12. Limbal stem cell deficiency

The loss or dysfunction of LSCs results in a condition known as limbal stem cell deficiency (LSCD). The imbalance of corneal-conjunctival homeostasis leads frequently to a process of re-epithelisation of the corneal surface by the conjunctival epithelial cells, a process called conjunctivalisation [154]. The cornea becomes covered by conjunctival epithelium and in more severe cases by the conjunctival substantia propria [155], Figure 10. This is accompanied by chronic inflammation, corneal scarring, vascularisation [156], resulting in vision loss and severe discomfort [157].

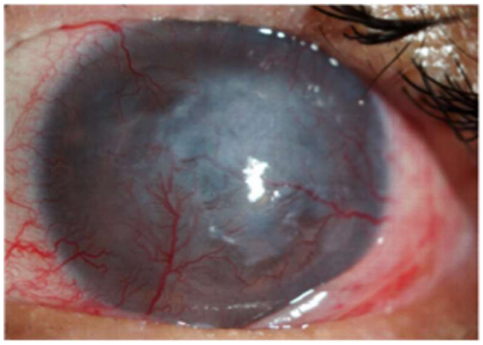

Figure 10 - Clinical image of a patient with limbal stem cell deficiency. The cornea loses its clarity, becoming covered by conjunctival epithelium and blood vessels.

Various causes and diseases, grouped into inherited or acquired, can lead to LSCD, Table 3. This condition can affect the corneal epithelium to various degrees depending on the extent of limbal involvement [158, 159]. The case where only a portion of the limbus and cornea is defective and possibly covered by conjunctival epithelium it is known as partial or focal LSCD. When the whole circumference of the limbus and corneal epithelium is affected it is known as total or diffuse LSCD [155].

Table 3 – Main ethiologies and pathological conditions for inherited and acquired limbal stem cell deficiency.

Heritable	Acquired		
Hereditary	**Injury**	**Iatrogenic**	**Inflammatory disease**
Aniridia	Mechanical trauma	Extensive limbal surgery	Stevens-Johnson syndrome
	Chemical or thermal burns	Therapeutic radiation	Cicatricial pemphigoid
		Cytotoxic agents	

Impression cytology of the corneal surface may support a clinical diagnosis of LSCD [141, 160, 161]. In this technique, a cellulose acetate filter is pressed onto the corneal surface under topical anaesthesia. The loose superficial corneal ECs are removed and subjected to histological and immunohistological analysis [160]. Healthy corneal epithelium is devoid of goblet cells and its differentiated cells lack KRT19, unlike those from the conjunctiva epithelium. Thus, the presence of goblet cells or KRT19 on impressions of the central cornea are indicators of conjunctivalisation, which may represent LSCD [161]. Although the presence of goblet cells is suggestive of LSCD, their absence does not exclude LSCD as one third of the

patients with clinical diagnosis of LSCD were not found to have goblet cells in their cornea [162].

In vivo confocal microscopy, has emerged as a promising tool for LSCD diagnosis [79]. This technique does not require the removal of corneal ECs but requires physical contact between the imaging probe and the ocular surface. This technique can distinguish the bright well-defined membrane corneal ECs from the hyper-reflective conjunctival ECs and goblet cells [79].

Mann and Pullinger [163] and later Friedenwald et al. [164] were the first to show that conjunctival ECs can migrate into the corneal region upon limbal injury. Later on, studies showed that the migrating cells can acquire an incomplete corneal-like phenotype being trapped in an incomplete metaplastic transition (later designated conjunctival transdifferentiation) between corneal and conjunctival type [165]. More recently, others have supported this hypothesis, showing that the migrating conjunctival cells differ from the normal corneal epithelium in glycogen metabolism and protein profiling [166-169]. Kurpakus et al. have suggested that conjunctival transdifferentiation is a result of environmental modulation, with the corneal BM playing a key role in such a process [170]. The environmental modulation of the corneal BM in the process of conjunctival transdifferentiation may have been ruled out in most of the previous studies as a total debridement of corneal epithelium and/or stroma may have occurred as a consequence of the mechanical or chemical corneal debridement prior the migration of conjunctival epithelium. The studies in this thesis will surpass this issue by recreating conjunctival or cornea microenvironments *in vitro*. Numerous studies have already addressed the importance of external cues, particularly ECM proteins, in cell fate modulation and differentiation utilizing a wide variety of cell types, including ECs from ocular surface [171-175], epidermal ECs [176], and endometrial ECs [177]. Very well documented observations also arise from SC differentiation in response to specific ECM proteins, where SC of various origins are driven into corneal epithelial-like cells upon culture on collagen type IV [178] or laminin-5 [179] and supplemented with limbal fibroblasts conditioned medium. However, the process of conjunctival transdifferentiation in response to extracellular cues has never been studied in *in vitro* culture systems. The studies in this thesis examined the plasticity of corneal and conjunctival ECs in response to various extracellular cues. To be able to do so, a panel of established markers to distinguish each cell type is required. Therefore, KRT3 and

KRT12 were used as markers for corneal ECs, KRT7 and KRT13 as markers for conjunctival ECs, and ΔNp63 and ABCB5 as putative markers for epithelial SCs.

1.12.1. Management of limbal stem cell deficiency

Four main approaches can be used for LSCD treatment: (i) non-surgical approaches [157, 180-182], (ii) whole tissue transplantation grafts [89, 183, 184], (iii) cell-based therapy [157, 185-187], and (iv) non-cultured cell based therapy [188, 189].

i. **Non-surgical approaches.** Non-operative or more conservative approaches have been used to treat milder cases of LCSD. These include intensive lubrication of the ocular surface to aid healing and reduce the discomfort from persistent epithelial defects [181], contact lenses to provide symptomatic relief from the epithelial irregularity [180], and antibiotic eye drops to prevent infections of the corneal surface in cases of epithelial failure [182].

ii. **Whole tissue transplantation.** Kenyon and Tseng were the first to propose the treatment of LSCD with healthy limbal tissue grafts [89]. They showed that limbal epithelial autograft from the healthy other eye of a patient could be used to treat unilateral LSCD with success. In cases of bilateral LSCD, the other eye cannot be used as a source of LSCs. Limbal epithelial allografts from a healthy matched living related or cadaveric donors have therefore been used with additional use of potent immune-suppression [183]. The main disadvantage of limbal epithelial grafting is the sizeable amount of healthy tissue required for the procedure. Animal studies have shown that the removal of large amounts of limbal epithelium from healthy eyes creates a considerable risk of LSCD in those eyes [184].

iii. **Cell-based therapy.** This approach is based on in vitro expansion of limbal ECs as firstly reported by Pellegrini et al. [185]. In this therapy a small biopsy of healthy human limbal epithelium from the patient's other eye (if healthy), a living related donor's eye, or a cadaveric tissue is harvested and expanded ex vivo (12-19 days) to form epithelial sheets. These epithelial constructs have successfully been used to restore the corneal epithelium of patients suffering LSCD [185]. The culture of limbal epithelium, and more importantly the LSCs, can be performed using co-culture with inactivated 3T3 mouse fibroblasts [185], AM alone [189, 190], or a combination of these two methods [191]. These methods enable the reconstruction of the ocular surface from a small biopsy of the donor eye minimizing the risk of SC failure in the healthy eye. However, the associated costs of a SC laboratory increase the price of this transplantation to €12000. Several studies have

addressed the success rate of ex vivo expansion of LSC all pointing to a success rate varying from around 75% to 100% [157, 186]. However, the follow-up time of the current clinical studies is usually less than one year and, as suggested by Sangwan et al., all the failures occurred within 20 months which may raise the need to extend the follow-up times [187]. The mechanisms by which the transplanted cells restore the ocular surface are still unknown. However, two main possibilities have been postulated: the transplanted LSC (i) replace the lost SCs or (ii) revitalize the dormant SCs [79]. Other sources of ECs have been used with varying rates of success. These include mucosal ECs [192], ESCs [193], bone-marrow-derived mesenchymal SCs [194, 195], and of bigger relevance for this study conjunctival ECs [196-198].

iv. **Non-cultured cell-based therapy**. A recent technique created by Sangwan et al. named Simple Limbal Epithelial Transplantation (SLET) has been shown to effectively treat unilateral LSCD in six human patients, with visual acuity improved from worse than 20/200 in all recipient eyes to 20/60, or even better in four eyes [188]. This method involves: (i) the removal of the fibrovascular tissue from the diseased cornea, (ii) the harvest of a biopsy of the limbal tissue from the contralateral eye, and (iii) the cutting of this biopsy in smaller pieces and their placement on amniotic membrane (AM) around the centre of the cornea. AM has long been used as a surrogate niche for LSC [189]. This substrate promotes epithelial healing, has low immunogenicity, anti-inflammatory, anti-angiogenic, and anti-scarring properties [199]. It also produces various growth factors, which have been shown to promote corneal epithelial wound healing. As there is no need for laboratory cell expansion, the SLET costs and time are reduced. In some severe cases of partial LSCD the above-mentioned approach may not be sufficient, and it is necessary to pursue with treatment options reserved for total LSCD.

v. **Potential new approaches.** Based on the relatively low efficiency of the aforementioned approaches [157, 186, 188], on the plasticity of conjunctival cells to differentiate into cornea epithelial-like cells [29, 30], and in the rationale that cells can respond to the extracellular cues [171-175], the studies in this thesis will assess a new method for conjunctival transdifferentiation based on cell response to extracellular cues (ECM proteins on Chapter 2 and 3 and extracellular vesicles on Chapter 4). This approach would lead to the implementation of a culture system to promote conjunctival differentiation into cornea epithelial-like cells that would have clinical potential. Additionally, bilateral cases of LSCD require the identification of alternative SC sources, other than autologous

limbal epithelium, for treatment. For this reason, the differentiation potential of human ESCs towards the conjunctival and corneal epithelial lineage was also investigated (Chapter 2).

1.13. Hypothesis

"The plasticity of the human ocular epithelial cells is modulated by extracellular cues"

1.14. Aims and objectives

The main aim of this work was to modulate the plasticity of ECs from human cornea and conjunctiva using extracellular cues. To achieve this, this thesis is broken down into 4 specific objectives:

i. **To determine if the differentation of human ECs from the conjunctiva and cornea can be modulated in response to ECM cues in vitro.** This was investigated in both established human conjunctival and corneal EC lines and primary cells, by culturing cells on ECM proteins previously deposited by alternative ECs. This is of importance due to its clinical significance. The studies in Chapter 2 investigate this aim.

ii. **To investigate the differentiation of human ESCs towards the conjunctival and corneal epithelial-like lineage.** hESCs were cultured on ECM proteins deposited by ECs to promote their differentiation towards conjunctiva epithelial-like or corneal epithelial-like cells. The studies in Chapter 2 also investigate this aim.

iii. **To assess the composition of the ECM that modulates the differentiation of the ECs from the human ocular surface.** This was investigated by analysing the differences in ECM composition produced by the two different cell lines (conjunctival and corneal ECs). The studies in Chapter 3 investigate this aim.

    a. **To identify the role played by several laminin isoforms in the modulation of cell differentiation.** This was achieved by culturing ECs on surfaces coated with all the commercially available human recombinant laminins.

    b. **To identify which signalling pathways are activated in response to the process of cell differentiation.** This was achieved by analysing the phosphorylation and

cleavage levels of 18 proteins known to play a role on cell differentation and/or growth.

iv. **To determine if the differentiation of human ECs from the conjunctiva and cornea can be modulated in response to extracellular vesicles in vitro.** Exosomes extracted from the above-mentioned cells lines were used to cross-modulate the differentiation of the two cell lines. The studies in Chapter 4 investigate this aim.

Chapter 2

Specific decellularized ECM promotes the plasticity of human ocular epithelial cells

2.1 Introduction

2.1.1. Cellular reprogramming

Since development is mainly dictated by genetic and epigenetic events, the process of cell differentiation is, in principle, reversible. Two main events in the history of genetics have confirmed this hypothesis. Firstly, the concept of nuclear transfer. Nuclear transfer is a two-step approach that requires the nuclei withdrawn from an egg cell and replacing it with a nucleus from an older donor cell [200] that induces the change in the gene expression pattern to that of an embryo state in response to the factors present in the transfected cell [201]. These studies demonstrated the feasibility of somatic nuclear reprogramming, although with low efficiency and better results by using nuclei from less differentiated cells, suggesting the involvement of epigenetic modifications [202]. Secondly, four transcription factors (Oct4, Sox2, Klf4, and c-myc) were shown to reprogram mouse fibroblasts into pluripotent SCs, the so-called induced pluripotent SCs (iPS) [203].

Three different approaches to address the process of cell reprogramming have been raised:

i. **Transdifferentiation.** The differentiated cells first dedifferentiate into an intermediate state with limited potency, prior re-differentiation into the second cell type [204], Figure 11A.

ii. **Direct reprogramming.** In this approach the differentiated cells directly differentiate from one cell type to another with no intermediate state of cell de-differentiation [205, 206], Figure 11B.

iii. **iPS technology.** In this approach a mature adult cell is reprogrammed to became pluripotent [203].

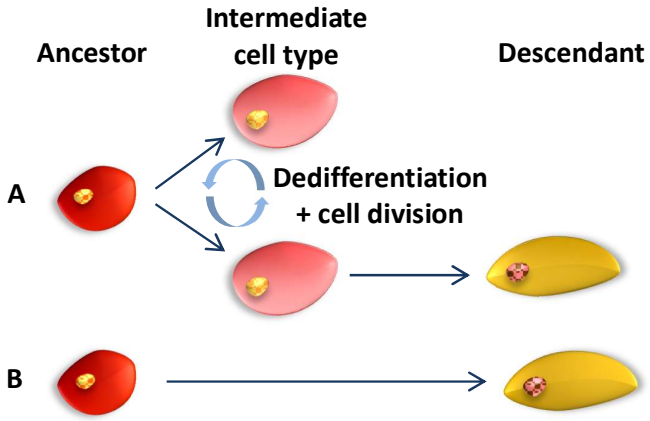

Figure 11 - Modes of cell reprogramming. Cell reprogramming can occur via two main mechanisms: (A) by requiring cell division and dedifferentiation as intermediate steps prior full re-differentiation into a different phenotype, a mechanism called transdifferentiation, (e.g. conversion of pigmented epithelial cells of the dorsal iris to lens fibers) or (B) alternatively it can occur without the requirement for cell division and dedifferentiation as intermediate steps, a process named direct reprogramming (e.g. conversion of pancreatic AR42J-B13 cells into hepatocytes).

2.1.1.1. Transdifferentiation

The irreversible switch mechanism from one differentiated cell into another is called transdifferentiation [207]. The term "transdifferentiation" was first used by Selman and Kafatos to describe the conversion of cuticle-producing cells into salt-secreting cells, using the silk moth during metamorphosis from the larval to the adult moth [208]. In the eye it was firstly reported by Wolff upon the finding that dorsal iris pigmented ECs transdifferentiated into crystalline lens during the regeneration of the crystalline lens cells of newts [209]. The first successful studies of *ex vivo* transdifferentiation were reported by Taylor and Jones in 1979. By inhibiting DNA methylation using 5-azacytidine, they converted cultured fibroblast cell lines into myocytes, chondrocytes, and adipocytes, suggesting a transdifferentiation under epigenetic control [210]. One decade later a transcription factor, called MyoD, was identified by its ability in transforming cultured fibroblasts into myoblasts by activating muscle-specific genes [211]. Dedifferentiation and cell division are intermediate processes in the switch in phenotype, but not obligatory in all cases [212]. At molecular levels, the cause of transdifferentiation has been associated with a change in the expression of a master switch gene, whose normal function is to distinguish the two cell types in normal development. Almost all studies on transdifferentiation required *in vitro* cell culture approaches prior to the transplantation of the transdifferentiated cells into the body. More recently, *in situ* induced transdifferentiation has shown promising results with cells within the tissue driven to transdifferentiate into the desired target cells [213-216]. Other instances

of transdifferentiation that involve the intermediate process of cell dedifferentiation include the conversion of pancreatic cells to hepatocytes [217] and vascular endothelium to smooth muscle [218].

2.1.1.2. Direct reprogramming

Direct reprogramming is generally accomplished through forced expression of lineage-specific transcription factors. These have been used successfully in reprogramming fibroblasts into various cell types *in vitro*, including skeletal muscle cells [211], hepatocytes [219], neurons [220], pancreatic islet cells [213], endothelial cells [221], smooth muscle cells [222], and cardiac muscle [223]. This technique is conceptually attractive as it does not require the reversion into a pluripotent state prior differentiation, avoiding any risks of teratoma formation [213]. This process involves the activation of target genes, within hours to days [220], does not require cell division and it is stable after removal of reprogramming factors [213, 219]. Direct reprogramming occurs at varying efficiency, however it is usually low and requires high expression of reprogramming factors [202]. Another drawback of this process is the epigenetic memory, also well documented in iPS cells [224, 225]. Despite induction of gene expression to another cell type, frequently some residual gene expression specific to the original cell type persists [226, 227]. The cell reprogramming works better when the progenitor and descendant cells share similar embryogenic germ layer origins. The mechanisms of direct reprogramming are poorly understood. While it is well established that transcription factors are the driving force with the contribution of microRNAs, it is less clear how cells maintain their descendant lineage. Direct reprogramming of patient-derived cells would facilitate the generation of clinically relevant cell therapies for regenerative medicine.

2.1.1.3. Metaplasia

Metaplasia is a wider class of cell transformation, which includes transdifferentiation and cases in which cells switch to a completely different cell type [228]. The term metaplasia was coined by Slack to describe anatomical and histological observations of unexpected appearance of foreign tissues in ectopic sites [229]. In some cases, metaplasia may be due to the presence of minor cell types within the given tissue, whose damage or regeneration triggers their outgrowth [230]. In human beings, one of the best studied examples of metaplasia is Barrett's metaplasia of the oesophagus. In this disease, the continuous damage due to reflux of the acid contents of the stomach causes the lower end of oesophagus, composed by stratified squamous epithelium, to become intestinal-type tissue.

2.1.1.4. Plasticity

The term plasticity has been suggested as an alternative to transdifferentiation and metaplasia. However, others have postulated that this new term is particularly applied to examples involving nuclear reprogramming [231]. One of the best studied cases of plasticity is the ectoderm to mesoderm lineage switch during tail regeneration of the axolotl upon injury [232]. Echeverri and Tanaka followed individual spinal cords during tail regeneration in the axolotl showing that they can generate muscle cells, chondrocytes and neurons, suggesting a switch in cell lineage in response to foreign environments [232].

2.1.2. Conjunctival transdifferentiation - early studies

Based on the notion that conjunctival epithelium can differentiate into a cornea epithelial-like phenotype by a process of transdifferentiation [233, 234], it was hypothesized that conjunctival epithelial grafts could be used as an approach to treat LSCD [235, 236]. However, it was later shown that conjunctival epithelial grafts are largely ineffective for the treatment of LSCD as the transdifferentiation to corneal epithelium appears to be incomplete [237]. The process of conjunctival transdifferentiation was first described by Mann and Pullinger [163] and Friedenwald [238]. By scraping off the corneal epithelium of six rabbits, Friedenwald showed a complete coverage of the corneal defect after 5-7 days. The appearance of the animals' eyes was entirely normal up to 2-3 weeks after injury, when the eyes acquire a roughened and more opaque appearance (conjunctiva-like) with the presence of typical goblet configuration cells. Four to five weeks after the abrasion, the corneal epithelium begins to assume a more normal appearance with still the persistence of some mucin-producing cells. Of significance is the presence of glycogen in the goblet cells' cytoplasm (goblet cells cytoplasm lacks glycogen), which suggests that the cells are trapped in the "process of metaplastic transition between corneal and conjunctival type of morphology and metabolism" [238]. Additionally, several reports have later shown that the resultant epithelium after conjunctival transdifferentiation differs from the normal corneal epithelium in glycogen metabolism [166], keratin profiling [167], general protein profile [168] and tensile strength [169], suggesting that the transdifferentiated epithelium is not a genuine corneal epithelium.

It has been suggested, in rabbits, that the retardation of conjunctival transdifferentiation into corneal epithelium-like is correlated with the corneal vascularization [239, 240]. Friedenwald observed that the conjunctival epithelium, which migrated onto the cornea after corneal abrasion, persisted in regions of superficial corneal vascularization and scar.

This was in contrast with the nearly complete process of conjunctival transdifferentiation observed in eyes with no signs of corneal vascularization or scar [238]. Kruse et al. explained this duality on corneal healing process based on the extent of limbal epithelium debridement: complete debridement would lead to corneal vascularization and conjunctivalisation and incomplete debridement (less than one third of the limbus [184]) would lead to non-vascularized corneas and conjunctival transdifferentiation [29]. Others have suggested that the limbus exerts an inhibitory growth pressure to prevent the migration of conjunctival ECs onto the cornea [234]. Tseng et al. showed, in rabbits whose corneas and limbus were totally removed, a rapid decline in goblet cell density accompanied by a complete transdifferentiation in non-vascularized corneas after 43 days of re-epithelialisation by conjunctival epithelium. On the other hand, vascularized corneas maintained high levels of goblet cell density and an epithelium that possesses conjunctival features until day 167 [239]. This evidence supports the theory that corneal vascularization may be a causative factor in modulating conjunctival transdifferentiation, inhibiting or reversing this process. Some authors have speculated that the persistence of goblet cells may be supported by factors from the blood circulation, namely vitamin A or other retinoids [241]. Others have shown that the goblet cells do not migrate onto the cornea, being instead formed *de novo* from non-goblet ECs. Loss of goblet cells during transdifferentiation occurs by desquamation and *in situ* cell death [242].

Dua has shown on a group of ten patients with various eye diseases that even after several months, the corneal surface covered by conjunctival cells remained relatively thin and irregular with no evidences of transdifferentiation [243]. Interestingly and supported by other studies [159], buds of corneal epithelium were detected protruding into the migrating conjunctival epithelium, all along the contact line between the two epithelial phenotypes [243]. These findings suggest that the healthy corneal epithelium may replace the conjunctival epithelium, with incomplete conjunctival transdifferentiation. These authors recommended that in cases with partial damage to the limbal epithelium accompanied by cornea conjunctivalisation, the conjunctival epithelium could be removed. This can be achieved by mechanically scrapping the migrating conjunctival epithelial until the migrating sheets of limbal epithelium have met, re-establishing the limbal barrier. In more severe cases limbal transplants or keratoepithelioplasty are needed [159].

2.1.3. Inhibitors of conjunctival transdifferentiation

A possible candidate for inhibiting conjunctival transdifferentiation, by maintaining the presence of goblet cells, is retinoid (including vitamin A). Retinoids are lipid-soluble vitamins present primarily in serum and epithelial tissues, which contain higher concentrations of retinol-binding proteins. They are essential for epithelial growth and differentiation [244]. The scleral and the conjunctival blood vessels are the major source of vitamin A in healthy corneas [245-247], providing ten times more than tears [248] and lacrimal gland fluid [249]. Deficiency of vitamin A either *in vitro* or *in vivo* causes keratinization of mucous membranes, and vitamin A in excess inhibits keratinization of epithelium and induces mucous metaplasia [244, 250]. Using rabbits as models, Tseng et al. showed maintenance of the conjunctiva-like epithelium (containing goblet cells) either in vascularized or non-vascularized corneas upon applying topically two different retinoids (13-cis retinoic acid and etretinate). These observations suggest the retinoids as one of the factors that inhibit conjunctival transdifferentiation maintaining goblet cell differentiation and controlling mucin expression, and conversely transdifferentiation can be induced in vascularised corneas by systemic vitamin A deficiency [241].

2.1.4. Conjunctival transdifferentiation - later studies

Recent studies have shown that the process of conjunctival transdifferentiation is incomplete. Moyer et al. showed that, after total corneal epithelium debridement, the regenerated epithelium of conjunctival origin does not express the corneal EC marker KRT12. However, in other milder corneal defects, when areas of LSCs are preserved, the expression of KRT12 is also preserved [251]. Other studies have shown that conjunctival transdifferentiation is a result of environmental modulation, where the presence or absence of the corneal BM might play a key role in determining the cell's fate [170]. Kurpakus et al. showed that conjunctival ECs cultured on top of intact corneal epithelial BM expressed KRT12 [170], suggesting a cell's fate modulation in response to the extracellular environment.

2.1.5. Microenvironment signalling cues in cells' fate modulation

Within the microenvironment, the ECM assumes to be the major support structure for the cells, providing dynamic signalling cues. Besides the support function, it also sequesters growth factors and other cytokines that can be released in response to a physiological alteration. In response to the ECM factors, the cells activate their biochemical and/or

mechanotransduction pathways that modulate their growth, survival, proliferation, migration, and differentiation [252]. Several studies have taken advantage of this to produce different types of matrices to modulate cell fate. These include the development of an acellular corneal matrix [171] to be used as a scaffold to induce the differentiation of mesenchymal SCs (MSCs) into cornea epithelial-like cells, which purely because of its physical and mechanical characteristics drive MSCs to express corneal epithelial markers KRT3 and KRT12 [253]. Others have differentiated amniotic ECs into conjunctiva epithelial-like cells (expressing KRT4 and KRT13) upon culture in decellularized conjunctival matrices [172]. Remarkably, Ang et. al have shown that AM sheets populated with human conjunctival ECs and transplanted into rabbit eyes with total LSCD have similar features to corneal epithelial tissues (including KRT3- and KRT12-positive events), suggesting these outcomes as possible clinical substitutes to corneal epithelial grafts [254].

Functionalized surfaces with major components of ECM, such as fibronectin, collagen, and laminins, are shown to either modulate ESCs to maintain their pluripotency or to differentiate into specific cell lineages [178, 255, 256]. The mechanism by which ECM modulates cell differentiation is attributed to integrins-cell cross-talk. Integrins are cell surface receptors that transduce a cascade of signals from the exterior to the intracellular space. When integrins bind to their ECM ligands they undergo conformational changes in both their extra and intracellular domains, which followed by the accumulation of cytoplasmic molecules and other adaptor proteins activates the downstream signalling pathways modulating their behaviour [257]. In addition to adhesion receptors, soluble growth factors can also bind to the ECM, which regulates their presentation, distribution, and activation.

2.1.6. Embryonic stem cells

ESCs are pluripotent SCs derived from the ICM of the blastocyst, Figure 12. The ICM of developing embryos gives rise to all three germ layers of the embryo itself: the endoderm, mesoderm, and ectoderm. Isolation and culture of the ICM, after physical separation of the rest of the embryo (particularly the trophectoderm), results in the formation of ESCs. Thomson et al. in 1998 first derived human ESCs (hESCs) using discarded *in vitro* fertilisation embryos [32].

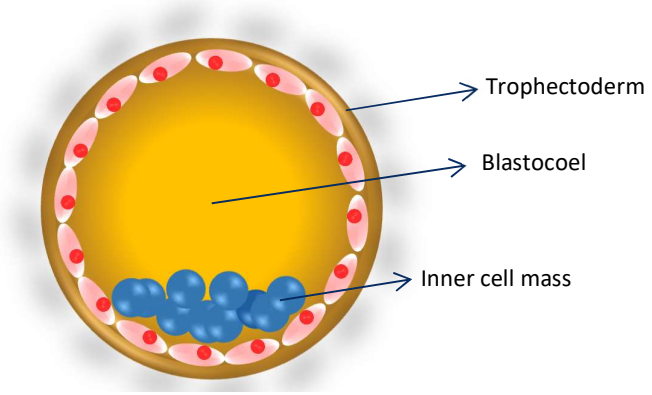

Figure 12 - The blastocyst. It consists of an outer trophoblast layer (named trophectoderm after blastulation), an inner cell mass and a fluid-filled cavity (blastocoel).

Undifferentiated ESCs possess intrinsic properties which distinguish them from more differentiated cells, as follows:

i. **Pluripotency genes.** Undifferentiated ESCs are known to express both the homeobox-containing transcription factor, Nanog [258, 259], and the POU domain class 5 transcription factor 1, POU5F1 (also known as octamer-binding transcription factor 4 (Oct4)) [260].

ii. **Cell surface markers.** The stage specific embryonic antigens (SSEA) 3 and 4 are glycolipids known to be expressed during the early stages of embryonic development and are down-regulated during hESCs differentiation [261, 262]. The tumour rejection antigens (TRAs) 160 and 181 are keratin sulphate associated antigens expressed by undifferentiated ESCs [261, 262].

iii. **Teratoma formation.** The pluripotency of ESCs can be confirmed by their injection into mice with severe combined immunodeficiency. This results in the formation of teratomas with cells and tissues from all three germ layers [263, 264].

2.1.6.1. The differentiation of embryonic stem cells

The predominant signalling pathways involved in pluripotency and self-renewal of hESC are transforming growth factor (TGF)-β, through SMAD2/3/4, and fibroblast growth factor receptor (FGFR), which activates the MAPK and AKT pathways [265]. The Wnt pathway is also known to promote ESC pluripotency, through a non-canonical mechanism that involves a balance between the transcriptional activator, TCF1, and the repressor, TCF3. The regulation of these pathways maintains the pluripotent state [265], which depends predominantly on three major transcription factors - OCT4, SOX2, and NANOG. These transcription factors activate expression of ESC-specific genes, regulate their own expression, repress genes involved in cell differentiation, and act as hESCs markers [266-269]. hESCs differentiation *in vitro* can be directed toward derivatives of the three primary germ layers [32]. The primary signalling pathway responsible for this is the BMP (bone morphogenetic proteins) pathway [270], through SMAD1/5/9 to promote differentiation by inhibiting the expression of NANOG and activating the expression of specific genes involved in differentiation [270, 271]. SMADs are intracellular proteins that transduce extracellular signals from TGF-β ligands to the nucleus activating downstream gene transcription [272-274]. The well conserved Notch signalling pathway also plays a role in differentiation through the Notch intracellular domain [275]. As the differentiation proceeds, lineage-specific pathways are activated.

Because of their potential to generate cells from the whole body, several studies have attempted to differentiate ESCs, including hESCs, into specific cell types with certain degrees of success. These include ESC differentiation towards skin and corneal epithelial-like cells using various methods [178, 193]. All the stated approaches have a transversal similarity; the mimicry of the extracellular environment where these differentiated cells reside. Amongst these are:

i. **Culture on fibroblast-deposited ECM proteins.** Undifferentiated mESCs cultured on top of ECM proteins derived from either human fibroblasts or 3T3 mouse fibroblasts differentiate into skin epithelial-like cells. Upon exposure to these ECMs, the differentiated mESCs expressed characteristic skin epithelial proteins KRT10 and KRT14 and showed formation of HDs [276]. Addition of either ascorbate or BMP4 to the culture further improved the formation of skin epithelial-like cells from mESCs [276]. Continued culture of the differentiating cells resulted in full thickness skin formation, including epithelial and sub-epithelial structures [276].

ii. **Culture on replicated limbal SC niche environment.** The SC niche refers to the specialized microenvironment where SCs reside, which interacts with SCs to regulate their fate [44] as in the case of the LSC niche [56]. Limbal fibroblast conditioned medium together with several proteins known to be part of the limbal SC niche have been used to induce differentiation of ESCs towards corneal-like ECs. These include fibronectin, human placental laminin, and collagen IV [178]. Further studies with collagen IV demonstrated considerable differentiation towards corneal-like ECs through a transient increase in the expression of the terminally differentiated corneal epithelial markers, KRT3 and KRT12, and a diminution in expression of the markers for ESCs, OCT4, NANOG, and SSEA4 [178]. Intriguingly, at the transcript level, after 18-21 days in culture, where KRT3 and 12 levels had returned to starting levels, increased expression of the suprabasal epithelial keratin, KRT10, was reported indicating incomplete differentiation [178]. The same studies showed highest CFE values at times when KRT3 and KRT12 protein expression was the highest, these are accompanied by high values of ΔNp63 expression after 7 days in culture. The expression of ΔNp63 then dropped significantly while CFE values are still high, suggesting incomplete differentiation [178].

iii. **Culture of embryoid bodies on replicated limbal SC niche environment.** Embryoid bodies, probably the most common method used to differentiate ESCs [277], are 3 dimensional aggregates of pluripotent SCs that can differentiate toward the three germ layers [278]. Homma et al. have used collagen IV coated dishes to differentiate mESCs derived embryoid bodies into corneal-like ECs, which expressed the terminally differentiated corneal EC marker KRT12 [193]. Moreover, the transplantation of such 8-day old differentiation cultures onto the surface of cornea denuded of its epithelium results in the formation of an epithelium showing morphological similarities to corneal epithelium 24 hours post-transplant [193].

2.1.6.2. Embryonic stem cell markers

In addition to the established markers used to identify adult epithelial SCs from the ocular surface, (addressed in section 1.9), it is of importance to discuss in detail markers used to identify undifferentiated hESCs. These include the following:

i. **POU5F1.** POU5F1 is a mammalian POU transcription factor expressed exclusively in pluripotent early embryo cells, blastomeres (type of cell produced by division of the zygote after fertilization), and in later germ cells [260, 279]. *In vivo* it is abundantly found

in the ICM of the early blastocyst but not in the trophectoderm, whereas nascent primitive endoderm in late blastocyst express Pou5f1 at even higher levels [266]. It regulates expression of several other transcription factors present in pluripotent cells, including Sox2 [280] and the E1A-like protein activity [281]. In the developing embryo, down-regulation of Pou5f1 expression is correlated with the loss of potential to form cells from the three germ layers, suggesting that Pou5f1 is a determinant of the germ line [267]. Niwa et al. suggest Pou5f1 to be the master regulator of pluripotency whose precise level governs 3 different distinct fates of ECs [282]. They found that when its expression was less than two-fold increase it caused differentiation of ESCs into primitive endoderm and mesoderm. On the other hand, the decreased expression of Pou5f1 induced loss of pluripotency and dedifferentiation of cells to trophectoderm [282]. Thus, a precise amount of Pou5f1 is required to sustain SC self-renewal.

ii. **SOX2 (SRY-related HMG box).** SOX2 is a member of the Sox gene family that encodes transcription factors with a single HMG (high motility group) DNA-binding domain [283]. It is associated with uncommitted dividing stem and precursor cells of the developing central nervous system [268]. It is also a marker for pluripotent lineage of the early mouse embryo, and similarly to Oct4 it is expressed in the ICM, epiblast, and in cells from the germinal layers. Unlike Oct4, Sox2 is also expressed by the multipotent cells of the extraembryonic ectoderm and in cells with limited developmental potential it is absent [283].

iii. **NANOG.** NANOG is a DNA binding homeobox transcription factor involved in the proliferation, self-renewal, and pluripotency of ESCs. During their differentiation, it is suppressed by p53 protein [269]. It also blocks ESCs differentiation and auto-represses its own expression in differentiating cells [258].

2.1.7. Aim

i. **To evaluate if the differentiation of ECs from the human cornea and conjunctiva can be modulated in response to ECM cues in vitro.** This was investigated in both established human corneal and conjunctival ECs lines and primary cells, by culturing those on the ECM proteins meshwork deposited by ECs. This is of importance due to the clinical relevance of plasticity and reversibility of corneal conjunctivalisation.

ii. **To investigate if hESCs can be differentiated towards conjunctival and corneal epithelial-like lineage in response to specific ECM proteins.** hESCs were cultured on

decellularized ECM proteins deposited by either conjunctival or corneal ECs to promote their differentiation accordingly.

2.2 Materials and Methods

2.2.1. Preparation of Media

Conjunctival medium consisted of Keratinocyte Serum-free medium without $CaCl_2$ (KSFM, Gibco ™ ThermoFisher Scientific, cat. Number 37010-022), supplemented with: 0.2% (V/V) Bovine Pituitary Extract (BPE), and 0.2ng/ml of epithelial growth factor (EGF) (all supplied with the medium), 1% (V/V) penicillin/streptomycin (P/S, Sigma-Aldrich, cat. Number P0781), and 0.4mM of $CaCl_2$ (Sigma-Aldrich, cat. Number 21114).

Corneal medium consisted of KSFM with $CaCl_2$ (Gibco ™ ThermoFisher Scientific, cat. Number 17005-042), supplemented with: 0.2% (V/V) BPE, 0.23ng/ml EGF (all supplied with the medium), and 0.06mM (0.13mM final concentration) of $CaCl_2$.

Freezing medium consisted of DMEM/F12 medium supplemented with: (%V/V) 20% of foetal calf serum (FCS, Gibco ™ ThermoFisher Scientific, cat. Number 26140-079) and 20% of dimethyl sulfoxide (DMSO, Sigma-Aldrich cat. Number D2650).

Basic medium consisted of high-glucose Dulbecco's Modified Eagle's Medium (DMEM, cat. Number 5671) without pyruvate, supplemented with: (%V/V) 10% FCS, 1% P/S, 1% fungizone (cat. Number A2942), and 8mM L-glutamine (cat. Number G7513) (all provided by Sigma-Aldrich, unless otherwise specified).

Supplemental hormonal epithelial medium (SHEM) was made up of three parts of low-glucose DMEM with pyruvate (Gibco Life Technologies, cat number 21885-025) and one part of Ham's F12 medium (cat. Number N6658) supplemented with: (%V/V) 10% FCS, 1% P/S, 0.4µg/mL hydrocortisone (cat. Number H2270), 5µg/mL insulin (cat. Number I9278), 1.4µg/mL tri-iodothyronine (cat. Number T5516), 24µg/mL adenine (cat. Number A9795), and 10ng/mL EGF (cat. Number E9644) (all provided by Sigma-Aldrich, unless otherwise specified).

The mTeSR™1 5X supplement was thawed overnight at 4°C, aliquoted, and kept at -20°C for a maximum of two months. The mTeSR™1 5X supplement was diluted accordingly in mTeSR™1 medium (cat. Number 05850, all provided by STEMCELL Technologies) and kept at 4°C for a maximum of two weeks.

2.2.2. Human conjunctival epithelial cell line (HCjE-Gi)

2.2.2.1. HCjE-Gi cell line

This cell line was obtained from primary cultures of conjunctival ECs derived from a conjunctival biopsy of an 82-year-old male. Prior immortalization by expression of telomerase reverse transcriptase (hTERT), abrogation of p16 and p53 functions was preformed [284]. Its differentiation characteristics can be found at Gipson et. al [152]. This cell line was kindly gifted by Ilene Gipson (Harvard Medical School, United States).

2.2.2.2. Maintenance of HCjE-Gi cultures

A frozen vial of HCjE-Gi cells was thawed by incubation in a water bath at 37˚C. The cell suspension was slowly mixed with conjunctival KSFM. The resulting suspension was centrifuged for 3 minutes at 1000 revolutions per minute (rpm). The supernatant was removed, and the resulting pellet re-suspended in 5mL of conjunctival KSFM. The cell suspension was then plated in a T-25cm^2 tissue culture flask at a density of 25000 cells/cm^2 and maintained at 37˚C, 5%CO_2 in a tissue culture incubator (In-VitroCell ES NU-5800 Direct Heat, NuAire, United States). The medium was changed the next day and then every other day. Upon 70-80% confluence, the medium was removed, and the culture flask washed once with phosphate buffered saline (PBS, Gibco™ Life Technologies, cat. Number 10010-015). 1.5mL of 1X trypsin-ethylene diaminetatraacetic (EDTA, Sigma-Aldrich cat. Number T4174) diluted in PBS was added and the flask placed in tissue culture incubator for 5-7 minutes. The trypsin inactivation was achieved by the addition of conjunctival KSFM. The resulting solution was centrifuged for 3 minutes at 1000 rpm. The supernatant was removed, and the resulting pellet re-suspended in 10mL of conjunctival KSFM. The cells plated in T-75cm^2 tissue culture flask at a density of 25000 cells/cm^2 were maintained at 37˚C, 5% CO_2 in tissue culture incubator and fed with fresh conjunctival KSFM every other day until further experiments.

2.2.2.3. Maintenance of HCjE-Gi frozen stocks

To maintain frozen stocks at each early passage, the cells were detached from the culture flasks by trypsin method as previously stated. After centrifugation, the supernatant was removed, and the resulting pellet re-suspended in equal volume of conjunctival KSFM and freezing medium. The resulting suspension was placed in a cryogenic vial (at density of 1x10^6 cells per vial) and the vial was stored at -80°C for 90 minutes and then stored in liquid nitrogen.

2.2.3. Human corneal epithelial cell line (hTCEpi)

2.2.3.1. hTCEpi cell line

This cell line was obtained from primary culture of ECs harvested individually from 21 donor eyes (ages ranging from 26-67 years). All corneas were obtained from the Tissue Transplant Services Lions' Eye Bank (Dallas, Texas) [285]. A stable clone from a 62-year-old white male was selected and immortalized by infection with hTERT. This cell line was kindly gifted by James Jester (University of Southern California, United States).

2.2.3.2. Maintenance of hTCEpi cultures

A frozen vial of hTCEpi cells was thawed by incubation in a water bath at 37˚C. The cell suspension was slowly mixed with corneal KSFM. The resulting suspension was treated as described previously, section 2.2.2.2.

2.2.3.3. Maintenance of hTCEpi frozen stocks

To maintain frozen stocks at each early passage, the cells were detached from the culture flasks by trypsin method as previously stated. After centrifugation, the supernatant was removed, and the resulting pellet re-suspended in corneal freezing medium consisting of corneal KSFM supplemented with 10% (V/V) DMSO. The resulting suspension was placed in a cryogenic vial (at density of $1x10^6$ cells per vial) and the vial stored in liquid nitrogen.

2.2.4. Mouse 3T3 fibroblasts cultures and preparation as feeder layers

2.2.4.1. 3T3 J2 cell line

3T3 cell line was firstly prepared from 17 to 19-day old Swiss mouse embryos. The whole embryo was minced and disaggregated using 0.25% trypsin. Upon confluence, the culture was put on a rigid transfer schedule (every 3 days). These cells were then plated at a density of $3*10^6$ cells per plate [286].

2.2.4.2. Maintenance of mouse 3T3 fibroblasts cultures

A frozen vial of mouse 3T3 J2 fibroblasts was thawed by incubation in a water bath at 37 ˚C. The cell suspension was slowly mixed with 1mL of basic medium. The resulting suspension was centrifuged for 3 minutes at 1000 rpm. The supernatant was removed, and the resulting pellet re-suspended in basic medium. The cell suspension was then plated in a T-25 cm^2 tissue culture flask and maintained at 37˚C, 5% CO_2 in a tissue culture incubator. The medium was changed every other day. Upon 70-80% confluence, the medium was removed from the culture flask and the cultures washed once with PBS. 1.5mL of 1X trypsin-EDTA solution was added and the flask placed in tissue culture incubator for 5 minutes. The trypsin inactivation

was achieved by the addition of basic medium. The resulting solution was centrifuged for 3 minutes at 1000 rpm. The supernatant was then removed, and the resulting pellet was re-suspended in basic medium. The 3T3 fibroblasts were then plated in T-75 cm^2 tissue culture flasks. The cells were maintained in a tissue culture incubator and fed with fresh basic medium every other day.

2.2.4.3. Maintenance of mouse 3T3 fibroblasts frozen stocks

To maintain frozen stocks at each early passage, the fibroblasts were detached from the culture flasks by trypsin method as previously stated. After the centrifugation step, the supernatant was removed, and the resulting pellet re-suspended in freezing medium consisting of basic medium supplemented with 5% (V/V) DMSO. The resulting suspension was placed in a cryogenic vial ($1x10^6$ cells per vial) and the vial was stored in liquid nitrogen.

2.2.4.4. Preparation of mouse 3T3 fibroblasts feeder cells

For this purpose, 3T3 fibroblasts cultures were maintained until confluence. Upon confluence, the cells were mitotically inactivated by incubation with 10µg/mL mitomycin C (Sigma-Aldrich, cat. Number M4287) in basic medium for 2 hours at 37˚C 5% CO_2. The medium was then removed, and the culture washed thrice with PBS. The fibroblasts were detached from the culture flasks by trypsin method as previously described. After cell counting, 25000 cells/cm^2 were seeded in tissue well plates in basic medium. The plates containing the inactivated cells were then placed back in the tissue incubator overnight.

2.2.5. Human primary limbal epithelial cultures

2.2.5.1. Suspension culture of human limbal epithelium

Cadaveric limbal tissue, remaining after removal of the central cornea for transplantation purposes and composed of peripheral cornea and limbus, was obtained from The Liverpool Research Eye Bank. Complete information about the donor can be found in Table 4. The deeper layers of the limbal rings were dissected away, and the remaining limbal tissue containing limbal epithelium was cut into (roughly) 1mm^2 pieces. The limbal pieces were incubated with 1X trypsin EDTA for 20 minutes in tissue culture incubator. The resulting cell suspension was removed and centrifuged for 5 minutes at 1000 rpm. The supernatant was removed, and the remaining cell pellet was re-suspended in SHEM medium. This trypsinization process was repeated four times using the same limbal tissue. The resulting limbal cell suspensions were then pooled together. The limbal ECs were added to tissue

culture well containing the previously mitotically inactivated 3T3 fibroblasts, Figure 13. This co-culture was placed in the incubator and the medium changed on the day after and then every other day.

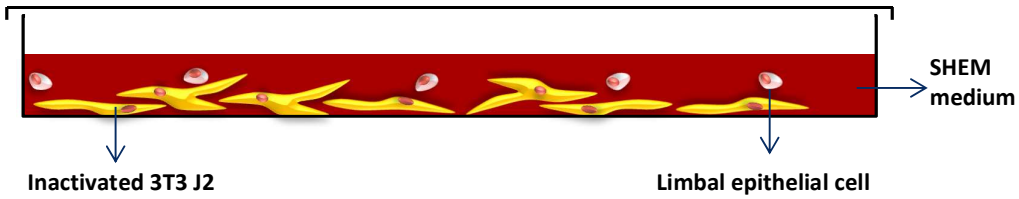

Figure 13 - Schematic illustration of the co-culture of limbal epithelial cells with 3T3 J2 mitotically inactivated fibroblasts using direct co-culture method. Abbreviations used SHEM: supplemented hormonal epithelial medium.

2.2.5.2. Sub-culturing

The original primary cultures, prior to confluence of the colonies, were sub-cultured. The cells were detached using the trypsinization method as previously described. After the centrifugation step the supernatant was discarded and the resulting pellet re-suspended in KSFM corneal medium supplemented with 1% P/S. The subcultures were then treated as the already stated hTCEpi cultures.

2.2.6. Human primary conjunctival epithelial cells

2.2.6.1. Suspension culture of human conjunctival epithelium

Cadaveric conjunctival tissue (bulbar and forniceal regions) was obtained from The Liverpool Research Eye Bank. Whenever possible the conjunctival and limbal tissues were retrieved from the same donor eye. Complete information about the donor can be found in Table 4. The adipose tissue layers and blood vessels of the conjunctival tissue were dissected away, and the remaining tissue containing conjunctival epithelium was cut into $1mm^2$ (roughly) pieces. The conjunctival pieces were incubated with 1X trypsin EDTA for 20 minutes in tissue culture incubator. The resulting cell suspension was removed and centrifuged for 5 minutes at 1000 rpm. The supernatant was removed, and the remaining cell pellet was re-suspended in SHEM medium. This trypsinization process was repeated four times using the same conjunctival tissue. The resulting cell suspensions were then pooled together. The conjunctival ECs were added to tissue culture wells containing the previously mitotically inactivated 3T3 fibroblasts, Figure 14. This co-culture was placed in the incubator and the medium changed on the day after and then every other day.

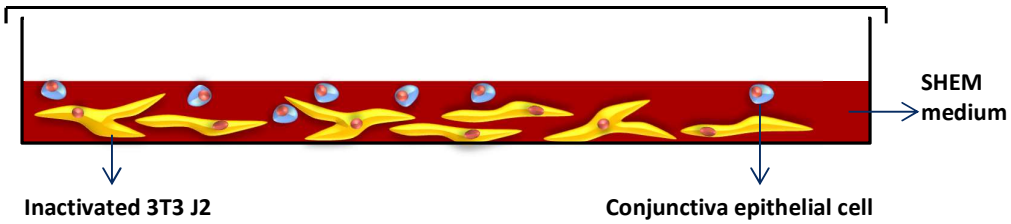

Figure 14 - Schematic illustration of the co-culture of conjunctival epithelial cells with 3T3 J2 mitotically inactivated fibroblasts using direct co-culture method. Abbreviations used SHEM: supplemented hormonal epithelial medium.

2.2.6.2. Sub-culturing

The original primary cultures, prior to confluence of the colonies, were sub-cultured. The cells were detached using the trypsinization method. After the centrifugation step the supernatant was discarded and the resulting pellet re-suspended in KSFM conjunctival medium. The trypsinization step was repeated twice to fully detach all cells from the culture well. The subcultures were then treated as the already stated HCjE-Gi cultures.

Table 4 - Donor information. Age, gender and post mortem interval are shown.

Donor	Age (years)	Gender	Post Mortem interval (hours)
14	84	Female	18
16	85	Male	22
17	76	Male	19.5
18	87	Male	17
20	62	Male	17
36	95-100	Female	16
37	80-85	Male	10

2.2.7. Human embryonic stem cells

HUES7 cells (obtained from Harvard University, HUES cells facility, Melton Laboratory, MA, USA) were kindly gifted by Professor Patricia Murray (Institute of Translational Medicine, University of Liverpool, UK). The full description on cell line preparation can be found at Baxter et al. [287]. Briefly, embryos were cultured in a series of sequential media, the zona pellucida and trophectoderm removed and the inner cell mass seeded onto mitotically inactivated mouse feeder layers for 8 days and the outgrowth passaged by manual dissection for the first 10 passages.

2.2.7.1. Coating of tissue culture plates with Matrigel®

Corning® Matrigel® hESC-qualified matrix (cat. Number 354277, lot number 5257004, Corning) was used for the coating of tissue culture plates. One aliquot (containing 263µL)

was thawed on ice and added to 24mL of cold DMEM/F12 (cat. Number 36254, STEMCELL Technologies). The resulting solution (1mL/well) was used to coat the 6 well plate cultureware (cat. number CLS3516-50EA, Corning® Costar® TC-Treated Multiple Well Plates). The cultureware was briefly swirled to evenly spread the Corning® Matrigel® across the surface. The resulting solution was incubated for one hour at RT, and the excess of Corning® Matrigel® solution removed. Specifications followed as per Technical Manual for Maintenance of human pluripotent stem cells in mTeSR™1 by STEMCELL™ Technologies.

2.2.7.2. Thawing of human embryonic stem cells

Complete mTeSR™1 and DMEM/F12 were brought to RT and Corning® Matrigel pre-coated cultureware was prepared beforehand. The cryovials containing hESCs were thawed in a 37°C water bath, and a 1mL micropipette was used to slowly transfer the contents into a conical tube containing the DMEM/F12 solution. The resulting solution was centrifuged for 5 minutes at 300xg. The supernatant was removed, the resultant pellet re-suspended in mTeSR™1 complete medium containing 10µM of Y-26632 (Dihydrochloride, cat. Number 72302, STEMCELL Technologies) and the cells seeded accordingly. The tissue culture flask was maintained at 37˚C, 5% CO_2 in tissue culture incubator and fed with fresh complete mTeSR™1 medium (without Y-26632) every day until further experiments.

2.2.7.3. Passaging of human embryonic stem cells

StemPro® Accutase® Cell Dissociation Reagent (cat. Number A1110501, ThermoFisher Scientific) was used. The culture well was washed with warmed PBS, the washing medium aspirated and cell dissociation reagent added. The cultureware was placed in a 37°C 5% CO_2 tissue incubator for approximately 5 minutes, when small gaps occurred between cells located on the edges of colonies. The resulting solution was harvested and the cultureware washed with DMEM/F12. The resulting solution was then centrifuged for 5 minutes at 300xg. The resultant pellet was re-suspended with complete mTeSR™1 supplemented with 10µM of Y-26632. The tissue culture flasks were maintained at 37˚C, 5% CO_2 in tissue culture incubator for 24 hours and fed with fresh complete mTeSR™1 medium (without Y-26632) every day until further experiments.

2.2.8. Cell doubling time

The cell doubling time was obtained by cell counting (trypan blue exclusion) at day 0 and day 6 and calculated as in Equation 2

$$DT = T * \frac{Ln(2)}{Ln(\frac{X_i}{X_o})}$$

Equation 2 – Doubling time calculation. Abbreviations used DT: doubling time, T: time, Xi: cell number at i time, Xo: cell number at time 0.

2.2.9. Cell seeding on ECM proteins

At desired time-points the cells were ruptured using the method described by Gospodarowicz [288] and Todorovic et al. [289] with small modifications. Briefly, the culture medium was removed and the cultureware briefly washed using sterile PBS. Cells were then treated with 20mM NH_4OH (cat. Number A669-212, Fisher Scientific) in sterile PBS for 5 minutes. The resulting cells ('de-roofed' cells) were washed away several times in sterile PBS followed by one wash with double distilled water (ddH_2O). This results in cultureware coated with ECM proteins. Viable cell count was performed using Trypan Blue exclusion (cat. Number T8154, Sigma-Aldrich). Briefly, 10µL of cell suspension were incubated with 10µL of Trypan blue for 1-2 minutes and then loaded into a Neubauer chamber. After counting, 25000 viable cells/cm^2 were seeded on top of ECM protein. The tissue culture flasks were maintained at 37˚C, 5% CO_2 in tissue culture incubator and fed with fresh KSFM (conjunctival or corneal accordingly) every other day until further experiments (at least three independent experiments were conducted with three technical replicates).

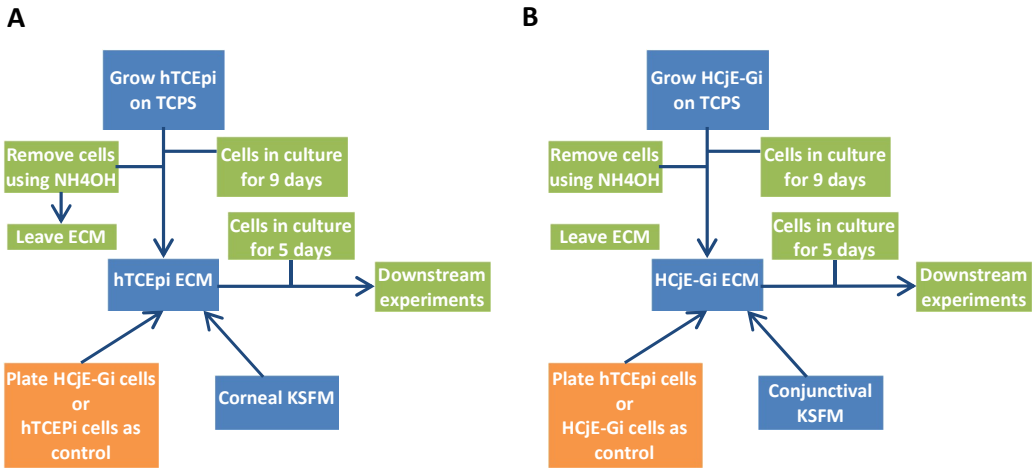

Scheme 1 – Cell seeding on ECM proteins experiment outlook. (A) hTCEpi cells were seeded for 9 days on TCPS. At this point cells were removed using NH4OH leaving the hTCEPi ECM proteins still attached to the TCPS. On top of these proteins, fresh HCjE-Gi cells (or hTCEPi cells as control) were seeded and fed with corneal KSFM for 5 days until further experiments. (B) HCjE-Gi cells were seeded for 9 days on TCPS. At this point cells were removed using NH4OH leaving the HCjE-Gi ECM proteins still attached to the TCPS. On top of these proteins, fresh hTCEpi cells (or HCjE-Gi cells as control) were seeded and fed with conjunctival KSFM for 5 days until further experiments Abbreviations used ECM: extracellular matrix, TCPS: tissue culture polystyrene.

2.2.10. RNA extraction

The tissue culture well was briefly washed with sterile PBS and incubated with 0.350mL of TRIzol® reagent (Invitrogen, cat. Number 15596-026) for 5 minutes at room temperature (RT). The resulting solution was collected into an Eppendorf and 200µL of chloroform (Sigma Chemicals, cat. Number C2432) was added. The tube was vortexed for few seconds, incubated at RT for 15 minutes and then centrifuged at 13000rpm for 15 minutes at 4˚C. The colourless aqueous (upper) phase of the centrifuged solution was transferred into a new collection Eppendorf and 500µL of 100% isopropyl alcohol (Sigma-Aldrich, cat. Number I9516) was added. The reaction was then incubated for 10 minutes at RT and then centrifuged at 13000 rpm for 10 minutes at 4˚C. The supernatant was discarded, and the resulting RNA pellet was washed with 75% (V/V) ethanol (Sigma-Aldrich, cat. Number E7023) in ddH_2O and centrifuged at 13000 rpm for 5 minutes at 4˚C. The supernatant was discarded, and the pellet allowed to air-dry for 15 minutes at RT. The dried pellet was dissolved in 20µL of DNAse, RNAse-free water (Ambion, cat. Number AM9937). Either this RNA mixture was stored at - 80˚C or reverse transcription was performed.

2.2.11. Reverse Transcription

Before reverse transcription, the concentration of RNA was assessed by analysing 1.5µL of the RNA solution using Nanodrop (ND100, Nanodrop Technologies). Subsequent steps were performed in accordance with the manufacturer's protocol by Primerdesign using *Precision nanoScript™* Reverse Transcription kit. Briefly, for the annealing step the volume correspondent to 2µg of RNA template and 1µL of reverse transcription primer was added into a 200µL PCR tube (Appleton Woods, cat. Number BS191). The final volume, 10µL, was completed with RNAse/DNAse-free water. The resulting solution was heated at 65˚C for 5 minutes. For the extension step, a mastermix containing 5µL of nanoScript 4X Buffer, 1µL dNTP mix 10mM, 4µL RNAse/DNAse-free water, and 1µL nanoScript2 enzyme was prepared and added into the resulting solution from the annealing step (all reagents were purchased from Primerdesign). The final solution was incubated at 42˚C for 20 minutes, and then at 72˚C for 15 minutes. The cDNA samples were then store at -20˚C until further utilization.

2.2.12. Reverse Transcriptase qPCR

96-well PCR microplates (LightCycler-type white, cat. Number I1402-9909, StarLab) were placed in cooled blocks, and each well was filled with 2.5µL (5ng) of cDNA template, 5µL SYBR® green, 0.5µL (30nM) of specific forward and reverse primers, and 2µL of RNAse/DNAse-free water. The filled LightCycler plates were briefly centrifuged on a mini-plate spinet (MPS1000, Labnet). The plates were then placed in a LightCycler 480 II (Roche).

qPCR was performed at 95˚C for 2 minutes for enzyme activation, followed by 45 cycles at 95˚C for 15 seconds, 60˚C for 60 seconds 72˚C for 1 second. To assess the purity of the amplicon, the melting curves were performed by continuously acquired fluorescence data until the temperature of 95˚C was achieved (at a 0.03˚C/s ramp rate). As housekeeping gene glyceraldehydes-3-phosphate dehydrogenase (GAPDH) was used for each investigated gene. The fold increase was calculated using ΔΔCt method [290]. Primer sequences are shown in Table 5.

Table 5 – List of primers used for Reverse Transcriptase quantitative PCR studies in Chapter 2. The primer sequences and the product size are included. Abbreviations used: GAPDH: glyceraldehyde-3-phosphate dehydrogenase, KRT: keratin, MUC5AC: mucin 5AC, ABCB5: ATP-binding cassette sub-family B member 5. # Sequences and product size of reference genes are not commercially provided by PrimerDesign.

Primer	Gene Sequence	Product size (bp)
GAPDH	F - # R - #	
KRT1	F - GTGGTGGTGGTGGTTTTGG R-T GCTCTGGTTGATAGTGACTTCTT	110
KRT3	F – TTCCATCTCAGGCACAAACAA R –CAGGTCCTCCATGTTCTTCAG	130
KRT7	F –CTCCCACCACTCCATCCT R - ATCACTTTCCAGACTGTCTCACT	105
KRT10	F- AAGAAGAACCACGAGGAGGAA R- ATGTTATTCAGAAGTTGAGTCAGATC	113
KRT12	F –CTCCAAATCACAAGCACAGTCA R - CCACCTCACCATTCACCATCT	98
KRT13	F –ATGCTGCTGGACATCAAGAC R -TCGTGGTAACAGAGGTGCTA	113
MUC5AC	F –CAGAGGGGTTGACAGTGAC R - GAACCGCATTTGGGCATC	113
ΔNp63	F –GGAAGGCGGATGAAGATAGC R - CATGTGTGTTCTGACGAAACG	96
ABCB5	F -GGAAAGAATTACCACTACCAAGAAGG R -TGGTAGCATCCAAATGGGCAAAC	119
SOX2	F – GGAGAGTAAGAAACAGCATGGA R -TTTGCGTGAGTGTGGATGG	128
OCT4	F - ATGTGGTCCGAGTGTGGTTC R - TGTGCATAGTCGCTGCTTGA	67
NANOG	F –GCTGTGTGTACTCAATGATAGATTT R -GAGGTTCAGGATGTTGGAGAG	85

2.2.13. Western Blot

2.2.12.1. Reagents

Running buffer was prepared by mixing 2L of methanol (cat. Number M/4000/PC17, Fisher Scientific UK), 300g of Tris (cat. Number T1503), 1440g of glycine (cat. Number G8898), and 100g of sodium dodecyl sulphate (SDS, cat. Number L4509), all provided by Sigma-Aldrich unless otherwise specified, the pH was then set to 8.3-8.7. The final volume was completed to 10L with ddH_2O. This stock solution was then diluted 10X in ddH_2O prior utilization.

Transfer buffer was prepared by mixing 2L of methanol with 30g of Tris and 144g of glycine. The final volume was completed to 10L with ddH_2O and kept at 4°C until usage.

Urea-SDS cell lysis buffer was prepared by mixing 40.08g of urea (cat. Number U5378), 1mL of 1M Tris/HCl (pH 6.8), 10mL of glycerol (cat. Number G8773), 5mL of 20% SDS in ddH_2O, all provided by Sigma-Aldrich.

Lower gel stock solution was prepared by mixing 90.8g of Tris (1.5M final concertation), 10mL of 20% SDS in ddH_2O. The final volume was completed to 500mL with ddH_2O. The resulting solution was stirred overnight at 4°C and the pH adjusted to 8.8.

Upper gel stock solution was prepared by mixing 30.275g of Tris (0.5M final concentration) and 10mL of 20% SDS in ddH_2O. The final volume was completed to 500mL with ddH_2O. The resulting solution was stirred overnight at 4°C and the pH adjusted to 6.8.

Buffer 1 consisted of (%V/V): 85% Urea-SDS buffer supplemented with 15% β-mercaptoethanol (cat. Number M6250), 50µM phenylmethanesulfonyl fluoride (cat. Number P7626), and 50µM *N*-ethylmaleimide (cat. Number E3876), all provided by Sigma-Aldrich.

2.2.12.2. Cell extracts

Cell preparations were extracted from a confluent T-25cm^2 tissue culture flask. The medium was removed, and the flask washed twice with sterile PBS to remove the serum and any other medium remains. 1mL of buffer 1 was added and the cells vigorously removed with the aid of a cell scraper (cat. Number 83.1830, Sarstedt).

2.2.12.3. SDS-PAGE

The extracts were then processed for SDS-PAGE. Acrylamide lower and upper gels were prepared as described in Table 6. 5µL of Spectra ™ multicolour Broad Range protein ladder (cat. Number 26634 Thermo Scientific) and 20µL of each sample were loaded in different

lanes and the gel ran for approximately 2 hours at 80V (PowerPac Basic ™, BioRad) in running buffer.

Table 6 – Western Blot 10% acrylamide gels recipe. Abbreviations used APS: ammonium persulfate, TEMED: N,N,N′,N′-Tetramethylethylenediamine.

Reagent	Lower gel	Upper gel	Cat. Number	Supplier
Stock	2mL	1.25mL	---	---
30% Acrylamide	2.75mL	0.75mL	A3699	Sigma-Aldrich
ddH_2O	3.25mL	3mL	---	---
10% APS	100µL	100µL	A/P470/46	Fisher Scientific
TEMED	4µL	5µL	T9281	Sigma-Aldrich

2.2.12.4. Immunoblotting

The Western immunoblotting was run for 2 hours at 110V in transfer buffer. The membranes (0.2µm cat. Number162-0112 BioRad) were then stained with Ponceau S solution (cat. number P7170, Sigma-Aldrich) for approximately 2 minutes and cut accordingly. Thereafter, the membranes were blocked in blocking solution containing 5% (W/V) skimmed milk diluted in 0.05% (V/V) PBSTween-20 (cat. number 9416, Sigma-Aldrich) solution for 30 minutes on the rocker and probed with primary antibody diluted in blocking solution overnight at 4˚C (Table 7). The membranes were then washed thrice using 0.05% (V/V) PBSTween-20 and incubated with the secondary antibody diluted in the blocking solution for one hour at RT (Table 8). The two horseradish peroxidase (HRP) chemicals SuperSignal® West Pico Chemiluminescent substrate (cat. Number 34080, Thermo Scientific) were mixed at ratio of 1:1 and poured over the membrane. The immunoblots were scanned using a Chemidoc (chemiDoc ™ XRS+, BioRad) and quantified using ImageLab 5.0 Software.

Table 7 - List of primary antibodies used for Western Blot studies in Chapter 2. Abbreviations used KRT: keratin, BS: blocking solution, ABCB5: ATP-binding cassette sub-family B member 5. # Kind gift from Professor Jonathan Jones (Northwestern University, Chicago, USA).

Antibody	Clone	Host	Blocking	Manufacturer	Dilution
KRT1	Polyclonal	Rabbit	BS	Abcam®	1:1000
KRT3	AE5	Mouse	BS	Abcam®	1:1000
KRT7	RCK105	Mouse	BS	Santa Cruz	1:1000
KRT12	J6	Rabbit	BS	#	1:1000
KRT13	Ks13.1	Mouse	BS	Santa Cruz	1:1000
ABCB5	5H3C6	Mouse	BS	Abcam®	1:1000
ΔNp63α	Poly6190	Rabbit	BS	Biolegend	1:1000
B-Actin	mAbcam 8224	Mouse	BS	Abcam®	1:5000

Table 8 - List of secondary antibodies used for Western Blot studies in Chapter 2.

Antibody	Host	Reactivity	Conjugate	#Catalogue	Manufacturer	Dilution
Anti-mouse	Horse	Human	HRP	7076	Cell Signalling	1:1000
Anti- rabbit	Goat	Human	HRP	7074	Cell Signalling	1:1000

2.2.14. Flow cytometry

A cell suspension was obtained by trypsinization (as previously described) and then centrifuged (all centrifugation steps were performed for 3 minutes at 1000 rpm at RT). The supernatant was then removed, and the cell pellet re-suspended in 100 µl of 1X FACS Permeabilizing Solution 2 (cat. Number 347692, BD Biosciences) in ddH_2O. The resultant suspension was incubated for 10 minutes at RT. After centrifugation, the supernatant was removed, and the remaining cell pellet re-suspended in 1ml of 5% (V/V) FCS in PBS. After centrifugation, the supernatant was discarded, and the cell pellet re-suspended in 100µL of primary antibody (Table 9) diluted in PBS. The resulting suspension was incubated in the dark for 30 minutes at 4°C. After adding 1ml of 5% (V/V) FCS in PBS to the cell suspension, centrifugation was performed, and the supernatant discarded. The resulting cell pellet was re-suspended in 100µL of appropriate secondary antibody (Table 10) diluted in PBS. This suspension was then incubated in the dark for 30 minutes at 4°C. 1ml of 5% (V/V) FCS in PBS was added to the cell suspension and centrifugation was performed. After discarding the supernatant, the cell pellet was re-suspended in 500µl of 5% (V/V) FCS in PBS. This final suspension was analysed using a BD Accuri C6 flow cytometer (BD Biosciences) and the results analysed using BD Accuri C6 software (BD Biosciences).

Table 9 – List of primary antibodies used for flow cytometry studies in Chapter 2. Abbreviations used KRT: keratin, ABCB5: ATP-binding cassette sub-family B member 5. # Concentration dependent on primary antibody.

Antibody	Clone	Host	Isotype	Manufacturer	Dilution
KRT3	AE5	Mouse	IgG	Abcam ®	1:1000
KRT7	RCK105	Mouse	IgG1	Santa Cruz	1:500
KRT12	J6	Rabbit			1:500
KRT13	Ks13.1	Mouse	IgG1	Santa Cruz	1:500
ABCB5	5H3C6	Mouse	IgG1	Abcam ®	1:1000
ΔNp63	Poly6190	Rabbit	IgG	Biolegend	1:1000
IgG	---	Mouse	---	ThermoFisher Scientific	#
lgG	---	Rabbit	---	ThermoFisher Scientific	#
IgG1	---	Mouse	---	ThermoFisher Scientific	#
IgG3	---	Mouse	---	ThermoFisher Scientific	#

Table 10 - List of secondary antibodies used for flow cytometry studies in Chapter 2. Abbreviations FITC: fluorescein isothiocyanate.

Antibody	Clone	Host	Reactivity	Conjugate	Manufacturer	Dilution
Anti-mouse	A-11005	Goat	Mouse	FITC	Life Technologies	1:1000
Anti-rabbit	F7512	Sheep	Rabbit	FITC	Sigma-Aldrich	1:1000

2.2.15. Statistical analysis

Kruskal-Wallis and Mann-Whitney tests followed by according post hoc analysis were used to determine statistically significant differences (GraphPad Prism 5, *p<0.05, **p<0.01, ***p<0.001). Data is expressed as median ± 5-95% percentile (unless otherwise specified). Non-parametric tests were chosen as these do not make the assumption about normally distributed data. Additionally, they are more robust when a small sample size is used and their outcome less affected by outliers.

2.3 Results

A process called 'de-roofing', derived from a protocol established by Gospodarowicz and Todorovic et al. with few modifications, was used to remove cells leaving only the ECM proteins (and other soluble factors) attached to the tissue polystyrene cultureware [288, 289]. On top of those ECM proteins, fresh cells were cultured, and the extent of differentiation assessed using various cell and molecular techniques. Six different markers were used for this purpose: KRT3 and KRT12 were used as markers for corneal ECs [106-108], KRT7 and KRT13 utilized as markers for conjunctival ECs [106], and ΔNp63 and ABCB5 as epithelial SCs markers [102, 103, 116]. The advantage of ABCB5 over ABCG2 (other marker for epithelial SCs) arises from the fact that ABCB5 is only expressed by the ΔNp63–positive cells [116]. MUC5AC was also investigated and used as a marker for the presence of goblet cells of conjunctival origin [132, 152]. This marker was only used at transcript levels as no suitable and reliable antibody can yet be found.

2.3.1. Cell doubling time

The doubling time showed non-significant differences between the two cell lines used, with cells needing approximately 2 days to go a full cell cycle, Figure 15. Since cell division is essential as an intermediate step for cell transdifferentiation, although not obligatory in all cases [212], cells were allowed in culture for 5 days (approximately two complete cell cycles).

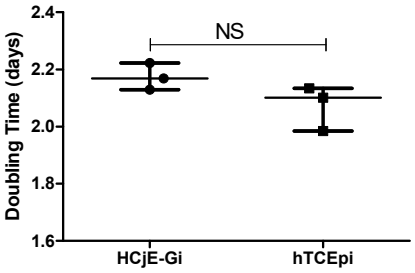

Figure 15 - HCjE-Gi and hTCEpi cells doubling time. (Data is represented as median ± interquartile range, n=3. Mann-Whitney test). Abbreviations used NS: non-significant.

2.3.2. hTCEpi ECM proteins drive higher expression of corneal and stem cell epithelial markers by HCjE-Gi cells than HCjE-Gi ECM proteins

The aim of these experiments was to identify the day of cell culture associated with the optimum time of ECM production and deposition for the modulation of KRTs and ΔNp63 expression.

hTCEpi cells were cultured over a desired period on TCPS. At each time-point the cultures were 'de-roofed' and HCjE-Gi cells cultured on hTCEpi ECM proteins for 5 days. HCjE-Gi cells cultured on their own ECM proteins were used as a control (dashed line). Day 9 appeared to be the only time-point whereupon KRT3 and was upregulated (1.4-fold increase, $p<0.05$) and KRT13 expression downregulated (6.2-fold decrease), Figure 16. No KRT12 expression was detected when HCjE-Gi cells were cultured on their own ECM proteins at day 9 (blue arrow) and as so no statistically analyses could be performed.

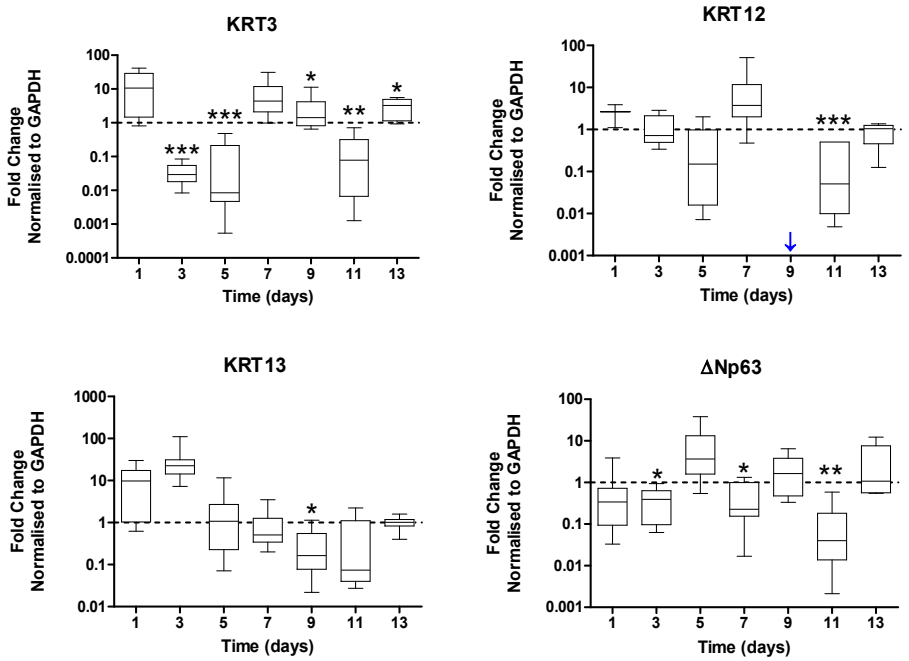

Figure 16 - The expression of epithelial cell markers by HCjE-Gi cells when cultured on hTCEpi ECM proteins compared to HCjE-Gi ECM deposited over time as assessed by Reverse Transcriptase qPCR. (Data is represented as median ± 5-95 percentile, n≥9, Mann-Whitney test, Bonferroni corrected p-value, *p<0.05, **p<0.01, ***p<0.001). Dashed line represents the basal expression of the markers of interest when cells are cultured on their own ECM proteins. Blue arrow represents expression not detected. Abbreviations used GAPDH: glyceraldehyde 3-phosphate dehydrogenase, KRT: keratin, ECM: extracellular matrix.

2.3.3. HCjE-Gi ECM proteins drives higher expression of conjunctival and stem cell epithelial markers by hTCEpi cells than hTCEpi ECM proteins

In this section, HCjE-Gi cells were cultured over a desired period on TCPS and at each time-point the cultures were 'de-roofed' and hTCEpi cells cultured on HCjE-Gi ECM proteins for 5 days. hTCEpi cells cultured on their own ECM proteins were used as a control (dashed line). KRT13 expression by hTCEpi cells at day 7 was upregulated (87-fold increase, $p<0.01$). Day 9

appeared to be the only time-point where KRT3 expression was downregulated (25-fold decrease) and KRT12 expression not detected (blue arrow), Figure 17.

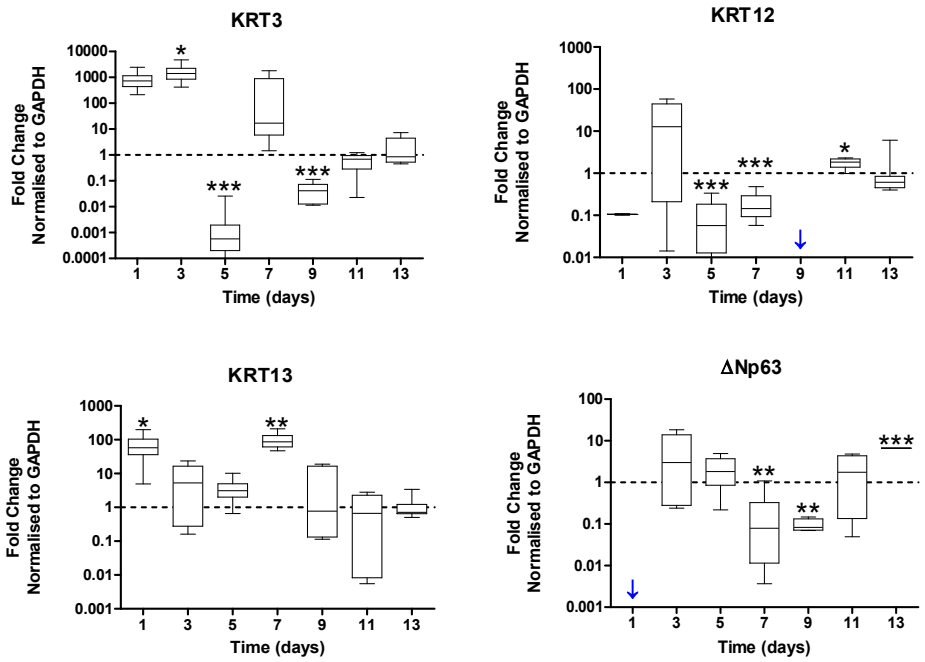

Figure 17 - The expression of epithelial cell markers by hTCEpi cells when cultured on HCjE-Gi ECM proteins compared to hTCEpi ECM deposited over time as assessed by Reverse Transcriptase qPCR. (Data is represented as median ± 5-95 percentile, n≥9, Mann-Whitney test, Bonferroni corrected p-value, *p<0.05, **p<0.01, ***p<0.001). Dashed line represents the basal expression of the markers of interest when cells are cultured on their own ECM proteins. Blue arrow represents expression not detected. Abbreviations used GAPDH: glyceraldehyde 3-phosphate dehydrogenase, KRT: keratin, ECM: extracellular matrix.

ECM proteins produced and deposited for 9 days were chosen as the preferred condition to further investigate the process of EC differentiation. The potential for EC differentiation of this system was further investigated. To further investigate the degree of cell differentiation, the expression of KRT7 (marker for terminally differentiated conjunctival ECs) and ABCB5 (marker for epithelial SC) will be addressed.

2.3.4. hTCEpi ECM proteins drive higher expression of corneal and stem cell epithelial markers by HCjE-Gi cells than the HCjE-Gi ECM

The results in this section were obtained by culturing HCjE-Gi cells on top of hTCEpi ECM proteins (produced and deposited by hTCEpi cells for 9 days) for 5 days. As internal control, the expression of the markers of interest by HCjE-Gi cells seeded on top of their own ECM proteins (deposited for 9 days) was used.

2.3.4.1. Reverse Transcriptase qPCR

The differentiation of HCjE-Gi cells into a cornea epithelial-like lineage was assessed by Reverse Transcriptase qPCR. By culturing HCjE-Gi cells on top of hTCEpi ECM proteins three different outcomes were appreciated at transcript expression levels compared with HCjE-Gi cells cultured on HCjE-Gi ECM and normalised to GAPDH levels:

i. significantly higher expression levels of the terminally differentiated corneal EC markers KRT3 (161-fold increase, $p<0.05$) and KRT12 (3.6-fold increase, $p<0.01$), Figure 18;

ii. significantly lower expression of conjunctival EC markers KRT7 and KRT13 (respectively 1.4 and 2.1-fold decrease, $p<0.05$), Figure 18;

iii. significantly higher expression levels of ABCB5 (1.8-fold increase, $p<0.05$), Figure 18.

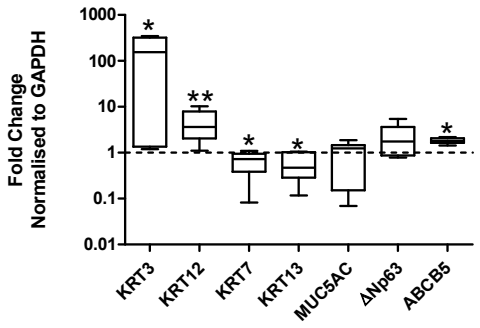

Figure 18 - The expression of epithelial cell markers by HCjE-Gi cells when cultured on top of hTCEpi ECM proteins compared with HCjE-Gi ECM as assessed by Reverse Transcriptase qPCR. Data normalised to GAPDH levels. (Data is represented as median ± 5-95 percentile, n≥6, Mann-Whitney test, *p<0.05, **p<0.01, ***p<0.001). Dashed line represents the basal expression of the markers of interest when cells are cultured on their own ECM proteins. Abbreviations used GAPDH: glyceraldehyde 3-phosphate dehydrogenase, KRT: keratin, MUC: mucin, ABCB5: ATP-binding cassette sub-family B member 5, ECM: extracellular matrix.

2.3.4.2. Western Blot

To further investigate the process of conjunctival differentiation into a corneal epithelial-like lineage, western blotting was performed. By seeding HCjE-Gi cells on top of deposited hTCEpi ECM proteins, and consistent with the transcript abundance data:

i. significant higher expression of corneal EC markers KRT3 and KRT12 ($p<0.05$) was appreciated, Figure 19;

ii. significant lower expression of KRT7 and KRT13 ($p<0.05$) was seen, Figure 19;

iii. significant higher expression of ABCB5 and ΔNp63 ($p<0.05$) was observed, Figure 19.

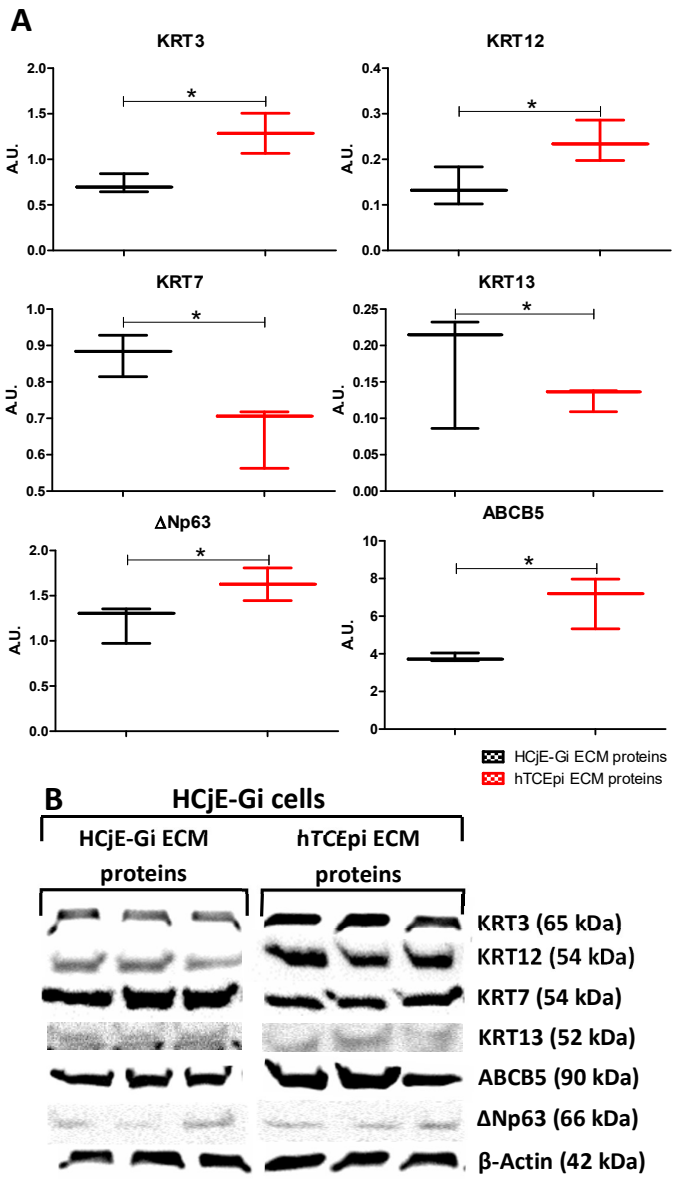

Figure 19 - The expression of epithelial cells markers by HCjE-Gi cells when cultured on top of hTCEpi ECM proteins compared with HCjE-Gi ECM as assessed by Western Blot. (A) Whiskers graphs showing the densitometry quantification of each protein, normalised against the expression of β-actin. (B) Western blots representative of three independent experiments. (Data is represented as median ± 5-95 percentile, n≥3, Mann-Whitney test, *$p<0.05$, ** $p<0.01$, *** $p<0.001$). Abbreviations used A.U.: arbitrary units, KRT: keratin, ABCB5: ATP-binding cassette sub-family B member 5, ECM: extracellular matrix.

2.3.4.3. Flow Cytometry

Flow cytometry corroborated the protein studies (Western blot) where the total protein content was assessed. The percentage of positive cells was defined by the subtraction of cells displaying expression for a given protein about a threshold given by its isotype control (see Appendix A.2 for details). By seeding HCjE-Gi cells on top of hTCEpi ECM proteins and

compared with HCjE-Gi cells cultured on their own ECM proteins, and consistent with Reverse Transcriptase qPCR and western blot data:

i. a significantly higher proportion of KRT12-positive cells was detected (30%, $p<0.05$), Figure 20.

ii. a significantly lower proportion of KRT7-positive and of KRT13-positive cells was also shown (10% for each protein, $p<0.05$), Figure 21,

iii. a significantly higher proportion of ΔNp63- and ABCB5-positive cells (nearly 25% for each marker, $p<0.01$) was observed, Figure 22.

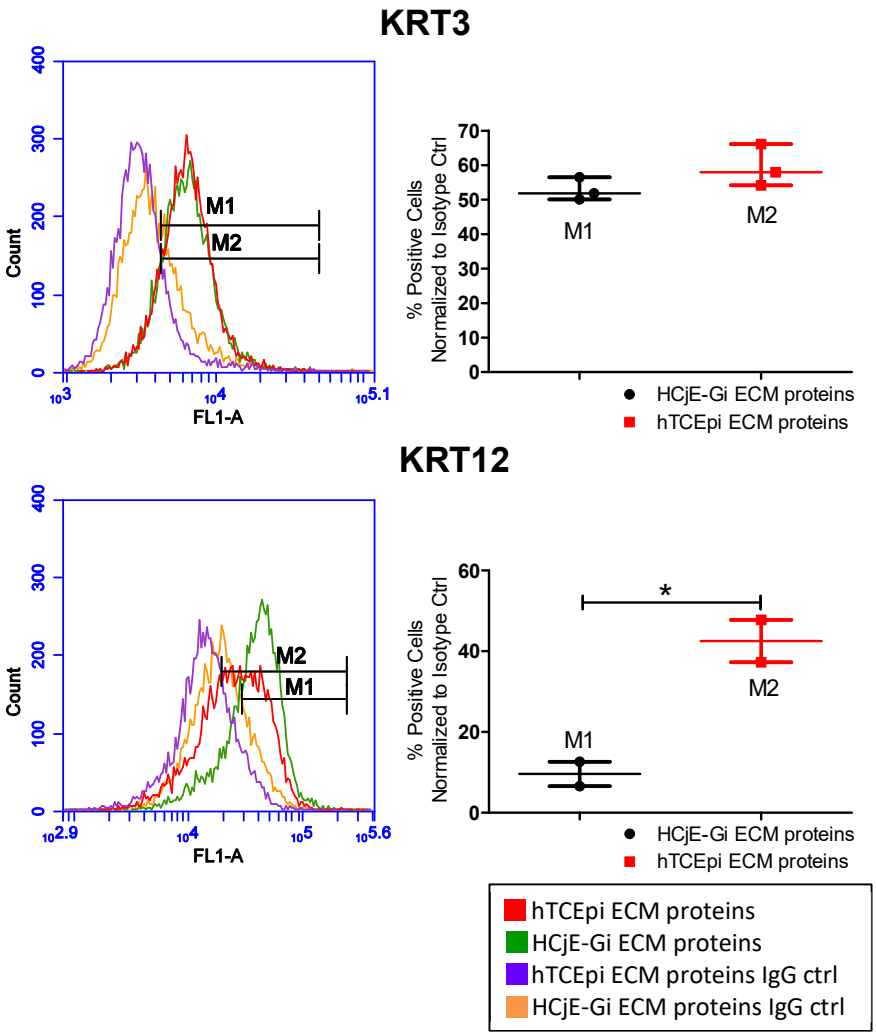

Figure 20 - The expression of corneal epithelial cells markers keratin 3 and keratin 12 by HCjE-Gi cells when cultured on top of hTCEpi ECM proteins compared with HCjE-Gi ECM as assessed by flow cytometry. The percentage of positive events normalised against isotype control is shown (M_x). (Data is represented as median ± 5-95 percentile, n≥3, Mann-Whitney test, *p<0.05, **p<0.01, ***p<0.001). Abbreviations used KRT: keratin, Ctrl: control, ECM: extracellular matrix.

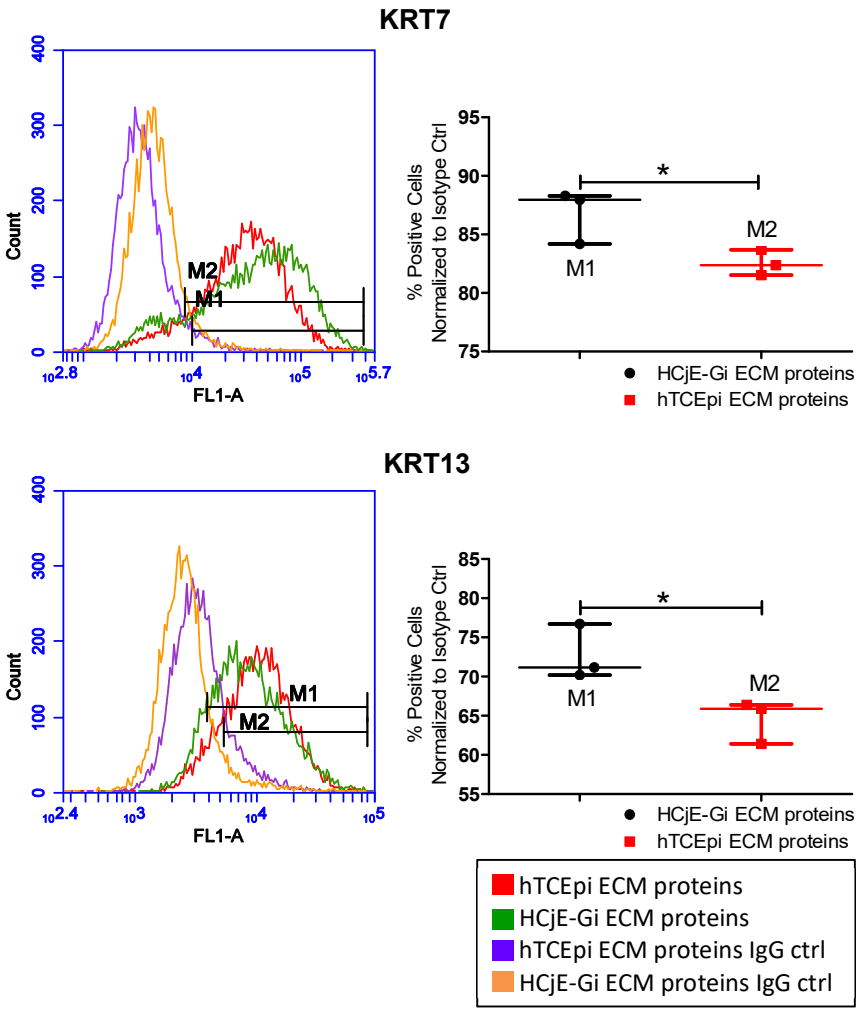

Figure 21 - The expression of corneal epithelial cells markers keratin 7 and keratin 13 by HCjE-Gi cells when cultured on top of hTCEpi ECM proteins compared with HCjE-Gi ECM as assessed by flow cytometry. The percentage of positive events normalised against isotype control is shown (M_x). (Data is represented as median ± 5-95 percentile, n≥3, Mann-Whitney test, *p<0.05, **p<0.01, ***p<0.001). Abbreviations used KRT: keratin, Ctrl: control, ECM: extracellular matrix.

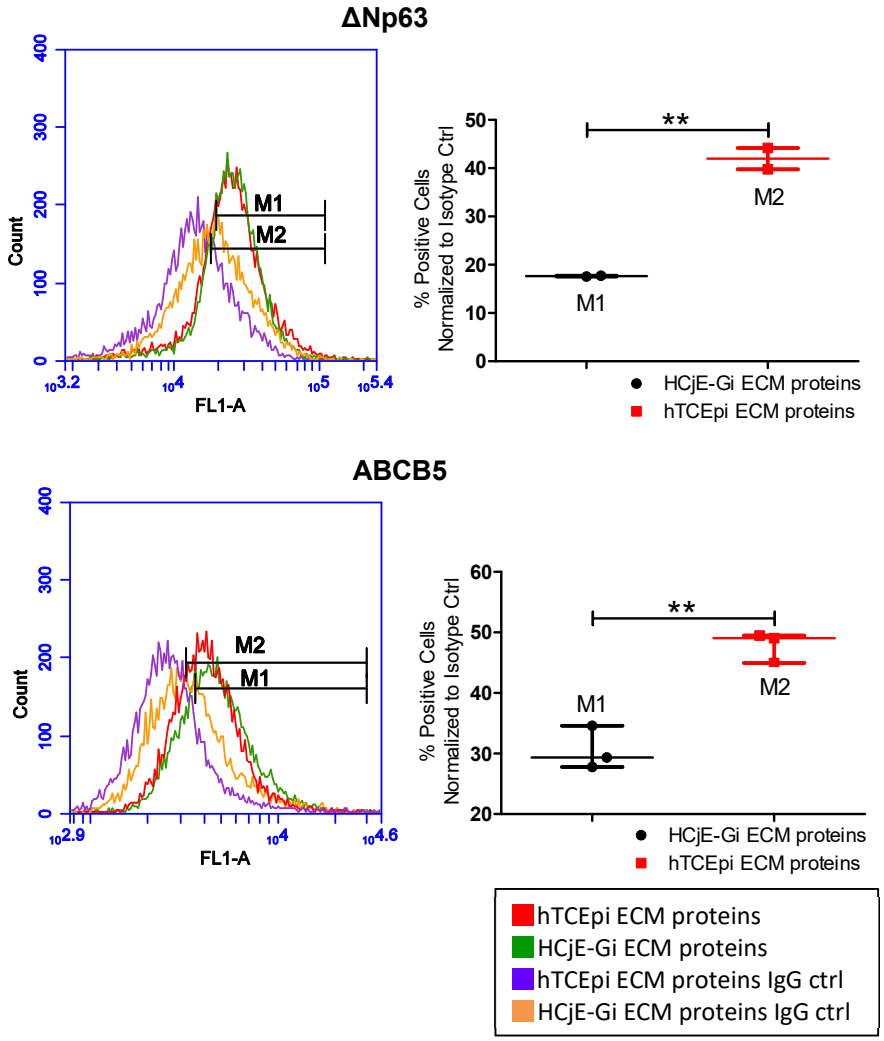

Figure 22 - The expression of epithelial stem cell markers ΔNp63 and ABCB5 by HCjE-Gi cells when cultured on top of hTCEpi ECM proteins compared with HCjE-Gi ECM as assessed by flow cytometry. The percentage of positive events normalised against isotype control is shown (M_x). (Data is represented as median ± 5-95 percentile, n≥3, Mann-Whitney test, *p<0.05, **p<0.01, ***p<0.001). Abbreviations used Ctrl: control, ABCB5: ATP-binding cassette sub-family B member 5, ECM: extracellular matrix.

2.3.4.4. Summary of results 1:

To summarize these results, by culturing HCjE-Gi cells on top of hTCEpi ECM proteins and compared to HCjE-Gi cells cultured on their own ECM proteins, there was a:

i. Higher expression of corneal EC markers.

ii. Lower expression of conjunctival EC markers.

iii. Higher expression of epithelial SC markers.

2.3.5. HCjE-Gi ECM proteins drive higher expression of conjunctival and stem cell epithelial markers by hTCEpi cells than the hTCEpi ECM

The results shown in this section were obtained by culturing hTCEpi cells on HCjE-Gi ECM proteins (produced and deposited by HCjE-Gi cells over 9 days) for 5 days. As internal control, the expression of the markers of interest by hTCEpi cells when seeded on top of their own ECM proteins (produced and deposited over 9 days) was used.

2.3.5.1. Reverse Transcriptase qPCR

By culturing hTCEpi cells on top of HCjE-Gi ECM proteins three different outcomes were appreciated at transcript expression levels compared with hTCEpi cells cultured on hTCEpi ECM and normalised to GAPDH levels: These are the opposite equivalent of the results shown in the previous sections:

i. significantly lower KRT12 transcript expression levels (4.0-fold decrease, $p<0.05$), Figure 23

ii. significantly higher levels of KRT7 and KRT13 expression (1.9- and 8.4-fold increase, respectively, $p<0.01$), Figure 23

iii. significant higher levels of ΔNp63 and ABCB5 expression (1.4-fold increase, $p<0.05$ and 1.4- fold increase, $p<0.001$ respectively), Figure 23.

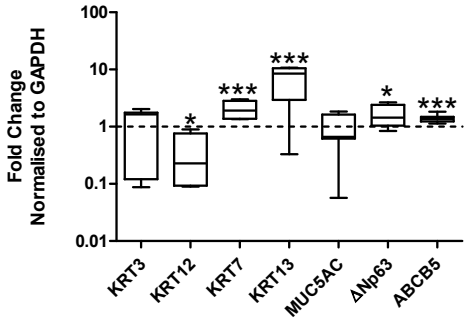

Figure 23 - The expression of epithelial cell markers by hTCEpi cells when cultured on top of HCjE-Gi ECM proteins compared with hTCEpi ECM as assessed by Reverse Transcriptase qPCR. Data normalised to GAPDH levels. (Data is represented as median ± 5-95 percentile, n≥4, Mann-Whitney test *p<0.05, **p<0.01, ***p<0.001). Dashed line represents the basal expression of the markers of interests when cells are cultured on their own ECM proteins. Abbreviations used GAPDH: glyceraldehyde 3-phosphate dehydrogenase, KRT: keratin, ABCB5: ATP-binding cassette sub-family B member 5, ECM: extracellular matrix.

2.3.5.2. Western Blot

Consistent with the transcript abundance data, significant lower values of KRT3 and KRT12 total protein expression ($p<0.001$ and $p<0.01$, respectively) accompanied by significant higher expression levels of KRT13 ($p<0.001$) and ABCB5 ($p<0.05$) were observed. Remarkably no KRT13 expression could be detected when hTCEpi cells were seeded on hTCEpi ECM proteins, Figure 24.

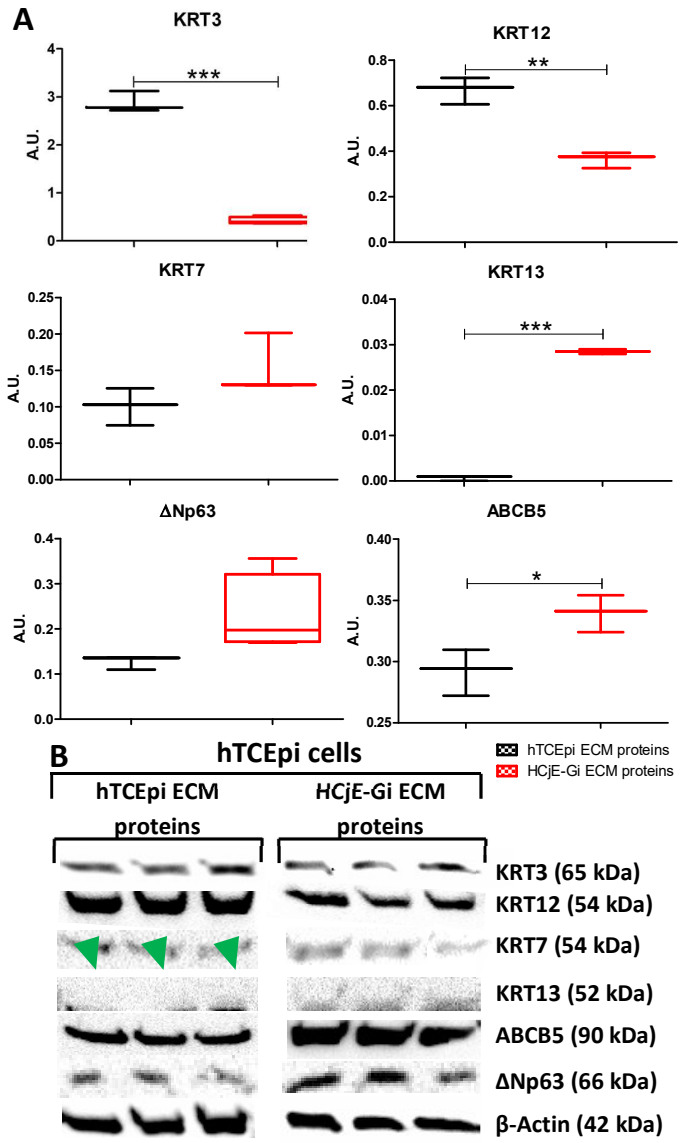

Figure 24 - The expression of epithelial cell markers by hTCEpi cells when cultured on top of HCjE-Gi ECM proteins compared with hTCEpi ECM as assessed by Western Blot. (A) Whiskers graphs showing the densitometry quantification of each protein normalised against the expression of β-actin. (B) Western blots representative of three independent experiments. Green arrowheads show no KRT13 expression when hTCEpi cells were seeded on hTCEpi ECM proteins. (Data is represented as median ± 5-95 percentile, n≥3, Mann-Whitney test, *p<0.05, ** p<0.01, *** p<0.001). Abbreviations used A.U. arbitrary units, KRT: keratin, ABCB5: ATP-binding cassette sub-family B member 5, ECM: extracellular matrix.

2.3.5.3. Flow Cytometry

Trends at protein levels assessed by flow cytometry are consistent with total protein data. By culturing hTCEpi cells on HCjE-Gi ECM proteins, and compared with hTCEpi cells cultured on hTCEpi ECM proteins, significant:

i. lower proportion of KRT3-positive cells (nearly 30%, $p<0.05$) and of KRT12-positive cells (20%, $p<0.05$) were observed, Figure 25.

ii. higher proportion of KRT7-positive cells was also appreciated (10%, $p<0.05$), Figure 26.

iii. higher proportion of ΔNp63-positive cells (25%, $p<0.05$) and of ABCB5-positive cells (nearly 40%, $p<0.01$) were observed, Figure 27.

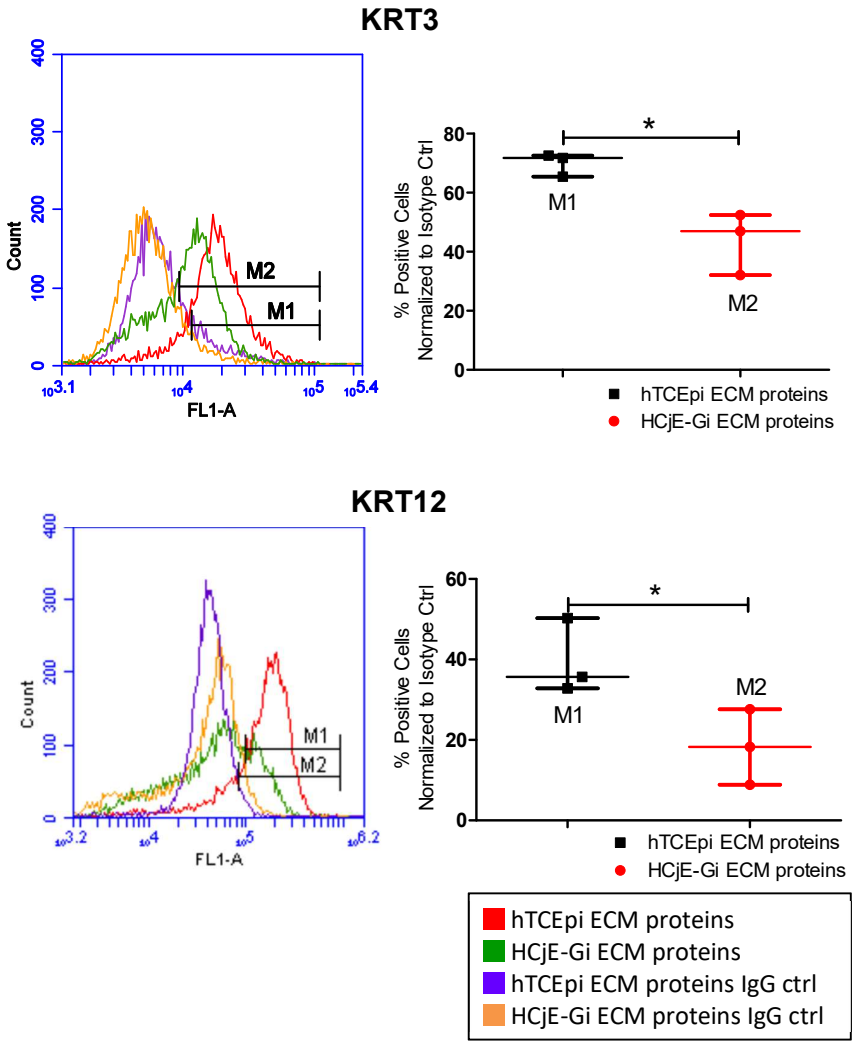

Figure 25 - The expression of corneal epithelial markers keratin 3 and keratin 12 by hTCEpi cells when cultured on top of HCjE-Gi ECM proteins compared with hTCEpi ECM as assessed by flow cytometry. The percentage of positive events normalised against isotype control is shown (Mx). (Data is represented as median ± 5-95 percentile, n≥3 Mann-Whitney test, *p<0.05, **p<0.01, ***p<0.001). Abbreviations used KRT: keratin, Ctrl: control, ECM: extracellular matrix.

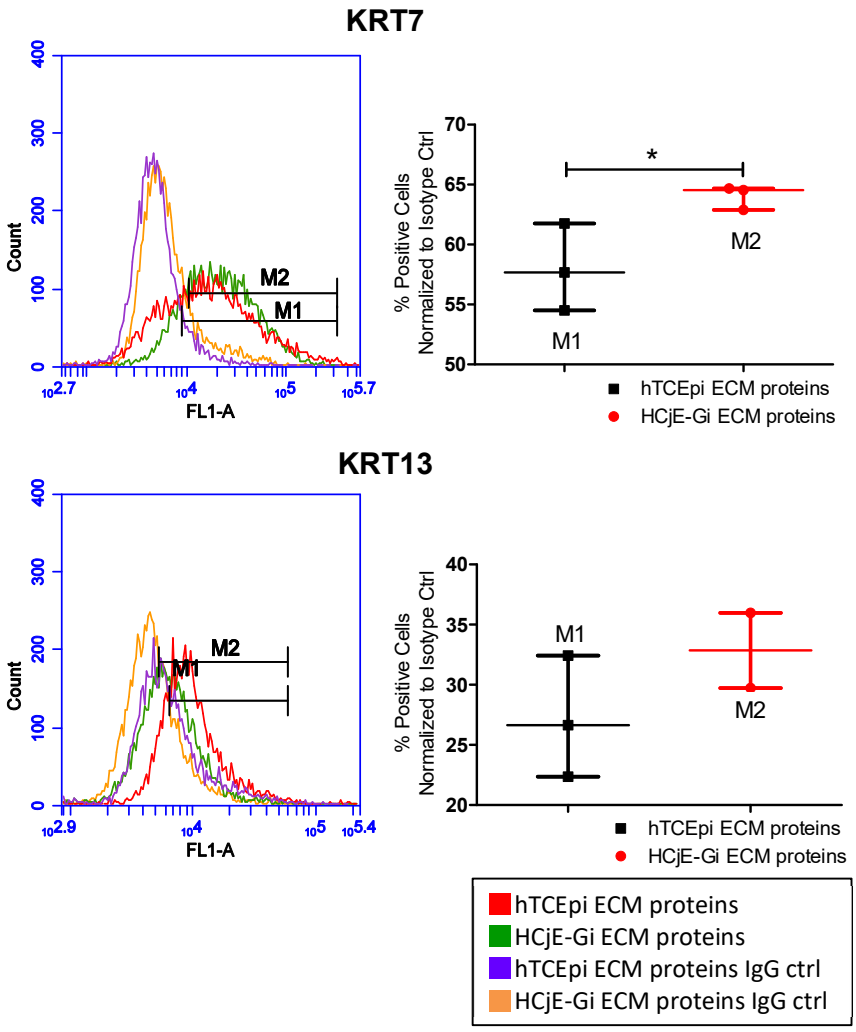

Figure 26 - The expression of conjunctival epithelial cell markers keratin 7 and keratin 13 by hTCEpi cells when cultured on top of HCjE-Gi ECM proteins compared with hTCEpi ECM as assessed by flow cytometry. The percentage of positive events normalised against isotype control is shown (Mx). (Data is represented as median ± 5-95 percentile, n≥3 Mann-Whitney test, *p<0.05, **p<0.01, ***p<0.001). Abbreviations used KRT: keratin, Ctrl: control, ECM: extracellular matrix.

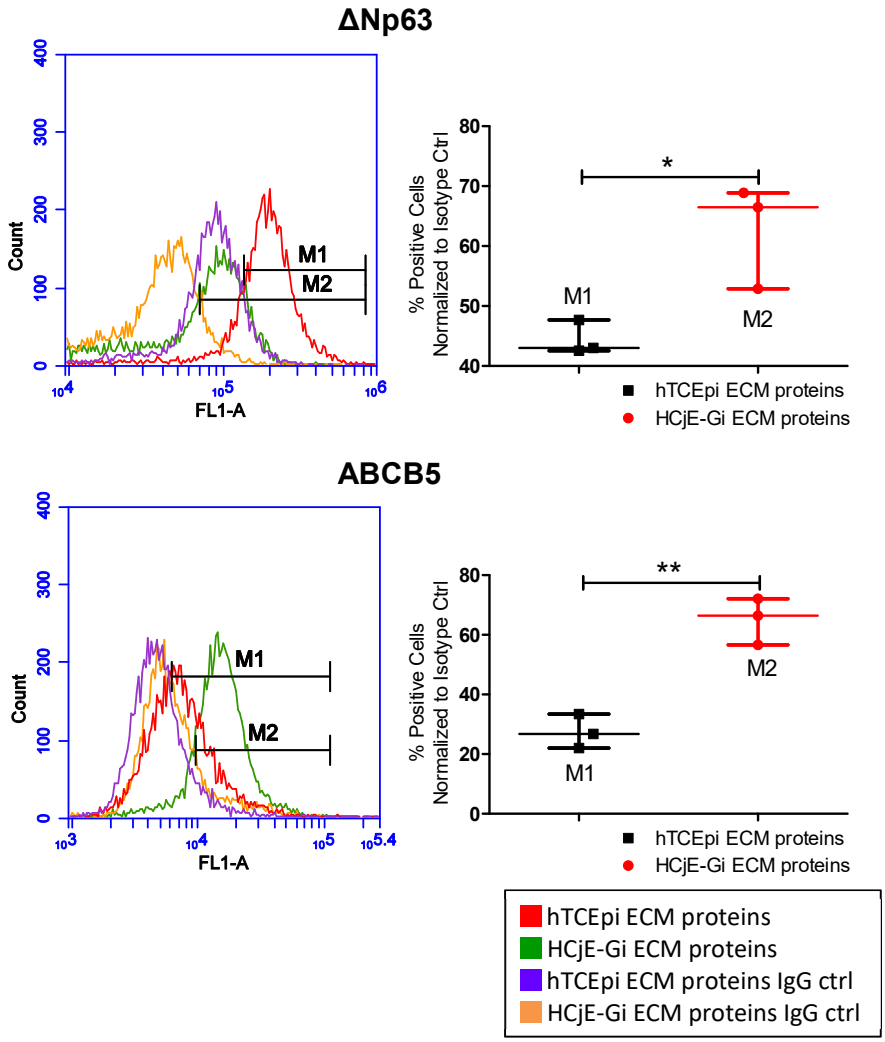

Figure 27 - The expression of epithelial stem cells markers ΔNp63 and ABCB5 by hTCEpi cells when cultured on top of HCjE-Gi ECM proteins compared with hTCEpi ECM as assessed by flow cytometry. The percentage of positive events normalised against isotype control is shown (Mx). (Data is represented as median ± 5-95 percentile, n≥3, Mann-Whitney test, *p<0.05, **p<0.01, ***p<0.001). Abbreviations used Ctrl: control, ECM: extracellular matrix, ABCB5: ATP-binding cassette sub-family B member 5.

2.3.5.4. Summary of results 2:

To summarize these results, by culturing hTCEpi cells on HCjE-Gi ECM proteins and compared to hTCEpi cells cultured on their own ECM proteins, there was a:

i. Lower expression of corneal EC markers.

ii. Higher expression of conjunctival EC markers.

iii. Higher expression of epithelial SC markers.

2.3.6. Corneal ECM proteins drive higher expression of corneal and stem cell epithelial markers by primary conjunctival cells than the conjunctival ECM

The results obtained with immortalized cell lines were further confirmed using primary cells. The experimental design used was the same as for cell lines: primary cells were cultured on regular TCPS cultureware for 9 days, the resulting culture was then "de-roofed". On top of the deposited ECM proteins, fresh cells (preferentially from the same donor) were cultured.

2.3.6.1. Reverse Transcriptase qPCR

Conjunctival primary cells from four different donors (six eyes called REBxx) cultured on corneal ECM proteins were used to assess the transcript expression profiles of the already stated markers of interest. All the comparisons were made against the expression of those markers by conjunctival cells cultured on conjunctival ECM proteins normalised to GAPDH levels. The results show:

i. Significant higher values of KRT3 expression in all eyes ($p \leq 0.05$), although at lower levels when compared to the fold increase observed in HCjE-Gi cells cultured on top of hTCEpi ECM proteins. The expression of KRT12 was, in two of the donors (REB17R and REB18R), significantly higher ($p < 0.01$), Figure 28.

ii. Significant lower levels of KRT7 expression ($p \leq 0.01$, 3 out of 6 eyes) and of KRT13 expression ($p \leq 0.05$, 4 out of 6 eyes). Relatively to the expression of MUC5AC, a significant higher expression of this transcript was observed ($p \leq 0.05$) in 5 out of 6 eyes, an exception is made for REB20L where lower values of its expression were observed ($p < 0.01$), Figure 28.

iii. Significant higher expression of ΔNp63 ($p \leq 0.05$, 4 out of 6 eyes) and ABCB5 ($p < 0.01$, 1 out of 6 eyes), Figure 28.

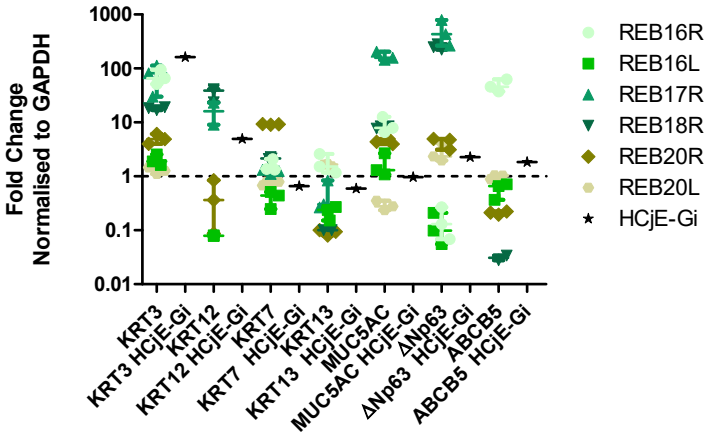

Figure 28 - The expression of epithelial cell markers by primary conjunctival cells when cultured on top of corneal ECM proteins compared with conjunctival ECM as assessed by Reverse Transcriptase qPCR. Data normalised to GAPDH levels (Data is represented as median ± interquartile range, n≥10). Dashed line represents the basal expression of the markers of interests when cells are cultured on their own ECM proteins. Abbreviations used GAPDH: glyceraldehyde 3-phosphate dehydrogenase, KRT: keratin, ABCB5: ATP-binding cassette sub-family B member 5, ECM: extracellular matrix.

2.3.6.2. Western Blot

Conjunctival primary cells extracted from six different donors (ten eyes) were used. Consistent with transcript abundance data, the total protein quantification results show:

i. Higher expression of KRT3 (8 out of 10 eyes) and KRT12 (9 out of 10 eyes). Noteworthy, no KRT12 expression was found when REB16R cells were seeded on conjunctival ECM proteins, Figure 29.

ii. Lower values of KRT7 (9 out of 10 eyes) and KRT13 expression (7 out of 9 eyes), Figure 29.

iii. Higher expression of ΔNp63 (7 out of 9 eyes) and ABCB5 (7 out of 10 eyes), Figure 29.

Ocular primary cells are not abundant in number and, when in culture, they quickly start to differentiate. Thus, *in vitro* expansion is difficult and therefore only one sample from each donor was reliable for western blotting. Consequently, no statistical analysis could then be performed

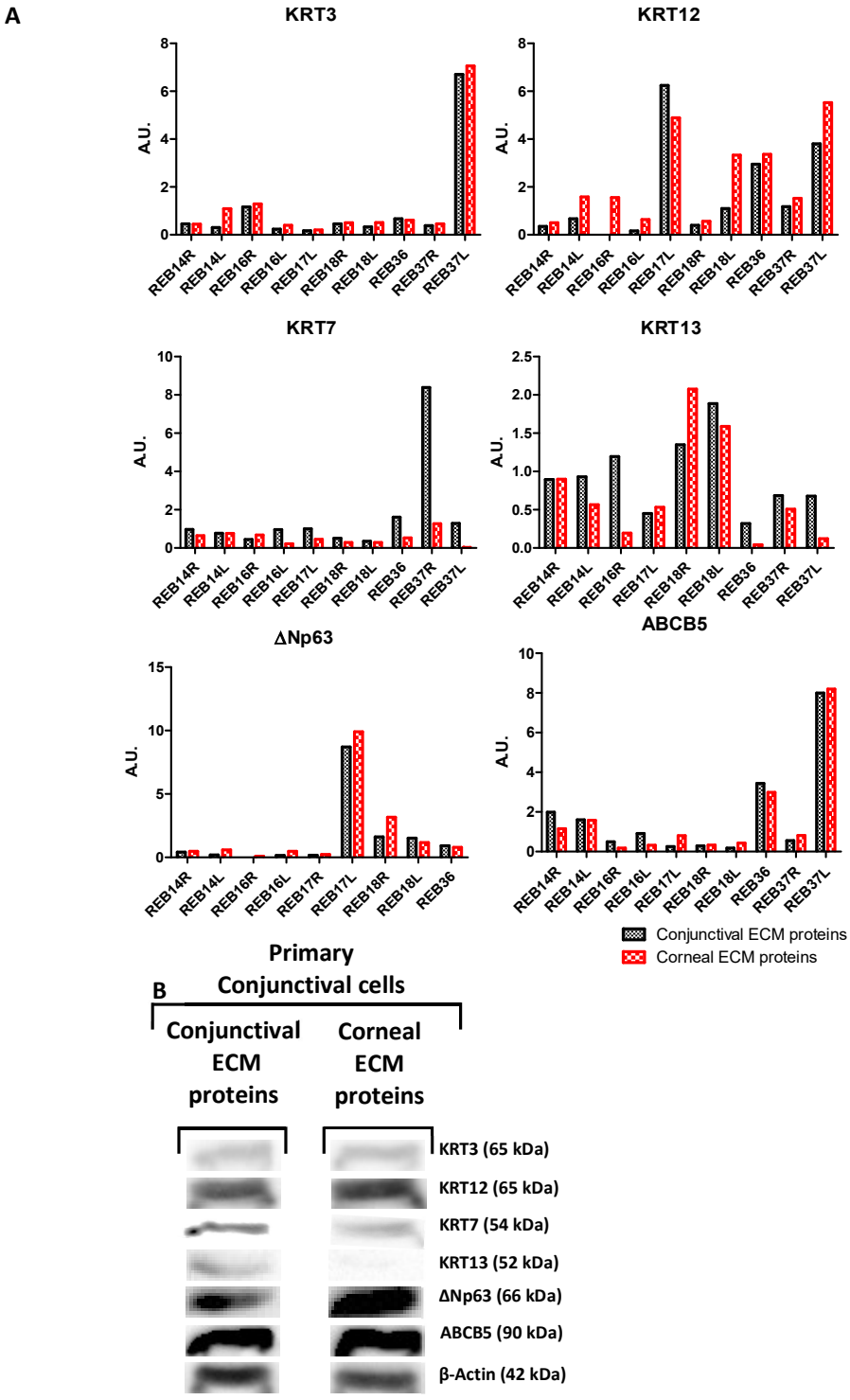

Figure 29 - The expression of epithelial cells markers by primary conjunctival epithelial cells when cultured on top of corneal ECM proteins compared with conjunctival ECM as assessed by Western Blot. (A) Bar graphs showing the densitometry quantification of each protein, normalised to the expression of β-actin. (B) Western blots representative of nine independent experiments. Abbreviations used A.U. arbitrary units, KRT: keratin, ABCB5: ATP-binding cassette sub-family B member 5, ECM: extracellular matrix.

2.3.6.3. Summary of results 3:

By culturing primary conjunctival ECs on top of deposited corneal ECM proteins and compared to conjunctival primary cells cultured on their own ECM proteins, there was a:

i. Higher expression of corneal EC markers.

ii. Lower expression of conjunctival EC markers.

iii. Higher expression of epithelial SC markers.

2.3.7. Conjunctival ECM proteins drive higher expression of conjunctival and stem cell epithelial markers by corneal primary cells than the corneal ECM

This next section addresses the results obtained by culturing primary corneal ECs obtained from four different donors (six eyes) cultured on conjunctival ECM proteins when compared to those obtained by primary corneal cells seeded on corneal ECM proteins.

2.3.7.1. Reverse Transcriptase qPCR

By seeding primary corneal ECs on conjunctival ECM proteins three outcomes arise:

i. Significantly lower levels of KRT3 expression were observed ($p \leq 0.01$, 4 out of 6 eyes). The expression of KRT12 was significantly lower ($p \leq 0.01$, 2 out of 6 eyes), Figure 30.

ii. Significantly higher values of KRT7 expression ($p \leq 0.01$, 2 out of 6 eyes) and of KRT13 expression values ($p \leq 0.05$, 6 out of 6 eyes) were also shown. Noteworthy, KRT13 expression was not detected for REB17R and REB20L corneal primary cells when seeded on their own ECM proteins. In addition, MUC5AC expression was higher in 2 out of 6 eyes ($p < 0.001$), Figure 30.

iii. The expression of ΔNp63 was only significantly higher in 1 out of 6 eyes ($p < 0.001$), this is accompanied by significant higher values in the expression of ABCB5 ($p \leq 0.05$, 4 out of 6 eyes). Moreover, no ABCB5 expression was detected for REB17R and REB20L primary corneal cells seeded on their own ECM proteins, Figure 30.

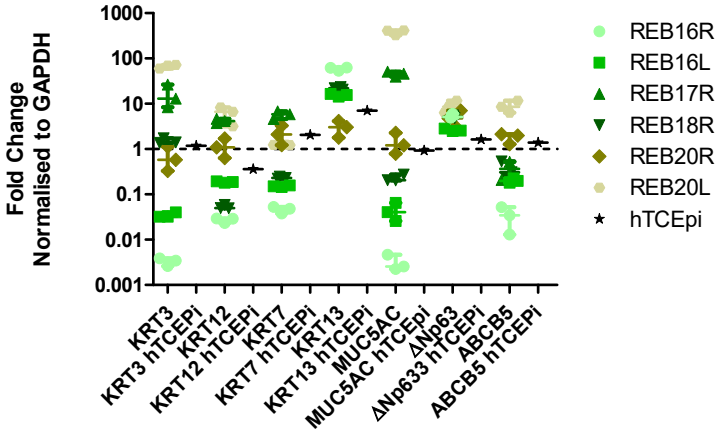

Figure 30 - The expression of epithelial cell markers by primary corneal cells when cultured on top of conjunctival ECM proteins compared with corneal ECM as assessed by Reverse Transcriptase qPCR. Data normalised to GAPDH levels. (Data is represented as median ± interquartile range, n≥12). Dashed line represents the basal expression of the markers of interests when cells are cultured on their own ECM proteins. Abbreviations used GAPDH: glyceraldehyde 3-phosphate dehydrogenase, KRT: keratin, ECM: extracellular matrix, ABCB5: ATP-binding cassette sub-family B member 5.

2.3.7.2. Western Blot

Primary corneal cells extracted from five donors (eight eyes) were cultured on top of conjunctival ECM proteins and their lysates compared against those extracted from primary corneal cells cultured on corneal ECM proteins. The results, consistent with transcript abundance data, showed:

i. Lower expression levels of KRT3 (6 out of 8 eyes) and KRT12 in all donors (8 out of 8 eyes), Figure 31.

ii. Higher expression of KRT7 and KRT13 (7 out of 8 eyes), Figure 31.

iii. Higher expression of ΔNp63 (4 out of 6 eyes) and ABCB5 (5 out of 8 eyes) when corneal primary cells were cultured on conjunctival ECM proteins, Figure 31

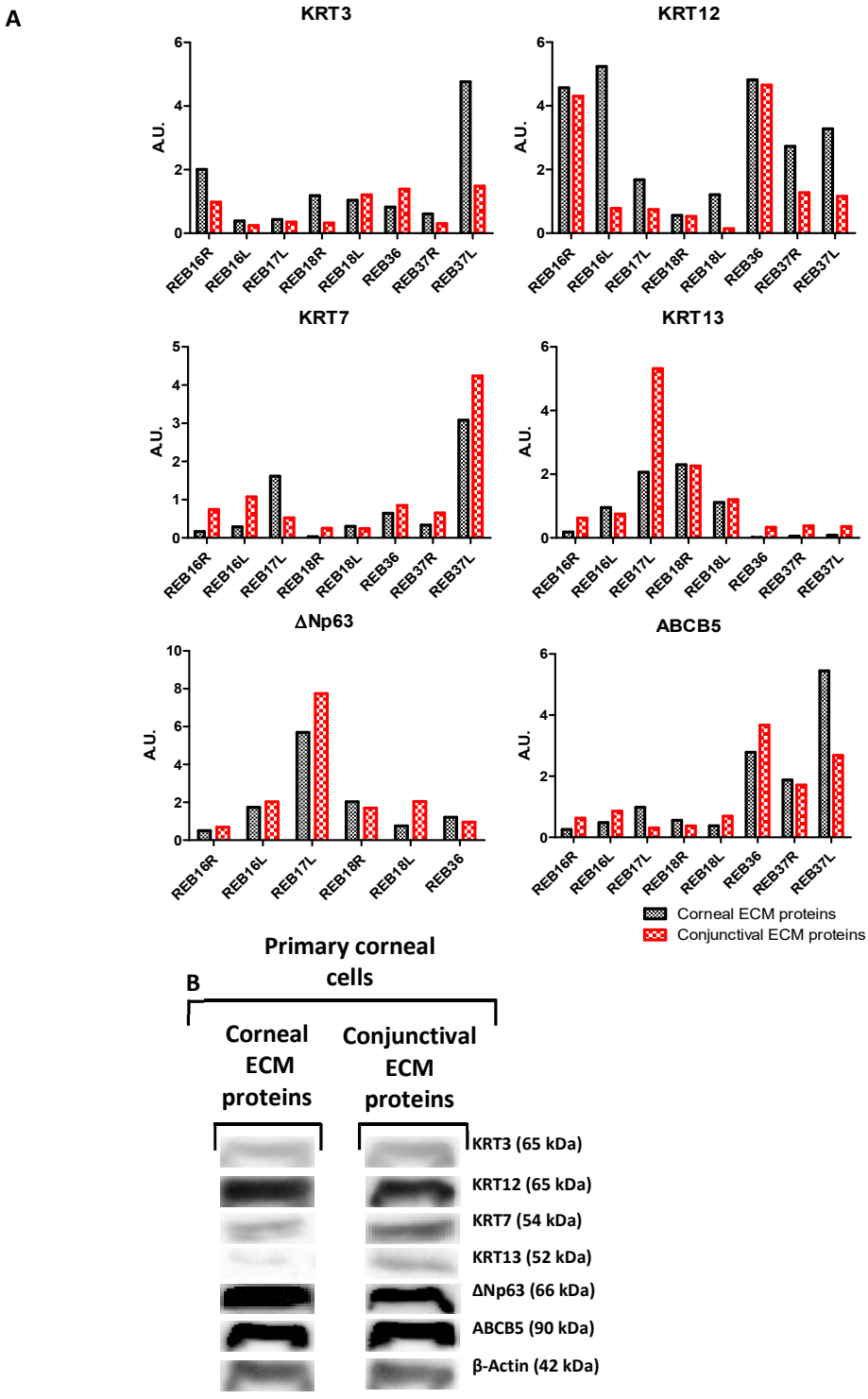

Figure 31 - The expression of epithelial cells markers by primary corneal epithelial cells when cultured on top of conjunctival ECM proteins compared with corneal ECM as assessed by Western Blot. (A) Bar graphs showing the densitometry quantification of each protein, normalised to the expression of β-actin. (B) Western blots representative of one independent experiments. Abbreviations used A.U. arbitrary units, KRT: keratin, ABCB5: ATP-binding cassette sub-family B member 5, ECM: extracellular matrix.

Yet again, no statistical analysis could here be performed because of the lack of cells necessary to run more than one reliable sample per donor.

2.3.7.3. Summary of results 4:

By culturing primary corneal ECs on top of deposited conjunctival ECM proteins and compared to corneal primary cells cultured on their own ECM proteins, there was a

i. Lower expression of corneal EC markers.

ii. Higher expression of conjunctival EC markers.

iii. Higher expression of epithelial SC markers.

2.3.8. The potential for cell differentiation of the "de-roofed" culture system was tested using other cell lines

To further understand the potential of the hereby developed system for cell differentiation two additional cell lines were tested: HaCaT and hESC cell lines.

2.3.8.1. HCjE-Gi ECM proteins drives higher expression of conjunctival epithelial markers by HaCaT cells than the HaCaT ECM

Since skin cells from the eye lids are in close contact with the conjunctival ECs, a process of conversion of skin cells into a conjunctival-like epithelium was tried based on modulation by the external environment. KRT1 and KRT10 are widely accepted as differentiation-specific markers for ECs lines from human skin (particularly HaCaT cell line) [291].

The layout of the experiments was the same as used in the foregoing sections: HaCaT and HCjE-Gi cells were separately grown for 9 days, submitted to the process of "de-roofing", and fresh cells cultured on the top of the deposited ECM proteins for 5 days.

2.3.8.1.1. Reverse Transcriptase qPCR

When HaCaT cells were cultured on top of conjunctival ECM proteins higher levels of KRT7 and KRT13 expression were observed (2.6- and 64-fold increase respectively, $p<0.01$). Interestingly, no KRT10 expression was found in such conditions (blue arrow) despite its expression to be found when HaCaT cells were cultured on their own ECM proteins, Figure 32.

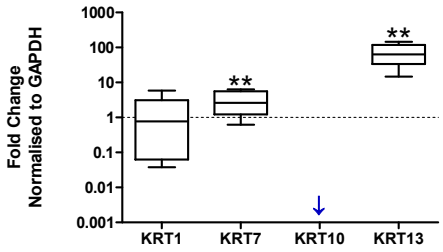

Figure 32 - The expression of a panel of keratin by HaCaT cells when cultured on top of HCjE-Gi ECM proteins compared with HaCaT ECM as assessed by Reverse Transcriptase qPCR. Data normalised to GAPDH. (Data is represented as median ± 5-95 percentile, n≥6, Mann-Whitney test *p<0.05, **p<0.01, ***p<0.001). Dashed line represents the basal expression of the markers of interests when cells are cultured on their own ECM proteins. Blue arrow denotes expression not detected. Abbreviations used GAPDH: glyceraldehyde 3-phosphate dehydrogenase, KRT: keratin, ECM: extracellular matrix.

2.3.8.1.2. Western Blot

Because KRT10 expression was not detected in Reverse Transcriptase qPCR, this marker was left out for western blotting. When HaCaT cells were cultured on HCjE-Gi ECM proteins, lower values of KRT1 expression and higher values of KRT13 expression were observed when compared to HaCaT cells cultured on their own ECM proteins ($p<0.05$ and $p<0.01$, respectively), Figure 33.

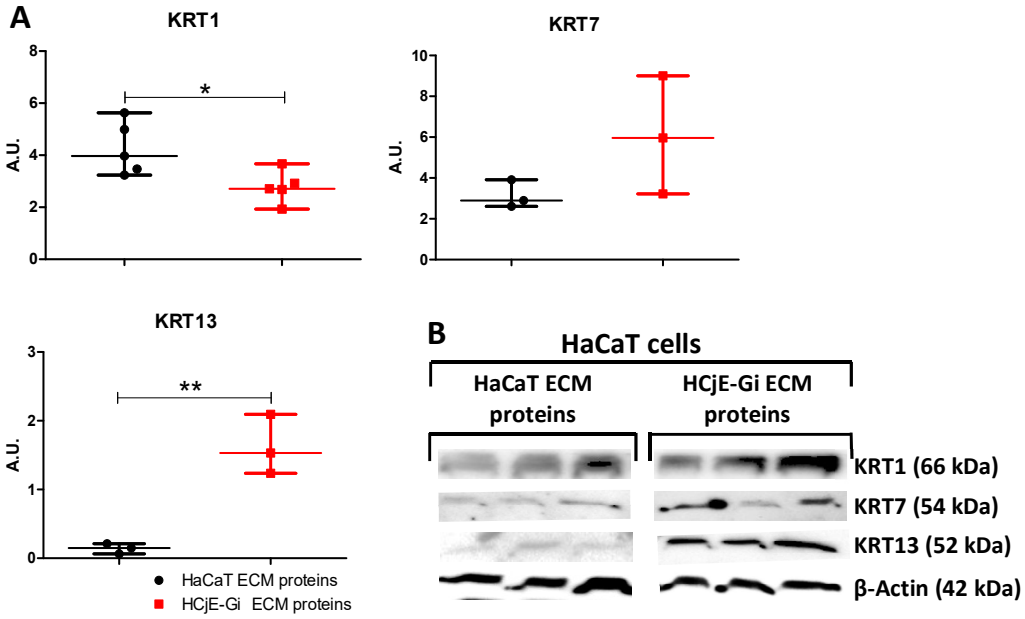

Figure 33 - The expression of a panel of keratins by HaCaT cells when cultured on top of HCjE-Gi ECM proteins as assessed by Western Blot. (A) Whiskers graphs showing the densitometry quantification of each protein, normalised to the expression of β-actin. (B) Western blots representative of three independent experiments. (Data is represented as median ± range, n≥3, Mann-Whitney test, *p<0.05, ** p<0.01, ***p<0.001). Abbreviations used A.U. arbitrary units, KRT: keratin, ECM: extracellular matrix.

2.3.8.1.3. Summary of results 5:

To summarize these results, by culturing HaCaT cells on HCjE-Gi ECM proteins and compared to HaCaT cells cultured on their own ECM proteins, there was a:

i. Higher expression of conjunctival EC markers.

ii. Lower expression of skin EC markers.

2.3.8.2. Differentiation of human embryonic stem cells towards conjunctival epithelial cells in response to specific ECM proteins

In the next section, the results obtained by culturing hESCs on ECM proteins produced and deposited by HCjE-Gi cells for 9 days will be addressed.

2.3.8.2.1. Culturing hESCs on ECM deposited by conjunctival cells drives the expression of conjunctival transcripts

The results in this section were obtained by comparing the expression of the genes of interest at a certain day of experiment against their expression at day 0 (RNA extracted from hESCs in suspension).

2.3.8.2.1.1. Stem cell marker expression

An up-regulation of ΔNp63 expression was only observed at day 1, 3, and 13 (nearly 10-fold increase, not statistically significant, NSS). An up-regulation of ABCB5 expression was seen at day 1 (2.8-fold increase, NSS) followed by a downregulation throughout the rest of the course of experiment (100 to 10-fold decrease, NSS). Moreover, the expression of undifferentiated hESCs markers, NANOG, SOX2, and OCT4 peaked at day 1 (9.6-, 2.6-, and 1.9-fold increase, respectively, NSS) and at day 9 (3.4-, 12-, and 6.8-fold increase, respectively, NSS). At day 3 a minimum in their expression levels was observed (lower than 10-fold decrease), Figure 34.

2.3.8.2.1.2. Corneal epithelial cell markers expression

A peak in expression of corneal epithelial marker KRT3 was observed at day 9 (9.7-fold increase, $p<0.05$ when compared to earlier time-points), while the expression of KRT12 was only detected in one sample at day 6 and day 9 (NSS), Figure 34.

2.3.8.2.1.3. Conjunctival epithelial cell markers expression

The expression of terminally differentiated conjunctival epithelial markers KRT7 and KRT13 peaked at day 9 (11- and 12-fold increase, respectively, NSS), Figure 34.

The results shown in this section were not statistically different of those obtained when RNA is extracted from hESCs in suspension (dashed line), however, a trend toward the differentiation, although incomplete, into epithelial-like cells is appreciated accompanied by a decrease in expression of epithelial and embryonic SC markers.

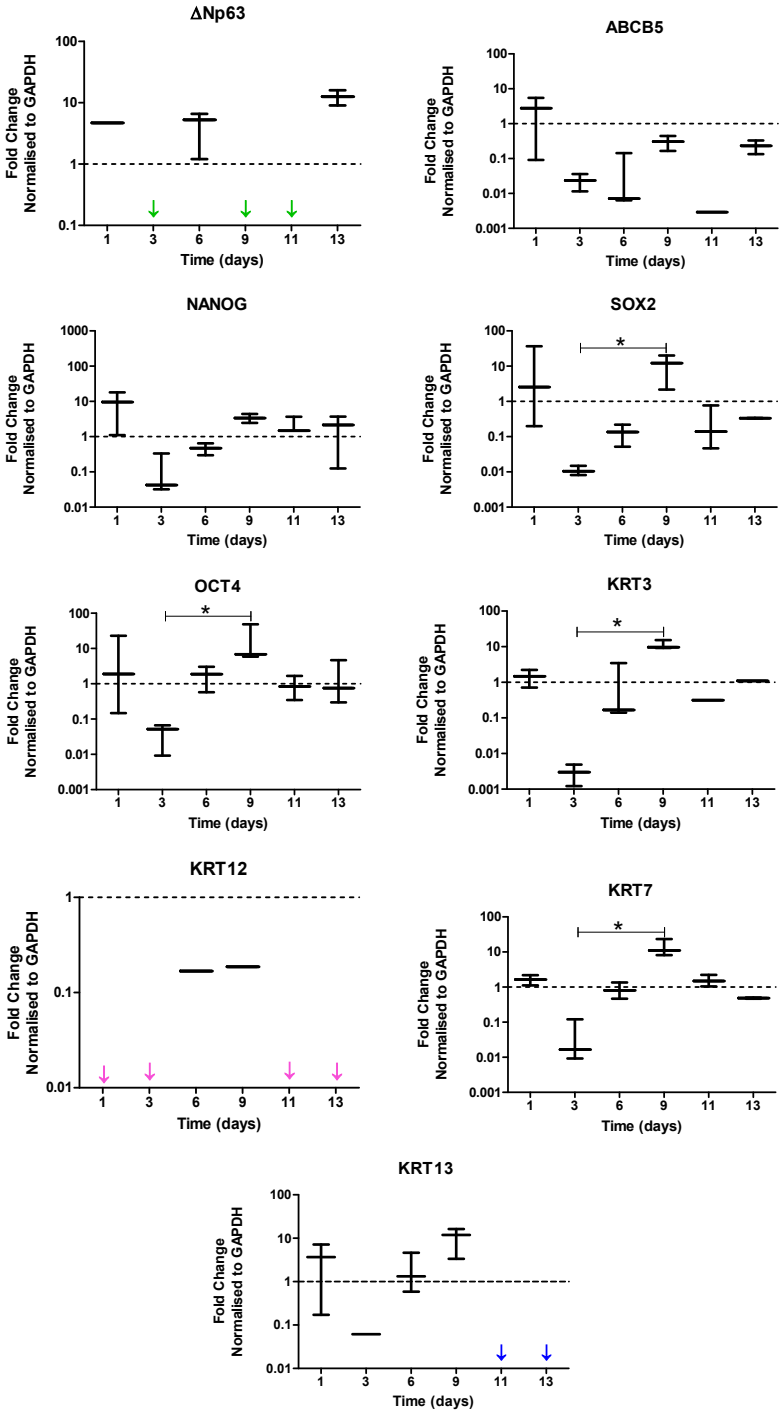

Figure 34 - The expression of epithelial and stem cell markers by human embryonic stem cells when cultured on top of HCjE-Gi ECM proteins compared with hESC ECM as assessed by Reverse Transcriptase qPCR. (Data is represented as median ± 5-95 percentile, n≥3, Kruskal-Wallis test followed by a Dunn's Multiple Comparison Test, Bonferroni corrected p-value, *p<0.05, **p<0.01, ***p<0.001). Dashed line represents the basal expression of the markers of interests at day 0. Arrows represent expression not detected. Abbreviations used GAPDH: glyceraldehyde 3-phosphate dehydrogenase, ABCB5: ATP-binding cassette sub-family B member 5, KRT: keratin, ECM: extracellular matrix.

2.3.8.3. Differentiation of human embryonic stem cells towards corneal epithelial cells in response to specific ECM proteins

In the next section, the results obtained by culturing hESCs on ECM proteins produced and deposited by hTCEpi cells for 9 days will be addressed.

2.3.8.3.1. Culturing hESCs on ECM deposited by corneal cells drives the expression of corneal transcripts

The results in this section were obtained by comparing the expression of the genes of interest at a certain day of experiment against their expression at day 0 (RNA extracted from hESCs in suspension).

2.3.8.3.1.1. Stem cell marker expression

Various peaks of ΔNp63 expression were observed throughout the course of the experiment (day 1 and day 6-9, NSS) with no expression being detected at day 3. A downregulation of ABCB5 to negligible values was seen throughout the whole course of experiment (0.0039- to 0.016-fold decrease, NSS). Moreover, the expression of undifferentiated hESC markers NANOG peaked at day 6-9 (13- 79-fold increase, respectively, NSS), SOX2 and OCT4 reached maximums of expression between day 6 and day 11 (NSS). Additionally, their expression showed minimums levels in the early time points (10-fold decrease, NSS), Figure 35.

2.3.8.3.1.2. Corneal epithelial cell markers expression

The expression of the differentiated corneal epithelial marker KRT3 peaked at day 9 (72-fold increase, NSS). Interestingly, no KRT12 expression was detected after day 1 (blue arrows), Figure 35.

2.3.8.3.1.3. Conjunctival epithelial cell markers expression

A peak in the expression of conjunctival epithelial marker KRT7 was observed at day 6-11 with little variations in its expression throughout the rest of the course of experiment (NSS), while the expression of KRT13 was only increased at day 6 (NSS), Figure 35.

The results shown in this section were not statistically different of those obtained when RNA was extracted from hESCs in suspension (dashed line), however, a trend towards the differentiation, although incomplete, into epithelial-like cells could be appreciated accompanied by a decrease in expression of epithelial SC markers.

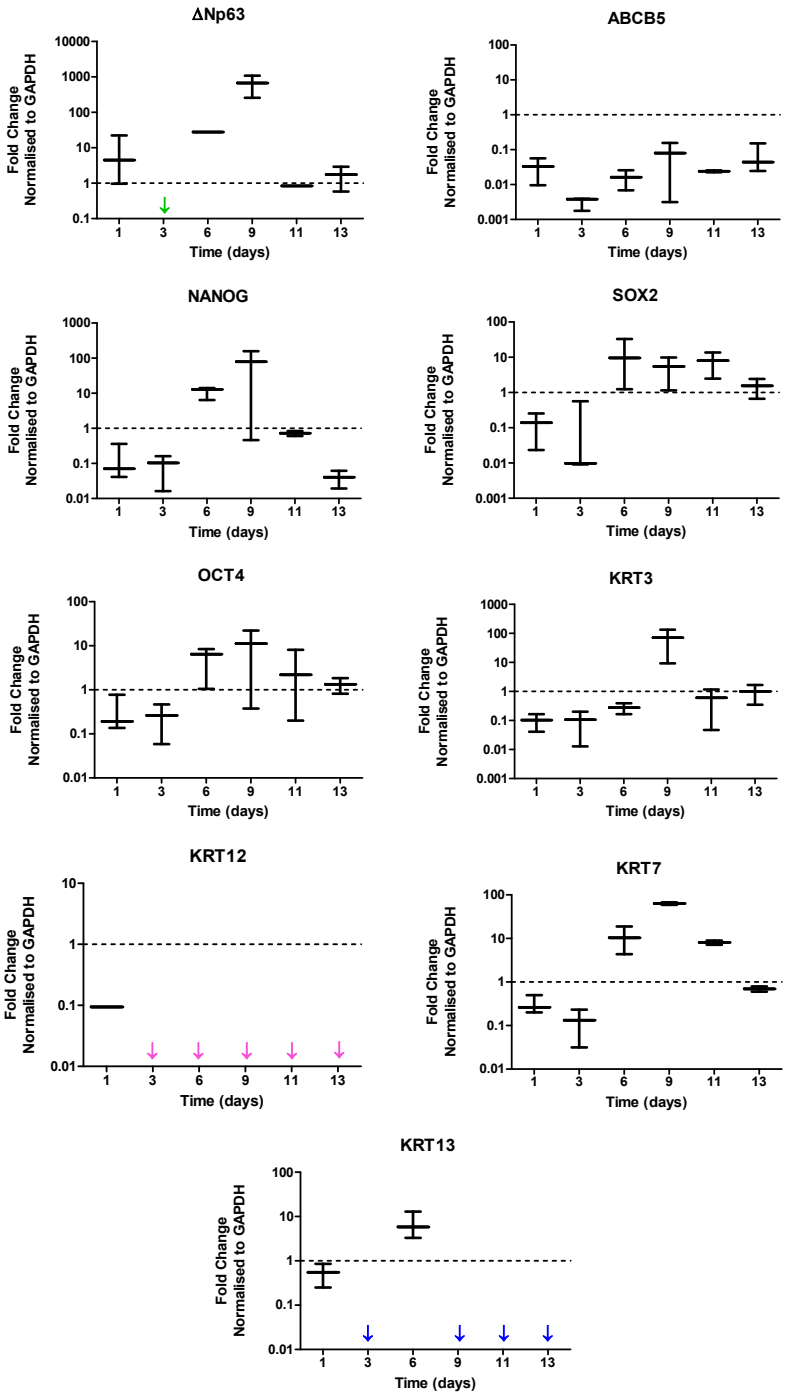

Figure 35 - The expression of epithelial and stem cell markers by human embryonic stem cells when cultured on top of hTCEpi ECM proteins compared with hESC ECM as assessed by Reverse Transcriptase qPCR. (Data is represented as median ± 5-95 percentile, n≥3, Kruskal-Wallis test followed by a Dunn's Multiple Comparison Test, Bonferroni corrected p-value, *p<0.05, **p<0.01, ***p<0.001). Dashed line represents the basal expression of the markers of interests at day 0. Arrows represent expression not detected. Abbreviations used GAPDH: glyceraldehyde 3-phosphate dehydrogenase, ABCB5: ATP-binding cassette sub-family B member 5, KRT: keratin, ECM: extracellular matrix.

2.3.9. Summary of results of Chapter 2:

To summarize these results, by culturing HCjE-Gi cells on top of hTCEpi ECM proteins and compared to HCjE-Gi cells cultured on their own ECM proteins:

i. The “de-roofed” culture system showed great potential in modulating the expression of several EC markers.

ii. HCjE-Gi cells cultured on top of hTCEpi ECM proteins were found to express corneal EC markers. Similar trends were observed when primary conjunctival cells were used.

iii. hTCEpi cells cultured on HCjE-Gi ECM proteins were found to express conjunctival EC markers. Similar trends were observed when primary corneal cells were used.

iv. The cell re-differentiation is preceded by a process of cell de-differentiation.

v. HaCaT cells cultured on HCjE-Gi ECM proteins were found to express conjunctival EC markers.

2.4 Discussion

Since ECs are closely associated with the connective tissue *in vivo,* others have suggested the possibility of ECM to be involved in specifying their pattern of keratin expression and phenotype [170], governing also cell migration [173] and differentiation [172, 174, 175, 253, 254]. The results outlined in this chapter highlight the role of ECM proteins for inducing the differentiation of ECs from the human ocular surface into a specific lineage, as assessed by various methods.

2.4.1. hTCEpi ECM proteins drive higher expression of corneal and stem cell epithelial markers by HCjE-Gi cells than the HCjE-Gi ECM

Reverse Transcriptase qPCR, total protein, and flow cytometry data show very consistent trends and results. Taken together the three data sets showed that when HCjE-Gi cells are cultured on hTCEpi proteins they show higher expression levels of corneal EC and epithelial SC markers (likely to indicate the emergence of early epithelial progenitor cells) and lower expression levels of conjunctival EC markers when compared to those obtained from HCjE-Gi cells cultured on HCjE-Gi ECM proteins. These data sets suggested that the HCjE-Gi cells, a conjunctival cell line, start to show corneal epithelial-like characteristics, losing their conjunctival epithelial phenotype in a process that involves an intermediate step of cell de-differentiation, an approach suggested by Kragl et al. in other organisms [204].

HCjE-Gi cells cultured on HCjE-Gi ECM proteins also expressed the 'specific' corneal epithelium-associated markers, although at lower levels when compared to those cultured on hTCEpi ECM proteins. Two different reasons help to explain these results. Firstly, the presence of ectopic clusters of KRT12-positive cells in human conjunctival tissue localized in the vicinity of SCs has been shown [292]. Secondly, KRT3 has also been shown to be expressed in bovine conjunctival epithelium *in vitro* but not *in vivo* [170]. These observations suggest that KRT3 may be antigenically masked *in vivo* and the detected expression may be a result of the KRT3 epitope "unmasking" in *in vitro* cultures, as seen in cells undergoing mitosis [293]. This would imply that KRT3 expression in conjunctiva is *in situ* inhibited by some sort of exogeneous factor and upon culture this exogenous factor is somehow lost. The source of this "negative" factor could be the vast blood vessel system present in the conjunctiva *in vivo*, which is absent in the cornea. However, the possibility that there may be an induction of KRT3 production *in vitro* by HCjE-Gi cells should not be ruled out.

The residual expression of conjunctival markers KRT7 and KRT13 by HCjE-Gi cells cultured on hTCEpi ECM proteins suggested that, although the major differentiating lineage is that of

corneal epithelium, it may not be the only one, with other epithelial lineages likely to be formed. Other explanation for this arises from the notion that proliferation and differentiation are not mutually exclusive processes, i.e. the expression of a new gene product is not necessarily linked to functional irreversibility [64]. Suggesting that whilst some conjunctival cells are differentiating towards the corneal epithelial-like lineage, a pool of conjunctival cells may still be proliferating, exhibiting the conjunctival-like characteristics.

Interestingly, Mackay et al. have compared the production of KRTs by cells seeded on Matrigel and on "de-roofed" matrices [294]. They have shown that cells seeded on Matrigel lack the production of several cytokeratins relative to the large amounts found on the "de-roofed" systems. These observations suggest that the structural integrity, subtle biochemical features of the intact BM, and other growth factors produced by cells and trapped within the BM (see mass spectrometry results on Chapter 3) are of crucial importance to trigger cell differentiation. In this regard, the hereby study overcomes this issue since the ECM is produced by the specific cell type that populates each structure of the ocular surface, maintaining its structural integrity and the inherent pool of soluble factors trapped within the ECM proteins. Taken together, the structural and the biochemical cues provided by the ECM show to be important trigger signals to induce cell differentiation. Supporting this idea are the studies from Kurpakus et al. [170] and Moyer et al. [251], who showed that conjunctival cells cultured on intact corneal BM express KRT12 [170] and, on the other hand, cultures lacking an intact corneal BM failed to trigger KRT12 expression [170, 251].

Specific components of the BM, such as several laminin isoforms or collagen types, have been used to trigger the expression of KRT12 by conjunctival ECs with no success [295]. Others have also showed that conjunctival cells in organotypic cultures failed to express KRT12 when they are subjected to air-liquid interphase, a method to promote KRT12 expression by corneal ECs [296].

2.4.2. HCjE-Gi ECM proteins drive higher expression of conjunctival and stem cell epithelial markers by hTCEpi cells than the hTCEpi ECM

Taken together the Reverse Transcriptase qPCR, Western blot, and flow cytometry data show that hTCEpi cells cultured on HCjE-Gi ECM express higher levels of conjunctival and SCs epithelial markers and lower levels of corneal epithelial markers when compared to those cultured on hTCEpi ECM proteins. These results suggested that the hTCEpi cells, a corneal cell line, show conjunctival epithelial-like characteristics, losing its corneal epithelial phenotype in a process that involves an intermediate step of cell de-differentiation.

Conversely, these are the equivalent opposite results of those obtained by HCjE-Gi cells, suggesting that the cell plasticity can be modulated in both ways when cells are given the appropriate extracellular cues.

The results obtained using cell lines as models were further confirmed using primary cells. Very similar trends were found, however, with greater variability, intrinsic to the utilization of primary (non-immortalized) cells. The variability of results can be consequence of several aspects including differences on post-mortem time of retrieval and other donor-to-donor variances (age, lifestyle, etc). However, primary cells retain normal cellular functions, signalling and genetic integrity, and are not genetically modified in any way beyond natural exposure to environmental insults typically encountered during the lifespan of the organism from which they were isolated. When compared, the results obtained by primary and cell lines showed an interesting trend. With exception of KRT3 (Figure 28) and ΔNp63 (Figure 30), the expression of all markers by the two cell lines showed to be close to an average value of the widespread values obtained by primary cells. This suggests that the used cells lines have a similar "average" behaviour when compared to the primary cells from the tissues that they were extracted from.

Previous experiments have led to the suggestion that cells, upon injury, dedifferentiate not into a complete pluripotent state but rather to restricted progenitor cells [204]. Accordingly, Tata et al. have shown the de-differentiation of committed airway luminal secretory cells into stable and functional SCs *in vivo* [297]. Garcia-Arraras et al. have also shown a process of dedifferentiation of ECs to mesenchymal phenotypes during intestinal regeneration [298]. Similar to those observations, the studies in this thesis suggested that the process of re-differentation may be preceded by an intermediate state of dedifferentiation as an increase in expression of putative epithelial SC markers was observed. However, the dedifferentiation and/or cell division are not obligatory processes in the conversion from one cell type into another [212].

The mechanisms involved in tissue-type cell differentation requires differential signal transduction from the ECM to the overlying cell layers [299, 300]. Proteins from the integrin family (reviewed in section 3.1.4) are the main candidates for the transduction of such signals [301, 302]. $\alpha_6\beta_4$ and $\alpha_3\beta_1$ integrins are two of the most common dimmers located along the region where ECs contact the BM [303]. Studies using conjunctival ECs have shown that by blocking β1 integrin chain, the focal adhesion kinase tyrosine (a protein involved in cell

adhesion) is phosphorylated, i.e. activated. The same results were not obtained when β4 integrin chain was blocked, suggesting that different integrins have different effects on cell adhesion [304]. The same studies have also shown that the EC adhesion to different laminins isoforms activate different intracellular signalling pathways [304], suggesting that different ECM proteins activate different signalling pathways, which can modulate EC differentiation via alternate signalling pathways.

The methods shown in this chapter open a new door for the possibility of promoting EC differentiation in *in vitro* culture models based on the cross-talk cell-ECM. The approach here applied showed that conjunctival ECs cultured *in vitro* can be triggered to express KRT3 and KRT12, although with no need for the presence of some sort of exogenous factor to trigger their expression as seen in *in vivo* systems [293].

2.4.3. HCjE-Gi ECM proteins drive higher expression of conjunctival markers by HaCaT cells than the HaCaT ECM

To further corroborate the ECM-driven differentiation, HaCaT cells were cultured on ECM proteins deposited by HCjE-Gi cells and the extent of differentiation assessed using specific markers for each epithelial population. Reverse Transcriptase qPCR and Western blot results confirmed this hypothesis. Both data sets showed a decrease in expression of skin epithelial markers KRT1 and KRT10 and a significant increase in expression of conjunctival markers KRT7 and KRT13 when HaCaT cells were cultured on HCjE-Gi ECM. These results suggest a differentiation toward the conjunctival epithelial-like lineage accompanied by a loss in skin epithelial-like features. Others have, however, showed that HaCaT cells express KRT13 [305] and low levels of KRT7 [306]. In the opposite direction, Wild et al. have yet shown that KRT1 and KRT10 may be expressed in conjunctival epithelium in result of focal inflammatory responses to environmental stresses [307].

These results showed that regardless the origin of the differentiated cells they can be induced to differentiate towards the lineage of cells that deposited the ECM proteins.

2.4.4. Potential of differentiating human epithelial cells towards a desired cell lineage

The studies in this chapter describe a new approach for the differentiation of ECs in response to the ECM composition and morphogenic cues in *in vitro* systems. This provides a further step towards refinement of protocols to produce techniques with potential therapeutic purposes. Several improvements need to be carried out:

i. **Functional studies to prove** functionality of the differentiated cells need to be carried out to prove that the differentiated cells can function as the target cell type.

ii. **Full differentiation** of the differentiating cells to prevent the risk of transplantation of early progenitor ECs that may led to the formation of tumours so that, either the process of differentiation must be refined or the cells expressing these markers selectively purified.

iii. **Double labelling of cells** for KRT3/12 plus KRT7/KRT13 to assess if the same differentiating cell express both corneal and conjunctival markers. Additionally, double labelling for corneal or conjunctival markers plus putative epithelial SC markers would unveil the percentage of dedifferentiating cells.

To conclude, two factors have been suggested to modulate the expression of corneal markers by conjunctival cells: (1) the morphological cues of the cornea BM and (2) and an exogenous factor that can trigger the expression of corneal epithelial markers when not in conjunctival environments. The hereby studies agreed with both these hypotheses, raising an approach suitable for cell culture and differentiation.

2.4.5. Specific ECM proteins promote the partial differentation of human embryonic stem cells

2.4.5.1. Expression of conjunctival epithelial associated markers by human embryonic stem cells

The studies outlined in this section highlight the importance of the HCjE-Gi ECM composition for inducing the differentiation of hESCs into conjunctival epithelial-like lineage. This was partially achieved by replicating the environment present in human conjunctival epithelium within the *in vitro* system by "de-roofing" the cell cultures and leaving the conjunctival-associated ECM proteins attached to the cultureware. The experiments suggested that the culture of hESCs on conjunctival ECM proteins results in an incomplete differentiation of these cells into conjunctival epithelial-like cells as assessed by Reverse Transcriptase qPCR. The observed peak in ΔNp63 and ABCB5 expression at earlier time-points (day 1 and day 1-3, respectively), however not statistically different, is likely to indicate the emergence of early epithelial progenitor cells. This is accompanied by a downregulation in expression of undifferentiated hESCs markers NANOG, SOX2, and OCT4. Additionally, the expression of OCT4 decreased to values less than 2-fold decrease (NSS) suggested a differentiation of hESCs into trophectoderm lineage [282]. This was also followed by the appearance of

terminally differentiated conjunctival EC markers KRT7 and KRT13 at day 9 (NSS). Additionally, the expression of KRT3 (a marker for terminally differentiated corneal ECs) was an indication of an ESC incomplete differentiation towards the conjunctival epithelial-like lineage. The non-significance of results may be result of the small number of reliable samples used (n=3), therefore a larger number of samples and protein data (Western blotting and/or flow cytometry) are of the upmost need. The mass spectrometry results, addressed in Chapter 3, showed a specific ECM composition for each cell line herein used. The specificity in composition is not only shown at protein but also at soluble factors levels, the latter produced by cells and trapped within the protein meshwork. The morphogenic cues provided by such composition may trigger the process of hESC differentiation, which has long been associated with interactions with external cues [178, 179, 308], in response to the mimicked conjunctival environment. In accordance with these observations, Wang et al. have yet suggested that the *in vitro* strategies for the differentiation of ESC toward the derivatives of all three germ layers are a recapitulation of biochemical cues present during embryogenesis [309].

2.4.5.2. Specific ECM proteins promote the expression of corneal epithelial associated markers by human embryonic stem cells

The studies outlined in this chapter highlighted the importance of the corneal ECM composition for inducing the differentiation of hESCs into corneal epithelial-like lineage. This was partially achieved by replicating the environment present in human corneal epithelium within the *in vitro* culture system. The observed peak in ΔNp63 and ABCB5 expression at earlier time-points (day 1 and day 1-3, respectively) is likely to indicate the emergence of early epithelial progenitor cells. This is accompanied by a downregulation in expression of undifferentiated hESCs markers NANOG, SOX2 and OCT4 at day 6 suggesting an early differentiation, however, the expression of these markers is shown to be upregulated at later time-points. This was accompanied by the expression of the terminally differentiated corneal EC marker KRT3 and markers for other epithelial lineages (KRT7 and KRT13). Based on this data it appears that differentiation towards an epithelial-like lineage is occurring in response to the mimicked human corneal environment. Yet again the non-significance of results may be result of the little number of samples used (n=3), and therefore a larger number of samples and protein data are of the upmost need to confirm this data.

2.4.5.3. Differences exist between the potential of the two ECM proteins meshwork used herein for the hESC differentiation

When the potential of the two decellularized ECM meshwork are compared, some differences in the magnitude of the fold changes are observed, despite the similar trends that were seen on gene expression profiling. Firstly, HCjE-Gi ECM appeared to promote a higher expression of ABCB5 by hESCs when compared to hTCEpi ECM suggesting an increased emergence of epithelial progenitor cells in the first condition. Secondly, the expression of undifferentiated ESC markers NANOG, SOX2, and OCT4 is higher at later time-points in hTCEpi ECM when compared to HCjE-Gi ECM, indicative of cells in less differentiated states. Thirdly, the expression of terminally differentiated ECs markers was lower in hTCEpi ECM, indicative of lower epithelial lineage commitment. The results in Chapter 3 showed a higher expression of laminin α5 by hTCEpi cells, as seen by the higher amount of protein detected in flow cytometry and ICC data and higher values of fold increase observed in Reverse Transcriptase qPCR data. Recent evidence has shown that this laminin isoform alone is sufficient to maintain the undifferentiated state and the pluripotency of ESC [310-313]. Taken together, these observations suggest a less differentiated state of hESCs and less commitment toward a differentiated epithelial-like lineage when cultured in hTCEpi ECM proteins possibly due to the higher amount of laminin α5 present in that condition. Further evaluation should then be performed in that regard.

2.4.5.4. Potential of differentiating human embryonic stem cells towards a desired cell lineage

The studies in this chapter assessed for the first time the differentiation of hESCs toward conjunctival and corneal epithelial-like lineages in response to the whole set of ECM proteins produced by two different EC lines – HCjE-Gi and hTCEpi. The non-significance of results and the expression of various hESC markers at later time-points may suggest that the ECM alone is not sufficient for hESCs differentiation toward the desired lineages. However, the combination with other external cues, such as conditioned medium and/or exosomes collected from differentiated conjunctival or corneal culture systems, may promote such process as shown by others with various degrees of success. These include, surface coating with collagen IV and use of limbal fibroblast medium [178], surface coating with laminin-332 [179], and co-culture of murine ESC with conjunctival ECs using transwell techniques [314]. Further improvements need to be carried out to fully characterize the technique hereby used, as follows:

i. **Studies at protein expression levels.** The transcript expression data need to be corroborated at protein expression levels (Western blot and/or flow cytometry).

ii. **Complete differentiation.** hESCs need to be fully differentiated toward the desired lineage, as the expression of some markers, such as KRT3 by hESCs cultured in HCjE-Gi ECM proteins, KRT7 and KRT13 by hESCs cultured in hTCEpi ECM are indicatives of incomplete differentiation.

iii. **Functional studies.** The differentiated hESCs need to the proven functional in the same way as the targeted lineage.

iv. **Expression of hESCs markers.** Some cells still expressed some of the undifferentiated hESCs markers. This can result in teratoma formation upon transplantation and therefore further purification and/or fully differentiation steps need to be carried out to eliminate this risk.

v. **Allogeneic source.** The differentiated cells, being of an allogeneic source, remain immunogenic and will require the use of potent immunosuppression drugs [315].

Chapter 3

Differences exist in the response of conjunctival and corneal epithelial cells to extracellular matrix proteins

3.1. Introduction

The ECM is a crucial part of the extracellular microenvironment, providing signalling cues to regulate many aspects of cellular behaviour. These include cell migration, adhesion, morphology, and differentiation [316-323]. The ECM is composed of a complex meshwork of several collagen types, proteoglycans, laminins isoforms and many other proteins produced within the cells and eventually released to the extracellular environment via exocytosis [324]. Broadly, the ECM includes the interstitial matrix, which constitutes the intercellular spaces, and the BM, where the cells rest promoting cell polarity. *In vivo* all cells are in close contact with the surrounding ECM, however striking spatial differences exist in the way different cell types interact with their ECM. While most cells are surrounded by their ECM, ECs only contact their matrix at the basal side with no contact at their apical side.

3.1.1. Cell-ECM interactions

Cell-ECM interactions are essential for many biological processes, including tissue development and repair, homeostasis, and response to injury [299]. The cell surface possesses two different groups of receptors that primarily mediate the interactions with the ECM: non-integrin and integrin receptors [325]. Non-integrin receptors include the syndecan family that may bind to collagens, fibronectin, thrombospondin, and bFGF [326]. Integrin-based adhesive complexes include focal adhesions, which link the ECM (via fibronectin adhesion motives) to the actin cytoskeleton within the cell, and hemidesmosomes, that connect the ECM to intermediate filaments, such as keratins. The integrins are responsible for passing information about the chemical and mechanical composition of the ECM into the cell [327]. Downstream to ECM-integrin binding, several processes may be activated, these include clustering of the receptors, activation of intracellular protein kinases, phosphorylation of cytoskeleton and other associated proteins, and transmission of the signal generated by receptor occupancy to the transcriptional machinery in the nucleus [328]. In addition to providing instructive signals through direct ligand interactions, the ECM can signal in a more indirect approach by sequestering different types of growth factors and cytokines, acting as a local reservoir releasing its contents in response to changes in

physiological conditions [329-331]. These molecules can activate classic signal-transduction pathways that induce cell growth, proliferation, and gene expression [327, 332, 333] but also regulate the transcription, translation, and post-translational modifications of ECM macromolecules [334]. The binding of growth factors to the ECM is mainly regulated by the side chains of glycosaminoglycans [335]. An extensive review of association of growth factors with ECM proteins can be found at Adams and Watt [299].

HDs are integrin-mediated adhesion complexes mainly found on the basal surface of specialized ECs, such as the intestine and skin [336]. They are responsible for firmly anchoring the ECs to the underlying BM, therefore increasing the overall rigidity of epithelial tissues. The cytoplasmic side of a HDs is composed of a plaque of adapter proteins attached to the end of a keratin filament [327, 337], Figure 36. Two types of HDs can be distinguished: type I present in the cornea and other epithelial tissues [4, 338] and type II present in intestinal epithelia [337]. The type I HDs correspond to the typical and conventional type of HDs, they are composed of 5 components (early named HD1-HD5): plectin, BP230, β4 integrin, collagen XVII, and α6 integrin, respectively. Type II HDs are negative for BP230 and collagen XVII and there is no direct evidence that type II HDs are involved in cell adhesion.

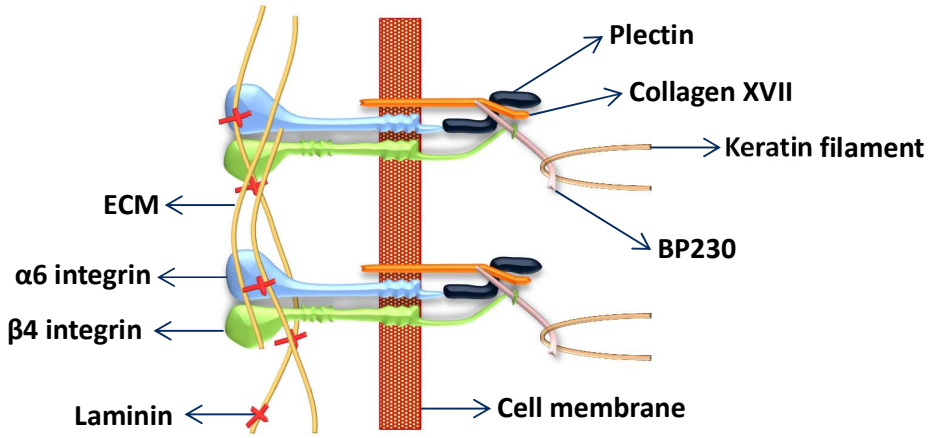

Figure 36 – Model for hemidesmosomes assembly. The association of the α6β4 integrin with the plectin plaque is essential for the formation of type II hemidesmosomes. When collagen XVII is present, it is incorporated into this complex through interactions with integrin and plectin. This is followed by the recruitment of additional plectin-collagen XVII complexes, resulting in further increase of size and stability of hemidesmosomes. The final step comprises the incorporation of BP230, and the hemidesmosomes containing α6β4 integrin, collagen XVII and plectin are turned into type I hemidesmosomes. Plectin and BP230 interact in the same site on collagen XVII, and it is likely they compete for this binding site. Abbreviations used ECM: extracellular matrix. Adapted from [3, 4].

3.1.2. ECM composition

The ECM is composed of two biochemically and morphologically separate structures, the interstitial matrix and the BM [339, 340]. The interstitial matrix is mainly composed of proteoglycans, mostly chondroitin sulphate and heparan sulphate [341], fibronectin [342], elastin, and collagens types I, III, V, VI, VII, and XII [339]. BM is a sheet-like deposition located at the interface between the ECs and the connective tissue. Its composition is tissue-specific and varies with the state of differentiation and development [343, 344]. Broadly, it contains collagen type IV [340, 345], a wide variety of laminin isoforms [340], and heparan sulphate [346]. Some ECM constituents help to protect cells against compression and shear forces, whilst others regulate several cell functions [179, 347, 348]. As the proteoglycans are negatively charged they attract the positively charged ions which in turn attract water molecules via osmosis, keeping the cells hydrated [349]. Elastin, as the name suggests, gives elasticity to the tissues [350]. Collagens are by far the most abundant component of ECM, around 90% of ECM is composed by those. They are present as fibrillary proteins giving structural support to the resident cells [347]. Heparan sulphate binds to variety of protein ligands and regulates several biological processes, such as development and angiogenesis [347, 348].

3.1.2.1. Basement membrane – cornea versus limbus

The corneal and limbal BMs are mainly composed of type IV collagen and laminins (the most abundant non-collageneous glycoproteins in the BM). Immunohistochemistry studies have shown a corneal BM mainly composed of collagen type IV α3, α4, α5, and α6 chains, and laminin α1, α3, α5, β1, β3, γ1, and γ2 chains. Moreover, the limbal BM contain additional collagen type IV α1 and α2 chains, and laminin α2 and β2 chains, but no collagen IV α3 and α4 chains. More importantly, limbal BM shows unique features, such as an increased expression of laminin α1, α2, β1 chains and a specific expression of laminin γ3, BM40/SPARC (which function as a modulator of cellular interactions with the ECM), and tenascin-C (a glycoprotein regulator of cell-matrix interactions), when compared to both corneal and conjunctival BM [46].

3.1.2.2. Basement membrane – limbus versus conjunctiva

Type IV collagen is also the major structural component of the conjunctival BM. The main differences on collagen composition arise from higher amounts of α5 and α6 chain of collagen IV and collagen type XVI in limbus BM when compared to conjunctiva BM [46]. Regarding the laminin composition, the main differences are the presence of laminin α1

chain in limbus but not in the conjunctiva, and the higher expression of laminin α2 chain and laminin β1 chain in the limbus BM. Laminin γ3 chain is shown at the anterior limbal zone and is confined to the base of the epithelial rete ridges in the posterior limbal region and to few isolated locations in the anterior conjunctiva. Studies by Schlötzer-Schrehardt et al. suggested the laminin-211 and laminin-213 as the most specific laminins for the limbal BM [46]. Clusterin (a glycoprotein that protects cell membrane and stabilizes cell-matrix interactions) was found at higher intensities in conjunctiva, with decreasing intensities in posterior limbus, being absent in the anterior limbus. Thrombospondin-4 showed an augmented labelling intensity in the posterior conjunctiva, when compared with the limbus and the anterior conjunctiva [46].

Besides these differences, there are features shared by the limbus and the conjunctiva BM, such as the pattern of collagen distribution (type IV chain α1, α2, α3, and α4 and type V, VI, and VII), the intensity of several glycoproteins, such as laminin-111, -322, α3, α5 chain, β2, β3, and γ2 chain, and thrombospondin -1. Regarding their composition in proteoglycans, the expression of type XV and XVIII collagen is also similar in both BMs [46]. Additionally, perlecan (the major BM heparin sulphate proteoglycan), fibronectin, nidogen-1 and -2 (glycoproteins with crucial roles in BM assembly by connecting collagen IV and laminin networks), and type VII collagen are found throughout the whole ocular surface BM [29, 351, 352]. A complete list of BM protein expression profile can be found in Table 11.

Table 11 - Localization of basement membrane components across the ocular surface. Abbreviations used: – no expression; -/+ weak expression; + moderate expression; ++ strong expression; BM: basement membrane. LAM: laminin. Adapted from [46].

BM component	Central cornea	Peripheral cornea	Anterior limbus	Posterior limbus	Conjunctiva
Collagens					
Collagen IV	+	+	+	+	+
Collagen IV α1 chain	-	-	+ or ++	+ or ++	+ or ++
Collagen IV α2 chain	-/+	-/+	++	++	++
Collagen IV α3 chain	+ or ++	+	-	-	- or -/+
Collagen IV α4 chain	- or -/+	- or -/+	-	-	- or -/+
Collagen IV α5 chain	++	++	++	++	++→+→-/+
Collagen IV α6 chain	++	++	++	++	+→-/+→-
Collagen V	+	+	-	-	-
Collagen VI	-	-	-	-	-
Collagen VII	++	++	++	++	++
Collagen XVI	-	+ (sub BM)	++ (sub BM)	-	-
Collagen XVII	+	+	+	+(gaps)	+
Glycoproteins					
LAM-111	+	+	+	+	+
LAM-332	++	++	++	++	++
LAMα1 chain	- or -/+	+	+	+	-
LAMα2 chain	-	- or -/+	+	++	+
LAMα3 chain	+	+	+	+	+
LAMα4 chain	- or -/+	- or -/+	-	-	-
LAMα5 chain	- or -/+	-/+ or +	+	+	+
LAMβ1 chain	-/+ or +	-/+ or +	++	++	+
LAMβ2 chain	-	-	+	+	+
LAMβ3 chain	+	+	+	+	+
LAMγ1 chain	-/+ or +	+	++	++	++
LAMγ2 chain	++	++	++	++	++
LAMγ3 chain	-	-	+	++ (focal)	+ (focal) or -
Fibronectin	+	+	++	++	+
Nidogen-1	+	+	++	++	++
Nidogen-2	-/+	+	++	++	++
Clusterin	+	++	-	+	++
Thrombospondin-1	+	+	-	-	-
Thrombospondin-4	-	+ (focal)	+ (focal)	+ (focal)	+ (focal)
Proteoglycans					
Perlecan	++	++	++	++	++
Collagen XV	+	+	+	+	+
Collagen XVIII	++	++	++	++	++

3.1.3. Laminins

Laminins are heterotrimeric molecules composed of one α, one β, and one γ chain, each derived from a different gene, which assemble into a disulphide-bonded heterotrimer with a cross-shaped structure [353]. The laminins have a central α chain (approximately 400KDa) with a varying number of globular regions and a β and γ chains (approximatively 200KDa)

with α-helical and globular regions. In higher organisms, 5α (*LAMA1–5*), 3β (*LAMB1–3*), and 3γ (*LAMC1–3*) chains have been identified [353]. Restrictions in the interaction potential and distribution patterns allow only 16 different laminins combinations to be found *in vivo*, despite the 51-possible different αβγ trimers combinations [353]. These proteins are named according to their chain composition, as follows: laminin-521 consists of a α5, β2 and γ1 chains [353]. Laminin trimers assemble and undergo glycosylation intracellularly, prior to secretion as intact heterotrimers into the ECM [354, 355]. Once secreted, higher order structures are formed, and some are proteolytically processed [356, 357], enabling interaction with other proteins. Cells interact with laminins through integrins forming complexes that mediate numerous cell functions, including embryonic development, cell migration, proliferation and differentiation, and BM assembly [299, 358]. The glutamic acid residue in the C-terminal region of the γ chain and the three globular modules in the α chain are necessary for binding to integrins [359]. Furthermore, the C-terminal region of the β chain possesses a short amino acid sequence to enhance laminin-integrin affinity [360].

Laminin γ1 chain is the widest expressed laminin subunit, being present in 10 out 16 known laminin isoforms [361, 362]. Laminin isoforms containing α1 and α3 chains are predominantly found in epithelia, whereas α2- and α4-containing laminins are mainly found in mesenchymal tissues. Additionally, laminins containing α5 chain are expressed in both epithelial and mesenchymal cells [361, 363, 364]. Within the cornea the most abundant laminin trimer is the laminin -332 with smaller amounts of laminin-111, laminin-311, and laminin-511 also being present [351, 352, 365, 366]. The conjunctival BM also contains the laminin-332 and laminin-111 [351, 352] but differs from the corneal BM by the expression of the α2- and β2-containing laminins, including laminin-211, laminin-221, and laminin-521 [46, 304].

Based on observations that laminin-511 contacts the inner cell mass of blastocysts in mice [367], this isoform has been used as substrates to enable mouse ESCs self-renewal for a period of over 5 months [311]. Others have used fragments of laminin-511, termed laminin E8 fragments, as alternatives to Matrigel® or to other feeder layers for culturing hESCs [313]. Cells cultured in these laminin fragments maintain high level expression of pluripotency markers even after 30 passages and show differentiating capacity into all three germ layers [313].

Table 12 - Laminins: its expression, and their receptors. Table adapted from [355, 363, 368-374]. A full description can be found at Li et. al [375].

Laminin isoform	Main site of expression	Integrin receptors
111	Embryonic and adult epithelium (kidney, liver, testis, ovary) including cornea	Integrins α1β1, α2β1, α6β1, α7β1, α9β1
121	Placenta	
211	Muscle, heart, peripheral nerve, testis	Integrins α1β1, α2β1, α6β1, α7β1
221	Muscle, heart, peripheral nerve, neuromuscular junction	
332	Major adhesive component of the epidermal BM, including cornea, conjunctiva, and limbal BM	Integrins α3β1 and α6β4
411	Endothelium, smooth muscle, fat, peripheral nerve	Integrins α6β1, α7β1
421	Endothelium, smooth muscle, neuromuscular junction	
511	Developing epithelium, mature epithelium, mature endothelium, smooth muscle	Integrins α2β1, α3β1, α6β1, α6β4, α7β1, αvβ3
521	Mature epithelium, mature endothelium, smooth muscle, neuromuscular junction, glomerular basement membrane	

Laminins are assembled intracellularly through a coiled-coil domain, termed LCC. They are then secreted as heterotrimeric molecules composed of one α, one β, and one γ chain [376]. The mechanisms by which cells deposit their laminins are not yet fully understood. However, two different mechanisms exist for laminin polymerization, these are self and co-polymerization. Self-polymerization involves the self-assembly of one certain heterotrimer, producing a matrix composed of only one laminin isoform. In contrast, co-polymerization requires the interaction of two or more laminin heterotrimers, resulting in a complex matrix composed by more than one isoform. These two processes exclude the formation of laminins containing α4 chain (truncated chain) and occur whilst the laminin chains are still bound to the receptors on the cell surface [377, 378].

3.1.4. Integrins

Integrins are a heterodimeric transmembrane molecules composed of an α and β chains non-covalently associated that facilitate cell-ECM adhesion [379, 380]. Integrins are classified according to their ligands, and in mammals at least 22 integrin heterodimers are known [327]. Their structure consists of a relatively large ectodomain, membrane-spanning helixes, and a relatively short cytoplasmic tail. Their ectodomain binds to ECM glycoproteins,

intercellular cell adhesion molecules, and other cellular receptors [379]. When triggered, integrins transduce the external signal to the intracellular space, through chemical pathways, providing information on its location, environment, adhesive state, and surrounding matrix. This information can result in changes of cell cycle, shape, motility, and differentiation [380]. They are also involved in the attachment of the cell, through microfilaments, to the ECM. The attachment to the substrate is helped by anchorage proteins, such as talin, vinculin, and paxillin, which together form a cell adhesion complex [381] whose association/disassociation plays a key role in cell migration [382]. For the scope of this study, laminin binding integrins include α3β1, α6β1, α6β4, and α7β1 [383]. Critical in the formation of HDs, integrin α6β4 loss results in a mechanically and functionally defective epithelium [384].

3.1.5. ECM transduction

Because cells sense the surrounding environment, functionalized substrates have been used to modulate cell behaviour, morphology, migration, and differentiation patterns. The cell's response is governed by various processes:

i. **Chemotaxis.** Chemotaxis refers to the movement of cells in response to chemical stimuli. The movement can be towards the source of the stimuli (chemoattractant) or in the opposite direction of the stimuli (chemorepellent) [316]. Chemotaxis is of critical importance in early development [317], actin filament rearrangements [318], immune response, and cancer metastasis [319, 320].

ii. **Haptotaxis**. Haptotaxis is the directional movement of cells in response to a gradient of cellular adhesion sites or other substrate-bound chemoattractants. Several biomaterials have been functionalized with a wide variety of attractants inducing cell motility, which can have a role in enhancing processes as wound healing [321] and immune response [322].

iii. **Mechanotaxis.** Mechanotaxis refers to the directed cell migration in response to mechanical cues, such as stiffness gradients or shear stress. This can be used to modulate vascular remodelling, where endothelial cells migration is stimulated in response to shear stress [323].

iv. **Differentiation**. Putting together the knowledge that cells actively respond to the underlying substrate, several authors have tried, with certain degree of success, to promote differentiation of SCs into more-differentiated cell lineages:

a. As mentioned on Chapter 1, the SCs for corneal epithelium reside in a very specialized niche, named the limbus. By exposing SCs, isolated from the bulge of hair follicles, to limbal specific environment cues (substrates functionalized with laminin-332) Blazejewska et al. induced these cells to differentiate into corneal epithelial-like cells [179].

b. In the same line of studies, Ahmad et al. induced two different hESC lines to differentiate into cornea epithelial-like cells by culturing them on collagen IV (major component of limbus) and feeding them with conditioned media obtained from limbal fibroblasts [178].

In both studies SCs lost their "stemness" observed by the decreased expression of SC markers, such as α6 integrin and KRT15 [179] and OCT4 and NANOG [178], and increase in expression of markers for differentiated corneal ECs, such as KRT3 and KRT12 [178, 179].

3.1.6. Intracellular signalling for cell growth and differentiation

In various non-ocular systems, it is very well documented that the ECM plays crucial roles in cell differentiation via integrin-mediated signaling pathways [299, 300]. Protein phosphorylation and proteolysis are the two major post-translational modifications for controlling cellular functions in response to extracellular stimuli [385]. It is recognized that tyrosine phosphorylation is the triggering signal in many signaling pathways. The majority of proteins that are downstream targets in these pathways are regulated by phosphorylation, not on tyrosine (Tyr) residues but on serine (Ser) and/or threonine (Thr) residues [386]. The mitogen-activated protein kinases (MAPKs) are focal points for the extracellular stimuli. Their activation is a downstream event of integrin ligation and results in the regulation of crucial cellular processes [387]. Three distinct subfamilies of the MAPKs have been described; the extracellular signal-regulated kinase (ERK), c-jun N-terminal or stress-activated protein kinases (JNK/SAPk), and the p38 group [388], which in resting cells are primarily located in the cell cytosol and translocate to the nuclei upon activation [389]. The ERK family has shown to be highly responsive to mitogen stimuli (such as growth factors) while JNK and p38 are activated by a variety of genotoxic stresses (including DNA repair and apoptosis) [390]. Remarkably, Lin et al. have observed that different laminin isoforms activate different intracellular signalling pathways, which support the hypothesis that ECM proteins modulate cell differentiation via alternate signalling pathways [304]. In this study, a MAPK/ERK signalling interactive pathway, whose roles are mainly involved in cell growth and

differentiation, was used. This assay allows for the simultaneous detection of the phosphorylation and cleavage levels of 18 signalling molecules, Table 13.

Table 13 - Target map of the PathScan® Intracellular Signalling Array Kit and their key roles in cell differentiation.

Target	Role	References
ERK1/2	Intermediate agent in response to extracellular signals. Its activation (phosphorylation) precedes cell growth and differentiation.	[389, 391-393]
STAT1 and STAT3	Involved in cell growth, apoptosis, and differentiation. STAT3 phosphorylation has a positive effect on EC differentiation from the lung.	[394-399].
AKT	AKT pathway activation (phosphorylation) induces EC differentiation and growth, and drives cancer SCs to lose their properties. Activated AKT results in phosphorylation of important downstream proteins involved in cell metabolism, proliferation, survival, and growth, such as GSK-3β (inhibition), PRAS40 (inhibition), BAD (inhibition), and S6 ribosomal protein.	[400-405].
mTOR	Regulates cell proliferation, metabolism, and survival. Dedifferentiation of RPE (retinal pigmented cells) is followed by mTOR activation.	[406, 407].
AMPKα	Its activation (phosphorylation) promotes epithelial differentiation and tight junction formation in gut epithelium.	[408]
S6	Its phosphorylation reflects mTOR pathway activation and predicts cell cycle progression. Differentiation agents in embryonic chicken cell lens triggered S6 phosphorylation.	[409]
P38 MAPK	Induces the differentiation of adipocytes, myoblasts, and SCs. p38δ played a role in regulating keratinocyte differentiation.	[410]
GSK-3β	Its inhibition (phosphorylation) prevents the epithelial-mesenchymal transition process, preventing ECs from losing their properties.	[411]
PRAS40	PRAS40 phosphorylation is increased in cells expressing KRT15 (a suggested epithelial SC marker).	[412]

3.1.7. Aims

i. **To identify how the ECM composition drives the differentiation of ECs from the human ocular surface.** This was investigated by assessing the differences on ECM composition produced by the two different cell lines (HCjE-Gi and hTCEpi).

ii. **To determine if the differentiation of human conjunctival and corneal ECs can be modulated in response to the laminin composition of the functionalized scaffolds.** This

was assessed by culturing the two cell lines on functionalized substrates with a range of different human recombinant laminins isoforms.

iii. **To identify which proteins are post-translationally modified in response to extracellular stimuli.** This was assessed by analysing the degree of phosphorylation and cleavage of 18 proteins upon culture of HCjE-Gi and hTCEpi cells on 4 different substrates.

3.2. Materials and Methods

3.2.1. Extracellular matrix protein extraction for LC-MS analysis

Basal cell protein proteolysis and extraction was performed according to the method described by Todorovic et al. [289] and Gospodarowicz [288] with small modifications. Briefly, after 9 days the culture medium was removed (T-25cm^2 flasks were used for this purpose) and the flask washed with sterile PBS. The cells were then ruptured by treatment with 20mM NH_4OH in sterile PBS for 5 minutes. The remaining ECM and basal cell components were washed several times in sterile PBS followed by ddH_2O. A solution of 50mM NH_4HCO_3 (cat. number 09830, Sigma-Aldrich) in ddH_2O, pH 8.0, containing: 0.02% (V/V) ProteaseMax surfactant (cat. number V2071, Promega), 0.33% (W/V) Trypsin Gold (Mass Spec grade, cat. number V5280, Promega) was added and the samples digested for 1 hour at 37°C in a humid chamber. The resulting solution containing the peptides was then transferred into tubes specially designed to prevent non-specific adsorption to the surface (Eppendorf LoBind cat. number Z666505, Sigma-Aldrich). The enzymatic reaction was stopped by adding acetic acid (cat. number 320099, Sigma-Aldrich) setting the pH to 3–4. 1% (V/V) of 0.5M 1,4-dithiothreitol (DTT, cat. number D5545, Sigma-Aldrich) was added for 20 minutes at 56°C to reduce the proteins. 2.5% (V/V) of 0.55M iodoacetamide (cat. number I149, Sigma-Aldrich) was added for 15 minutes at RT in the dark to alkylate the proteins. 0.3125% (W/V) of Trypsin Gold and 0.00625% (V/V) ProteaseMax Surfactant were added and the solution heated at 37°C for 3 hours for protein digestion. Trifluoroacetic acid (TFA, cat. number 40967, Sigma-Aldrich) was added to a final concentration of 0.5% (V/V) to inactivate the trypsin. The samples were frozen at -20°C until further analysis.

3.2.2. Liquid chromatography–mass spectrometry analysis

LC-MS analysis was performed using an Ultimate 3000 RSLCnano system (Dionex, Thermo Fisher Scientific) coupled to a hybrid linear ion trap/Orbitrap mass spectrometer (LTQ Orbitrap XL; Thermo Fisher Scientific). Digested samples were sonicated to ensure an even suspension and 1µg of digested proteins was loaded onto a C18 trap column (C18 PepMap, 300µm i.d. × 5mm, 5µm particle size, 100µm pore size; Dionex) and desalted for 3 minutes at a flow rate of 25µL/min using 2% acetonitrile containing 0.1M TFA. The trap column was then switched online with the analytical column (PepMap C18, 75µm i.d. × 500mm, 3µm particle, and 100µm pore size; Dionex), and peptides were eluted in a 180 minutes gradient at a flow rate of 300nL/minute using 2% acetonitrile with 0.1% formic acid (FA) to 50%

acetonitrile containing 0.08% FA. Mass Spectrometry Data was acquired with Xcalibur software, version 2.0.7 (Thermo Fisher Scientific). The mass spectrometer was operated in data-dependent mode and externally calibrated. MS1 survey scan (m/z 400–1200) was set at a resolution of 30 000 in the Orbitrap, followed by ten MS2 scans using CID activation mode in the ion trap. The dynamic exclusion was enabled with the following settings: repeat count, 1; repeat duration, 30 seconds; exclusion list size, 500; and exclusion duration, 40 seconds. The activation time was 30 milliseconds, with an isolation width of 2 Da for ITMS; the normalized activation energy was 32%, and the activation (q) was 0.25. The LC-MS analysis was performed at Dublin City University by Dr Finbarr O'Sulllivan and Dr Paula Meleady.

3.2.3. Data analysis – Database Search and Postsearch Filtering Analysis

Proteome Discoverer (PD) version 2.1.0.81 (Thermo-Scientific) was used to perform the database search against the human sequences in the UniProt Swiss-Prot protein database (version January 2016 with 20 151 entries) for the Mass Spectrometry raw data files. The search engines SEQUEST-HT and Mascot (version 2.4.0) were utilised in PD. The search parameters used were as follows: 20ppm tolerance for precursor ion masses, 0.6Da for fragment ion masses analysed by ion trap. A total of two missed cleavages were permitted for fully tryptic peptides. Carbamidomethylation of cysteines (+57.0215 Da) was set as a fixed modification, and variable modifications of methionine oxidation (+15.9949 Da) and N-terminal acetylation (+42.0106 Da) were allowed. The false discovery rate (FDR) was determined by using a target–decoy search strategy using Percolator in PD2.1. The sequence database contains each sequence in both forward and reverse orientations, enabling FDR estimation. The FDR was set to 0.01 at both the peptide and the protein levels. The LC-MS data analysis was performed at Dublin City University by Dr Finbarr O'Sulllivan and Dr Paula Meleady.

3.2.4. Reverse Transcriptase qPCR

Reverse Transcriptase qPCR and all the previous steps (RNA extraction and cDNA synthesis) were done as outlined in sections 2.2.10, 2.2.11, and 2.2.12 respectively. Table 14 shows the set of primers used for the studies performed in this chapter.

Table 14 –List of primers used for Reverse Transcriptase qPCR studies in Chapter 3. The primer sequences and the product size are included. Abbreviations used GAPDH: glyceraldehyde-3-phosphate dehydrogenase, COL: collagen, LAM: laminin. # Sequences and product size of reference genes are not commercially provided by PrimerDesign.

Primer	Gene Sequence	Product size (bp)
GAPDH	F - # R - #	#
COLXVIIα1	F - GGAGTACCCTCGGAAGGAATTT R- ACGCTTAACATCATCCAATTCTGT	133
LAMα5	F – GGCTTCTACCGCTCTCCCA R – GTAGCATCGACCCGTCAGG	114
LAMβ1	F- GAGAGGAAAGTCAGCGAGATAAA R - GAGCCATCATTTCTGTAACATCTTT	127
LAMβ2	F- CCTTGAGCCTGGTATCTCCTAC R - AGATTATTCACCGAGTCAATGAGC	117

3.2.5. Flow cytometry

Flow cytometry was done as outlined in section 2.2.14. Table 15 and Table 16 show the antibodies used for the studies performed in this chapter.

Table 15 – List of primary antibodies used for flow cytometry studies in Chapter 3. Abbreviations used COL: collagen, LAM: laminin.

Antibody	Clone	Source	Isotype	Manufacturer	Dilution
COLXVIIα1	EPR18614	Rabbit	IgG	Abcam	1:500
LAMα5	2F7	Mouse	IgG1	Sigma-Aldrich	1:500
LAMβ1	Polyclonal	Rabbit	IgG	ThermoFisher Scientific	1:500
LAMβ2	CL2979	Mouse	IgG2a	Abcam	1:500
IgG	Isotype Control	Rabbit	---	ThermoFisher Scientific	0.49µg/µL
IgG1	Isotype Control	Mouse	---	ThermoFisher Scientific	0.2µg/µL
IgG2a	Isotype Control	Mouse	---	ThermoFisher Scientific	2µg/µL

Table 16 - List of secondary antibodies used for flow cytometry studies in Chapter 3. Abbreviations used FITC: fluorescein isothiocyanate.

Antibody	Host	Reactivity	Conjugate	Manufacturer	Dilution
A-11005	Goat	Mouse	AlexaFluor 594	Life Technologies	1:400
F7512	Sheep	Rabbit	FITC	Sigma-Aldrich	1:400

3.2.6. Immunocytochemistry on ECM proteins

Cells were seeded on a glass coverslip (22x22mm cat. Number 408/0187/33, Thickness No.1, BDH) over a desired number of days. The culture medium was removed, and the wells briefly

washed once in sterile PBS. The cells were then ruptured using 20mM NH_4OH for 5 minutes in sterile PBS. The remaining extracellular matrix and basal cell components were washed several times in sterile PBS followed by ddH_2O. The wells were incubated with ice-cold methanol (cat. Number M/4000/PC17, Fisher Scientific UK) for 10 minutes at RT (all steps were performed at RT unless otherwise specified), followed by three washing steps with PBS for 5 minutes. The wells were then blocked using 2% goat serum (cat. Number G9023, Sigma-Aldrich) diluted in PBS for one hour, followed by three washing steps with PBS for 5 minutes. Primary antibody diluted in PBS was added and incubated overnight at 4°C in the dark, Table 17. The following day, the primary antibody was removed from the culture well and the well washed thrice with PBS for 5 minutes. The well was incubated with conjugated secondary antibody diluted in PBS for one hour in the dark, Table 18. After removal of the secondary antibody and washing in PBS for 5 minutes, the coverslip was removed from the well and mounted in a slide (cat. Number 631-0102, SuperFrost 1mm thick, VWR International) using VECTASHIELD (cat. Number H-1000, Vector Laboratories). The coverslips were then viewed using an ECLIPSE Ti-E inverted Microscope System (Nikon, USA).

Table 17 - Table of primary antibodies used for the ICC studies in Chapter 3. Abbreviations used COL: collagen, LAM: laminin

Antibody	Clone	Source	Isotype	Manufacturer	Dilution
COLXVIIα1	EPR18614	Rabbit	IgG	Abcam	1:1000
LAMα5	2F7	Mouse	IgG	Sigma-Aldrich	1:1000
LAMβ1	Polyclonal	Rabbit	IgG	ThermoFisher Scientific	1:1000
LAMβ2	CL2979	Mouse	IgG2a	Abcam	1:1000

Table 18 - Table of secondary antibodies used for the ICC studies in Chapter 3. Abbreviations used FITC: fluorescein isothiocyanate.

Antibody	Host	Reactivity	Conjugate	Manufacturer	Dilution
A-11005	Goat	Mouse	AlexaFluor 594	Life Technologies	1:400
F7512	Sheep	Rabbit	FITC	Sigma-Aldrich	1:400

3.2.7. Coating with human recombinant laminins

Most laminin isoforms, except for LAM-111, are extremely difficult to extract from tissues due to the high degree of cross-linking with other laminins and other molecules. Only recently, a few forms of recombinant laminins have successfully been produced [413-415]. Solutions containing recombinant LAM-111, -121, -211, -221, -411, -421, -511, and -521 isoforms were used (cat. Number KT202, BioLamina). All steps were done in accordance with the manufacturer's protocol. Briefly, the stock solutions were thawed on ice prior to use and

then diluted in 1xDPBS with Ca^{2+} and Mg^{2+} (cat. number 14040091, ThermoFisher) to a final concentration of 10µg/mL (9.8µg/cm^2) unless otherwise specified. The final solution was added to the culture dishes. These were sealed with Parafilm ® and incubated overnight at 4°C. On the next day cells were seeded accordingly at density of 25000 cells/cm^2, the medium changed every other day until further experiments.

3.2.8. PathScan ® Intracellular Signalling Array Kit

PathScan® Intracellular Signalling Array Kit (Chemiluminescent Readout, cat. Number 7323, Cell Signalling Technology) was used for this purpose. All steps were done in accordance with the manufacturer's protocol at RT. Briefly, cells were washed with ice-cold PBS and lysed with ice-cold 1X Cell Lysis buffer supplemented with a cocktail of protease and phosphatase inhibitors (cOmplete Tablets Mini and PhosSTOP EASYpack, Roche). The Array Blocking Buffer was added and incubated for 15 minutes on an orbital shaker. The protein lysate was added and incubated for two hours. After washing, the Detection Antibody Cocktail was added and incubated for 1 hour on an orbital shaker. HRP-linked streptavidin was added and incubated for 30 minutes. LumiGLO®/Peroxidase reagent was added and images captured immediately after, using a Chemidoc (chemiDoc ™ XRS+, BioRad) and quantified using ImageLab 5.0 Software.

3.2.9. Statistical analysis

Kruskal-Wallis test followed by a Dunn's multiple comparison test (unless otherwise specified) were used to determine statistically significant differences (GraphPad Prism 5, *p<0.05, **p<0.01, ***p<0.001). Data is expressed as median ± 5-95% percentile (unless otherwise specified).

3.3. Results

3.3.1. ECM composition by mass spectrometry analysis

ECM composition was assessed by mass spectrometry. In total 444 different entries were detected: 107 being shown to be found only on HCjE-Gi ECM, 152 exclusively on hTCEpi ECM, and 185 found in both matrices preparations, Figure 37.

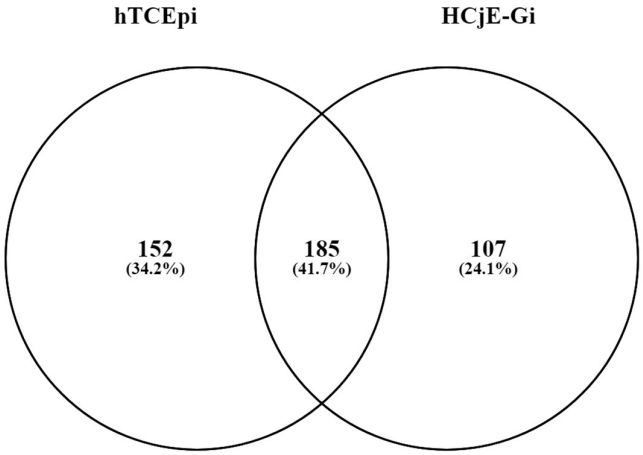

Figure 37 - Venn diagram of unique and shared ECM proteome as assessed by mass spectrometry. A total of 444 entries were detected: 107 were only found on HCjE-Gi cells-produced ECM, 152 on hTCEpi cells-produced ECM, and 185 detected in both ECM preparations.

Interestingly, amongst the heavy subset of ECM proteins, various growth factors and other soluble molecules were detected (data not shown). These include TGF-β, insulin-like growth factor binding protein, epidermal growth factor receptor (EGFR), fibroblast growth factor (FGF), interleukin enhancer-binding factor 2, and 3, amongst many others. These soluble factors produced by cells and trapped within the ECM proteins meshwork provide chemical cues, additional to those provided by the ECM proteins, for the differential keratin expression [294]. However, additional studies needed to be performed to understand the role played by such molecules.

Very similar results were found for the biological processes associated with the proteins derived from either ECM preparations. The majority of the ECM proteins seem to be mainly involved in processes of cell adhesion, ECM organization and signal transduction, Figure 38. The main cellular components associated with the proteins detected in both ECM proteins are shown on Figure 39. Noteworthy is the presence of a large number of proteins associated with exosomes.

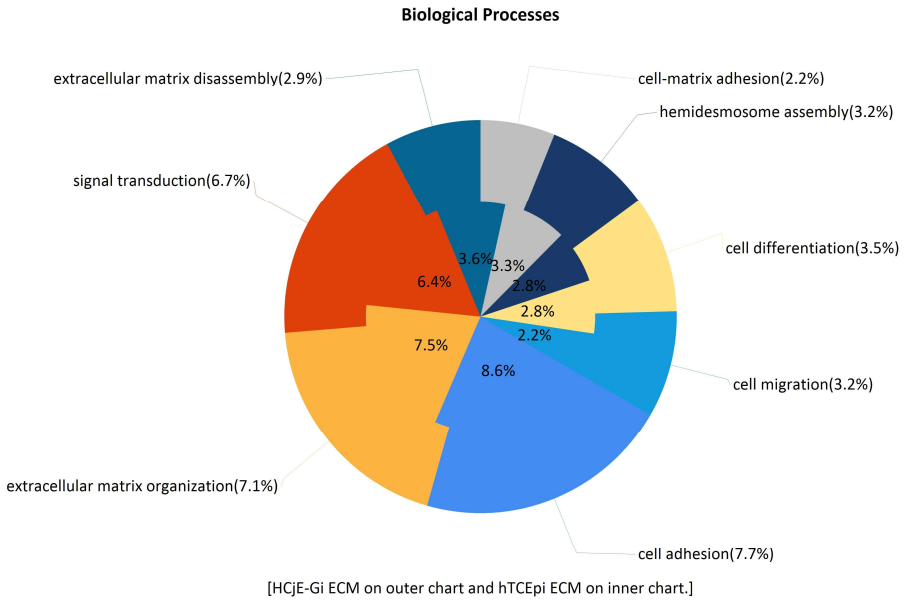

Figure 38 - Biological processes associated with the proteins detected on HCjE-Gi and hTCEpi ECM preparations. Inner and outer chart show the percentages relatively to hTCEpi ECM proteins and HCjE-Gi ECM proteins, respectively. Data analysed using FunRich version 3.0 with Gene Ontology database [416].

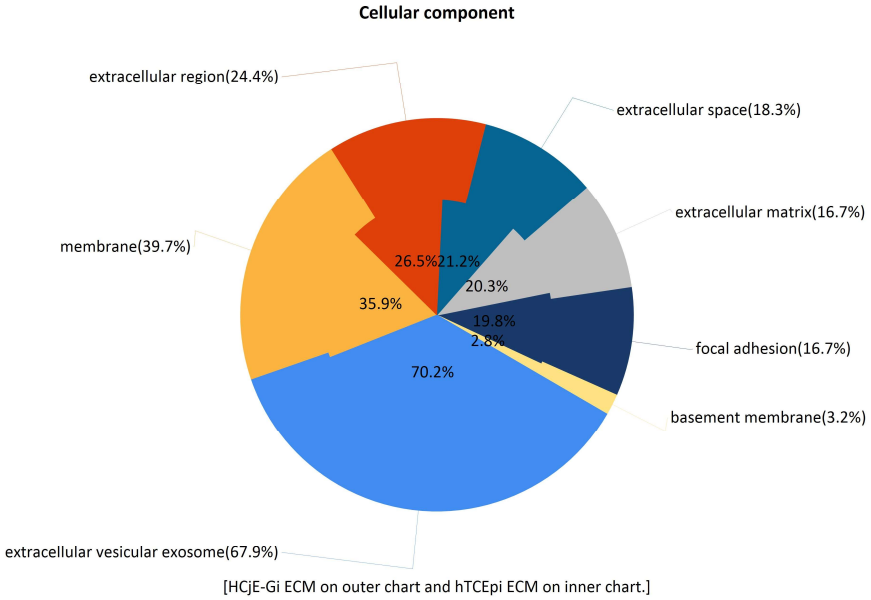

Figure 39 – Cellular components associated with the proteins detected on HCjE-Gi and hTCEpi ECM preparations. Inner and outer chart show the percentages relatively to hTCEpi ECM proteins and HCjE-Gi ECM proteins, respectively. Data analysed using FunRich version 3.0 with Gene Ontology database [416].

Since ECM produced by one cell type induced such an alteration in the other cell type behaviour, as shown in Chapter 2, a detailed study was carried on the expression and production of proteins that were specifically produced by each cell line and thus more likely to be involved in the process of cell differentiation towards a specific cell lineage. Thus, from the 107 proteins produced only by HCjE-Gi cells, laminin (LAM)α5 was chosen. Regarding the proteins exclusively detected on the hTCEpi ECM, collagen (COL)XVIIα1 and LAMβ1 were chosen. Since laminins appear as heterotrimeric proteins, LAMβ2 expression was also a subject of study as it trimers with LAMα5 and LAMγ1 to form LAM-521, a protein already found on conjunctival BM [417].

Collagens are trimeric structures composed of three polypeptide α chains, which account a total of 28 collagen members in vertebrates [418]. Unlikely most of the collagen types, collagen XVII (also known as BP180) is a transmembrane protein with an intracellular domain [419]. It is a homotrimer composed of three α1 chains identified as a structural component necessary for the stable attachment of HDs type I to the keratin filaments [420]. It occurs in two forms: as a full-length transmembrane protein and as a soluble ectodomain [421]. Mutations in the collagen XVII gene are associated with both generalized atrophic benign and junctional epidermolysis bullosa [419] and recurrent erosion of the corneal epithelium [422, 423]. Due to its role played in the integrity of epithelial tissues, its expression profile was subject of this study. Moreover, laminins are known to be involved in many crucial cell processes including cell proliferation and differentiation (see section 3.1.3), thus their choice as subject of study appeared of understandable interest.

3.3.2. mRNA expression levels for ECM proteins show to be different in HCjE-Gi and hTCEpi cells - Reverse Transcriptase quantitative PCR

Reverse Transcriptase qPCR was performed within a certain window of time (Ct values obtained at day 0 were used for normalisation). The expression of COLXVIIα1 by HCjE-Gi cells, although not detected on mass spectrometry, was detected by Reverse Transcriptase qPCR since early time points. However, its abundance levels did not vary significantly through time. On the other hand, an increase in its transcript expression levels was observed from day 3 to day 6 on hTCEpi cells (126-fold increase, $p<0.05$), Figure 40.

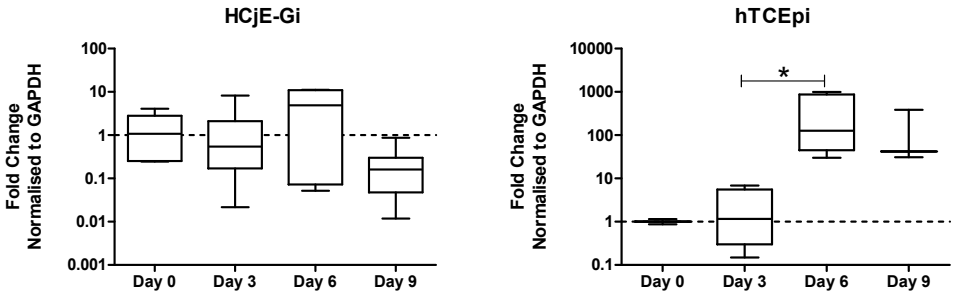

Figure 40 - The expression of collagen XVII α1 by HCjE-Gi and hTCEpi cells over 9 days as assessed by Reverse Transcriptase qPCR. (Data is represented as median ± 5-95 percentile, n≥6, Kruskal-Wallis test followed by a Dunn's Multiple Comparison test, *p<0.05, **p<0.01, ***p<0.001). Dashed line represents the basal expression of the gene of interest at day 0. Abbreviations used GAPDH: glyceraldehyde 3-phosphate dehydrogenase.

No significant differences in LAMα5 transcript abundance levels by HCjE-Gi cells were detected until day 9 when it drops significantly (p<0.05). In contrast, a continuous increase in its expression levels by hTCEpi cells was appreciated from days 0-3 until day 6-9 (p≤0.01), Figure 41.

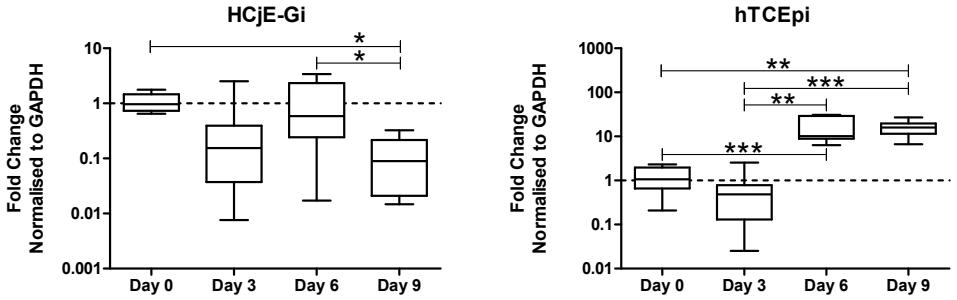

Figure 41 - The expression of laminin α5 by HCjE-Gi and hTCEpi cells over 9 days as assessed by Reverse Transcriptase qPCR. (Data is represented as median ± 5-95 percentile, n≥6, Kruskal-Wallis test followed by a Dunn's Multiple Comparison test, *p<0.05, **p<0.01, ***p<0.001). Dashed line represents the basal expression of the gene of interest at day 0. Abbreviations used GAPDH: glyceraldehyde 3-phosphate dehydrogenase.

As abovementioned, LAMβ1 trimers with LAMα5 and LAMγ1 to form LAM-511 and consequently their pattern of expression is expected to be similar. Consistent with this, a decrease in its expression levels was observed from day 0 to day 9 by the HCjE-Gi cells (25-fold decrease, p<0.05). On the other hand, a continuous increase in its expression levels by hTCEpi cells was observed from day 0 until day 6 when it peaks (698-fold increase, p≤0.001), Figure 42.

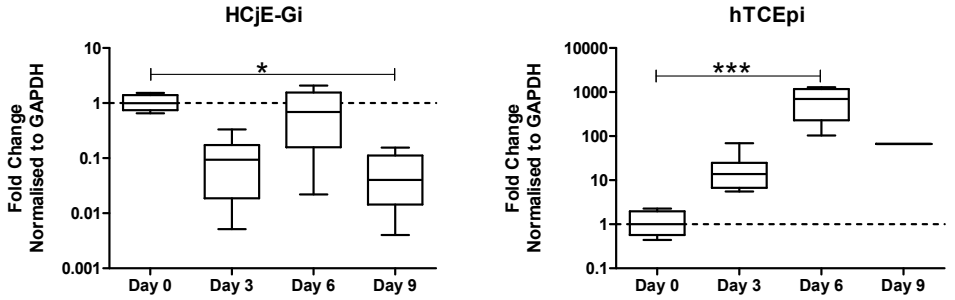

Figure 42 - The expression of laminin β1 by HCjE-Gi and hTCEpi cells over 9 days as assessed by Reverse Transcriptase qPCR. (Data is represented as median ± 5-95 percentile, n≥6, Kruskal-Wallis test followed by a Dunn's Multiple Comparison test, *p<0.05, **p<0.01, ***p<0.001). Dashed line represents the basal expression of the gene of interest at day 0. Abbreviations used GAPDH: glyceraldehyde 3-phosphate dehydrogenase.

LAMβ2 also forms a trimer with LAMα5 and LAMγ1 to form yet a different laminin isoform (LAM-521). A continuous decrease in its expression levels was observed for the HCjE-Gi cells throughout the course of the experiment (p<0.01). Regarding its expression by hTCEpi cells, a peak was observed at day 6 (206-fold increase, p≤0.05) when it plateaus, Figure 43.

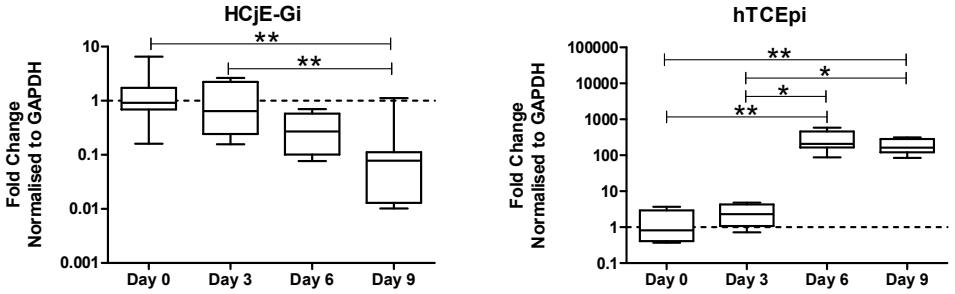

Figure 43 - The expression of laminin β2 by HCjE-Gi and hTCEpi cells over 9 days as assessed by Reverse Transcriptase qPCR. (Data is represented as median ± 5-95 percentile, n≥6, Kruskal-Wallis test followed by a Dunn's Multiple Comparison test, *p<0.05, **p<0.01, ***p<0.001). Dashed line represents the basal expression of the gene of interest at day 0. Abbreviations used GAPDH: glyceraldehyde 3-phosphate dehydrogenase.

When the fold change values of the two cell lines are plotted together, additional and complementary trends are observed. These include higher COLXVIIα1, LAMα5, LAMβ2 transcript levels expressed by hTCEpi cells at day 6 and 9 (p≤0.05), and higher LAMβ1 and LAMβ2 transcript levels expressed by hTCEpi cells at day 3 (p≤0.05), Figure 44.

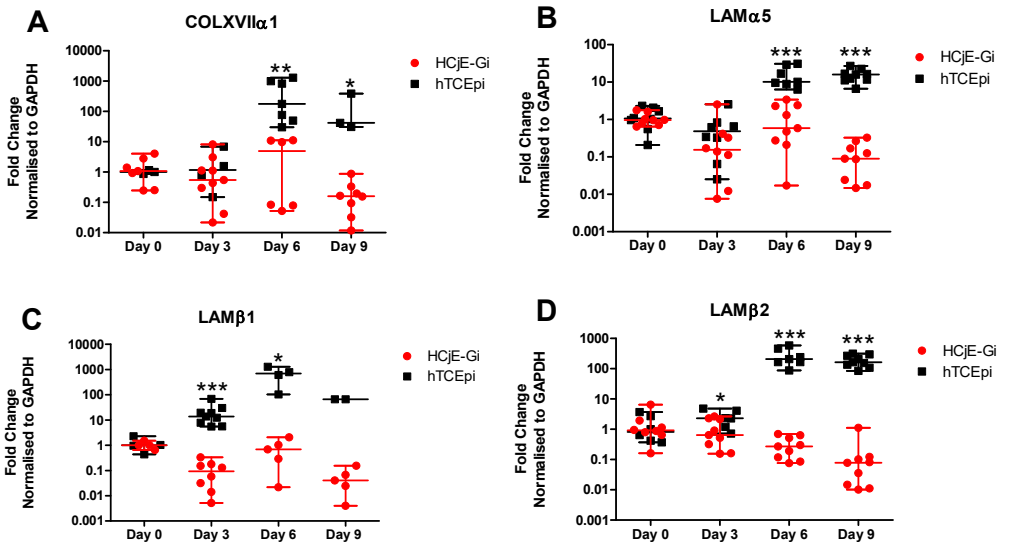

Figure 44 - The expression of transcripts produced by HCjE-Gi and hTCEpi cells over 9 days as assessed by Reverse Transcriptase qPCR. (Data is represented as median ± range, n≥3, Mann Whitney test, *p<0.05, **p<0.01, ***p<0.001). Abbreviations used COL: collage, LAM: laminin.

3.3.2.1. Summary of results 6:

To summarize these results, the expression levels of:

i. COLXVIIα1 and LAMα5 in HCjE-Gi cells were relatively constant until day 6, when it decreased.

ii. LAMβ2 by HCjE-Gi cells decreased over time.

iii. COLXVIIα1, LAMα5, LAMβ1, and LAMβ2 in hTCEpi cells increased over time, plateauing at day 6-9.

iv. COLXVIIα1, LAMα5, LAMβ2 were higher in hTCEpi cells at day 6 and 9 when compared to those expressed by HCjE-Gi cells.

v. LAMβ1 and LAMβ2 were higher in hTCEpi cells at day 3 when compared to those expressed by HCjE-Gi cells.

3.3.3. The percentage of positive events for ECM proteins is shown to be different in HCjE-Gi and hTCEpi cells – Flow Cytometry

Protein expression levels in terms of positive events were assessed by flow cytometry. Here BD FACS™ permeabilizing solution 2 was used to detect both membrane and cytosolic epitopes.

Consistent with Reverse Transcriptase qPCR results, no appreciable changes in the percentage of COLVXIIα1-positive events can be seen on HCjE-Gi cell preparations over time, Figure 45A and C. Regarding its expression by hTCEpi cells, significant lower levels of the percentage of COLXVIIα1-positive events were shown from day 0 to day 3 (decrease of 70%, $p<0.01$), followed by a steady increase until day 9 (NSS), Figure 45B and D.

Regarding the expression of LAMα5 by HCjE-Gi cells, and consistent with Reverse Transcriptase qPCR results, significant lower levels in the percentage of positive events were observed from day 0 to day 9 ($p<0.05$, corresponding to a decrease of 15% in LAMα5-positive events), Figure 46A and C. A decrease in its expression levels was also shown on hTCEpi cells although non-significant throughout the course of the experiment, Figure 46B and D.

The abundance of LAMβ1-positive events in HCjE-Gi cell preparations were shown not to significantly vary over the time course analysed, Figure 47A and C. Concerning its expression by hTCEpi cells a significant decrease in the percentage of LAMβ1-positive events from day 0 to day 3 ($p<0.01$, reduction of 60% in positive events) was observed, Figure 47B and D.

The levels of LAMβ2-positive events by HCjE-Gi cells was shown to increase over time (although not statistically different between time-points), Figure 48A and C. Regarding its expression by hTCEpi cells a decrease in the levels of LAMβ2-positive events at day 3 was followed by a constant increase in their expression up to day 9 (although not statistically different between time-points), Figure 48B and D.

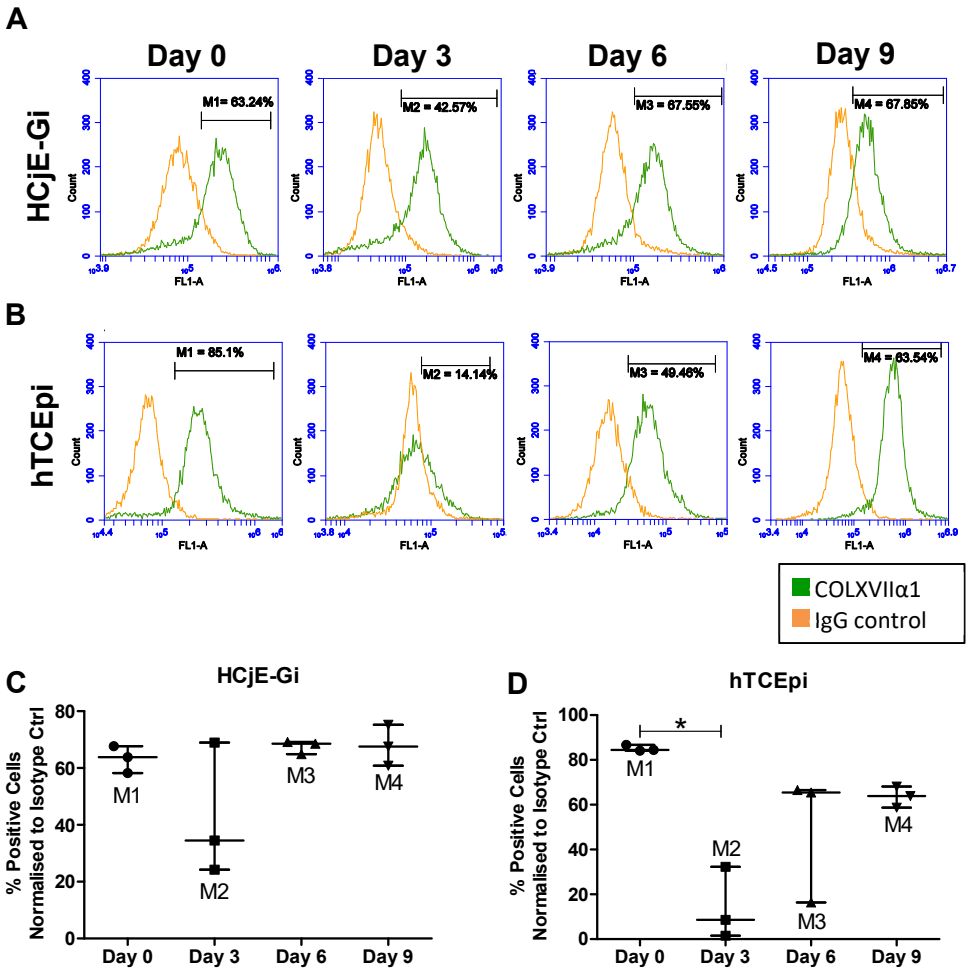

Figure 45 –The expression of collagen XVII α1 by HCjE-Gi and hTCEpi over 9 days as assessed by flow cytometry. The percentage of positive events normalized against isotype control is shown (M_x). (Data is represented as median ± range, n≥3, Kruskal-Wallis test followed by a Dunn's Multiple Comparison test. (Data is represented as median ± range, n=3, Mann-Whitney test) *p<0.05, **p<0.01, ***p<0.001). Abbreviations used COL: collagen, Ctrl: control, A.U. arbitrary units.

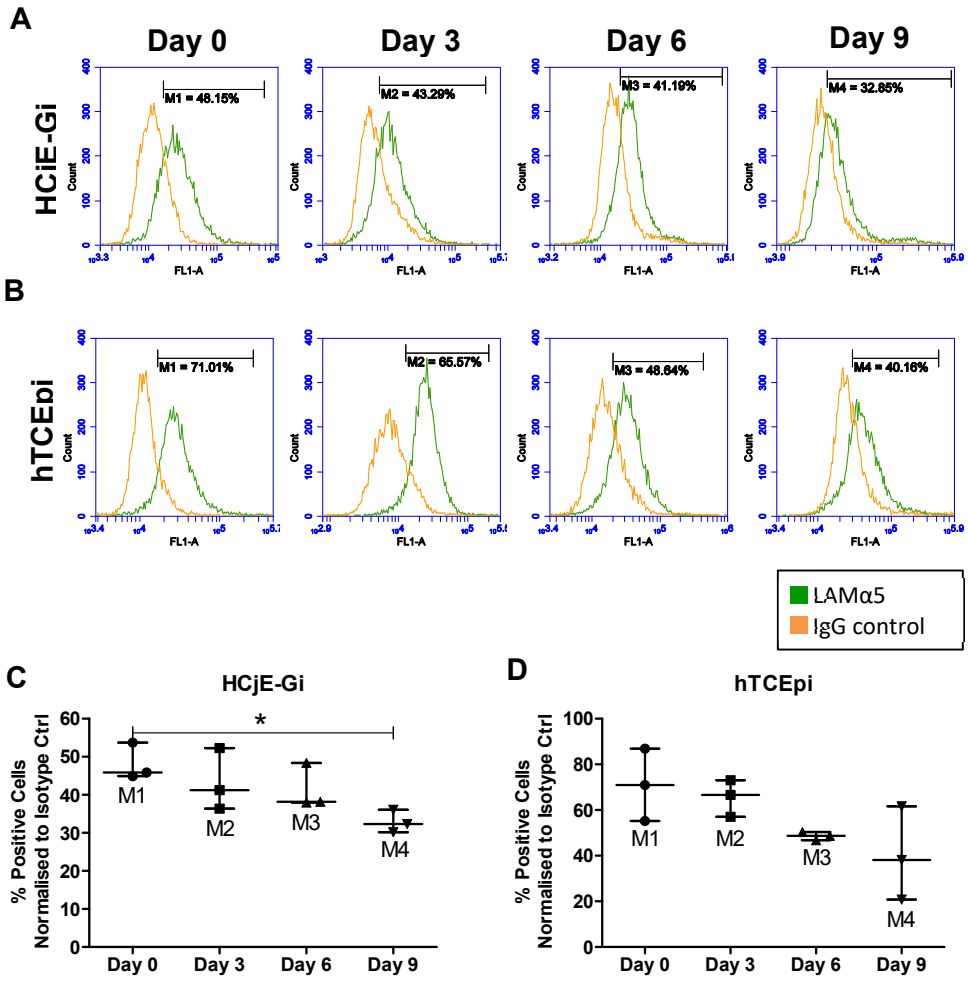

Figure 46 - The expression of laminin α5 by HCjE-Gi and hTCEpi over 9 days as assessed by flow cytometry. The percentage of positive events normalized against isotype control is shown (M_x). (Data is represented as median ± range, n≥3, Kruskal-Wallis test followed by a Dunn's Multiple Comparison test. (Data is represented as median ± range, n=3, Mann-Whitney test) *p<0.05, **p<0.01, ***p<0.001). Abbreviations used LAM: laminin, Ctrl: control, A.U. arbitrary units.

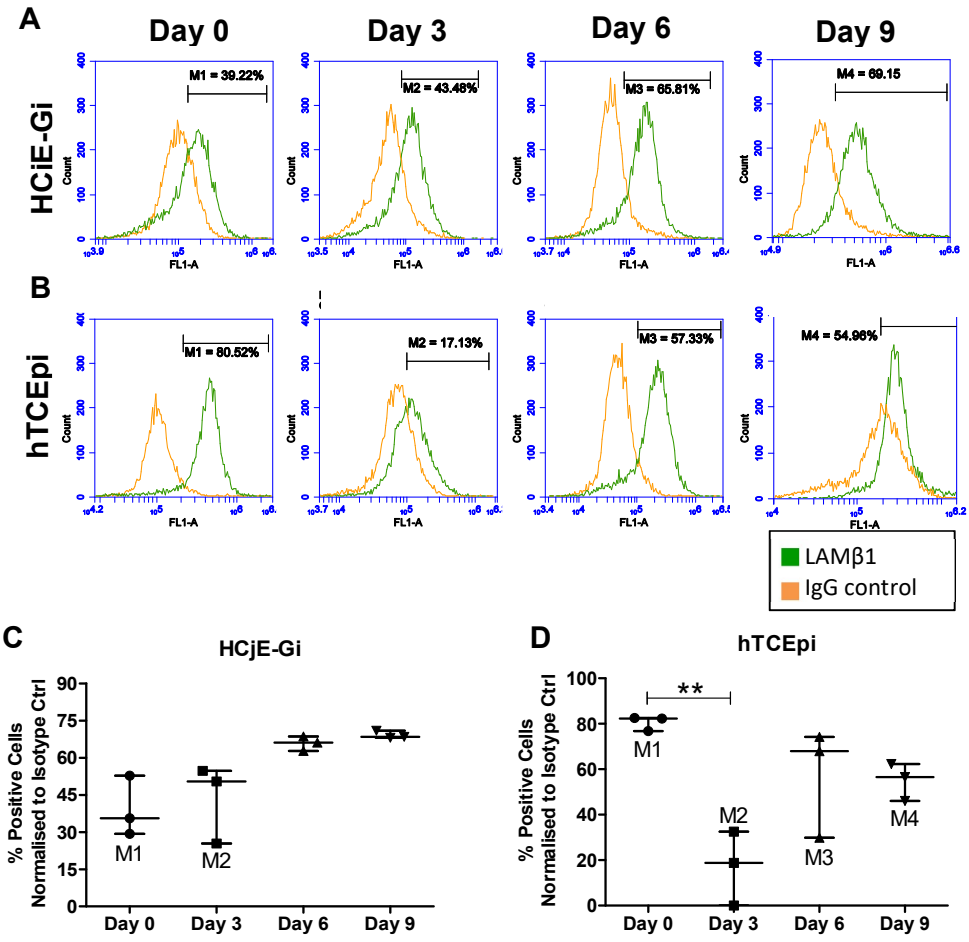

Figure 47 - The expression of laminin β1 by HCjE-Gi and hTCEpi over 9 days as assessed by flow cytometry. The percentage of positive events normalized against isotype control is shown (M_x). (Data is represented as median ± range, n≥3, Kruskal-Wallis test followed by a Dunn's Multiple Comparison test. (Data is represented as median ± range, n=3, Mann-Whitney test) *p<0.05, **p<0.01, ***p<0.001). Abbreviations used LAM: laminin, Ctrl: control, A.U. arbitrary units.

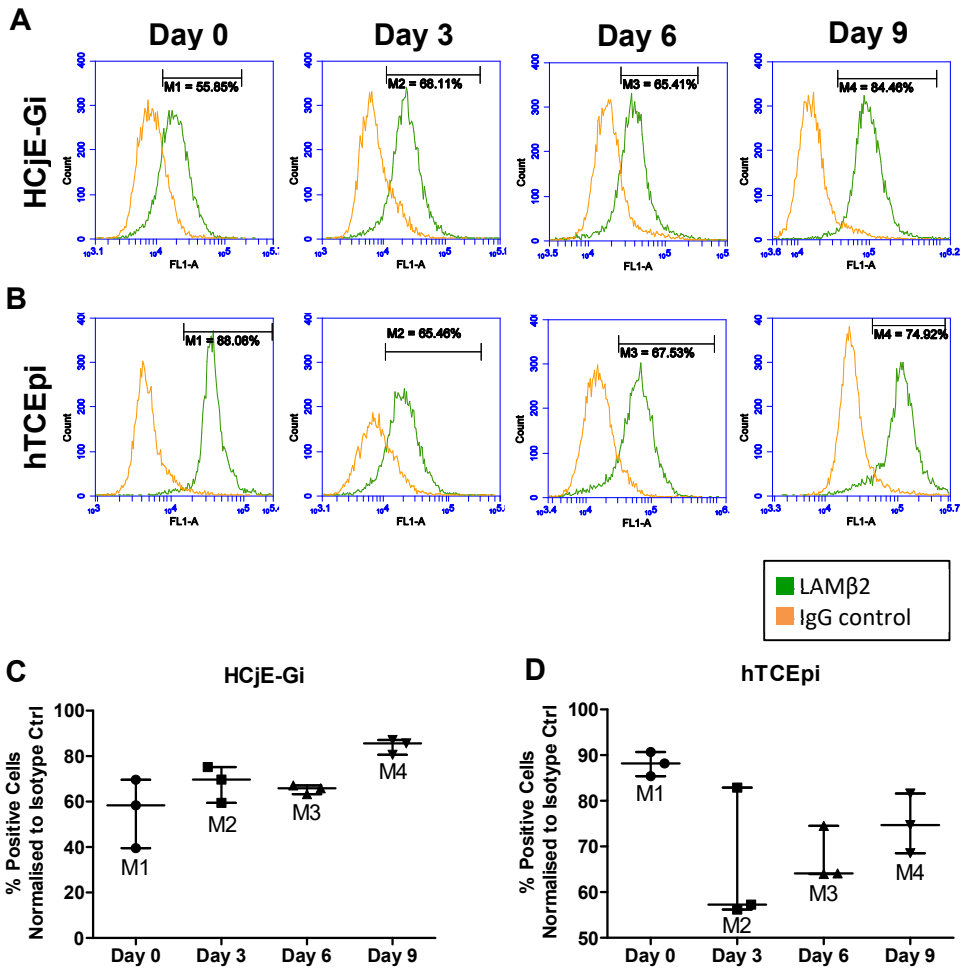

Figure 48 - The expression of laminin β2 by HCjE-Gi and hTCEpi over 9 days as assessed by flow cytometry. (A-D) The percentage of positive events normalized against isotype control is shown (M_x). (Data is represented as median ± range, n≥3, Kruskal-Wallis test followed by a Dunn's Multiple Comparison test. (Data is represented as median ± range, n=3, Mann-Whitney test) *p<0.05, **p<0.01, ***p<0.001). Abbreviations used LAM: laminin, Ctrl: control, A.U. arbitrary units.

When the percentage of positive events detected on the two cell lines is plotted together additional and complimentary trends are observed. These include a significant higher percentage of COLXVIIα1-positive events at day 0 detected on hTCEpi cells (p<0.01, which corresponds to a difference in nearly 20% of COLXVIIα1-positive events between the two cell lines), Figure 49A; a significant difference at day 3 on percentage of LAMα5-positive events (p<0.05) equivalent to a difference in nearly 25% more LAMα5-positive events detected on hTCEpi cell preparations, Figure 49B; a higher percentage of LAMβ1-positive events at day 0 detected on hTCEpi cell preparations (difference in nearly 40% more LAMβ1-positive events detected in hTCEpi cells, p<0.05), Figure 49C; and a difference at day 0 on the percentage of

LAMβ2-positive events ($p<0.05$, corresponding to 30% more LAMβ2-positive events being detected on hTCEpi cell preparations), Figure 49D.

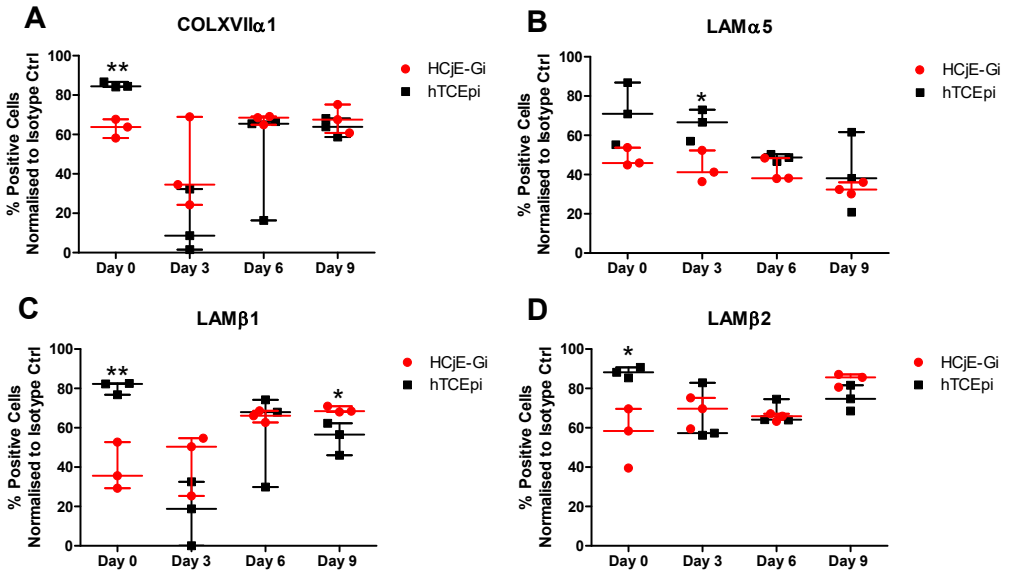

Figure 49 - The expression of ECM proteins produced by HCjE-Gi and hTCEpi cells over 9 days as assessed by flow cytometry. The percentage of positive events normalized against isotype control. (Data is represented as median ± range, n=3, Mann-Whitney test, *p<0.05, **p<0.01, ***p<0.001). Abbreviations used ECM: extracellular matrix, Ctrl: control, COL: collagen, LAM: laminin.

3.3.3.1. Summary of results 7:

To summarize these results, the percentage of:

i. COLXVIIα1-, LAMβ1- , and LAMβ2-positive events was higher in hTCEpi cell preparations at day 0 when compared to HCjE-Gi cell preparations.

ii. LAMα5-positive events was higher in hTCEpi cell preparations at day 3 when compared to HCjE-Gi cell preparations.

3.3.4. ECM characterization by immunocytochemistry

At desired time points, cell cultures were "de-roofed" and specific ECM proteins immunostained and visualized.

3.3.4.1. Collagen XVIIα1

Noteworthy is the absence of COLXVIIα1 at day 0 on both HCjE-Gi and hTCEpi ECM. Its production appears to increase with time in both matrices, showing a punctate pattern (zoomed image). Additionally, on hTCEpi ECM the pattern soon appears to bear a

resemblance to a rosette shape (typical shape of laminin chains with which this protein interacts to form HDs), Figure 50.

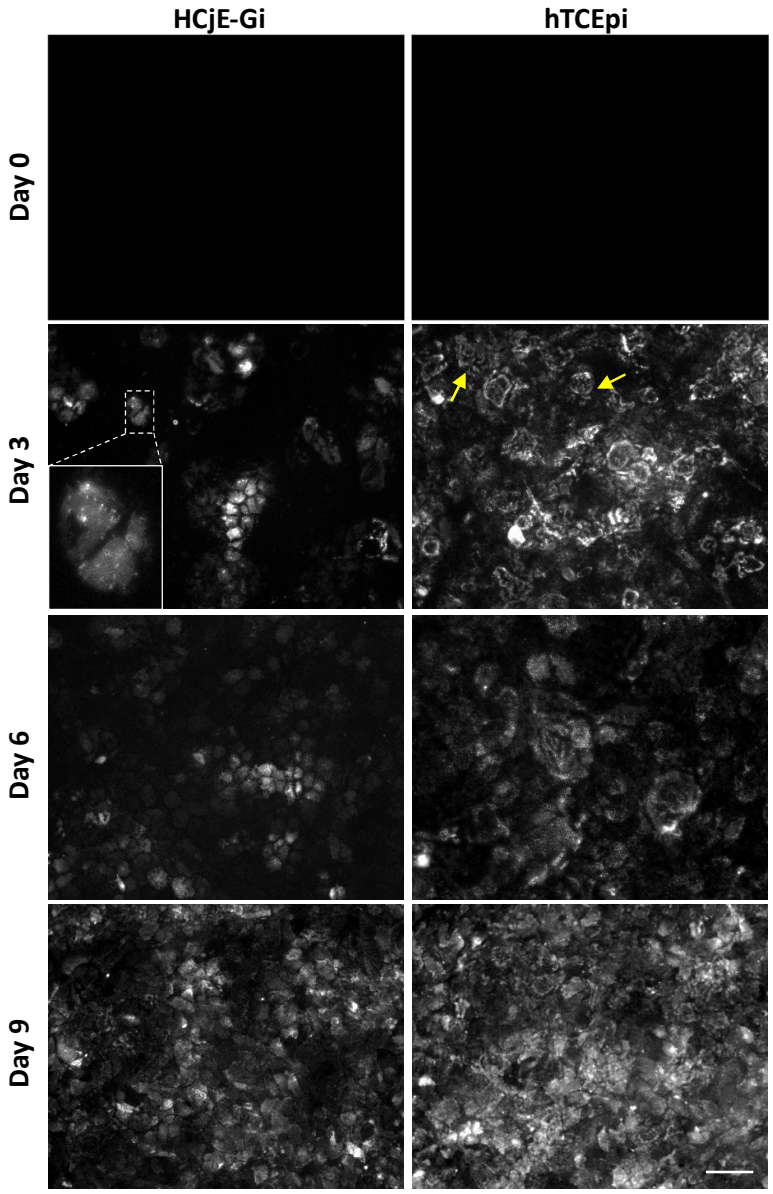

Figure 50 - The deposition of collagen XVIIα1 by HCjE-Gi and hTCEpi cells over 9 days as assessed by immunocytochemistry. Cells plated onto a glass coverslip were de-roofed and analysed by immunofluorescence at the showed time-points. Box shows a zoomed typical collagen XVIIα1 punctuated structure. Yellow arrows show a rosette shape resulting from the interaction of collagen XVIIα1 with matrix laminins, (scale bar 50µm).

3.3.4.2. Laminin α5

Regarding LAMα5, its deposition increased over time with incomplete rosette shapes observed at day 0 (green arrows) and cloudy appearances at day 9 in both ECMs. The production of this laminin chain appeared to be higher by hTCEpi cells, consistent with the flow cytometry data. The cloudy appearance is result of the high production and deposition of this protein. At intermediate time points, clear rosette shapes can be observed, Figure 51.

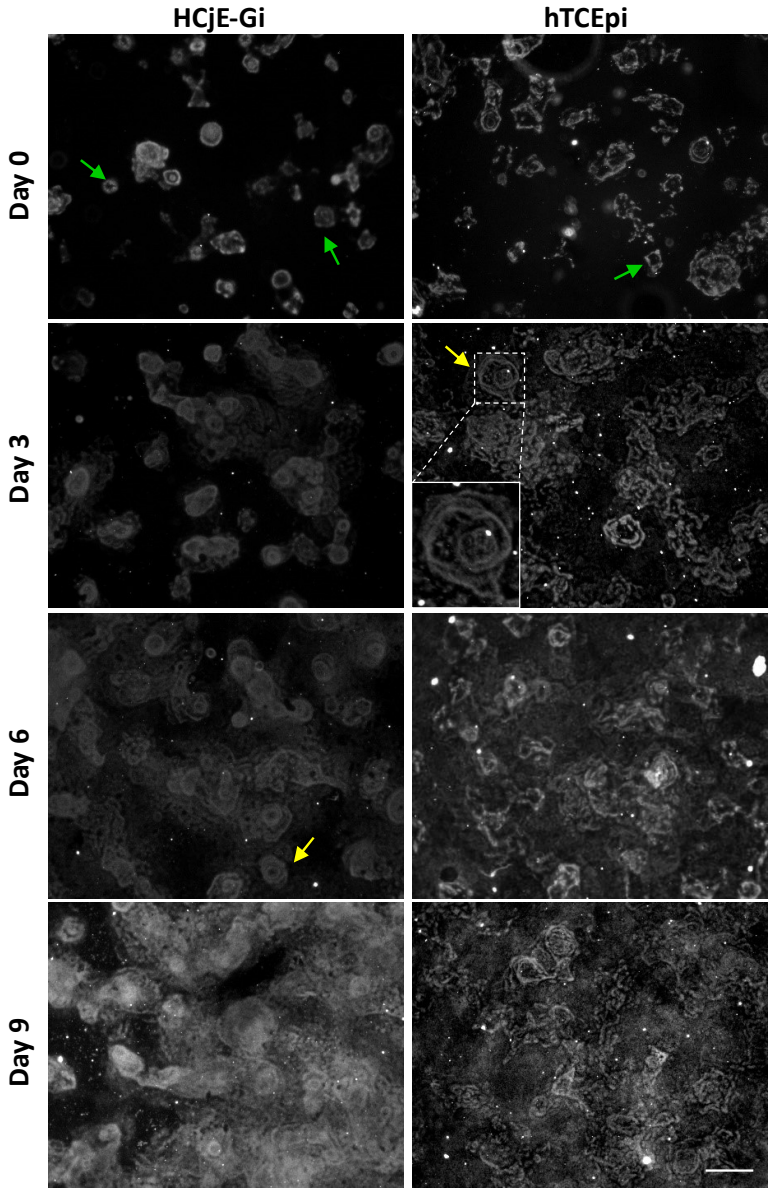

Figure 51 - The deposition of laminin α5 by HCjE-Gi and hTCEpi cells over 9 days as assessed by immunocytochemistry. Cells plated onto a glass coverslip were de-roofed and analysed by immunofluorescence at the showed time-points. Zoomed box and yellow arrows show a typical laminin rosette structure. Green arrows show an incomplete laminin rosette structure, (scale bar 50µm).

3.3.4.3. Laminin β1 and Laminin β2

Concerning LAMβ1 and LAMβ2 chains, complete rosette shapes can only be observed at day 3 on HCjE-Gi ECM contrasting with the earlier appearance of these structures on hTCEpi ECM at day 0. Consistent with the flow cytometry data, its deposition appeared also to be more accentuated at earlier time points by hTCEpi cells when compared to HCjE-Gi cells, Figure 52 and Figure 53.

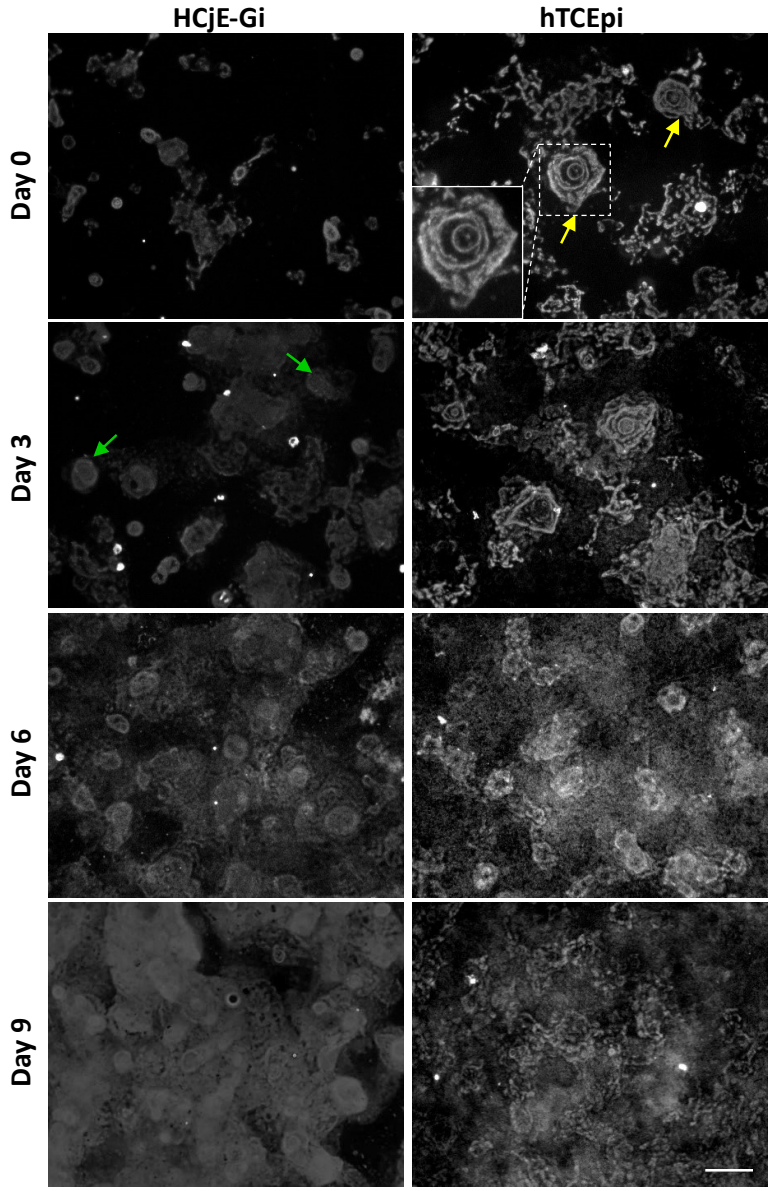

Figure 52 - The deposition of laminin β1 by HCjE-Gi and hTCEpi cells over 9 days as assessed by immunocytochemistry. Cells plated onto a glass coverslip were de-roofed and analysed by immunofluorescence at the showed time-points. Zoomed box and arrows show a typical laminin rosette structure, (scale bar 50µm).

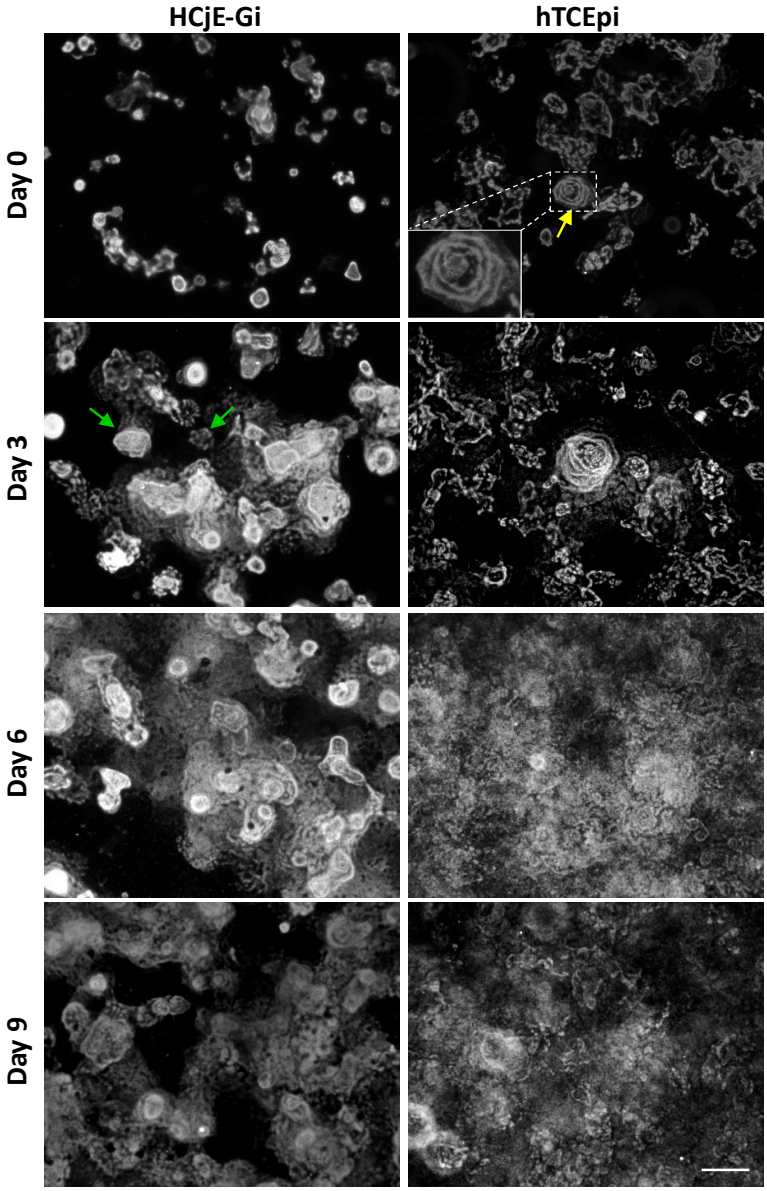

Figure 53 - The deposition of laminin β2 by HCjE-Gi and hTCEpi cells over 9 days as assessed by immunocytochemistry. Cells plated onto a glass coverslip were de-roofed and analysed by immunofluorescence at the showed time-points. Zoomed box and arrows show a zoomed typical laminin rosette structure, (scale bar 50μm).

3.3.4.4. Summary of results 8:

i. The COLXVIIα1 was only detectable in HCjE-Gi and hTCEpi ECM after 3 days.

ii. The LAMα5 chain was detectable at day 0 in both cell lines with different shape appearances throughout the time window analysed.

iii. LAMβ1 and LAMβ2 chains were both detected at the earliest time-point with their deposition to be more accentuated by hTCEpi cells.

3.3.5. Coating plates with recombinant human laminins isoforms

3.3.5.1. General laminin screening – HCjE-Gi cells show different epithelial marker expression when cultured on different human recombinant laminins

Laminins are, together with collagen fibres, the most abundant components of the BM [347]. By binding to integrin receptors and other membrane molecules, they critically regulate cell attachment, differentiation, migration and other cell functions [424]. Additionally, specific laminins have been robustly demonstrated as regulating agents of the differentiation of several cell types, including conjunctival ECs [425]. Moreover, different preparations of mixed laminins have previously been shown to modulate ocular surface EC differentiation via alternate signalling pathways, however these studies involved crude preparations of mixed laminins [304]. Therefore, they are good candidates for contributing to the differentiation process. In this study, the cultureware was coated with a single recombinant laminin isoform for a better specificity and controlled studies. In this study all the commercially available laminin isoforms were tested for a more complete screening of their potential on modulating cell differentiation. The expression of six epithelial transcripts by HCjE-Gi cells when cultured in 8 human recombinant laminin isoforms was assessed by Reverse Transcriptase qPCR and normalised to the GAPDH levels of HCjE-Gi cells cultured on TCPS.

3.3.5.1.1. Expression of corneal epithelial cell markers

HCjE-Gi cells cultured on LAM-111 and LAM-211 showed higher levels of KRT3 transcript levels when compared to those in TCPS ($p<0.001$); additionally, KRT3 transcript expression to be higher in cells cultured on LAM-211 when compared to LAM-121, -221, -411, and -521 ($p\leq0.05$), Figure 54. HCjE-Gi cells cultured on LAM-121 showed higher levels of KRT12 expression when compared to those in TCPS, Figure 54.

3.3.5.1.2. Expression of conjunctival epithelial cell markers

Regarding the expression of KRT7 and KRT13 transcripts, their levels appeared to be higher when HCjE-Gi cells are cultured on LAM-111, -211, and -421 than those cultured in LAM-121, -221, -411, -521, and TCPS ($p\leq0.05$), Figure 54.

3.3.5.1.3. Expression of epithelial stem cell markers

No significant differences were appreciated on ΔNp63 levels between the various conditions; although the expression of ABCB5 was shown to be higher on LAM-421 when compared to the other coating proteins ($p\leq0.05$), Figure 54. Noteworthy is the absence of ΔNp63

transcript expression by HCjE-Gi cells cultured on LAM-121 and LAM-221 (blue arrows), Figure 54.

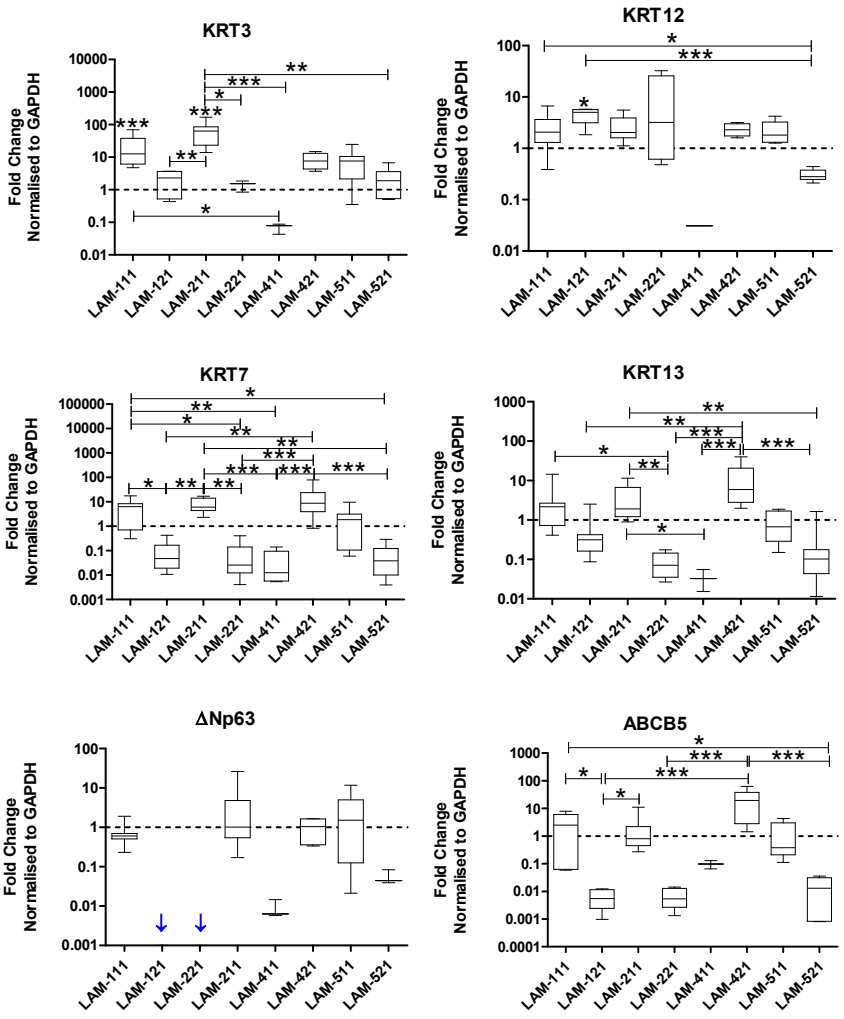

Figure 54 - The expression of epithelial cell markers by HCjE-Gi cells when cultured on top of several recombinant laminin isoforms as assessed by Reverse Transcriptase qPCR. (Data is represented as median ± 5-95 percentile, n≥6, Kruskal-Wallis test followed by Dunn's Multiple comparison test, *p<0.05, **p<0.01, ***p<0.001). Dashed line represents the basal expression of the markers of interests when cells are cultured on TCPS. Arrows represent gene expression not detectable in that laminin isoform. Abbreviations used GAPDH: glyceraldehyde 3-phosphate dehydrogenase, LAM: laminin, KRT: keratin, ABCB5: ATP-binding cassette sub-family B member 5, TCPS: tissue culture polystyrene.

3.3.5.2. General laminin screening – hTCEpi cells show different epithelial marker expression when cultured on different human recombinant laminins

The expression levels of the same six epithelial transcripts by hTCEpi cells when cultured in 8 human recombinant laminin isoforms were assessed by Reverse Transcriptase qPCR. Their expression was normalised to the GAPDH levels of hTCEpi cells cultured on TCPS.

3.3.5.2.1. Expression of corneal epithelial cell markers

hTCEpi cells cultured on LAM-111, -211, -521 showed higher levels of KRT3 expression than those cultured on LAM-411, and those cultured on LAM-511 expressed higher levels of KRT12 than those cultured on LAM-411 ($p<0.05$), Figure 55.

3.3.5.2.2. Expression of conjunctival epithelial cell markers

hTCEpi cells seeded on LAM-121, -221, and -411 expressed lower levels of KRT7 than those cultured on LAM-211, -421, and TCPS ($p\leq0.05$). hTCEpi cells cultured on LAM-411 expressed lower levels of KRT13 than those cultured on LAM-421, -511, -521, and TCPS ($p\leq0.05$), Figure 55.

3.3.5.2.3. Expression of epithelial stem cell markers

Cells cultured on LAM-411 showed lower expression of ΔNp63 than those on LAM-421 and LAM-511; and lower levels of ABCB5 than those cultured on TCPS, Figure 55. Noteworthy was the absence of KRT12, ΔNp63, and ABCB5 transcript expression by hTCEpi cells when cultured on LAM-221 (blue arrows), ΔNp63 and ABCB5 when in LAM-521 (red arrows), Figure 55.

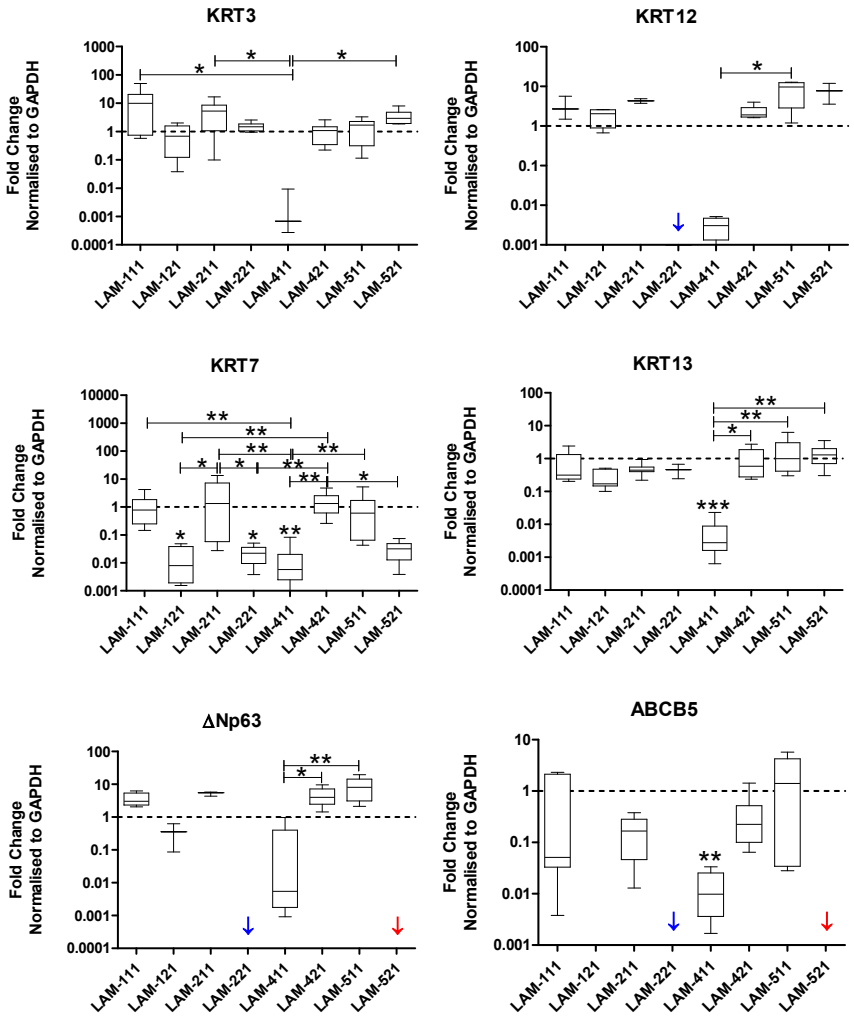

Figure 55 - The expression of epithelial cell markers by hTCEpi cells when cultured on top of several recombinant laminin isoforms as assessed by Reverse Transcriptase qPCR. (Data is represented as median ± 5-95 percentile, n≥6, Kruskal-Wallis test followed by Dunn's Multiple comparison test, *p<0.05, **p<0.01, ***p<0.001). Dashed line represents the basal expression of the markers of interests when cells are cultured on TCPS. Arrows represent gene expression not detectable in that laminin isoform. Abbreviations used GAPDH: glyceraldehyde 3-phosphate dehydrogenase, LAM: laminin, KRT: keratin, ABCB5: ATP-binding cassette sub-family B member 5, TCPS: tissue culture polystyrene.

Taken together, the previous observations suggest that cells cultured in LAM-511 did not retain fully differentiated characteristics as seen by the high expression of putative SC markers. In conjunction with these results and based on others' investigations related to its distribution throughout the surface of human eye [46] and its role in maintaining the overlying cells in an undifferentiated state [310, 311, 426, 427], this isoform was chosen to further investigate its role on modulating EC differentiation.

3.3.6. HCjE-Gi cells respond differently to different concentrations of LAM-511

HCjE-Gi cells were cultured on surfaces functionalized with different concentrations of LAM-511 and the transcript expression of six epithelial markers was normalized to the expression of GAPDH of HCjE-Gi cells cultured of TCPS.

HCjE-Gi cells cultured on surfaces coated with 10µg/mL showed higher levels of expression of all keratin transcripts when compared to those seeded on TCPS and on surfaces functionalized with lower LAM-511 concentrations ($p \leq 0.05$, with some exceptions). Noteworthy was the absence of KRT12 expression when HCjE-Gi cells were cultured on 2.5µg/mL coated cultureware (blue arrow). Regarding the expression of epithelial SC markers, HCjE-Gi cells cultured on 2.5µg/mL showed higher expression of ΔNp63 (10-fold increase, $p \leq 0.05$), and 10µg/mL led to higher levels of ABCB5 expression when compared to cells cultured on surfaces coated with 1µg/mL and 5µg/mL of LAM-511 (8.8-fold increase, $p \leq 0.01$), Figure 56.

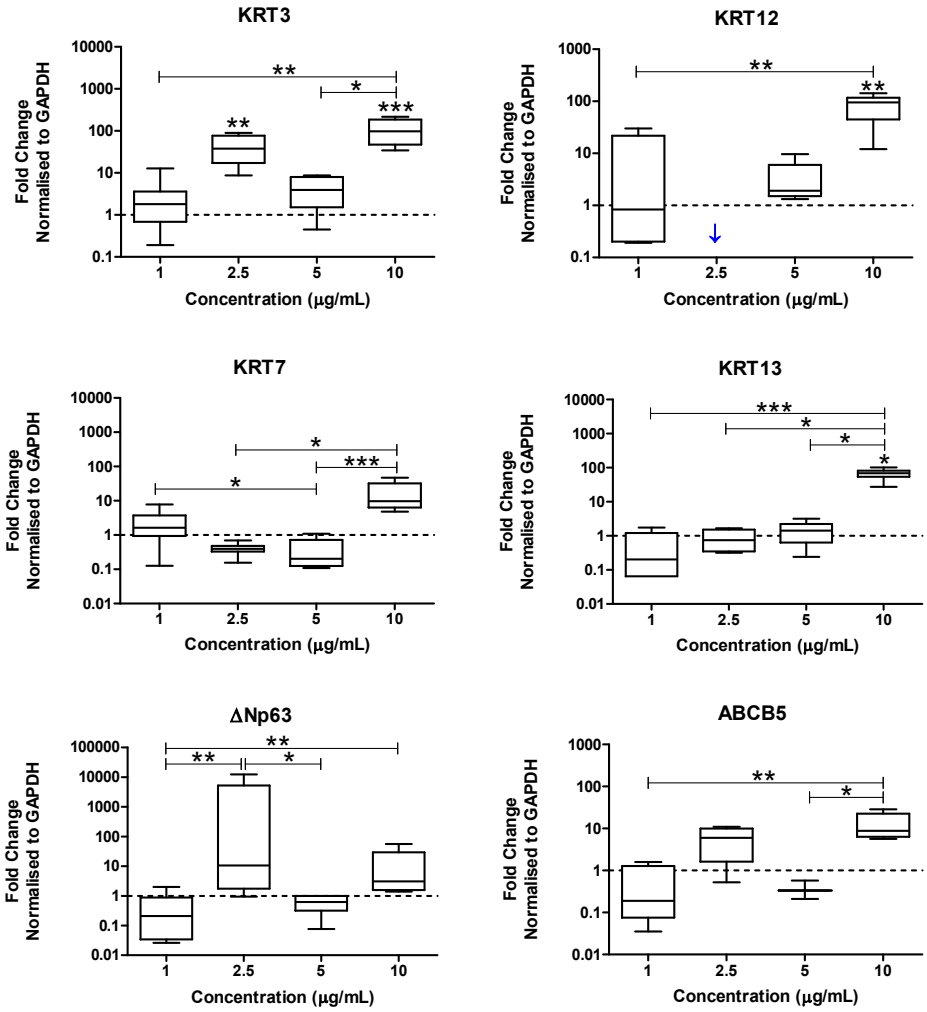

Figure 56 - The expression of epithelial cell markers by HCjE-Gi cells when cultured on top of surfaces coated with various concentrations of human recombinant laminin-511 as assessed by Reverse Transcriptase qPCR. (Data is represented as median ± 5-95 percentile, n≥6, Kruskal-Wallis test followed by a Dunn's Multiple Comparison test, *p<0.05, **p<0.01, ***p<0.001). Dashed line represents the basal expression of the markers of interests when cells are cultured on TCPS. Arrows represent gene expression not detectable in that laminin concentration. Abbreviations used GAPDH: glyceraldehyde 3-phosphate dehydrogenase, KRT: keratin, ABCB5: ATP-binding cassette sub-family B member 5, TCPS: tissue culture polystyrene.

3.3.7. hTCEpi cells respond differently to different concentrations of LAM-511

hTCEpi cells were cultured on surfaces functionalized with different concentrations of LAM-511 and the transcript expression of six epithelial markers was normalized to the expression of GAPDH levels of hTCEpi cells cultured on TCPS.

hTCEpi cells cultured on 5µg/mL coated surfaces showed changes in keratin expression profile. Briefly, significant higher levels of KRT3, KRT12, and KRT13 expression on 5µg/mL coated surfaces were observed when compared to cells seeded on others LAM-511 concentrations. Regarding the expression of epithelial SC markers, hTCEpi cells cultured on lower concentrations of LAM-511 (2.5-5µg/mL) appeared to express higher levels of ΔNp63 and ABCBC5 when compared to those cultured on other LAM-511 concentrations, Figure 57.

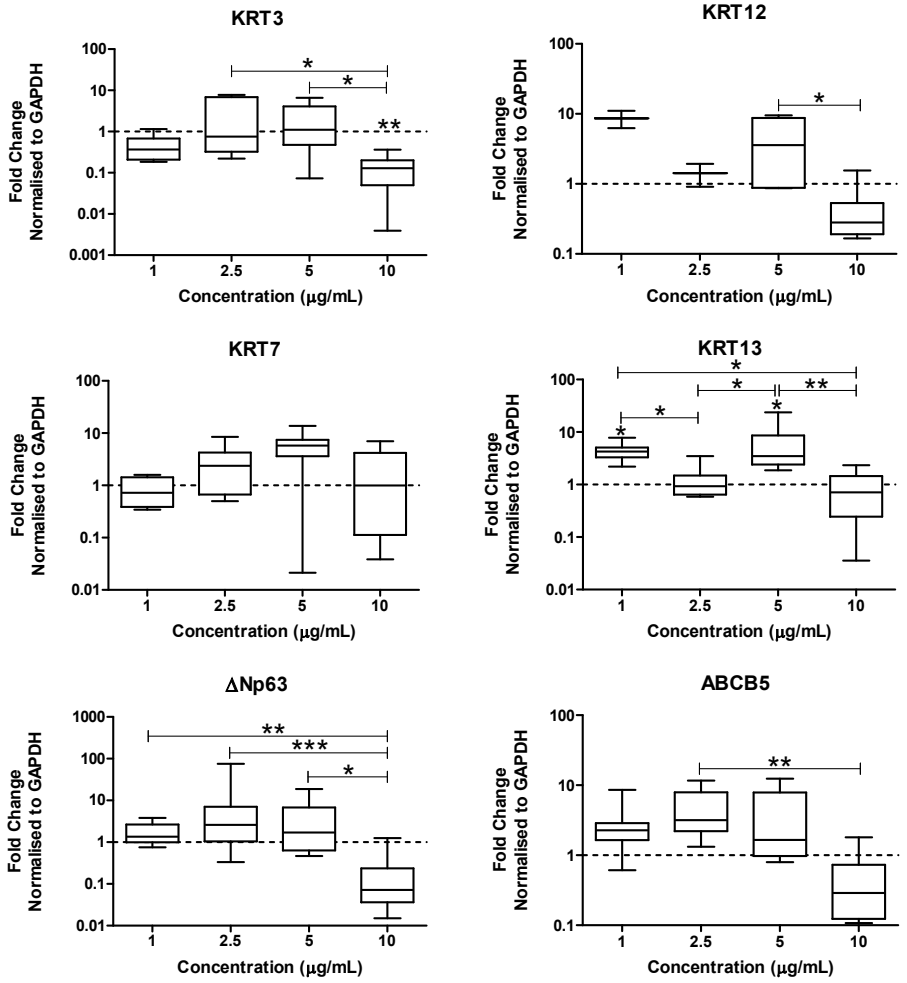

Figure 57 - The expression of epithelial cell markers by hTCEpi cells when cultured on top of surfaces coated with varied concentrations of human recombinant laminin-511 as assessed by Reverse Transcriptase qPCR. (Data is represented as median ± 5-95 percentile, n≥6, Kruskal-Wallis test followed by a Dunn's Multiple Comparison test, *p<0.05, **p<0.01, ***p<0.001). Dashed line represents the basal expression of the markers of interests when cells are cultured on TCPS. Abbreviations used GAPDH: glyceraldehyde 3-phosphate dehydrogenase, KRT: keratin, ABCB5: ATP-binding cassette sub-family B member 5, TCPS: tissue culture polystyrene.

3.3.7.1. Summary of results 9:

i. HCjE-Gi cells cultured on surfaces coated with 10µg/mL of LAM-511 showed higher levels of EC markers transcripts, including corneal (KRT3 and KRT12), conjunctival (KRT7 and KRT13), and SC (ABCB5) epithelial markers.

ii. hTCEPi cells cultured on surfaces coated with 5µg/mL of LAM-511 exhibited higher levels of transcripts that encode for corneal (KRT3 and KRT12) and conjunctival (KRT7 and KRT13) epithelial markers.

iii. Cell response to functionalized surfaces is LAM-511-concentration dependent.

3.3.8. HCjE-Gi cells' response to LAM-511 functionalized substrates is time-dependent

Because cell response showed to be laminin isoform and concentration-dependent, the time-dependency was considered and further investigated. For this purpose, HCjE-Gi cells were cultured on top of cultureware coated with 10µg/mL of LAM-511, the transcript expression of six epithelial markers was then assessed over 5 days and normalised to the expression of GAPDH levels of HCjE-Gi cells cultured of TCPS.

HCjE-Gi cells cultured on LAM-511 for 3 days showed higher expression levels of KRT3 and ΔNp63 than those kept in culture for 5 days (24- and 2-fold increase, respectively $p<0.001$). Additionally, the expression levels of KRT3 by HCjE-Gi cells cultured on functionalized scaffolds for 3 days were higher than those observed for HCjE-Gi cells cultured on TCPS (24-fold increase, $p<0.05$), Figure 58. No KRT12 transcript expression was detected when HCjE-Gi cells were cultured on TCPS for 3 days, consequently no statistical analysis could be performed (blue arrows), Figure 58.

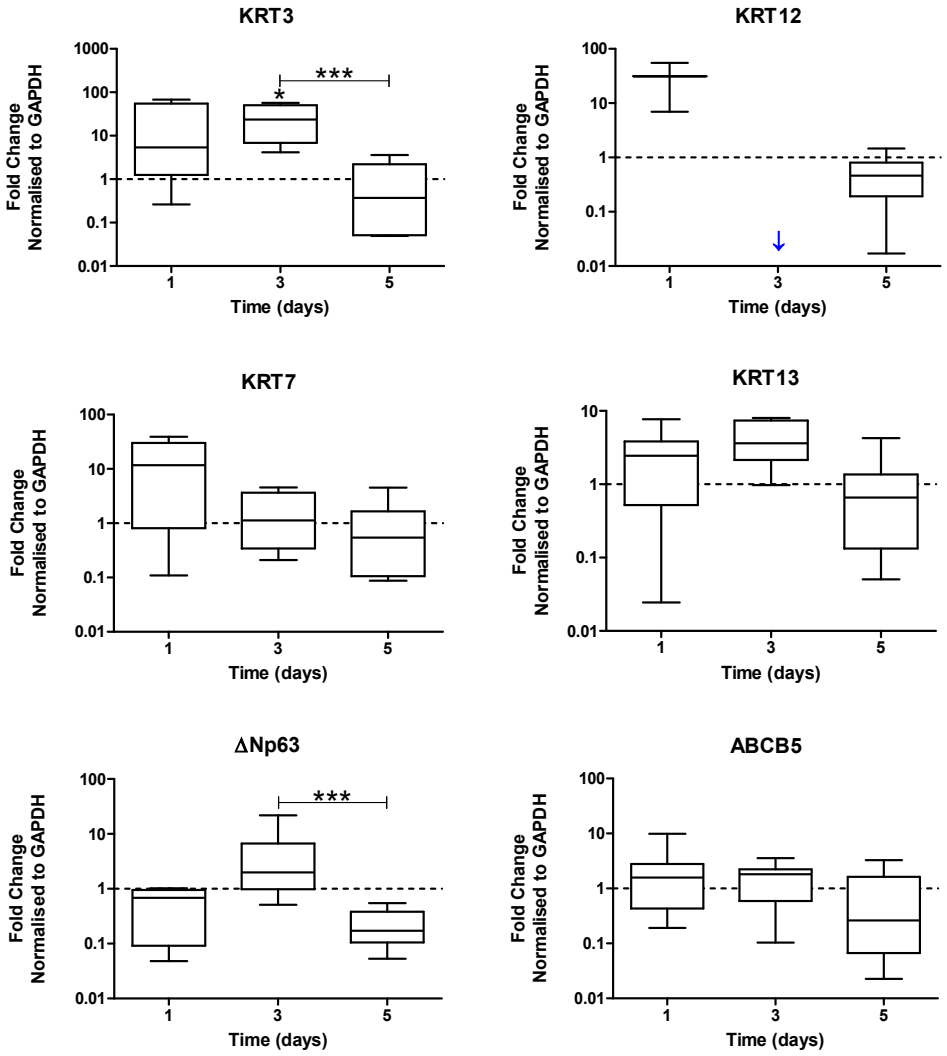

Figure 58 - The expression of epithelial cell markers by HCjE-Gi cells when cultured on top of recombinant laminin-511 over 5 days as assessed by Reverse Transcriptase qPCR. (Data is represented as median ± 5-95 percentile, n≥6, Kruskal-Wallis test followed by a Dunn's Multiple Comparison test, *p<0.05, **p<0.01, ***p<0.001). Dashed line represents the basal expression of the markers of interests when cells are cultured on TCPS. Arrows represent gene expression not detectable in that time point. Abbreviations used GAPDH: glyceraldehyde 3-phosphate dehydrogenase, TCPS: tissue culture polystyrene, KRT: keratin, ABCB5: ATP-binding cassette sub-family B member 5.

3.3.9. hTCEpi cells' response to LAM-511 functionalized substrates is time-dependent

In this section, hTCEpi cells were cultured on top of cultureware coated with 5µg/mL of recombinant LAM-511, the transcript abundance of six epithelial markers was then assessed over 5 days and normalized to the expression of GAPDH levels of hTCEpi cells cultured on TCPS.

hTCEpi cells cultured on LAM-511 for 3 days showed higher expression levels of KRT3, KRT7, and ABCBB5 than those left in culture for 5 days (5.1-, 6.4-, and 2.3-fold increase respectively, p≤0.05). Additionally, the transcript abundance of KRT12, KRT7, and KRT13 by hTCEPi cells (12-, 6.4-, and 3.8-fold increase respectively, p≤0.01) was also higher for cells kept in culture for 3 days when compared to those maintained in culture for 1 day only, Figure 59.

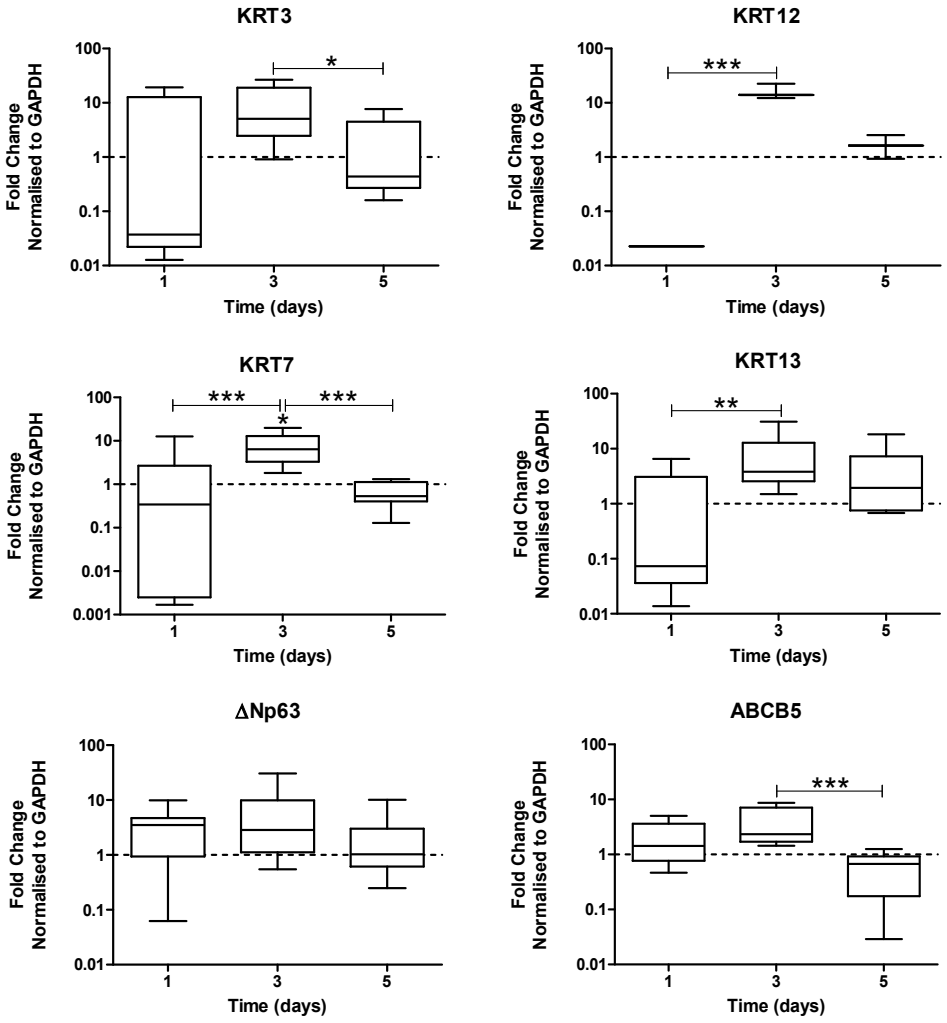

Figure 59 - The expression of epithelial cell markers by hTCEpi cells when cultured on top of recombinant laminin-511 over 5 days as assessed by Reverse Transcriptase qPCR. (Data is represented as median ± 5-95 percentile, n≥6, Kruskal-Wallis test followed by a Dunn's Multiple Comparison test, *p<0.05, **p<0.01, ***p<0.001). Dashed line represents the basal expression of the markers of interests when cells are cultured on TCPS. Abbreviations used GAPDH: glyceraldehyde 3-phosphate dehydrogenase, TCPS: tissue culture polystyrene, KRT: keratin, ABCB5: ATP-binding cassette sub-family B member 5.

3.3.9.1. Summary of results 10:

i. HCjE-Gi cells seeded for 3 days on surfaces functionalized with 10µg/mL of LAM-511 showed significant alterations in their EC markers expression profile.

ii. hTCEpi cells cultured on surfaces coated with 5µg/mL of LAM-511 for 3 days showed significant alterations in their expression profile of EC markers.

iii. Cell response to functionalized substrates is time-dependent.

3.3.10. The protein residues' phosphorylation and cleavage levels are reduced when cells are cultured on surfaces coated with ECM proteins

PathScan® Intracellular Signalling Array Kit was used to monitor the expression of 18 signalling molecules that are phosphorylated or cleaved in response to signal-transduction pathway activation, Figure 60. Different conditions were selected for these studies following the modulation observed at keratin profiling: HCjE-Gi and hTCEpi cells cultured on TCPS (control), HCjE-Gi and hTCEpi cells cultured on HCjE-Gi ECM proteins and on hTCEpi ECM proteins for three days, following "de-roofing", and HCjE-Gi and hTCEpi cells cultured for three days on surfaces coated with 10µg/mL and 5µg/mL of LAM-511, respectively.

A significant decrease in phosphorylation or cleavage levels of nearly all proteins was observed when HCjE-Gi cells were seeded in pre-coated cultureware, regardless the ECM proteins preparation. This trend was not observed in the levels of p70 S6 kinase, p53, p38, SAP/JNK, and caspase-3 residue phosphorylation. Very similar results were seen for the hTCEpi cells. Additionally, no changes in STAT1, S6 ribosomal protein, mTOR and PARP residue phosphorylation or cleavage levels were shown when hTCEpi cells were cultured on pre-coated cultureware, Figure 61.

A

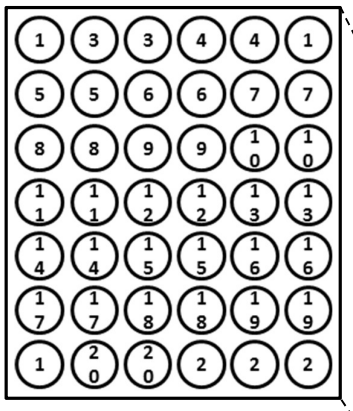

B

	Target	Phosphorylation site
1	Positive Control	N/A
2	Negative Control	N/A
3	ERK1/2	Thr202/Tyr204
4	Stat1	Tyr701
5	Stat3	Tyr705
6	Akt	Thr308
7	Akt	Ser473
8	AMPKα	Thr172
9	S6 Ribosomal protein	Ser235/236
10	mTOR	Ser2448
11	HSP27	Ser78
12	Bad	Ser112
13	p70 S6 Kinase	Thr389
14	PRAS40	Thr246
15	P53	Ser15
16	P38	Thr180/Tyr182
17	SAPK/JNK	Thr183/Tyr185
18	PARP	Asp214
19	Caspase-3	Asp175
20	GSK-3β	Ser9

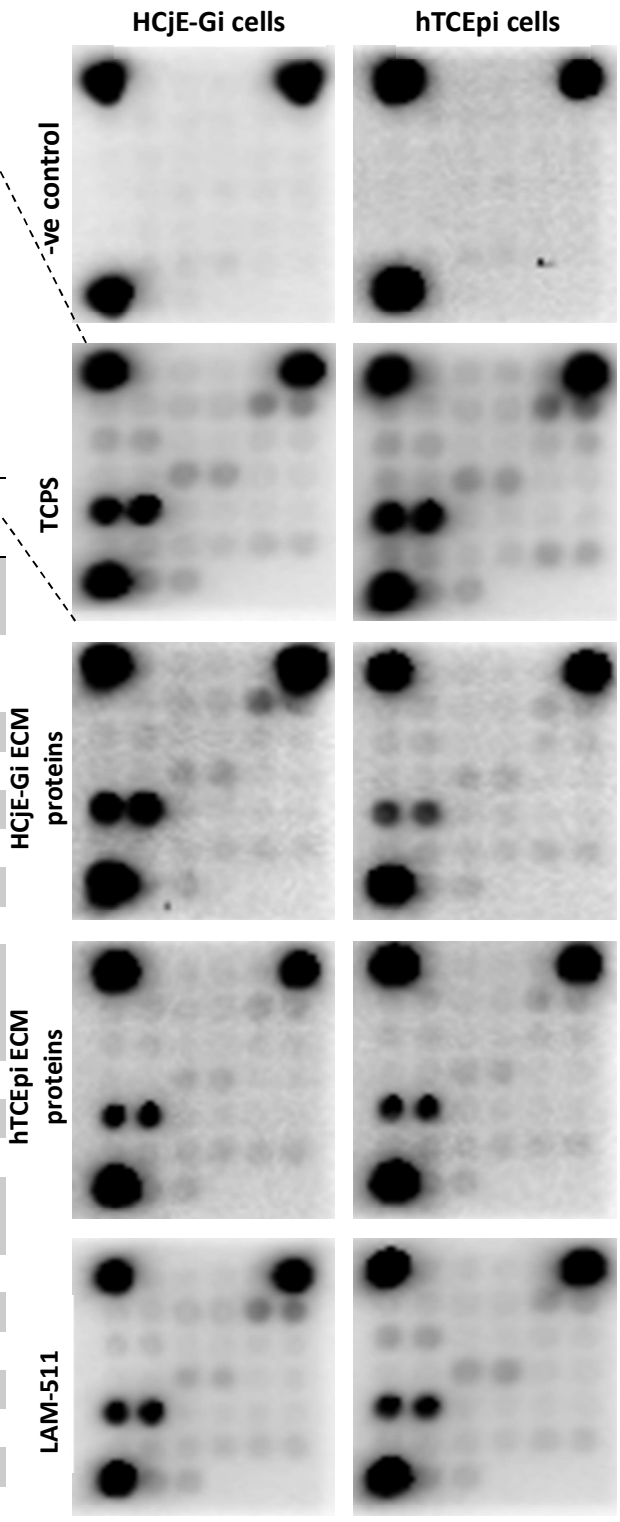

Figure 60 - PathScan® Intracellular Signalling Array. (A) Target map (B) Chemiluminescent readout (C) immunoblotting. Abbreviations used: TCPS: tissue culture polystyrene, ECM: extracellular matrix, LAM: laminin.

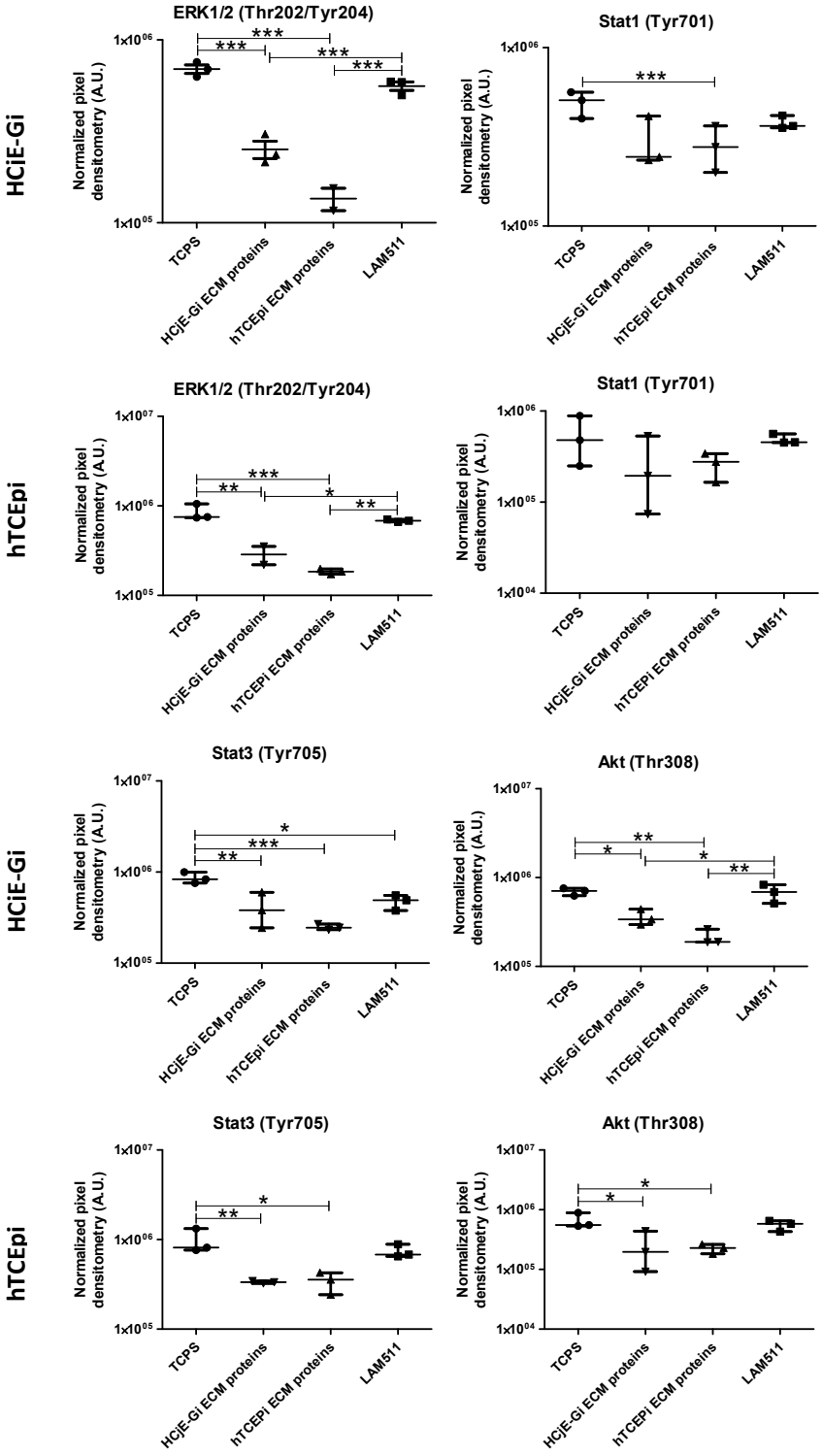

Figure 61 (continued) 1/5 - Densitometry quantification of PathScan® Intracellular Signalling Array of HCjE-Gi and hTCEpi cells when cultured in different matrices. (Data is represented as median ± 5-95 percentile, n≥3, One-way ANOVA followed by Tukey's Multiple Comparison Test, *p<0.05, ** p<0.01, *** p<0.001). Abbreviations used A.U. arbitrary units, ECM: extracellular matrix, LAM: laminin.

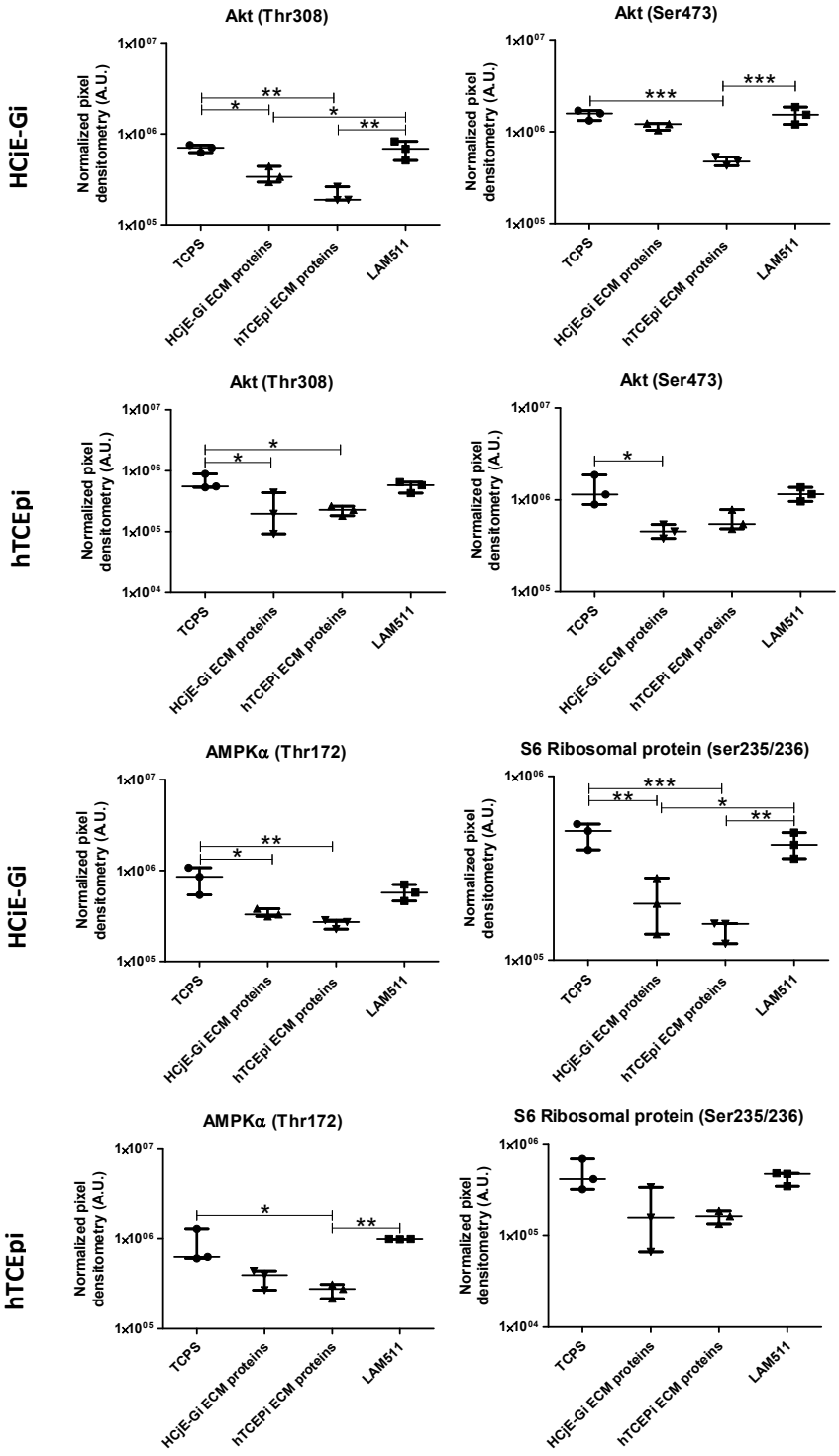

Figure 61 (continued) 2/5 - Densitometry quantification of PathScan® Intracellular Signalling Array of HCjE-Gi and hTCEpi cells when cultured in different matrices. (Data is represented as median ± 5-95 percentile, n≥3, One-way ANOVA followed by Tukey's Multiple Comparison Test, *p<0.05, ** p<0.01, *** p<0.001). Abbreviations used A.U. arbitrary units, ECM: extracellular matrix, LAM: laminin.

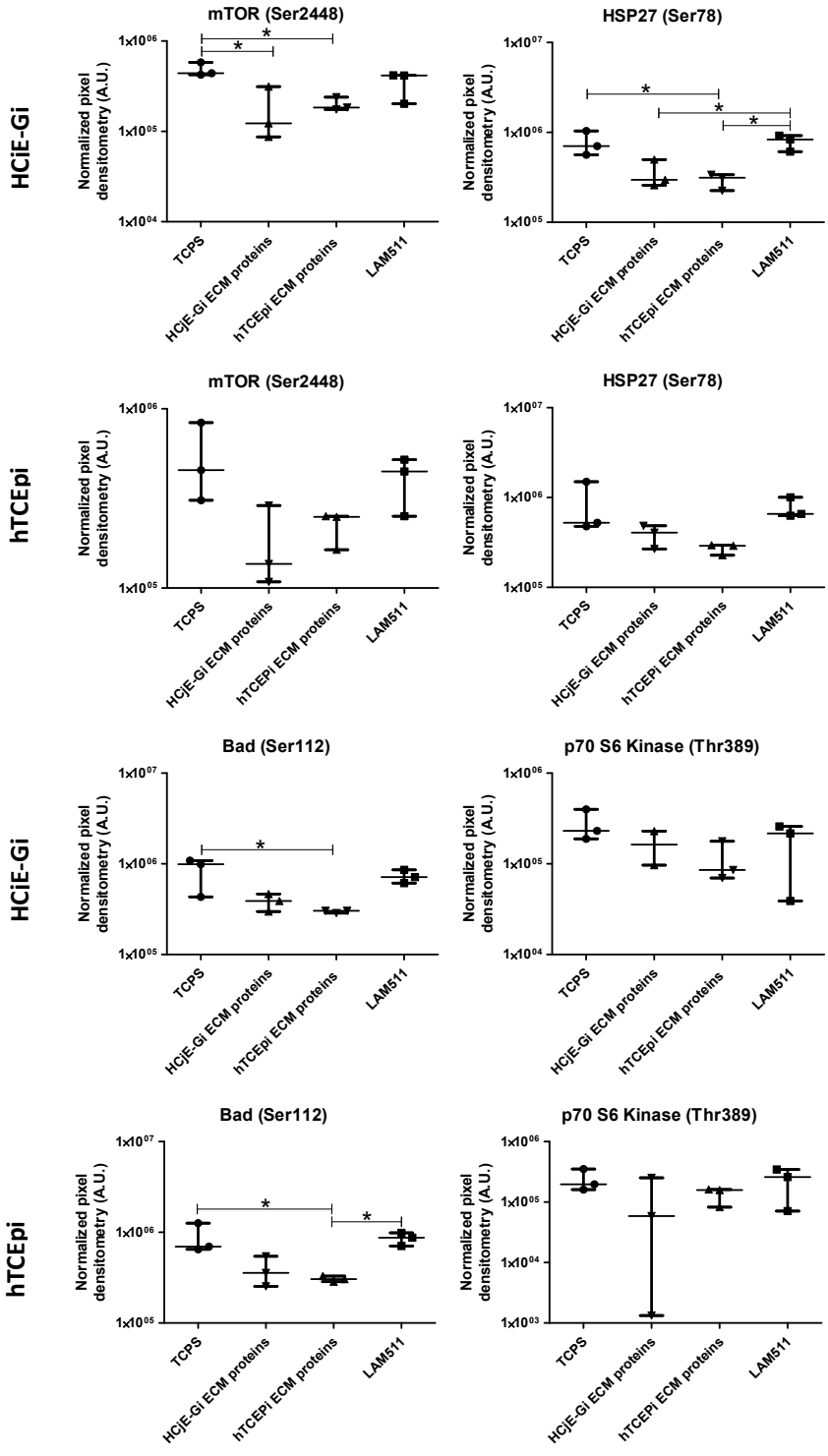

Figure 61 (continued) 3/5 - Densitometry quantification of PathScan® Intracellular Signalling Array of HCjE-Gi and hTCEpi cells when cultured in different matrices. (Data is represented as median ± 5-95 percentile, n≥3, One-way ANOVA followed by Tukey's Multiple Comparison Test, *p<0.05, ** p<0.01, *** p<0.001). Abbreviations used A.U. arbitrary units, ECM: extracellular matrix, LAM: laminin.

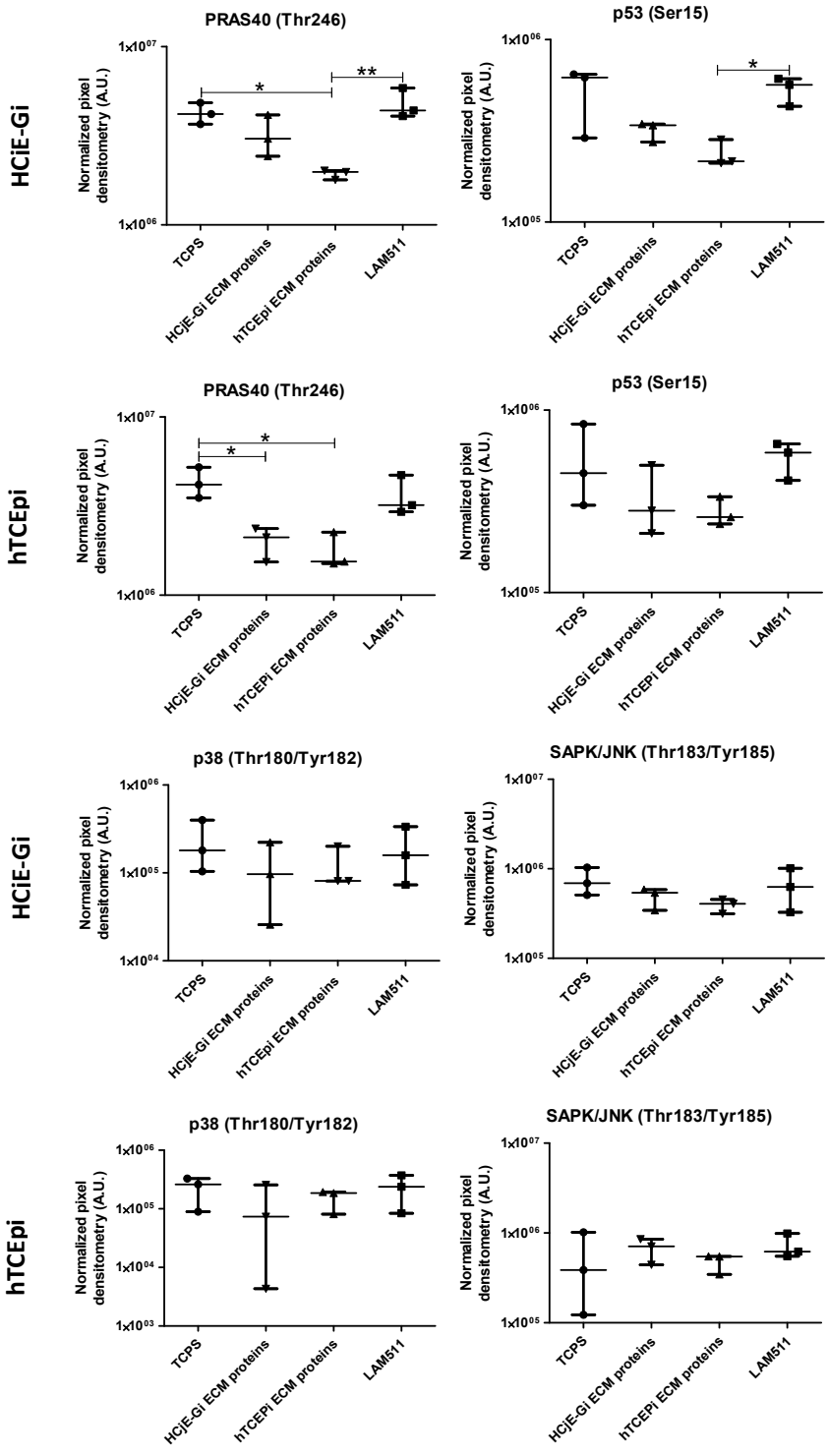

Figure 61 (continued) 4/5 - Densitometry quantification of PathScan® Intracellular Signalling Array of HCjE-Gi and hTCEpi cells when cultured in different matrices. (Data is represented as median ± 5-95 percentile, n≥3, One-way ANOVA followed by Tukey's Multiple Comparison Test, *p<0.05, ** p<0.01, *** p<0.001). Abbreviations used A.U. arbitrary units, ECM: extracellular matrix, LAM: laminin.

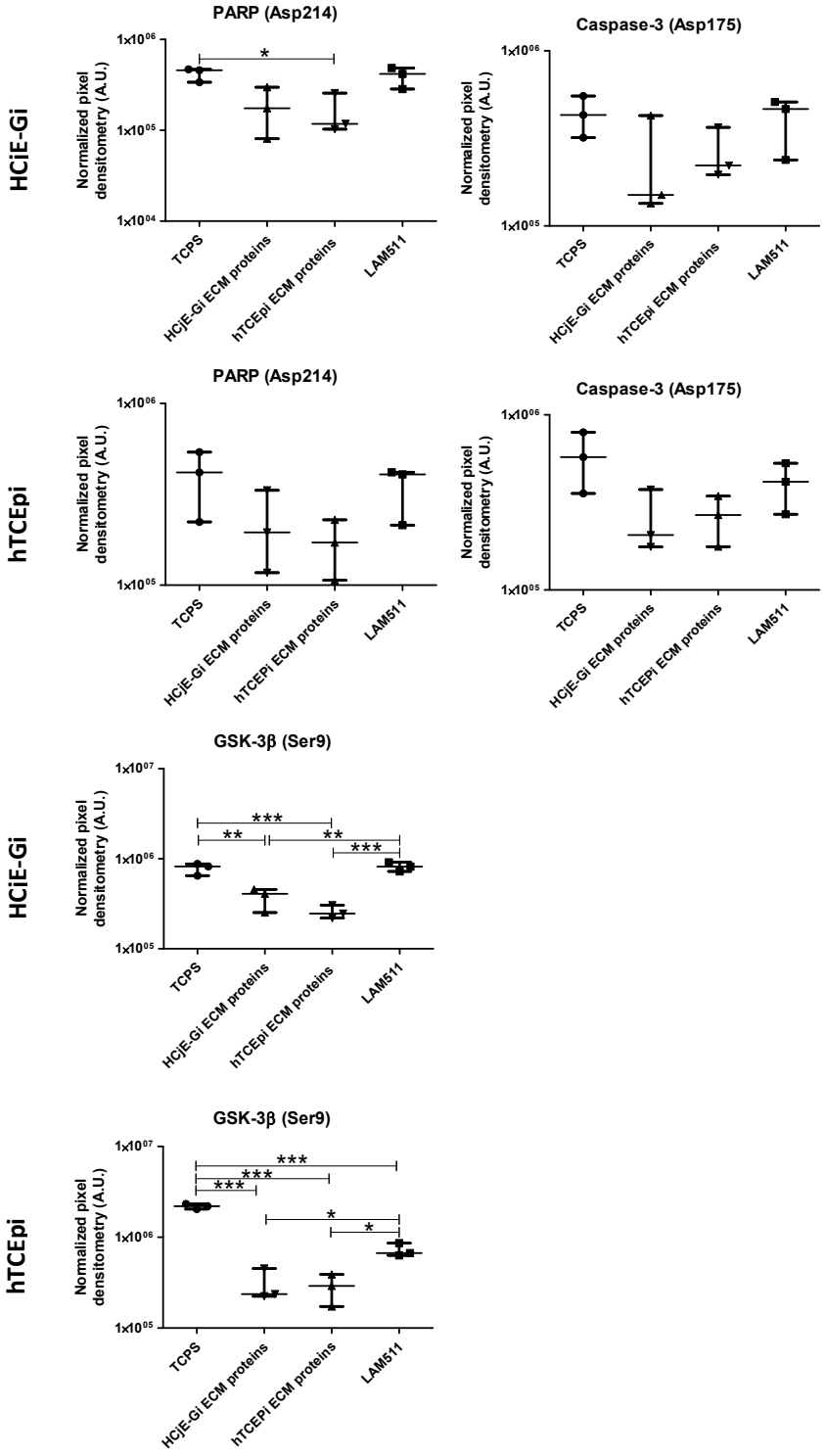

Figure 61 (continued) 5/5 - Densitometry quantification of PathScan® Intracellular Signalling Array of HCjE-Gi and hTCEpi cells when cultured in different matrices. (Data is represented as median ± 5-95 percentile, n≥3, One-way ANOVA followed by Tukey's Multiple Comparison Test, *p<0.05, ** p<0.01, *** p<0.001). Abbreviations used A.U. arbitrary units, ECM: extracellular matrix, LAM: laminin.

3.3.10.1. Summary of results 11:

i. A significant decrease in phosphorylation and cleavage levels of nearly all protein residues was observed when HCjE-Gi and hTCEpi cells were seeded in pre-coated cultureware, regardless the ECM preparation used.

ii. Similar signalling pathways were activated in the differentation of the two cell lines used.

3.3.11. Summary of results of Chapter 3:

i. The "de-roofing" method showed to be reliable as a vast subset of ECM proteins and growth factors were found by mass spectrometry in both cell lines lysates.

ii. The expression of COLXVIIα1, LAMα5, LAMβ1, and LAMβ2 over-time appeared to be cell-dependent.

iii. Cells were sensitive to the underlying substrate, i.e. surfaces coated with different laminin isoforms induced different keratin profiling expression.

iv. The cell response to LAM-511 functionalised substrates was concentration and time in culture-dependent.

v. A decrease in residue phosphorylation and cleavage levels was observed for both cell lines when cells were cultured on pre-coated cultureware, regardless of the ECM preparation used.

3.4. Discussion

The studies in this chapter assessed the composition of ECM produced by the two cell lines and the plasticity of two terminally differentiated ECs towards desired epithelial lineages upon culture on substrates functionalized with one single laminin isoform.

3.4.1. Characterization of the ECM produced by the two cell lines

Mass spectrometry data showed a cell-dependent ECM composition, despite some proteins were shown to be present in both matrices. The most abundant proteins found in both matrices, and therefore unlikely to be involved in the process of differentiation into specific lineage, include fibronectin, the three chains that comprise LAM-332, various integrin chains, tenascin, and thrombospondins. Fibronectin [46], LAM-332 [46], and integrin α3β1, α6β1, and α6β4 [428] were all also found by others to be present in the conjunctival and corneal BM. On the other hand, tenascin-C and thrombospondin-1, here found in both matrices, are suggested to be enriched in the limbal and cornea regions, respectively [46].

Mass spectrometry results showed COLXVIIα1, LAMα5, and LAMβ1 to be specific for one or another ECM, and therefore likely to be involved in the process of cell differentiation. For this reason, their production and expression was further investigated.

COLXVIIα1 is a protein involved in the formation of HDs and consequently involved in the adhesion of cells to the underlying substrate [420]. Its higher expression levels detected in hTCEpi cells (Reverse Transcriptase qPCR and flow cytometry) suggest a stronger and more cohesive interaction cell-substrate. These results were expected since conjunctiva is a looser structure when compared to cornea [8, 429]. Others have suggested, not only the presence of COLXVIIα1 in human corneal tissues, but also a close regulation of mRNA and protein levels with increases and decreases in mRNA preceding those of the protein by approximately 2 days [430].

LAMα5 isoform trimers with LAMβ1 and LAMγ1 to form LAM-511 or with LAMβ2 and LAMγ1 to form LAM-521 [353], thus the expression profile of their individual chains should follow similar trends. The transcript expression of LAMα5 and LAMβ1 by HCjE-Gi cells showed a better match than LAMα5 and LAMβ2, which may suggest that LAM-511 is produced at higher levels than LAM-521 by those cells.

Immunocytochemistry (ICC) results confirmed the production of all four proteins by the two cell lines. Others have also localized COLXVIIα1, LAMα5, and LAMβ1 within both the cornea

and conjunctival BM [46, 431]. LAMβ2, on the other hand, has been mostly localized in the conjunctiva [46, 304, 352] and limbus BM [46]. COLXVIIα1 presence in the ECM appears to be delayed in comparison with all other three laminin chains.

Based on mass spectrometry, Reverse Transcriptase qPCR, flow cytometry, and ICC data, the four proteins are produced by the two cell lines. However, their production levels appear to be cell and time-dependent. Briefly, the latter three data sets showed higher expression of the four proteins by hTCEpi cells over time. The time specificity and differences in protein production profiles may be the trigger agent to the different cell responses upon culture in the different matrices. Others have yet suggested that even in similar matrices, the organizational states of the common ECM molecules and/or the way such components interact with each other and/or with other soluble factors may provide tissue specificity [170, 294]. However, the results in this section not only considered the potential interactions between all the proteins present in the ECM but also their interactions with growth factors and other soluble factors, as these were shown not to be washed away by the "de-roofing" method.

3.4.2. Cell response to the functionalized substrate is laminin isoform-dependent

Functionally, laminin isoforms are known to regulate the differentiation of ECs [432]. Differences in the laminin composition of the conjunctival and corneal BM provide circumstantial evidences for some external modulation of EC differentiation [30, 425]. Consistent with these observations, our experiments showed that different recombinant laminins isoforms have different effects on the expression profiles of various EC markers.

Cells cultured on LAM-411 showed the lowest expression of epithelial markers. One study has shown this isoform to have the lowest binding affinity to integrins [433], which may impair the formation of adhesion complexes and *per se* the integrity of overlying cultured ECs.

HCjE-Gi cells cultured on functionalized substrates that contain LAMβ2 showed higher levels of corneal EC markers KRT3 and KRT12 and lower levels of conjunctival EC markers KRT7 and KRT13 when compared to cells cultured on uncoated substrates. These results are in some way contradictory with the work of Kurpakus and Lin, who showed that the lack of LAMβ2 is correlated with the loss of expression of KRT4 [425], that dimers with KRT13 to form intermediate filaments. Two different reasons may explain these differences; firstly, the time

in culture; 5 days in the herein studies versus the 14 days on Kurpakus and Lin's work; secondly, they used a purified LAMβ2 chain whilst here was used a whole laminin isoform that contain that specific chain. Interestingly, it is in the substrates that contain both LAMβ2 and LAMγ1 (LAM-121, -221, and -521) that HCjE-Gi express higher values of the corneal markers and lower values of conjunctival markers. Very scarce information is published on the effects of LAMγ1 in the ocular cell differentiation. It is present in both cornea and conjunctival BM [46] and its knockout is lethal [434] due to the lack of BM formation [435]. It was also associated with the differentiation of Schwann cells [436]. The results may suggest that HCjE-Gi cells cultured in LAM-111, -211, and -421 are in a less differentiation state as they expressed not only the conjunctiva-associated markers, KRT7 and KRT13, but also the associated corneal markers KRT3 and KRT12. Similar observations were obtained by Wei et al., who by culturing conjunctival ECs on feeder layers observed the expression of KRT5/14, hyperproliferative keratins KRT6/16, small amounts of KRT3 and KRT12, and KRT8/18 [30]. Suggesting that in appropriate culture conditions conjunctival ECs do not retain fully differentiation characteristics [30] and consequently they may either be in a hyperproliferative or in a dedifferentiation state.

On the opposite equivalent direction, hTCEpi cells cultured on LAM-111, and LAM-511 expressed higher levels of corneal markers and lower levels of conjunctival markers. These two laminin isoforms, are together with LAM-332, the most abundant in the cornea BM [352, 366, 437]. These observations suggested that the mimicry of the corneal environment, by using these two isoforms, is correlated with the differentiation of corneal ECs, as shown by others using different systems [425]. Moreover, when hTCEpi cells were cultured on the suggested conjunctival laminin isoforms (LAM-121, -221, and -521 [46, 438]) the expression levels of the conjunctival markers were not statistically different. Despite being observed, the expression levels of such markers was lower when compared to the results seen in Chapter 2. Two reasons may explain these results; firstly, the cells in Chapter 3 were cultured on single laminin isoforms and not in the protein and growth factor meshwork as in Chapter 2; secondly, the cells were kept in culture for 5 days, whilst others' studies have cultured cells in crude laminin preparations for longer (9-14 days) [425]. Taken together these observations suggested that, despite cell responsiveness to the external environment, single laminin isoforms are not sufficient to promote complete cell differentiation into specific lineages.

To assess the issues related with time and concentration-dependent response, cells were cultured in surfaces coated with different LAM-511 concentrations and for variable periods of time. LAM-511 was chosen for substrate functionalization because its role in maintaining the undifferentiated state of mESCs [311], hESC [313] and to be efficiently used as substrate for the *ex vivo* expansion of human limbal epithelial progenitor cells [439].

LAM-511 has been located in conjunctival, corneal and limbal BM, but appears to be enriched in the latter [46], which helps to understand why cells cultured in substrates functionalized with such laminin isoform start to lose their differentiation characteristics to gain those associated with dedifferentiated cells. Indeed, our results showed that both cell lines when cultured in LAM-511 express several keratins, including KRT3, KRT12, KRT7, and KRT13 suggesting that the cultured cells did not retain fully differentiated characteristics. To further corroborate these results, the expression of the two epithelial SC markers showed the highest levels under the same conditions where the keratin expression levels were also the highest. These results suggested an emergence of progenitor ECs. Others have showed an optimal concentration of this protein to support the efficient adhesion and expansion of human pluripotent SCs ranging from 3-6µg/cm^2 (equivalent to roughly 30-60µg/mL) [313], considerably higher than the used in the hereby studies.

The mechanism of differentiation appears to be concentration dependent, with 10 and 5µg/mL inducing the highest expression of epithelial markers by HCjE-Gi and hTCEpi cells, respectively. Additionally, the cell response to LAM-511 seems also to be time-dependent, with both cell lines showing higher expression of ECs' markers at day 3. Some investigators have suggested that the process of cell re-differentiation may be preceded by an intermediate step of cell de-differentation requiring cell division, however not obligatory in all cases [212]. Both cell lines used in this study show a doubling time of around 2 days (see section 2.3.1). The cell doubling observations together with the higher expression of SC markers within the first 3 days suggest that after the first full cell cycle the cells are in a less differentiated state. Interestingly, it has been shown that the process of differentiation and proliferation are not mutually exclusive [64]. Being that said, while some cells are differentiating and expressing new gene products, others may still be expressing their "native" characteristics. Yet again, the differences observed in the gene profiling of cells cultured in LAM-511 substrates were not as dramatic as the ones observed in Chapter 2. Lack of appropriate structural and biochemical cues for cell differentiation in the LAM-511 culture conditions may be a reason for such difference. Only one study has briefly compared two

similar culturing systems with very similar findings; the lack of structural and biochemical cues on Matrigel coated substrates led cells (mouse mammary ECs) to produce relatively large amounts of cytokeratins when compared to those cultured on "de-roofed" ECM proteins[440], suggesting a hyperproliferative cell state in the first condition. However, in those studies, the expression of SC markers was not addressed.

Cell interactions with laminins and other ECM proteins are mainly mediated through integrins [380]. ECs synthetize various integrin subunits, including integrin α6 and β1 chains, both detected by mass spectrometry in either matrices. Integrin α6β1 is the main receptor to mediate cell-laminins interactions, including cell-LAM-511 interactions [310, 311]. Integrin αVβ1, only detected in hTCEpi ECM, also contributes to cell adhesion [311]. Others have shown that by blocking integrin β1 chain the cell adhesion to LAM-511 is completely inhibited, whereas integrin αV and α6 chain blocking partially inhibited cell adhesion to LAM-511 coated surfaces [311]. Others have yet suggested that β1 but not β4 integrin mediated the adhesion of conjunctival ECs to LAM-511 and LAM-521 [304]. These observations suggest that integrin β1 chain may be the main protein involved in cell-surface cross-talk. By assessing the laminin-integrin binding affinity, Nishiuchi et al. have suggested that LAM-511 and LAM-521 are the preferred ligand for all the laminin-binding integrins, on other hand LAM-411 was the poorest ligand, showing the lowest integrin binding affinity [433]. These observations may help to understand the lack in keratin expression by cells cultured on LAM-411 as the cell integrity and adhesion may have been compromised due to the poor cell-substrate interaction. Additionally, Polisetti et al. have shown that epithelial stem progenitor cells cultured on LAM-411 have the lowest covered area, cell adhesion, BrdU proliferation and amount of Ki67-positive cells (proliferating cells) when compared to cells cultured on other laminin isoforms [439]. Using a different corneal EC line, Kurpakus et al. have shown that it is integrin α3 chain (detected by mass spectrometry in both ECM preparations) that plays a major role in mediating cellular adhesion to LAM-111 and placental laminin (mainly composed of LAM-511 and LAM-521) [438]. However, these results are conflicting with others', who showed that the blocking of this chain does not affect the adhesion of mammary ECs to LAM-111 [441] but affects the adhesion of human foreskin keratinocytes [442]. It is then reasonable to affirm that integrin specificity for laminin isoforms is cell type-dependent. Further investigations should then be performed to characterize cell integrity and morphology on the different substrates.

The clinical applications of laminin molecules still present technical difficulties as they are large proteins that require three different genes, each encoding the α, β, and γ chain [353]. Recent studies have reported the successful culture and expansion of hESCs and hiPSCs using recombinant laminin E8s isoforms [313]. E8s are truncated proteins consisting of the C-terminal regions of the α, β, and γ laminin chains. They contain the active integrin-binding site composed of the laminin globular domains of the α chain and the glutamate residue of the γ chain [443]. These E8 laminin fragments showed robust capacity to be used in therapeutic applications as they still retain the α6β1 integrin binding site and do not present the risk of contamination with xenogeneic pathogens and immunogens [313].

3.4.3. The protein residues' phosphorylation and cleavage levels are reduced when cells are cultured on coated surfaces

Upon extracellular stimulation, MAPK/ERK signalling module is activated by dual phosphorylation of the Thr202 and Tyr204 residues by the dual specificity kinases MEK1 and MEK2, which lead to EC differentation [389, 393]. Additionally, growth of undifferentiated ESC is enhanced by culture with PD098059, a MEK inhibitor [444], and MEK pathway inhibition promotes murine ESC self-renewal [444]. Studies in PC12 cells have shown that inhibition of ERK activity results in enhanced STA3-mediated transcription [445], suggesting that the antagonism between STAT3 and ERK signalling could account for the effect of PD098059 in ESCs. In accordance with these observations, HCjE-Gi and hTCEpi cells when cultured on coated substrates showed lower levels of ERK1/2, STAT1, and STAT3 phosphorylation, suggesting that cells lost their differentiated state, gaining undifferentiated characteristics as seen by the high levels of keratin, either corneal and conjunctival, and putative SC markers expression.

AKT and mTOR regulation are intricately linked, with AKT functioning upstream of mTOR complex 1 (mTORC1) and mTORC2 regulating AKT activation. mTORC2 phosphorylates the AKT serine residues Ser473 and Ser450. Phosphorylation of both serine residues stimulates phosphorylation at Thr308 residue by PDK1 (3-phosphoinositide-dependent protein kinase-1) that leads to full AKT activation, which in turn phosphorylate (activity inhibition) GSK-3β, PRAS40, BAD and S6 ribosomal protein [402, 403], consistent with these observations are the similar trends followed by the phosphorylation profiles of those five proteins. AKT can also activate mTORC1 by phosphorylating PRAS40, thereby relieving the PRAS40-mediated inhibition of mTORC1 [446]. mTORC1 phosphorylates p70 S6 kinase leading to cell cycle progression. S6 ribosomal protein, found downstream p70 S6 kinase reflects mTOR pathway

activation and predicts cell cycle progression. The activation (phosphorylation) of these proteins have effects on cell differentiation [404, 405, 447]. Together, and consistent with the others' observations [405, 447], these data support the model that low levels of AKT activation (phosphorylation) inhibit cell differentiation, whereas high AKT activation may be necessary for cell differentiation.

GSK-3β inhibitors act as mimetics of Wnt stimulation and consequently support expansion of mouse and human ESC keeping their undifferentiated state [448]. Wnt/β-catenin signalling has also been correlated with an increase in the proliferation of LSC while maintaining the positive LSC markers expression [449].

The phosphorylation and cleavage levels of all protein residues point all in one single direction; cells cultured on coated surfaces exhibit undifferentiated characteristics – high levels of keratins and putative SC markers expression. Additionally, the low levels of AMPk, HSP27, and PARP phosphorylation also corroborated that hypothesis [408, 450-452].

When the three different coating methods are compared, a striking trend is observed; cells cultured on "de-roofed" culture systems showed lower levels of protein residue phosphorylation and cleavage when compared to LAM-511 coating substrates. These observations suggest that cells cultured on ECM proteins appear to be in a less differentiated state than those cultured on LAM-511. This may be explained by the lack of structural and chemical cues on LAM-511 coating method, whereas "de-roofed" cultures systems not only provide morphogenic information resultant from the interaction between all the proteins produced, but also provide a pool of soluble factors produced by cells and trapped within the ECM. These cues have been shown to regulate central cell processes (reviewed in [299]), including cell differentiation, as seen on Chapter 2, in a process that involves an intermediate step of cell de-differentiation. On the other hand, LAM-511, despite lack of structural and chemical cues, has a differentiation inhibitory potential that allows cells to preserve their undifferentiated state [310-312] as seen by the expression of SC markers (ΔNp63 and ABCB5) albeit, at lower levels than the cells cultured on the "de-roofed" systems. TCPS, here used as control, did not provide any cues, either biochemical or structural, and therefore is the one condition showing higher levels of post-translational protein modifications, mostly indicative of a fully differentiated cell state. Consistent with this, Wei et al. have shown that conjunctival ECs cultured on TCPS are in a hyperproliferative state in contrast to the undifferentiated state of those cultured on feeder layers [30]. Taken altogether, these

observations have suggested that cells cultured on different ECM proteins meshwork (regardless the producing cell) may be in a less differentiated state when compared to those on TCPS, however further investigations on the expression of different epithelial SC markers should be conducted.

3.4.4. Potential of differentiating human epithelial cells towards a desired cell lineage

The studies in this chapter addressed the response of ECs upon culture on different laminin isoforms regarding their potential for cell differentiation and protein post-translational modifications. However, several improvements are needed:

i. **Coating substrates with a combination of several laminin isoforms.** The data showed that the protein production profiles are cell type-dependent. Useful information would arise from culturing cells in substrates functionalized with a combination of laminin isoforms that better modulate the keratin expression in accordance with one's need.

ii. **Specific antibody blocking of certain laminin chains.** To better understand the cell response to the laminin isoforms, antibody blocking of laminin chains could be performed to assess if cell's phenotype can be recovered after differentiation.

iii. **Blocking of certain signalling pathways.** Useful data would result from experiments in which certain pathways and/or small branches of these pathways were blocked by antibody binding to, therefore, investigate whether the same type of response would be given without the interference of the extracellular cues.

Chapter 4

Epithelial cell-derived exosomes trigger the differentiation of two epithelial cell lines.

4.1. Introduction

Intercellular communication in multicellular organisms is mediated through three different mechanisms: (i) direct cell-cell contact, (ii) transfer of secreted molecules, and the recently proposed mechanism (iii) the transfer of extracellular vesicles (EVs) [5]. EVs, released by the so-called secreting cell, bind to the receptors on the membrane of the recipient cell, eventually releasing their cargo and ultimately modifying the recipient's physiological state [453]. Exosomes are a specific subtype of secreted EVs. The term exosome, coined by Trams et al., was firstly used to name vesicles ranging from 40 to 1000nm diameter carrying 5'-nucleotidase [454]. In more recent years, the term exosome has been adapted and adopted to designate vesicles whose diameter ranges from 40 to 100nm. Such vesicles have been found and isolated from several body fluids, including blood plasma [455], saliva [456], semen [457], and tears [458]. Most of these studies referred to these vesicles as exosomes because of their exosome-like protein content. However, these populations are likely to be composed of a mixture of exosomes and other membrane vesicles, as the isolation and purification methods used do not allow to fully discriminate between these two classes of vesicles within the same population.

4.1.1. Exosomes and other secreted vesicles

EVs are small membrane vesicles released from the surface of many different cell types including B lymphocytes, dendritic cells, Schwann cells, intestinal ECs, and many others [459, 460]. Produced by different mechanisms, three classes of EVs have been identified: (i) apoptotic bodies (diameter ranges from 1 to 5µm) released by cells undergoing apoptosis, (ii) microvesicles (MVs, whose diameter goes up to 1µm) and (iii) exosomes (40 to 100nm in diameter) [461, 462]. MVs are a heterogeneous population of EVs formed by the outward budding and shedding from cells' plasma membrane in a calcium and enzymatic-dependent way. Exosomes are a heterogenous population of EVs of endosomal origin. They are formed intracellularly by the inward budding on the limiting membrane of endocytic compartments leading to the synthesis of vesicles-containing endosomes, the multivesicular bodies (MVBs). The MVB will eventually fuse with the plasma membrane of the secreting cell releasing their

content, i.e. the exosomes [463]. When viewed under electron microscopy, quickly frozen exosomes have a perfectly rounded shape [464] and not the “saucer-like” shape, erroneously considered as the typical shape of exosomes [5]. Hereby, the term exosome will exclusively refer to EVs of endocytic origin.

4.1.2. The molecular composition of exosomes

4.1.2.1. Exosome membrane

The exosome lipid bilayer is decorated with tetraspanins, a protein superfamily that organizes membrane microdomains termed tetraspanin-enriched microdomains (TEM) by forming clusters and interacting with a large variety of transmembrane and cytosolic proteins [465]. A wide variety of tetraspanins (cluster of differentiation (CD)9, CD63, and CD81) [466], and cytosolic proteins, including endosome or membrane-associated proteins are shown to be present at the exosome membrane [5]. It is becoming clear that these proteins are not exosome-specific markers but rather exosomes-enriched proteins. To describe and characterize an exosome-containing solution both transmembrane and cytosolic proteins with membrane or receptor binding capacities are required to be found positive. In addition, the level of proteins not expected to be enriched in exosome populations of endosomal origin should also be determined, these include proteins associated with compartments other than plasma membrane or endosomes [467].

CD63 is a member of the transmembrane 4 superfamily characterized by the presence of four hydrophobic domains [468]. Being a tetraspanin, CD63 interacts with different proteins, including integrins (α4β1 and α6β1) and has been linked with exosome docking at the recipient cell [468]. CD63’s role in exosome function has also been associated with protein transporting and sorting [468, 469]. Tumour susceptible gene (TSG)101 is a component of the endosomal sorting complexes required for transport (ESCRT)-I complex, being involved in the regulation of vesicular trafficking process [470]. It binds to the ubiquitinated cargo proteins and is required for sorting of endocytic cargos into MVBs [470, 471]. Glucose-regulated protein (GRP)94 (also known as endoplasmin and HSP90 β family member 1) is a molecule chaperone whose functions are related with the processing and transport of secreted proteins [472].

In accordance with the gold standards proposed by the International Society for Extracellular Vesicles [467], the hereby structures referred to as exosomes are those that demonstrated

to be CD63 and TSG101 (endosome-binding and cytosolic protein, respectively) positive and GRP94 (endoplasmic reticulum protein) negative.

Purified exosomes should be completely devoid of serum proteins and other proteins associated with intracellular compartments, such as endoplasmic reticulum, mitochondria, nuclei, and Golgi-apparatus [473]. In addition to the already mentioned tetraspanins and endosome-associated proteins, exosomes are highly enriched in cholesterol, sphingomyelin, and hexosylceramides when compared to the plasma membrane [474, 475]. The fatty acids in exosomes are mostly saturated or monounsaturated. This high fatty acid concentration together with high cholesterol composition has been suggested to be important for their segregation into exosomes during their formation at MVBs [5].

4.1.2.2. Exosome cargo

Exosomes carry a cargo that appears to be not only cell-type dependent but can even differ from parent to daughter cells [476, 477]. The cargo includes mRNA and miRNA molecules, often small amounts of DNA, transcription factors, cytokines, and growth factors [453]. More recently, deep sequencing approaches have demonstrated that EVs also contain a large variety of other small noncoding RNA species, including RNA transcripts overlapping with protein coding regions, repeated sequences of structural RNAs, tRNA fragments, and small interfering RNA [478, 479]. Many RNA molecules are selectively incorporated into EVs as they are found to be enriched relatively to the RNA profiles of the originating cell [479-481].

How miRNA molecules are selectively incorporated into exosomes is still unknown. However, recent studies suggested that miRNAs in EVs share common specific sequence motifs (more poly(U) than poly(A)) at the 3'-end of the molecule, which may act as cis-acting elements for targeting to EVs [482]. Similarly, Villarroya-Beltri et al. have suggested that this mechanism involves the recognition of specific sequence motifs (GGAG) over-represented in miRNAs, called EXOmotifs [483]. These motives are recognized by hnRNPA2B1, a heterogenous nuclear ribonucleoprotein, and loaded into exosomes [483]. Others have further suggested a role of sphingomyelinase 2 on miRNA secretion into exosomes [484]. The cargo can be delivered to the recipient cells in remote locations inducing intracellular signalling changes and modification of their physiological state [485]. To increase the specificity of cargo delivery, MVs are decorated with cellular receptors and transmembrane proteins from the secreting cells. Furthermore, after transferring mouse exosomal RNA into human cells, mouse proteins were found in the recipient cells, suggesting that the transferred exosomal

RNA is translated after entering the recipient cell in the presence of the necessary machinery [480, 486].

4.1.2.2.1. mRNAs

Several studies have shown that mRNA molecules are confined inside exosomes and are functional and translated into proteins in the presence of the necessary machinery [480, 486]. These are as follows:

i. Exosomes treated with RNase showed no difference in RNA degradation when compared to non-treated exosomes [480].

ii. Exosomes treated with trypsin also showed that exosomal RNA is resistant to the treatment [480].

4.1.2.2.2. MicroRNAs

miRNAs are small (20-22 nucleotides long) non-coding RNAs molecules acting as post-transcriptional repressors by binding to 3'UTR of the target mRNA [1]. They derive from transcripts that fold back on themselves to form distinctive hairpin structures [2]. Once processed from the hairpin, the miRNAs pair with the mRNAs to direct transcriptional modification, Figure 62 [1]. The degree of complementarity (through Watson-Crick base pairing) determines the fate of mRNA molecules. Lower rates of miRNA-mRNA sequence pairing results in translation repression and mRNA degradation, whereas higher rates of complementarity results in mRNA cleavage and degradation [1]. However, in very few cases miRNAs also target coding regions upregulating the expression of their target mRNAs [487, 488]. Each miRNA may bind to several mRNAs targets, and one mRNA may be targeted by multiple miRNA molecules [1]. Found in all multicellular eukaryotes species, they regulate important biological processes, including cell growth, development, proliferation, and differentiation. Nearly 1100 human mature microRNAs have been identified and are proposed to regulate more than 30% of human transcriptomes [489].

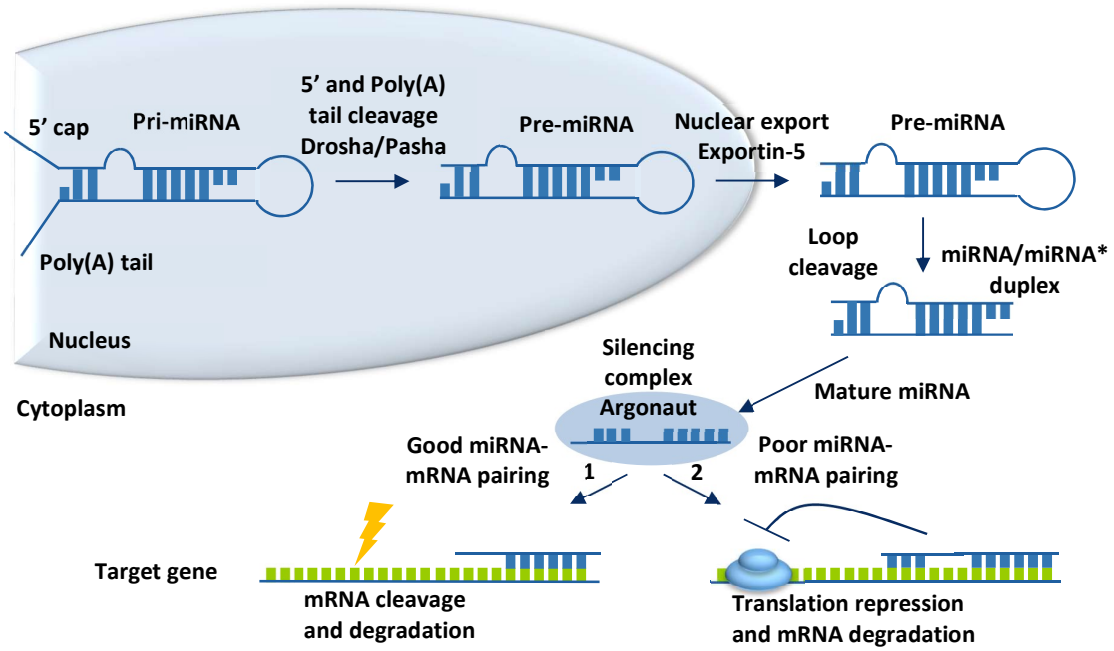

Figure 62 - Processing of a typical miRNA. The miRNA is transcribed from its own gene or a host gene as a long pri-mRNA transcript. This is processed to pre-miRNA by the protein pair Drosha/Pasha and then transported to the cytoplasm by Exportin-5, where it undergoes further modifications to form the final miRNA molecule (miRNA* molecule is often degraded). The miRNA can base-pair with any target mRNA that contains the complementary sequence. The miRNA prevents gene expression by degrading the target mRNA (1) or by blocking its translation (2). Adapted from [1, 2].

Despite the amount of publications related to miRNA biology and functions over the last two decades, the research on miRNA biology in the human eye is still very scarce. An extensive list of significant pathways and biological functions potentially affected by differentially expressed miRNAs in corneal epithelium can be found at Teng et al. [490] and their roles in eye disorders at Raghunath et al. [491]. Others have assessed the miRNA content in human corneal [490-495] and conjunctival [496, 497] tissues and/or cells using several techniques. Table 19 shows the miRNA signature found in human ocular epithelium.

The most expressed miRNA molecule in the cornea is miR-184 and it is mainly located at the basal and immediately suprabasal cells of the corneal epithelium but not in the superficial cells of the cornea, limbus and conjunctiva [493]. Different observations were made by Derrick et al. who have shown its expression also in conjunctival clinical samples [497]. It has been suggested that miR-184 is involved in the terminal differentiation of the corneal epithelium [498] and is down-regulated during corneal re-epithelization in the early stages of wound healing, suggesting that its expression is independent of the proliferative status of the corneal epithelium [493]. Comparative studies have shown a higher abundance of miR-184, miR93b, miR-149 and miR-575 at central cornea epithelium when compared to limbal

epithelial [490], suggesting that those miRNAs may be involved in the terminal differentiation processes seen at the central cornea. Because of its similar expression profiles in cornea and lens, miR-184 may be involved in some unique common features of these two structures, including transparency and avascularity. The limbal regions have been shown to be enriched in miR-145, miR-143, miR-126, miR-338, miR-10b, miR142-3p, miR142-5p, miR-377, and miR-376a [490], which because of their preferred location may be associated with undifferentiated cell states. miR-205 and miR-217 are expressed throughout the entire corneal, limbal and conjunctival epithelium [493]. In human conjunctival specimens, miR-1274B has been shown to have the highest overall expression, followed by miR-151-3p, miR-378, miR-720, and miR-184 [496]. Only two miRNAs have been associated with the regulation of adult epidermal SCs: miR-203 as it targets p63, the regulator of epithelial SC maintenance and differentiation [499, 500], and miR-125b as it targets Blimp1, responsible for maintaining the epithelial SCs in a hair follicle lineage [501]. Only recently, miR-103/107 family has been shown to be preferentially expressed in the basal cells of the limbal epithelium, targeting p90RSK2 a protein that helps to maintain a slow-cycling phenotype. Other molecules have also been identified as targets of this miRNA family, including NEDD9 and m(PTPRM) both shown to somehow be involved in SC-enriched epithelia [495]. Others have shown a gradual increase in expression of miR-24, mir-27b, and miR-184 during hESCs differentiation toward corneal epithelial-like lineages, with the knockdown of miR-184 resulting in reduced levels of KRT3 expression and therefore affecting the normal corneal epithelial commitment [494]. The same studies have shown miR-450b-5p as a PAX6-repressing miRNA and, accordingly, the absence of miR-450b-5p is required for PAX6 expression in the developing eye surface. They suggested that PAX6 repression by miR-450b-5p contributed to the pluripotent state of SCs and its decrease allows the cells to exit from this undifferentiated state [494].

Table 19 – Signature miRNAs in human ocular epithelium. ++++ strong expression, +++ high expression, ++ moderate expression, + residual expression, - down-regulated, NA not assessed. Adapted from [490-498, 502].

miRNA	Cornea	Limbus	Conjunctiva
miR-145	+	+++	NA
miR-143	-/+	+++	NA
miR-126	-/+	+++	NA
miR-338	-	++	NA
miR-10b	--	++	NA
miR-142-3p	-	+	NA
miR-142-5p	-	+	NA
miR-377	-	+	NA
miR-376a	--	+	NA
miR-146a	--	+	NA
miR-139	--	+/-	NA
miR-211	--	+/-	NA
miR-155	--	+/-	NA
miR-127	--	-	NA
miR-184	++++	+++	+
miR-193b	+++	++	NA
miR-149	+	+ (+/-)	NA
miR-575	++	+	NA
miR-1274b	NA	NA	++++
miR-151-3p	NA	NA	+++
miR-378	NA	NA	++
miR-720	NA	NA	+
miR-190b	NA	NA	+
miR-31	++	-	NA
miR-103	++	+++	NA
miR-99a	+ (-/+)	+	NA
miR-21-5p	NA	NA	++
miR-141-3p	NA	NA	+
miR-26-5p	NA	NA	+
miR-22-3p	NA	NA	+
miR-27b-3p	NA	NA	+
miR-191-5p	NA	NA	+

4.1.2.2.3. Proteins

Exosome preparations are devoid of any proteins of nuclear, mitochondrial, endoplasmic-reticulum or Golgi-apparatus origin [503]. All exosomal proteins identified to date have been found in the cytosol, in the membrane of endocytic compartments or at the cell membrane [473]. Other studies have analysed the protein content of exosomes using Western blotting [466, 504, 505] and flow cytometry [506-508]. An extensive table containing proteins present in exosome preparations can be found at Thery et al. [473]. Noteworthy is the absence of any lysosomal proteases and other soluble endocytic residents [473]. How the cytosolic content is recruited into the exosomes is still unclear. However, recent observations indicate

that ubiquitination of the cytosolic domain of selected proteins triggers the partitioning of some, but not all, membrane proteins into vesicles of endosomal origin [509-511]. It may also involve association of exosomal membrane proteins with chaperones, such as Hsc70, known to be found in exosomes of most cells [506]. A small subset of other cytosolic proteins, together with tetraspanins (a review can be found at Andreu and Yanez-Mo [512]), has been suggested to play a role in exosomes sorting. These include the already mentioned Hsc70, the Hsc90, and the PKM2 [513].

4.1.3. Exosome biogenesis

The endosomal origin is the most accepted hypothesis for the origin of exosomes, several studies have solidified this:

i. **Exosome membrane composition.** Exosome specific membrane composition lacks some abundant cell-surface proteins, such as CD28, CD40L, and CD45 in T-cell derived exosomes [514] and transferrin receptor in B-cell-derived exosomes [508, 515]. These studies suggested that exosomes are not simply fragments of the cell membrane.

ii. **Exosome cargo.** Many of the cytosolic proteins that are found in exosomes have been found in the endocytic pathway, these include annexin II, RAB5/RAB7, and TSG101 [516]. These observations suggested an endocytic step at some point in the formation of exosomes.

Late endosomes bud off parts of their limiting membrane into their lumen forming intraluminal vesicles (ILVs), which can accumulate hundreds of vesicles. This late structure termed the MVB will eventually fuse with the cell membrane, in an exocytic manner, releasing their content, i.e. the exosomes, Figure 63. Two pathways have been suggested to rule MVBs' fate. The first one, called secretory pathway, leads to the secretion of MVBs to the extracellular milieu. The second one, named lysosomal pathway, leads to the fusion of the MVBs with lysosomes for degradation of their contents [5]. These two different fates arise from distinct populations of MVBs that coexist within the same cell [5, 517]. Furthermore, co-localization of cholesterol with the toxin perfringolysin O indicates one cholesterol-rich MVB population for exosome secretion, and another, although morphologically identical, but cholesterol-poor population for lysosomal targeting [5, 517].

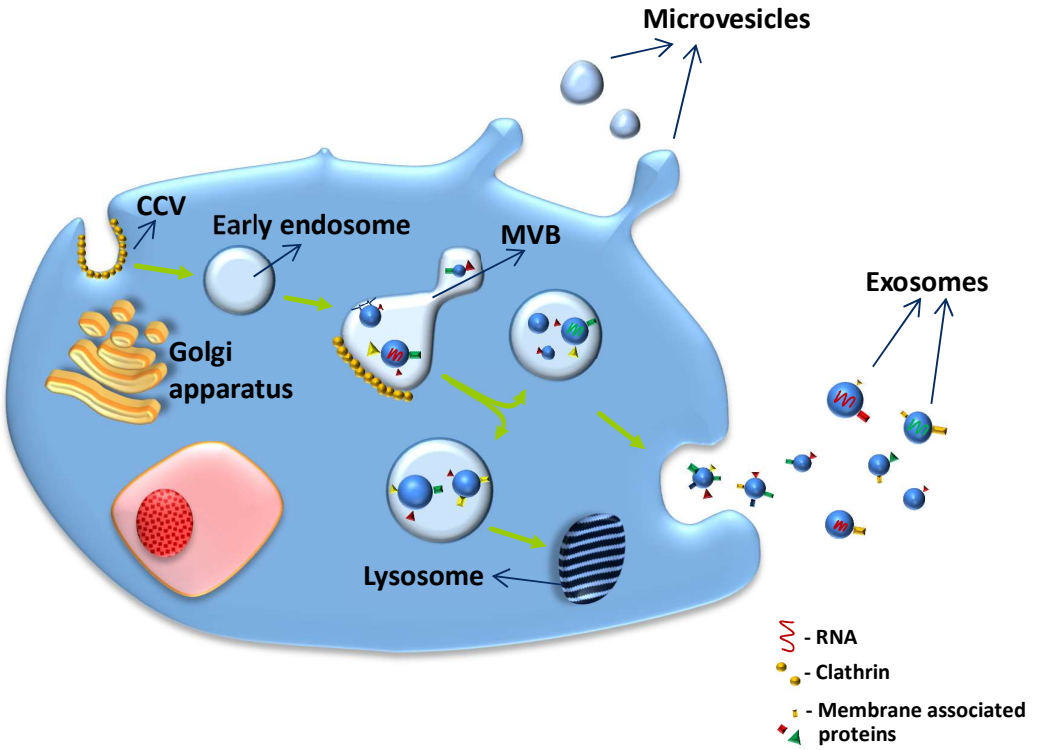

Figure 63 – Schematic release of MVs and exosomes. MVs bud directly from the cell membrane, whilst exosomes are formed by budding into early endosomes and are released by fusion of MVB with the cell membrane. Other MVBs can follow the lysosomal pathway for degradation of their contents. Abbreviations used CCV: clathrin-coated vesicles, MVB: multivesicular body. Adapted from [5].

4.1.3.1. ESCRT-dependent pathways

In exosome biogenesis, well-conserved proteins assemble into four multiprotein complexes, known as ESCRT-0, -I, -II, and –III that are associate with various other proteins [518]. ESCRT-0, -I, and -II complexes recognize and sequester ubiquitinated proteins at the endosomal delimiting membrane, the ESCRT- I and -II complexes are, in addition, responsible for membrane deformation into buds with sequestered cargo [509, 519, 520]. The ESCRT-III complex is responsible for the actual scission of the vesicles [521]. Different members of the ESCRT machinery have been involved in exosome biogenesis and secretion in different cell types [522].

4.1.3.2. ESCRT-independent mechanisms

It has been demonstrated that in some cells types, such as oligodendroglial cells, the depletion of subunits belonging to the four ESCRT complexes does not totally impair the formation of MVBs, suggesting that other ESCRT-independent mechanisms can operate for exosomes biogenesis. These are known to be dependent on a sphingomyelinase, a ceramide-producing enzyme [523]. Ceramide is a lipid with a cone-shaped structure that possibly

facilitates the membrane invagination of ILVs. These observations are consistent with the presence of great concentrations of ceramides and its derivatives in exosomes [523]. Other have shown that syntenin stimulates the production of exosomes and it is also required for the budding of CD63-positve ILVs into the MVB, playing an important role in anchoring receptor proteins of the membrane to cytoskeletal components [471]. Syntenin is a protein present at great concentrations in exosome populations and its effects on exosome production depends on the interaction with an auxiliary component of the ESCRT complexes [471]. In addition, syntenin has been shown to bind to membrane receptors, as syndecans and CD63 [471], suggesting a direct role on exosomal sorting. Additionally, certain mammalian cells have developed pathways for MVBs formation independently of both ESCRT complexes [524] and ceramide pathways [469]. Tetraspanins, highly enriched in MVBs, have been proposed to function as sorting machines in the formation of exosomes in those cells being involved in the organization of large molecular complexes and membrane subdomains [459]. Exosome secretion has been shown defective in CD9 knockout mice [525]. In contrast, the absence of CD81 in lymphocytes does not have an effect on exosome release [526].

4.1.4. Exosome secretion

The release of a vesicle requires its mobilization to the cell periphery, its docking and its fusion with the cell membrane. These processes involve cytoskeleton rearrangements (mediated by actin and microtubules) associated with molecular motors (regulated by kinases and myosin), cell membrane fusion components (regulated by SNAREs and tethering factors), and molecular switches [527]. Most of the intracellular transport is controlled by well conserved cytosolic proteins, including small GTPases of the Rab family. Rab proteins control various steps of vesicular trafficking, including budding, motility, and docking of several classes of vesicles with the cell membrane [528]. Proteins of the Rab family are suggested to be required for exosome secretion. It is thought that Rab27 is involved directly or indirectly in the transportation and tethering of the secretory MVBs at the cell periphery. By silencing the two Rab27 effectors, the Slp4 and Slac2b, Ostrowski et al. have shown a decrease in exosome secretion, with no modifications in their protein content or morphology [529]. In addition, exosomes produced by Rab27a knockdown cells appeared to be larger when compared to control but homogenously distributed within the cell. On the other hand, exosomes extracted from Rab27b knockdown cells showed asymmetrical perinuclear distribution with no changes in their size [529]. These results suggest that these two proteins

have different roles in the biogenesis and release of such EVs. In addition, the same group has shown that Rab27a is preferentially associated with CD63-positive MVBs, whereas Rab27b has a minor co-localization with CD63-positive events. In the same line of studies, Hsu et al., by knocking down the Rab GTPase-activating proteins, Rab35, and interfering with its effector, showed an inhibition of exosome secretion and an intracellular accumulation on endosomal vesicles [530]. Inactivation of Rab11 (although controversial), Rab27, and Rab35, is apparently involved in exosome secretion, not causing a complete cessation of exosome secretion, albeit reducing it to some extent [529-531]. Since other Rab GTPases (Rab7 and Rab11), associated with the endocytic system, have not shown any effect on exosome secretion, others have suggested that a particular subset of MVBs participates in the generation of exosomes [529]. The role of GTPase-activating proteins can then be complimentary or indirectly altered by regulating secretory pathways upstream of those involved in exosome secretion.

Exosome secretion follows the same rules as excretory-lysosome fusion, i.e. they fuse with MVB membrane after activation in a Ca^{2+}-dependent manner [5]. The mechanism by which MVBs fuse with the plasma membrane of the donor cell is still mostly unknown. The SNARE complex involved in Ca^{2+}-regulated exocytosis of conventional lysosomes includes VAMP7 and Ca^{2+} binding synaptotagmin VII [532]. Little is known if the exocytic fusion of MVB is controlled by the same process and the results are controversial. One study showed that exosome secretion by reticulocytes appeared to be VAMP7-dependent [533], whereas in kidney ECs (MDCK cells), the expression of the Longin domain of VAMP7 (negatively regulating its interaction abilities) selectively impaired the lysosomal secretion but not the exosomes release [534]. Release of MVs can be stimulated in response to certain receptors in different cell populations. For instance, platelets release more exosomes in response to thrombin receptor activation [535] and dendritic cells increase their vesicle release in response to lipopolysaccharides [536]. One common signal that triggers the release of EVs is the increase of intracellular Ca^{2+} concentration [504, 531].

To better understand their biogenesis and release, other groups have reported the secretion of vesicles of endocytic origin [537]. Using immunoelectron microscope techniques they have observed the destination of an internalized transferrin-receptor antibody - a marker used to follow endocytosis and the recycling of cell-surface proteins [463, 538]. At 0 hours, the antibody binds to the cell surface. In cells incubated at 37°C for 15 minutes after antibody binding, the antibody is found in large empty vesicles, which may correspond to early

endosomes. After one hour at 37°C the antibody is then found in endosomes containing internal vesicles (likely corresponding to the MVB) and is mainly localized at the surface of the internal vesicles. After 3 hours, some of the MVBs fuse with the cell membrane, releasing their contents, the exosomes [463].

4.1.5. Interactions with recipient cells

To perform their functions the exosomes must interact with the recipient cells to release their cargo, Figure 64. Exosome anchoring to the recipient cell is likely to be determined by interactions of different tetraspanins (including CD63, CD81, and CD9) and adhesion molecules, such as integrins and ICAMs, present in the EVs membrane [465, 512]. After binding to the recipient cell, EVs may follow four different paths: (i) remain stably associated with the plasma membrane, (ii) directly fuse with the plasma membrane, (iii) be internalized through endocytic or micropinocytic pathways, and (iv) fuse with the delimiting membrane of an endocytic compartment [5]. After being endocytosed, the EVs may fuse with the endosomal delimiting membrane where their content may be released and translated or targeted for lysosomal degradation [5]. Recent studies have shown a more efficient fusion of exosomes with the limiting membrane of endocytic organelles in acidic environment due to changes in recipient cell membrane rigidity [539]. Of interest is the selective incorporation of specific exosomes by some cell types. For example, exosomes extracted from B cells selectively bind to follicular dendritic cells in lymphoid follicles [540]; and EVs extracted from intestinal ECs bind preferentially to dendritic cells rather than to B or T lymphocytes [541].

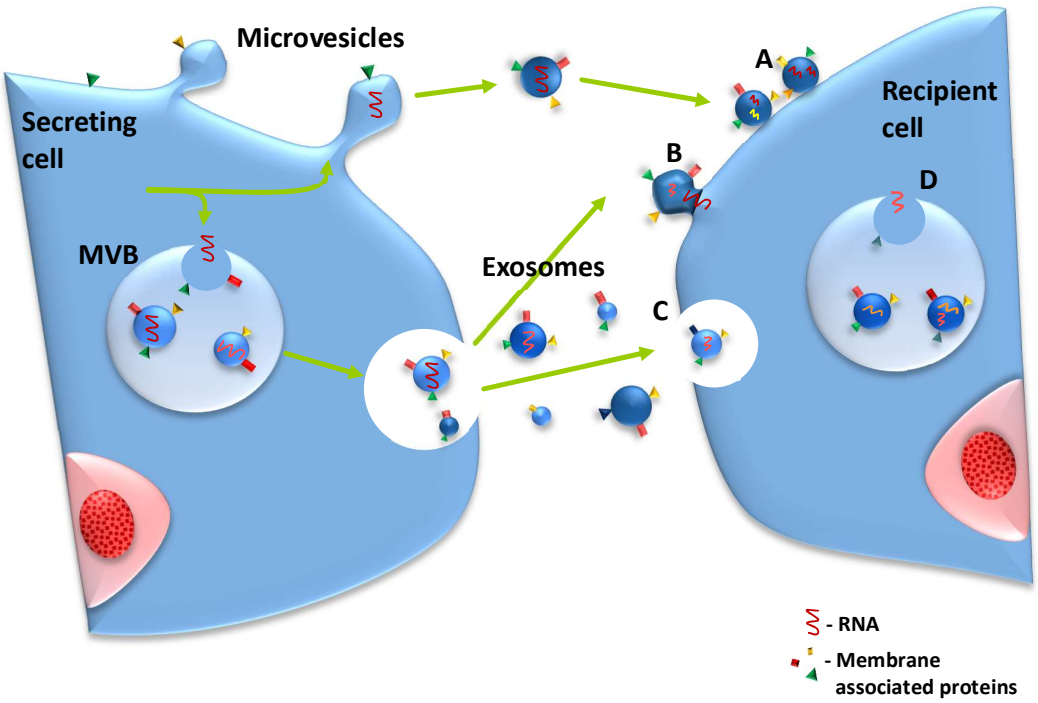

Figure 64 - Cargo transfer by EVs and exosomes. RNA molecules and proteins are selectively incorporated into MVBs, which will eventually fuse with the plasma membrane to release exosomes into the extracellular space. The MVs and exosomes may follow four different paths: (A) remain stably associated with the plasma membrane, (B) directly fuse with the plasma membrane, (C) be internalized through endocytic or micropinocytic pathways, and (D) fuse with the delimiting membrane of an endocytic compartment. Abbreviations used MV: microvesicle, MVB: multivesicular body.

4.1.6. Functions of EVs

Since exosome content varies from one cell type to another, their functions are also likely to be different. Firstly, exosomes can facilitate intercellular communication whether locally or at a certain distance, without the need for direct cell-cell contact, by exchanging proteins and nucleic acids between the exosome-producing and the recipient cell. Secondly, their secretion could function as a mechanism of protein and/or obsolete molecules elimination alternative to lysosomal degradation [463, 542, 543]. Others have, more recently, demonstrated that cancer cells release EVs to increase the tumour progression by promoting angiogenesis and tumour cell migration in metastases [544, 545]. The release of EVs by intestinal ECs, whether apically or basolaterally, appear to be involved in antigen presentation under inflammatory conditions, allowing these static cells to act at distance [546]. Studies with Chinese-hamster ovary cells and blood mononuclear cells, cells that produce CC-chemokine receptor 5 (CCR5) [547], strongly supported the importance of MV transfer between cells. In these studies, large vesicles bearing CCR5 released by hamster ovary cells and blood mononuclear cells, transfer CCR5 to monocytes and endothelial cells

(cells that do not express this receptor), rendering them sensitive to infection with macrophage-tropic HIV-1 virus [547].

4.1.7. Uses of EVs – clinical point of view

EVs can be used as therapeutic agents with potential advantages over cell therapies. Exosome cargo can be tailored for each patient, their lipid composition allows high stability (longer than 6 months), they are enriched in major histocompatibility complex (MHC), their membrane express ligands for NK receptors (molecules involved in the prevention of nausea and vomiting associated with chemotherapy), and they do not respond to immunosuppressive molecules [548, 549]. A phase II clinical trial used autologous dendritic cell (DC)-derived exosomes for the treatment of cancer. This trial launched in November 2009 at Gustave Roussy and Curies Institutes used DC-derived exosomes purified from autologous maturing monocyte derived-DC. [550]. DC-derived exosomes express high levels of functional MHC class-I and -II peptide complexes, that can in theory substitute for DC to elicit tumour rejection. Results from phase II studies showed that 32% of the patients had stable disease after 4 months and 1 patient had a grade-3 hepatotoxicity [551, 552]. Others phase I trials have recently been concluded with promising results [553-556].

One may ask the reason why exosomes were chosen over other EVs populations, particularly MVs. Bruno et al. compared the renal regenerative potential of either exosomes enriched populations and MVs enriched populations [557]. They have shown that the exosome enriched population not only induce renal regeneration but also showed higher expression of pro-proliferative molecules. On the other hand, MVs enriched populations were unable to induce renal regeneration [557]. Similar observations were made elsewhere where exosome-containing solutions were shown to be more effective than those containing only MVs [558-560]. These studies supported the choice of exosomes over MVs. Nevertheless, others have yet shown a synergetic effect of exosomes and MVs in reversing the effect of radiation in marrow hematopoietic cells [561]. In the latter, preparations containing both exosomes and MVs showed to be more effective that either exosomes or MVs alone.

4.1.8. Aim

i. **To determine if exosomes are produced by cultured ocular surface epithelial cells.** Exosomes were extracted from the aforementioned cell lines using differential ultracentrifugation and characterized in terms of their transmembrane protein content and size.

ii. **To determine if the differentiation of human epithelial cells from the conjunctiva and cornea can be modulated in response to different extracellular vesicles populations in vitro.** Exosomes extracted from the aforementioned cell lines were used to cross-modulate the differentiation of the two cell lines.

iii. **To characterize the cargo of exosomes extracted from cultured ocular surface epithelial cells.** Exosomal miRNA cargo was characterized using next generation sequencing approaches.

4.2. Materials and Methods

4.2.1.Cell culture

Human conjunctival ECs (HCjE-Gi) [152] and human corneal ECs (hTCEpi) [562] were cultured as described in section 2.2.2 and 2.2.3, respectively.

4.2.2.Exosome extraction

The most commonly used protocol for exosome extraction and purification involves several centrifugation and ultracentrifugation steps [6, 515, 563], described in Figure 65. Briefly, upon 80% confluence cells were cultured in BPE–depleted KSFM (exosomes-free medium) for 72 hours. The conditioned medium was then collected and centrifuged at 500xg (Centrifuge 5417, Eppendorf) for 5 minutes at 4°C to remove any dead cells, the resulting supernatant was collected and centrifuged at 2000xg for 10 minutes at 4°C and the pellet discarded to remove cell debris. The resulting supernatant was filtered using a 0.22 µm filter (cat. Number SLGP033RS, Merck Millipore). A total of 32mL of conditioned medium per condition was collected into OptiSeal ™ tubes (cat. Number 361623, Beckman Coulter) and ultracentrifuged at 100000xg (90Ti fixed angle rotor, Beckman Coulter) for 2 hours at 4°C. The resulting pellet was re-suspended in PBS and once again ultracentrifuged at 100000xg (90Ti fixed angle rotor) for 2 hours at 4°C. The resulting pellet was re-suspended in 200µL of PBS and stored at -80°C until further experiments.

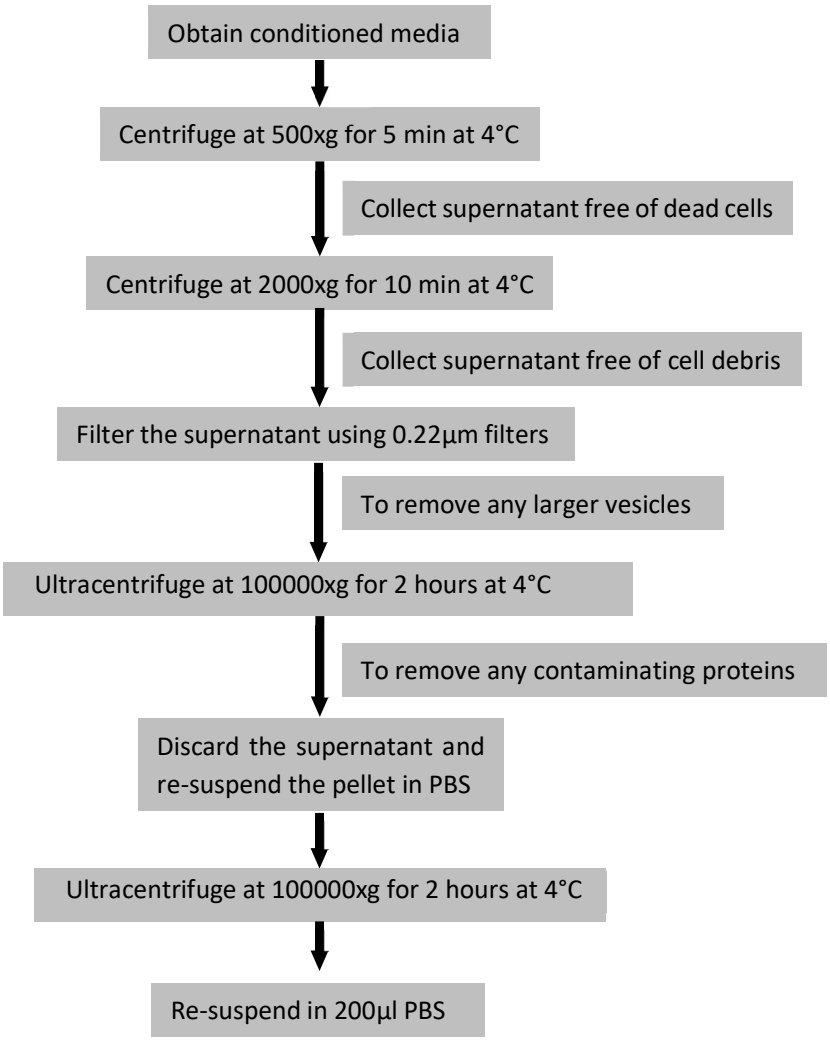

Figure 65 - Exosome extraction protocol using differential ultracentrifugation. In differential centrifugation exosomes and microvesicles are isolated based on their size upon a sequence of centrifugation steps. The resulting solution has been shown to have high purity and high enrichment isolation [6].

4.2.3.Exosome characterization by flow cytometry

The exosome-containing suspension was incubated with 10µL of aldehyde/sulphate latex beads (cat. number A37304, Life Technologies) for 15 minutes at RT. PBS was then added to a final volume of 1mL and the solution incubated overnight at 4°C on a test tube rotator wheel at 20rpm (Stuart® Equipment). To saturate any remaining free-binding sites on beads, glycine (cat. Number 67419, Sigma-Aldrich) was added to a final concentration of 100mM and the resulting solution incubated at RT for 30 minutes. The solution was then centrifuged (all centrifugation steps were performed for 3 minutes at 4,000 rpm at RT). The supernatant was then removed, and the remaining pellet was re-suspended in 1ml of 0.5% (W/V) BSA

(cat. Number A9085, Sigma-Aldrich) in PBS, this step was repeated thrice. The resulting pellet was then re-suspended in 100µL of primary antibody (Table 20) diluted in 0.5% (W/V) BSA in PBS and incubated in the dark for 30 minutes at 4°C. After adding 1ml of 0.5% (W/V) BSA in PBS to the suspension, centrifugation was performed. After removal of the supernatant, the pellet was re-suspended in 100µL of appropriate secondary antibody (Table 21) diluted in 0.5% (W/V) BSA in PBS. This suspension was then incubated in the dark for 30 minutes at 4°C. After the addition of 1ml of 0.5% (W/V) BSA in PBS to the suspension, centrifugation was performed. The resulting pellet was re-suspended in 500µl of 0.5% (W/V) BSA in PBS. This final suspension was analysed using a BD Accuri C6 flow cytometer (BD Biosciences) and the results analysed using BD Accuri C6 (BD Biosciences).

Table 20 – List of primary antibodies used for exosome characterization using flow cytometry.

Antibody	Clone	Host	Isotype	Manufacturer	Dilution
CD63	Polyclonal	Mouse	IgG	Santa Cruz Biotechnology	1:1000
TSG101	4A10	Mouse	IgG1	Abcam	1:1000
GRP94	9G10	Rat	IgG2a	Abcam	1:1000
IgG	---	Mouse	---	ThermoFisher Scientific	0.2µg/µL
IgG1	---	Mouse	---	ThermoFisher Scientific	1µg/µL
IgG2a	---	Rat	---	ThermoFisher Scientific	1µg/µL

Table 21 - List of secondary antibodies used for exosome characterization using flow cytometry.

Antibody	Clone	Host	Reactivity	Conjugate	Manufacturer	Dilution
Anti-mouse	A-11005	Goat	Mouse	FITC	Life Technologies	1:1000
Anti-rat	F7512	Sheep	Rabbit	FITC	Sigma-Aldrich	1:1000

4.2.4.Quantification and sizing of exosomes by NanoSight® analysis

750µL of the exosome-containing suspension (dilution factor 1:150) was used for NanoSight® analysis following the manufacturer's protocol (NanoSight NS300 instrument, NanoSight Ltd. Minton Park, Amesbury, UK). The camera used was a sCMOS type camera and a red type laser. The temperature was kept constant at 22°C and the water viscosity kept at 0.953cP. For analysis 1498 frames were used at a rate of 25 frames per second.

4.2.5.Reverse Transcriptase qPCR

Reverse Transcriptase qPCR and all the previous steps (RNA extraction and cDNA synthesis) were done as outlined in sections 2.2.10, 2.2.11, and 2.2.12, respectively. Table 22 shows the set of primers used for these studies.

Table 22 – List of primers used for Reverse Transcriptase qPCR studies in Chapter 4. The primer sequences and the product size are included. Abbreviations used: GAPDH: glyceraldehyde-3-phosphate dehydrogenase, KRT: keratin, ABCB5: ATP binding cassette sub-family B member 5. # Sequences and product size of reference genes are not commercially provided by PrimerDesign.

Primer	Gene Sequence	Product size (bp)
GAPDH	F - # R - #	
KRT3	F – TTCCATCTCAGGCACAAACAA R –CAGGTCCTCCATGTTCTTCAG	130
KRT7	F –CTCCCACCACTCCATCCT R - ATCACTTTCCAGACTGTCTCACT	105
KRT12	F –CTCCAAATCACAAGCACAGTCA R - CCACCTCACCATTCACCATCT	98
KRT13	F –ATGCTGCTGGACATCAAGAC R -TCGTGGTAACAGAGGTGCTA	113
ΔNp63α	F –GGAAGGCGGATGAAGATAGC R - CATGTGTGTTCTGACGAAACG	96
ABCB5	F - GGAAAGAATTACCACTACCAAGAAGG R - TGGTAGCATCCAAATGGGCAAAC	119

4.2.6.Flow cytometry of ocular surface epithelial cells

Flow cytometry was performed as outlined in 2.2.14. Table 23 and Table 24 show the set of primary and secondary antibodies used for these studies, respectively.

Table 23 – List of primary antibodies used for flow cytometry studies in Chapter 4. # Concentration dependent on primary antibody. Abbreviations used KRT: keratin

Antibody	Clone	Host	Isotype	Manufacturer	Dilution
KRT3	AE5	Mouse	IgG	Abcam ®	1:1000
KRT7	RCK105	Mouse	IgG1	Santa Cruz	1:500
KRT12	J6	Rabbit	IgG		1:1000
KRT13	Ks13.1	Mouse	IgG1	Santa Cruz	1:500
ΔNp63α	Poly6190	Rabbit	IgG	BioLegend	1:1000
IgG	---	Mouse	---	ThermoFisher Scientific	#
IgG	---	Rabbit	---	ThermoFisher Scientific	#
IgG1	---	Mouse	---	ThermoFisher Scientific	#

Table 24 - List of secondary antibodies used for flow cytometry studies in Chapter 4. Abbreviations used FITC: fluorescein isothiocyanate

Antibody	Clone	Host	Reactivity	Conjugate	Manufacturer	Dilution
Anti-mouse	A-11005	Goat	Mouse	FITC	Life Technologies	1:1000
Anti-rabbit	F7512	Sheep	Rabbit	FITC	Sigma-Aldrich	1:1000

4.2.7.XenoLight DiR labelling

After differential ultracentrifugation, the exosome-containing solution was incubated with 2µM of XenoLigth DiR Fluorescent Dye (cat. Number 125964, PerkinElmer) diluted in diluent C (cat. Number CGLDIL, Sigma-Aldrich) for 30 minutes. The resulting solution was then washed twice in sterile PBS (100000xg for 2 hours at 4°C). The labelled exosomes were diluted in appropriate exosome-free KSFM and used in further investigations.

4.2.8.End-point PCR

After differential ultracentrifugation, the exosome-containing solution was used for RNA extraction and cDNA synthesis as outlined in 2.2.10 and 2.2.11, respectively. 18ng of cDNA (correspondent to 2.5µL) was added to a 200µL PCR tube (Appleton Woods, cat. Number BS191) together with 12.5µL of REDTaq® ReadyMix ™ (cat. Number R2523, Sigma-Aldrich), 5µL of primer pair and 5µL of nuclease-free ddH_2O (cat. Number AM9937, Ambion). End-point PCR temperatures were in accordance to section 2.2.12.

4.2.9.Agarose gel

5µL of HyperLadder 100bp (cat. Number BIO-33056, Bioline) and 10µL of end-point PCR products were loaded into different lanes of a 2% TAE agarose gel (cat. Number A9639, Sigma-Aldrich) supplemented with 0.0036% (V/V) ethidium bromide (cat. Number E1510, Sigma-Aldrich) and run for approximately 1 hour at 100V (PowerPac Basic ™, BioRad). TAE buffer was prepared as follows: 40mM Tris (cat. Number 93362, Sigma-Aldrich), 20mM acetic acid (cat. Number 320099, Sigma-Aldrich), and 1mM EDTA (cat. Number EDS, Sigma-Aldrich), pH adjusted to 8.6.

4.2.10. Next Generation Sequencing - Exosomal RNA sequencing

10 mL of cell culture media was centrifuged at 1500xg for 5 minutes to remove residual cells and debris. The supernatant was transferred to a new 50mL conical tube for exosome isolation. ExoQuick-TC (System Biosciences, Palo Alto, CA) was added to the supernatant at 1:5 ratio (ExoQuick:Supernatant), mixed gently, and allowed to incubate overnight at 4°C. On

the next day, the admixture was centrifugated at 1500xg for 30 minutes to recover exosomes for total RNA isolation.

Please refer to page 5 of the SeraMir Exosome RNA Amplification User Manual (https://www.systembio.com/downloads/Manual_SeraMir_web_ver12.pdf) for detailed information on isolation of exo-RNA from exosomes. The key information is presented on Steps 7-22. 1µL of total exo-RNA was utilized for measurement of small RNA concentration by Agilent Bioanalyzer Small RNA Assay using Bioanalyzer 2100 Expert instrument (Agilent Technologies, Santa Clara, CA).

Next generation sequencing libraries were generated with the TailorMix Micro RNA Sample Preparation version 2 protocol (SeqMatic LLC, Fremont, CA). Briefly, 3'-adapter was ligated to the RNA sample and excess 3'-adapters were removed subsequently. 5'-adapter was then ligated to the 3'-adapter ligated samples, followed by first strand cDNA synthesis. cDNA library was amplified and barcoded via enrichment PCR. Final RNA library was size-selected on an 8% TBE polyacrylamide gel. Sequencing was performed on the Illumina NextSeq 500 platform at a readlength of 1x75bp single-end at SR50.

The isolation method used for this analysis (performed by the manufacturer) was different from the method used in the remaining studies of this thesis.

4.2.11. Statistical analysis

A Mann-Whitney analysis followed by Dunn's multiple comparison test (unless otherwise specified) were used to determine statistically significant differences (GraphPad Prism 5, *$p<0.05$, **$p<0.01$, ***$p<0.001$). Data is expressed as median ± 5-95% percentile (unless otherwise specified).

4.3. Results

4.3.1. Exosome characterization by flow cytometry

To ensure that the feeding medium is *per se* exosome-free, flow cytometry was performed on the solution resultant of ultracentrifugation of fresh medium depleted from BPE. Both conjunctival and corneal KSFM (BPE-depleted) showed to be negative for the exosome-enriched solution markers CD63 and TSG101, and negative for GRP94, Figure 66A and B respectively. These results suggested that the feeding media is then exosome-free and any vesicle thereafter detected resulted from cell production and release.

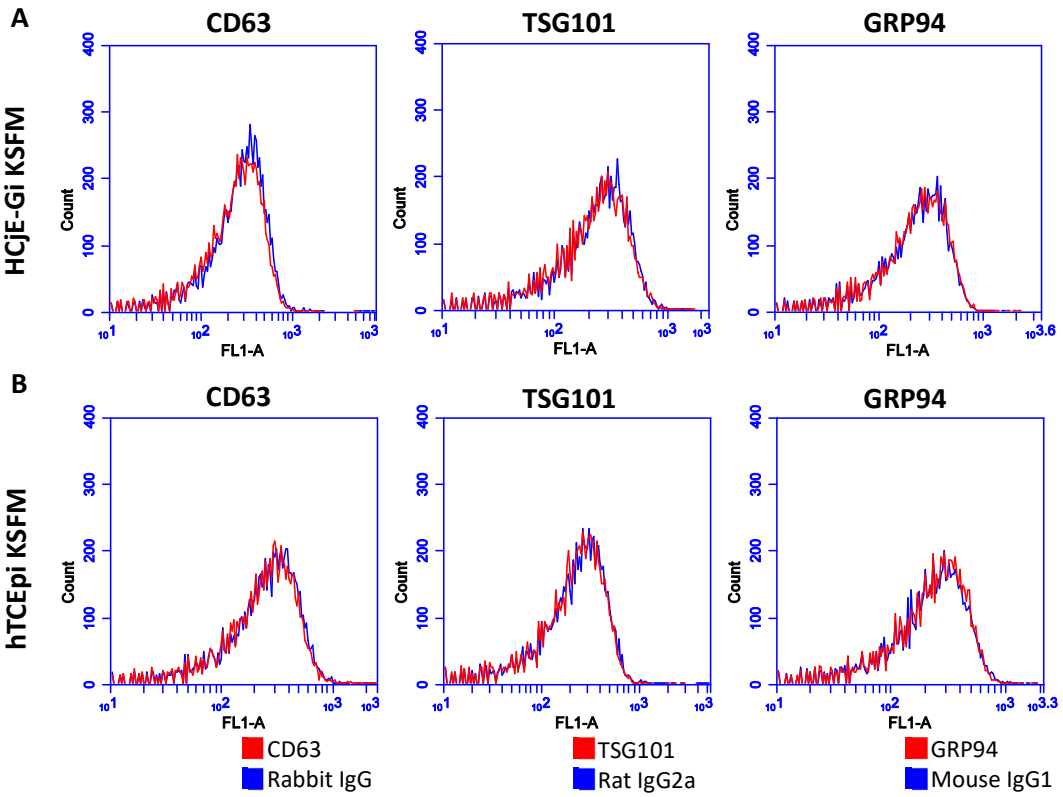

Figure 66 - Characterization of particles extracted from fresh (A) HCjE-Gi and (B) hTCEpi BPE-depleted KSFM assessed by flow cytometry. Abbreviations used BPE: bovine pituitary extract.

4.3.1.1. HCjE-Gi cells-derived exosomes are CD63 and TSG101 positive and GRP94 negative

Upon 80% of confluence, cells were cultured in BPE–depleted KSFM (exosome-free medium). The conditioned medium was then collected at day 1, 2, and 3 and the exosomes extracted using differential ultracentrifugation. Flow cytometry was performed to characterize the resulting solution.

The percentage of CD63-positive events in the HCjE-Gi cells-derived population increased over time, ranging from 9.84% at day 1 to 65.33% at day 3 ($p<0.05$). Regarding TSG101, its expression peaks at day 3, with 24.64% of vesicles shown to be TSG101-positive ($p<0.05$). The expression of GRP94 was shown to be negative throughout the entire course of the experiment, Figure 67.

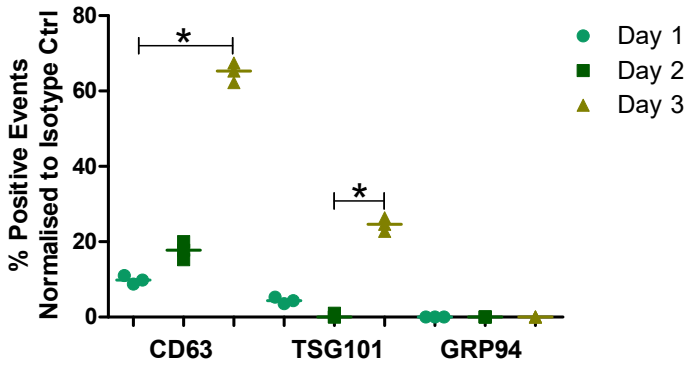

Figure 67 - Characterization of HCjE-Gi-derived exosomes extracted from conditioned medium over 3 days as assessed by flow cytometry. The percentage of positive events normalised against isotype control is shown. (Data is represented as median ± 5-95 percentile, n=3, Kruskal-Wallis test followed by Dunn's Multiple comparison test, *p<0.05, **p<0.01, ***p<0.001).

4.3.1.2. hTCEpi cells-derived exosomes are CD63 and TSG101 positive and GRP94 negative

Concerning the hTCEpi-derived exosomes, an increase in the percentage of CD63-positive events can be appreciated over time, ranging from 8.18% at day 1 to 45.55% at day 3 ($p<0.05$). Regarding TSG101, its expression increased within the time window analysed, peaking at day 3, with 12.27% of vesicles shown to be TSG101-positive ($p<0.05$). The expression of GRP94 was shown to be negative throughout the whole-time course, Figure 68.

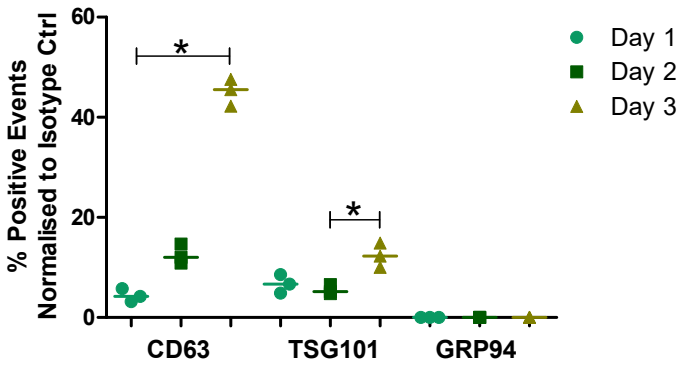

Figure 68 - Characterization of hTCEPi exosomes extracted from conditioned medium over 3 days as assessed by flow cytometry. The percentage of positive events normalised against isotype control is shown. (Data is represented as median ± 5-95 percentile, n=3, Kruskal-Wallis test followed by Dunn's Multiple comparison test, *p<0.05, **p<0.01, ***p<0.001).

4.3.1.3. Summary of results 12:

i. The percentage of CD63- and TSG101-positive events (markers for exosome-enriched solutions) peaked in the exosome populations extracted from cells kept in culture for 3 days.

ii. The percentage of GRP94-positive events showed to be zero throughout the whole experiment.

4.3.2. Exosome characterization by NanoSight

To further characterize the exosome population in terms of size distribution and concentration, the conditioned medium was collected at day 1, 2, and 3. After extraction, the exosome-enriched solutions were viewed under NanoSight®.

4.3.2.1. HCjE-Gi derived exosomes' size ranges from 81 to 96nm

Regarding the HCjE-Gi-derived exosome population, the particles concentration seemed not to differ much from day 1 to day 2. However, an increase in particle concentration is observed at day 3, Figure 69C. In terms of size distribution, 10% of the particles (D10) had a diameter that ranges from 81 to 96nm (or smaller), within the expected size range of exosomes, Figure 69. A snapshot captured during the collection of the data is shown in Figure 69D. As expected, since the solution under visualization has a certain "tridimensionality", some vesicles appeared out of focus (red arrowhead) which may have biased the expected size of exosomes.

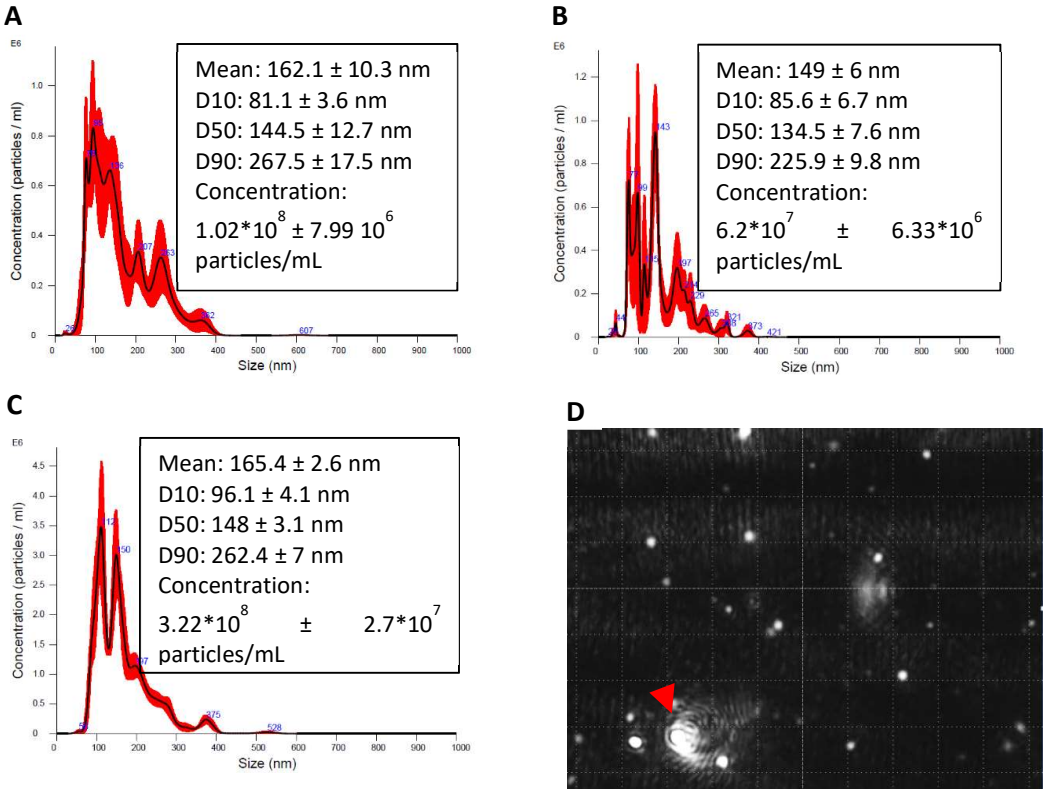

Figure 69 - Characterization of HCjE-Gi cells-derived exosomes extracted from conditioned medium as assessed by NanoSight. (A-C) The size distribution and concentration of particles extracted from conditioned medium kept in culture for 1, 2, and 3 days is shown, respectively (merged mean of 3 individual samples). (D) Snapshot captured whilst sample was being analysed. Red arrowhead shows the particles "off-focus". D10, D50, and D90 indicates the percentage undersize, i.e. for example if D50 is 100nm that means that 50% of analysed vesicles are 100nm or smaller.

4.3.2.2. hTCEpi exosomes derived exosomes' size ranges from 97 to 124nm

The hTCEpi-derived exosomes populations showed little differences in particle concentration observed from day 1 to day 3. In terms of size distribution, 10% of the particles had a diameter that ranges from 97 to 124.7nm (or smaller), within the expected size range of exosomes, Figure 70

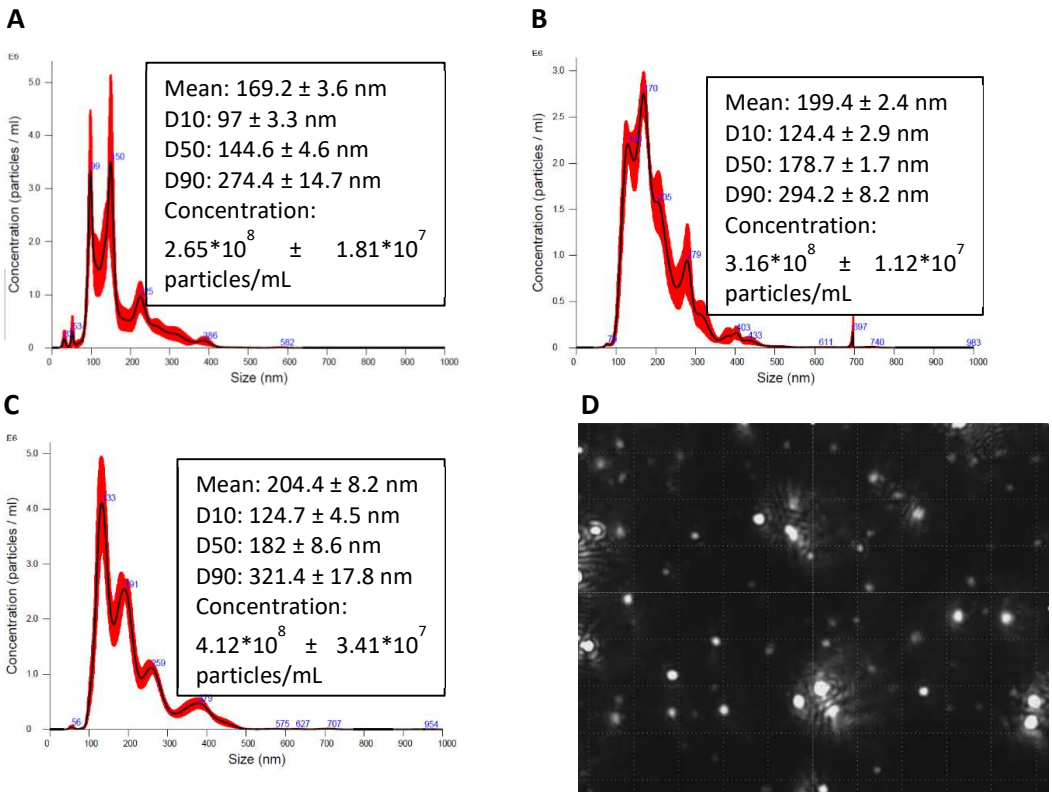

Figure 70 - Characterization of hTCEpi cells derived exosomes extracted from conditioned medium as assessed by NanoSight. (A-C) The size distribution and concentration of particles extracted from conditioned medium kept in culture for 1, 2, and 3 days is shown, respectively (merged mean of 3 individual samples). (D) Snapshot captured whilst sample was being analysed. D10, D50, and D90 indicates the percentage undersize, i.e. for example if D50 is 100nm that means that 50% of analysed vesicles are 100nm or smaller.

Putting together this information, the exosomes used in the downstream experiments were the ones extracted from the conditioned medium collected after 3 days of cell culture.

4.3.2.3. Summary of results 13:

i. Higher concentrations of exosomes were obtained from conditioned medium collected from cells kept in culture for 3 days.

ii. The diameter of vesicles falls within the range of the expected size for exosomes.

4.3.3. Exosome internalization studies- XenoLight DiR-labelled exosomes

To better understand the internalization of exosomes through time, a dye used for lipid bilayer staining was used. The labelled exosomes, diluted accordingly in KSFM, were incubated in culture for a desired period and the percentage of positive events assessed using flow cytometry.

The percentage of DiR-labelled hTCEpi-derived exosomes internalized and/or docked to the cell membrane of HCjE-Gi cells increased over-time peaking at 24 hours ($p<0.05$), Figure 71A. Very similar results were obtained when hTCEpi cells were cultured with labelled HCjE-Gi derived exosomes, Figure 71B.

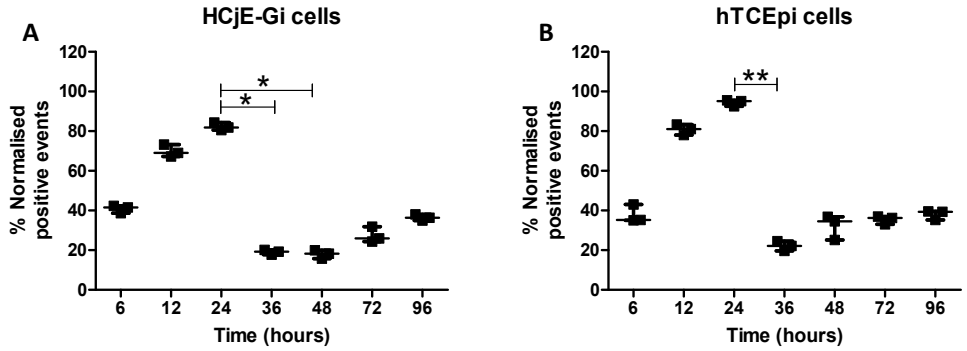

Figure 71 – Internalization and/or docking profiles of XenoLight DiR labelled exosomes. (A) hTCEpi-derived exosomes by HCjE-Gi cells. (B) HCjE-Gi-derived exosomes by hTCEpi cells. Results are normalised against non-labelled exosomes (Data is represented as median ± range, n=3, Kruskal-Wallis test followed by Dunn's Multiple Comparison Test, *p<0.05, **p<0.01, ***p<0.001).

Another membrane labelling dye (PKH26) was used elsewhere to assess the time-response to exosome uptake by bladder cancer cells [564]. Very similar results were there shown, with a peak in number of spots (supposedly exosomes) detected inside the cells after 14 hours of incubation with PKH26-labelled exosomes. The same study showed a dose-dependency in exosome uptake, with more vesicles being detected as its concentration increases. The decrease in the percentage of internalized vesicles can be explained by the incorporation of the exosomes by the cell which will eventually result in the release of their cargo.

4.3.4. Culturing HCjE-Gi cells with hTCEpi-derived exosomes drives higher expression of corneal epithelial markers than the HCjE-Gi-derived exosomes.

This section addresses the results obtained when HCjE-Gi cells were cultured in hTCEpi-derived exosomes containing medium. $3.22x10^8$ particles per 25000 cells were used. The extent of differentiation was assessed by studying the expression of a wide range of well-accepted markers for ECs; KRT3 and KRT12 were used as markers for terminally differentiated corneal ECs [107, 108] while KRT7 and KRT13 were used as markers for terminally differentiated conjunctival ECs [106]. As markers for epithelial SCs ΔNp63 and ABCB5 were used.

4.3.4.1. Reverse Transcriptase qPCR

4.3.4.1.1. Expression of corneal epithelial cell markers

hTCEpi-derived exosomes appeared not to induce significant changes in the levels of expression of KRT3 and KRT12 when compared to HCjE-Gi cell-derived exosomes (dashed line), exception is made for the significant lower levels of KRT3 expressed at 36 hours (25-fold decrease, $p \leq 0.05$). However, an increase in the levels of KRT12 appeared to be occurring at later time-points (NSS). Remarkably, no KRT12 expression was detected at 6 hours when medium containing HCjE-Gi-derived exosomes was used (blue arrow), Figure 72.

4.3.4.1.2. Expression of conjunctival epithelial cell markers

Regarding the expression of KRT7, two different outcomes can be observed. In the first one, up to 12 hours, an increase in its expression levels was observed when medium containing hTCEpi cells-derived exosomes was used compared to HCjE-Gi-derived exosomes containing medium (NSS). This is followed by a significant decrease in KRT7 expression at 24 and 96 hours when hTCEpi-derived exosomes were used and compared to HCjE-Gi derived exosomes (7.7- and 2.6- fold decrease respectively, $p \leq 0.05$). Similarly, the expression of KRT13 was significantly lower at 12 and 48 hours when hTCEpi-derived exosomes were used (1.8- and 2.8- fold decrease respectively, $p \leq 0.001$), Figure 72.

4.3.4.1.3. Expression of epithelial stem cell markers

Several peaks in ΔNp63 expression were appreciated at 6 and 48 hours when hTCEpi cells-derived exosomes were used (4.1- and 12-fold increase respectively, NSS). The expression of ABCB5 peaked at 36 hours, being significantly increased when hTCEpi-derived exosomes were used and compared to HCjE-Gi-derived exosomes (329-fold increase respectively, $p < 0.01$), Figure 72.

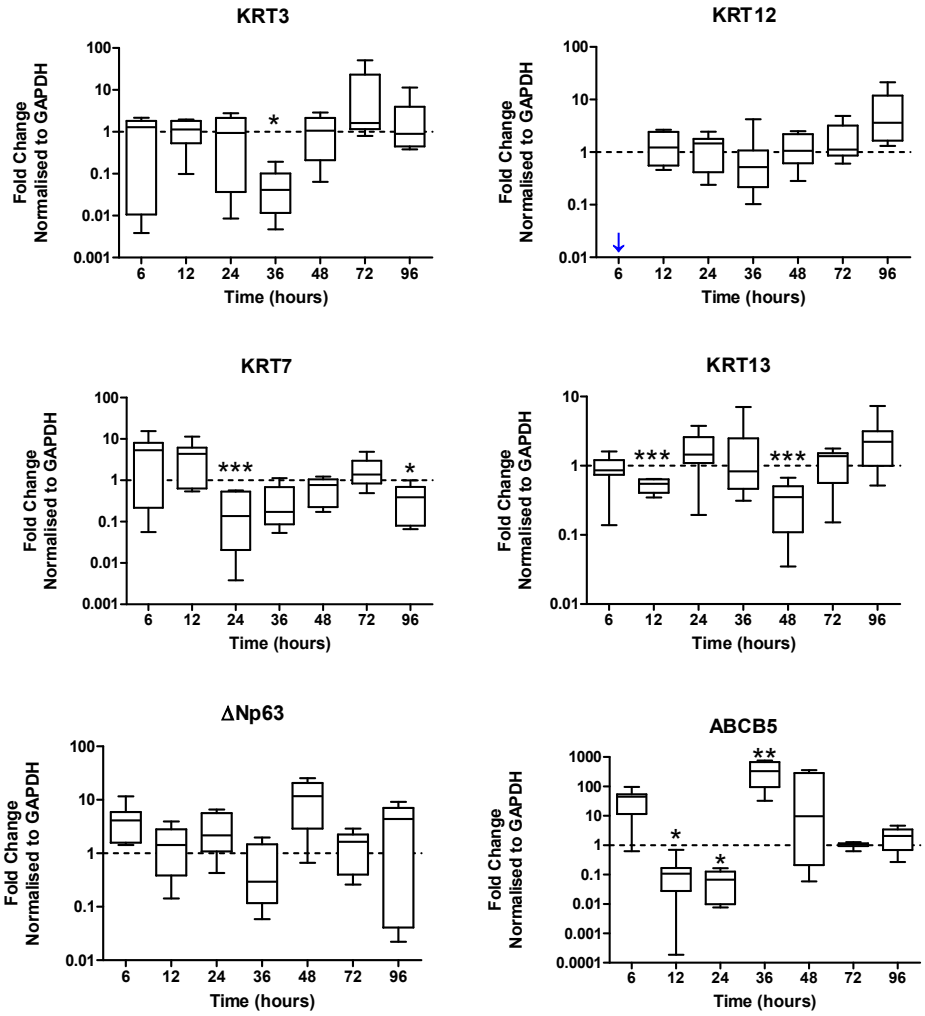

Figure 72 - The expression of epithelial cell markers by HCjE-Gi cells when cultured in medium containing hTCEpi-derived exosomes compared to medium containing HCjE-Gi-derived exosomes over 96 hours as assessed by Reverse Transcriptase qPCR. (Data is represented as median ± 5-95 percentile, n≥6, Mann-Whitney test, Bonferroni corrected p-value, *p<0.05, **p<0.01, ***p<0.001). Dashed line represents the basal expression of the markers of interests when cells are cultured on their own exosomes-containing medium. Abbreviations used GAPDH: glyceraldehyde 3-phosphate dehydrogenase, KRT: keratin, ABCB5: ATP-binding cassette sub-family B member 5.

4.3.4.2. Flow cytometry

4.3.4.2.1. Expression of corneal epithelial cell markers

By culturing HCjE-Gi cells in hTCEpi-derived exosomes containing medium an increase in expression of KRT3 was induced after 36 hours (translated in an increase in 35% of KRT3-positive events, p<0.001) and 96 hours (increase in nearly 10% of KRT3-positive events, p<0.001). A continuous diminution in the expression levels of KRT3 is observed from 6 hours to 96 hours, regardless the exosome population, with no expression detected at 48 and 72

hours. Regarding the expression of KRT12, a continuous increase in its expression was observed over time when hTCEpi-derived exosomes were used. Remarkably, the hTCEpi-derived exosomes induced HCjE-Gi cells to significantly increase the percentage of KRT12-positive cells at 36 hours ($p<0.05$), Figure 73.

4.3.4.2.2. Expression of conjunctival epithelial cell markers

In terms of KRT7 overall expression, a relative plateau in the percentage of positive events is seen throughout the time-window analysed until 48 hours when a drop in its levels is observed. Moreover, the only significant differences between the two exosome populations arrived at 12 hours when the hTCEpi-derived exosomes induced a decrease in KRT7 expression levels (nearly 30% of positive events, $p<0.001$). Regarding the percentage of KRT13-positive events, a drop in its levels was already observed at 6 hours and 24 hours (decrease in nearly 40% and 10% of KRT13-positive cells, respectively, $p\leq0.05$) when hTCEpi-derived exosomes were used, Figure 73.

4.3.4.2.3. Expression of epithelial stem cell markers

At 24 hours a significant increase in the levels of ΔNp63-positive events (5%, $p<0.05$) was observed when hTCEpi-derived exosomes were used. This increase came to a halt between 24 and 48 hours followed by a significant increase in the levels of expression at 72 hours (increase in 10% of ΔNp63-positive events, $p<0.01$) when hTCEpi-derived exosomes were used, Figure 73.

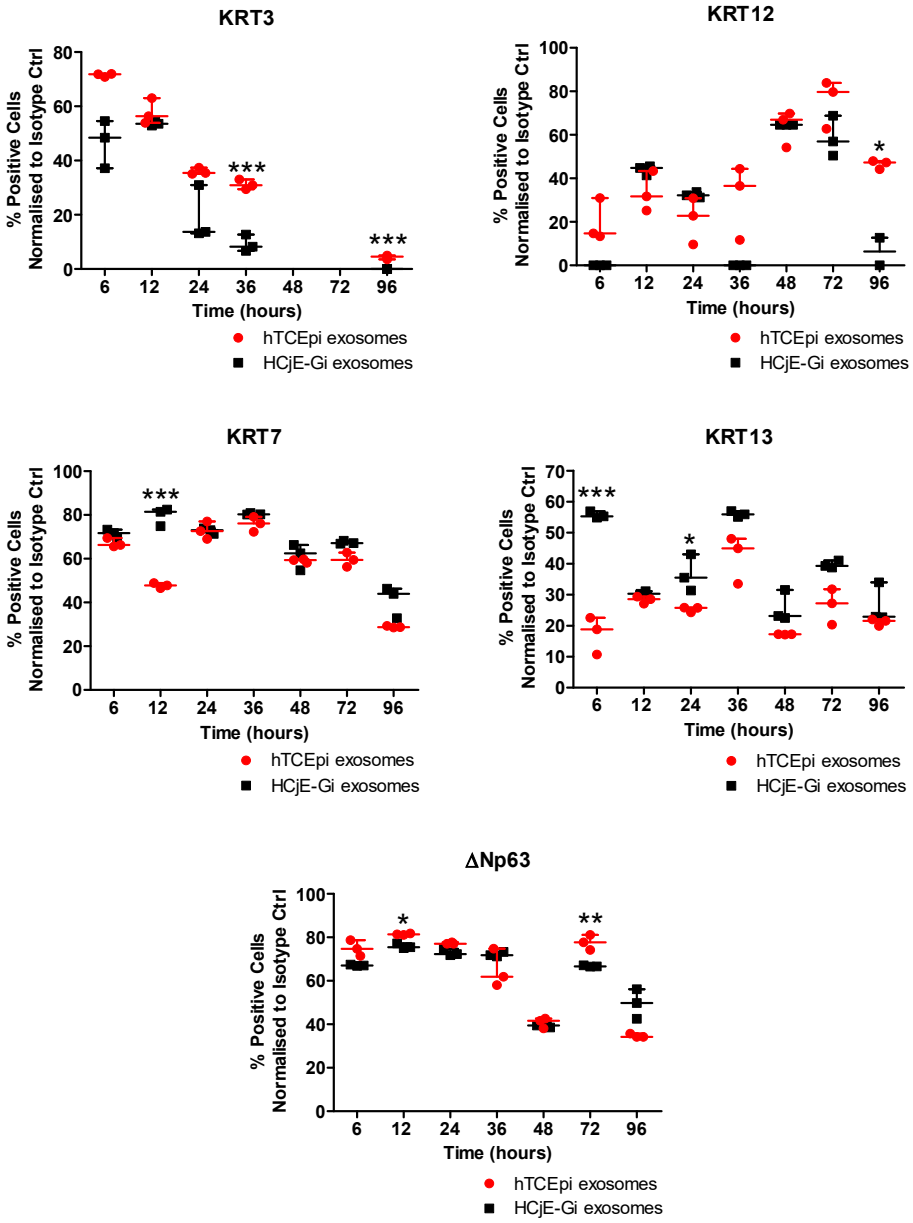

Figure 73 - The expression of epithelial cell markers by HCjE-Gi cells when cultured in medium containing hTCEpi-derived exosomes compared to medium containing HCjE-Gi-derived exosomes over 96 hours as assessed by flow cytometry. The percentage of positive events normalised against isotype control is shown. (Data is represented as median ± interquartile range, n≥3, Mann-Whitney test, Bonferroni corrected p-value, *p<0.05, **p<0.01, ***p<0.001). Abbreviations used Ctrl: control, KRT: keratin.

4.3.4.3. Summary of results 14:

HCjE-Gi cells cultured in medium containing exosomes extracted from hTCEpi cells showed:

i. An increase in expression of corneal EC markers.

ii. A decrease in expression of conjunctival EC markers.

iii. An increase in expression of epithelial SC markers.

4.3.5. Culturing hTCEpi cells with HCjE-Gi cells-derived exosomes drives higher expression of conjunctival epithelial markers than the hTCEpi-derived exosomes

The results in this section were obtained by culturing hTCEpi cells with medium containing HCjE-Gi-derived exosomes and compared to hTCEpi cells cultured with hTCEpi-derived exosomes over a desired period. $3.22x10^8$ particles per 25000 cells were used.

4.3.5.1. Reverse Transcriptase qPCR

4.3.5.1.1. Expression of corneal epithelial cell markers

Little changes on KRT3 and KRT12 expression were appreciated until 48 hours, when a peak in their expression was observed (18- and 40-fold increase respectively). This was followed by a significant decrease in their expression to negligible values (100-fold decrease for both markers, $p \leq 0.01$), Figure 74.

4.3.5.1.2. Expression of conjunctival epithelial cell markers

The HCjE-Gi-derived exosomes appeared to significantly induce an increase in KRT7 and KRT13 expression over time, peaking at 48 hours (8.1- and 17-fold increase respectively, $p \leq 0.05$), followed by a significant decrease in their expression to negligible values (nearly 100-fold decrease for both markers, $p \leq 0.001$), Figure 74.

4.3.5.1.3. Expression of epithelial stem cell markers

Regarding ΔNp63 expression, a significant peak in its levels was appreciated at 12 and 48 hours when hTCEpi cells were cultured with HCjE-Gi-derived exosomes (7.8- and 66-fold increase respectively, $p<0.005$). Very similar results were found for the other SC marker, ABCB5, Figure 74.

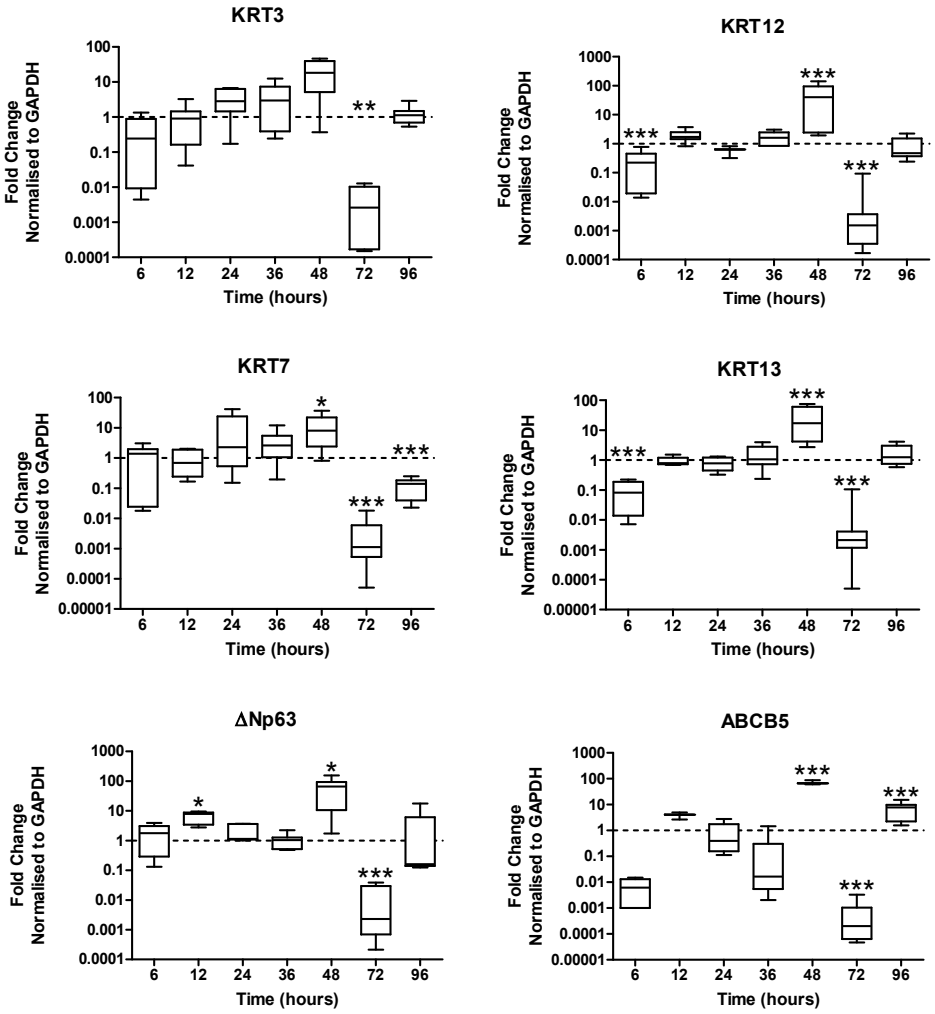

Figure 74 - The expression of epithelial cell markers by hTCEpi cells when cultured in medium containing HCjE-Gi-derived exosomes compared to medium containing hTCEpi-derived exosomes over 96 hours as assessed by Reverse Transcriptase qPCR. (Data is represented as median ± 5-95 percentile, n≥6, Mann-Whitney test, Bonferroni corrected p-value, *p<0.05, **p<0.01, ***p<0.001). Dashed line represents the basal expression of the markers of interests when cells are cultured on their own exosomes-containing medium. Abbreviations used GAPDH: glyceraldehyde 3-phosphate dehydrogenase, KRT: keratin, ABCB5: ATP-binding cassette sub-family B member 5.

4.3.5.2. Flow cytometry

4.3.5.2.1. Expression of corneal epithelial cell markers

By culturing hTCEpi cells with medium containing HCjE-Gi cells-derived exosomes a decrease in the percentage of KRT3-positive events was seen after 6 hours (decrease of 20% in KRT3-positive cells, $p<0.05$). This decrease was also appreciated after 96 hours (diminution of 10% in positive events, $p<0.05$). The only appreciable changes in KRT12 expression induced by HCjE-Gi-derived exosomes were observed after 96 hours (decrease of 10% in KRT12-positive

cells, p<0.001). Interestingly, a negligible percentage of KRT12-positive events was observed at 96 hours when the hTCEpi cells were seeded with HCjE-Gi-derived exosomes containing medium (blue arrow). Moreover, the percentage of KRT12-positive events appeared to increase throughout the time-window analysed until 72 hours, Figure 75.

4.3.5.2.2. Expression of conjunctival epithelial cell markers

Regarding the percentage of KRT7-positive events no significant changes could be appreciated until 72 hours where a significant increase in its percentage was seen (corresponding to an increase of 10% in positive events, p<0.01). In respect to KRT13, a significant increase in its expression levels is observed after 24, 48, and 96 hours when HCjE-Gi cells-derived exosomes were used (corresponding to an increase of nearly 15% in KRT13-positive cells, p≤0.05). Remarkably, negligible percentages of KRT13-positive events were detected at 48 hours when medium containing hTCEpi-derived exosomes was used (green arrow), Figure 75.

4.3.5.2.3. Expression of epithelial stem cell markers

Concerning the expression of ΔNp63 a cyclic trend could be observed, i.e. a decrease in its expression levels was followed by an increase for either exosomes-containing medium used. At 96 hours the HCjE-Gi-derived exosomes induced a significant increase in its expression levels by hTCEPi cells (equivalent to an increase in 20% of positive events, p<0.001), Figure 75.

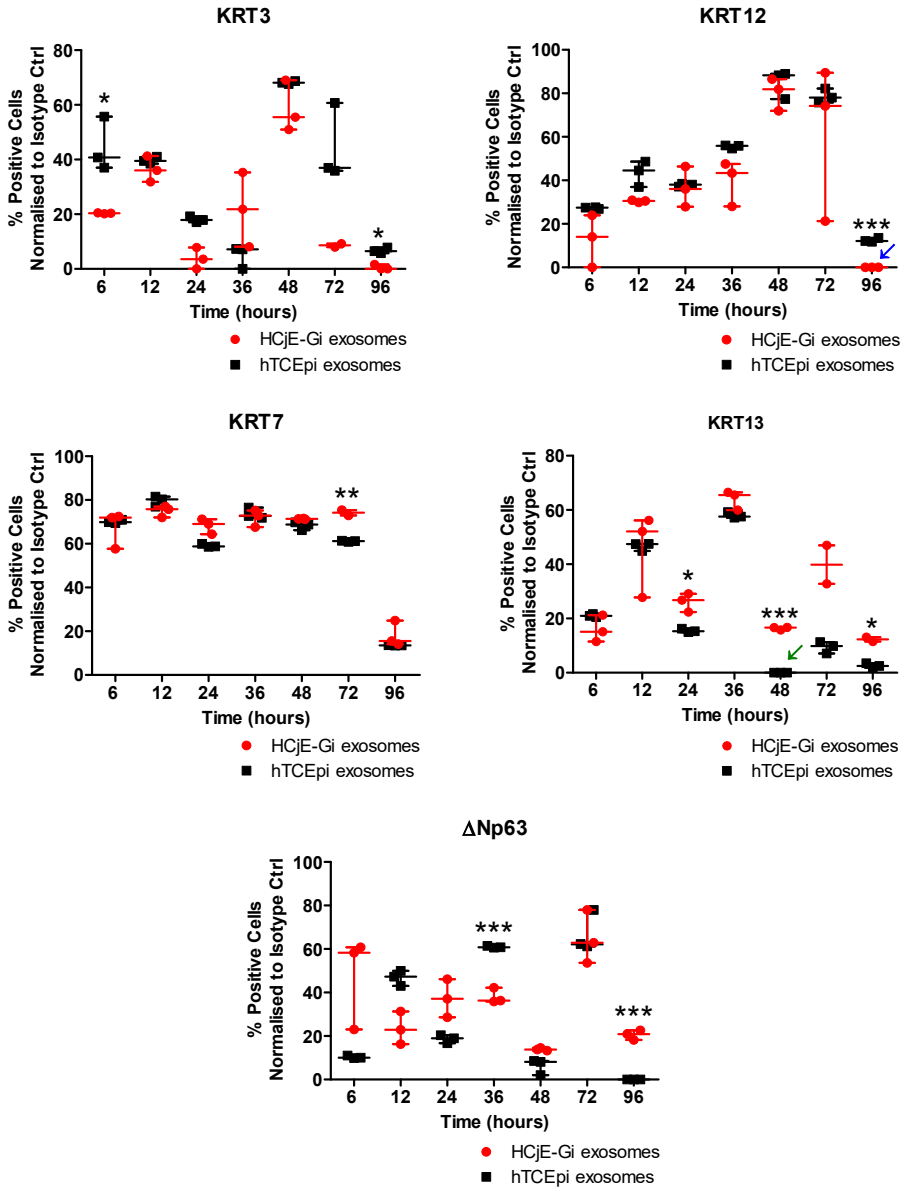

Figure 75 - The expression of epithelial cell markers by hTCEpi cells when cultured in medium containing HCjE-Gi cells-derived exosomes compared to medium containing hTCEpi cells-derived exosomes over 96 hours as assessed by flow cytometry. The percentage of positive events normalised against isotype control is shown. (Data is represented as median ± range, n≥3, Mann-Whitney test, Bonferroni corrected p-value, *p<0.05, **p<0.01, ***p<0.001). Abbreviations used Ctrl: control, KRT: keratin.

4.3.5.3. Summary of results 15:

hTCEpi cells cultured in medium containing exosomes extracted from HCjE-Gi cells showed:

i. A decrease in expression of corneal EC markers.

ii. An increase in expression of conjunctival EC markers.

iii. An increase in expression of epithelial SC markers.

4.3.6. Exosome cargo - End-point PCR

Several studies have shown that mRNA molecules are confined inside the exosomes and can be translated into proteins in the presence of the necessary machinery [480]. In this section, PCR products were probed for the encoding genes for the EC markers used throughout this study.

4.3.6.1. HCjE-Gi-derived exosomes contain mRNA molecules

Exosomes produced by HCjE-Gi cells contain mRNA from all studied genes with exception for KRT12 and KRT13 (blue arrows), Figure 76.

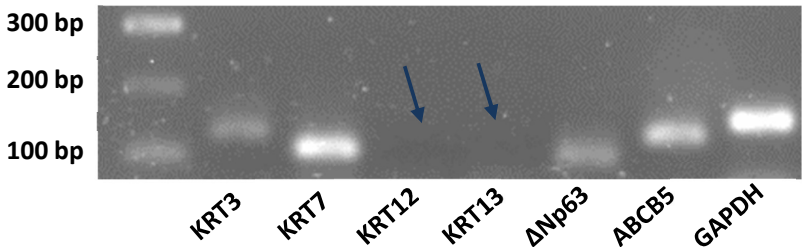

Figure 76 - Polymerase chain reaction products extracted from exosomes produced by HCjE-Gi cells. First lane shows a 100bp ladder. Abbreviations used bp: base pairs, KRT: keratin, ABCB5: ATP-binding cassette sub-family B member 5, GAPDH: glyceraldehyde 3-phosphate dehydrogenase.

4.3.6.2. hTCEpi-derived exosomes contain mRNA molecules

Exosomes produced by hTCEpi cells showed to contain mRNA from all studied genes with exception for KRT12 and KRT13 (green arrows), Figure 77.

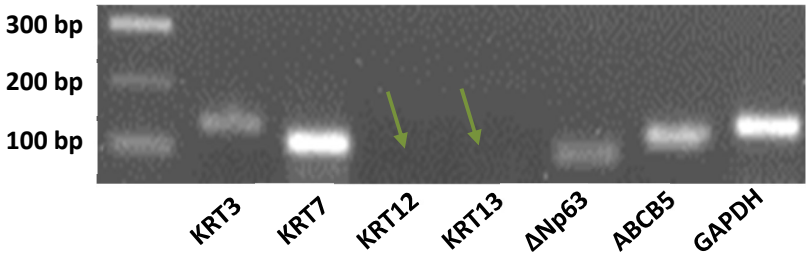

Figure 77 - Polymerase chain reaction products extracted from exosomes produced by hTCEpi cells. First lane shows a 100bp ladder. Abbreviations used bp: base pairs, KRT: keratin, ABCB5: ATP-binding cassette sub-family B member 5, GAPDH: glyceraldehyde 3-phosphate dehydrogenase.

4.3.6.3. Negative control

The presence of the mRNA for the transcripts of interest was not detected, Figure 78.

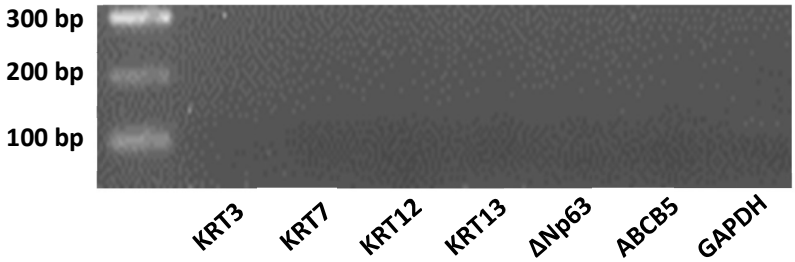

Figure 78 – Negative control for polymerase chain reaction products. First lane shows a 100bp ladder. Abbreviations used bp: base pairs, KRT: keratin, ABCB5: ATP-binding cassette sub-family B member 5, GAPDH: glyceraldehyde 3-phosphate dehydrogenase.

4.3.7. Exosome cargo - Exo-NGS Exosomal miRNA Sequencing

NGS sequencing results showed the presence of 22 different RNA types in both exosome populations, being the miRNA (mild blue) a small percentage of the total molecules detected, Figure 79.

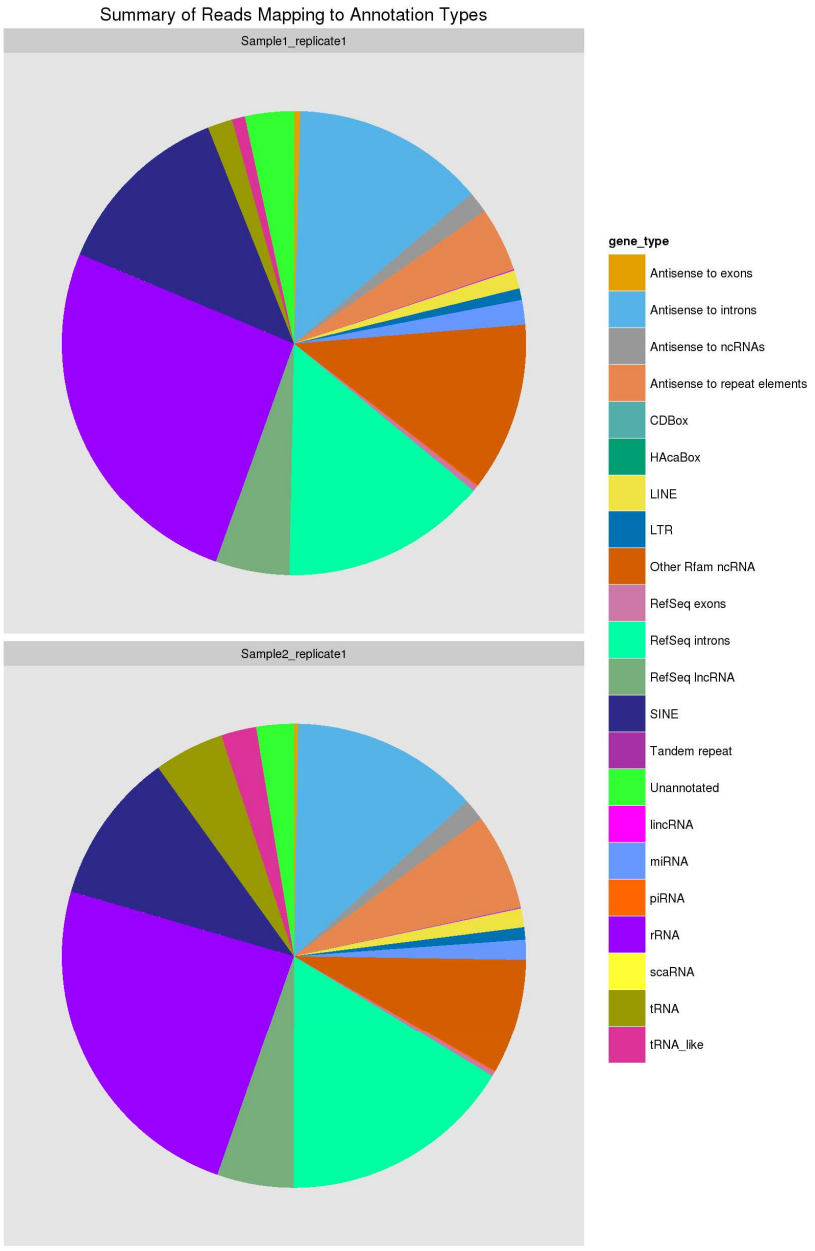

Figure 79 - Pie chart summarizing the number of reads mapping to each annotation type in each sample. Sample1 and Sample2 indicate HCjE-Gi and hTCEpi-derived exosomes, respectively.

The relative abundance in miRNA content of the two exosome populations was assessed by NGS exosomal miRNA sequencing. A total of 1668 different miRNA molecules (precursor and mature) were detected: 337 showed to be present only on HCjE-Gi-derived exosomes, 282 on hTCEpi -derived exosomes, and 1049 to be shared by both populations, Figure 80. Table 25 shows the presence of 11 miRNA molecules (precursor and mature), with significant

differences in their relative abundance between the two populations ($p<0.05$). The abundance of mir-146a, miR-146a-5p, mir-155, miR-155-5p, mir-9-5p, mir-9-1, mir-9-3, and mir-9-2 was significantly higher on the HCjE-Gi-derived exosome populations ($p<0.05$). On the other hand, the abundance of mir-598, miR-598, miR-34c-3p, and mir-34c was shown to be significantly higher on hTCEpi- derived exosomes population ($p<0.05$).

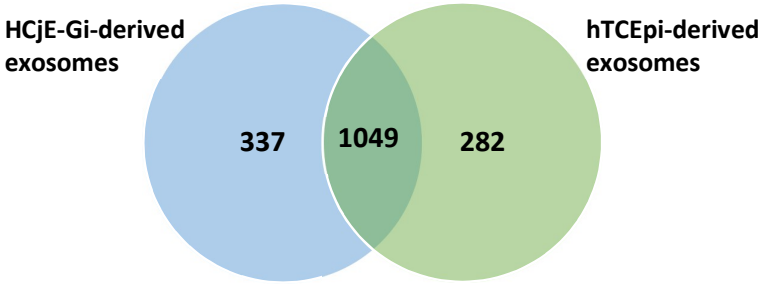

Figure 80 - Venn diagram presentation of miRNAs content detected in both exosome populations. 337 molecules were only detected on HCjE-Gi-derived exosomes (blue), 282 molecules detected only on hTCEpi-derived exosomes (green), and 1049 molecules were shown to be shared by both exosome populations (dark green).

Table 25 - miRNA content of the two exosome populations as assessed by NGS. mir denotes precursor miRNA molecules, miR denotes mature miRNA molecules.

miRNA	Abundance HCjE-Gi	Abundance hTCEpi	p-value	Log_2 fold change	Role
miR-598	Residual	111.74	0.048	infinity	Down-regulated in cancer tissues
miR-34c-3p	46.56	1548.96	0.011	5.1	Up-regulated in cell differentation
mir-34c	116.39	2713.78	0.029	4.5	Up-regulated in cell differentation
mir-146a	10080.83	510.48	0.048	-4.3	Upregulated in stem cell maintenance homeostasis
miR-146a-5p	10080.83	510.48	0.048	-4.3	Upregulated in stem cell maintenance homeostasis
mir-155	703.82	4.38	0.0001	-7.3	Upregulation represses cell differentiation
miR-155-5p	703.82	4.38	0.0001	-7.3	Upregulation represses cell differentiation
miR-9-5p	86.27	Residual	0.03	infinity	Probably involved in cell differentiation
mir-9-1	98.59	Residual	0.018	infinity	Probably involved in cell differentiation
mir-9-3	98.59	Residual	0.018	infinity	Probably involved in cell differentiation
mir-9-2	98.59	Residual	0.018	infinity	Probably involved in cell differentiation

4.3.8. Summary of results of Chapter 4:

i. An optimized percentage of CD63- and TSG101-positive events (markers for exosome-enriched solutions) was obtained from vesicles extracted from conditioned medium collected after 3 days in culture.

ii. The percentage of GRP94 -positive events showed to zero throughout the whole experiment.

iii. The internalization of DiR-labelled exosomes by both cell lines peaked after 24 hours.

iv. By seeding HCjE-Gi cells with medium containing exosomes extracted from hTCEpi cells:

- **a.** An increase in expression of corneal EC markers was observed.
- **b.** A decrease in expression of conjunctival EC markers was seen.
- **c.** An increase in expression of epithelial SC markers was appreciated.

v. By seeding hTCEpi cells with medium containing exosomes extracted from HCjE-Gi cells:

- **a.** A decrease in expression of corneal EC markers was seen.
- **b.** An increase in expression of conjunctival EC markers was appreciated.
- **c.** An increase in expression of epithelial SC markers was observed.

vi. Exosomes extracted from the two cells lines contained mRNA to encode for KRT3, KRT7, ΔNp63, and ABCB5.

vii. The miRNA content carried by the two exosomes populations showed to be different.

4.4. Discussion

Countless studies have already suggested EVs, and particularly exosomes, as agents to transfer bioactive molecules between different cells to play important roles in angiogenesis [565], wound healing [566], cancer metastasis [567, 568], amongst many other processes. The studies outlined in this chapter addressed for the first time the role played by the exosomes to induce the differentiation of two EC populations from the human ocular surface. The extent of differentiation and the characterization of exosomes cargo was assessed by a range of different techniques.

The mass spectrometry results, addressed in Chapter 3 (section 3.3.1), showed the presence of exosome-associated proteins present in the HCjE-Gi and hTCEpi ECM preparations. These observations were the first indicative of the production and release of exosomes by the two cell lines.

4.4.1. Exosomes were successfully extracted from the conditioned media obtained from the two cell lines

Flow cytometry results revealed a successful extraction of EVs with the properties of exosomes-enriched populations: (i) presence of CD63- and TSG101-positive events and (ii) absence of GRP94-positive events [503]. The percentage of CD63 and TSG101-positive events was shown to increase with the time that cells are kept in culture, which may be a result of more exosome-like vesicles being produced over time. Co-localization of CD63 and TSG101, to address the double-positivity, would give better insights regarding the real percentage of exosomes that can be extracted from conditioned medium and therefore a better approach to distinguish them from other EVs. NanoSight® data showed that the extracted EVs have diameters that fall within the expected size of an exosome (40-100nm) [473, 569]. However, bigger events are detected which are likely the result of off-focus particles detected and analysed by the NanoSight® software. Based on these two sets of data, exosomes-containing populations can be extracted from conditioned medium, collected as early as day one, obtained from the two cell lines (HCjE-Gi and hTCEpi).

Thery et al. have shown that clathrin coated vesicles, which will later mature into MVBs, are internalized by cells in 15 minutes [473] and PKH26-labelled exosomes are detected within different cell types just one hour after incubation [570]. In accordance with these studies, the herein internalization studies have shown an increase in DiR-labelled vesicles from, as early as 6 hours until 24 hours, when the percentage of positive events dropped significantly.

This reduction may be attributed to degradation of exosome membrane due to their fusion with the cell membrane or other intracellular compartments, resulting in exosome cargo release. Because of their content and rapid internalization by cells, exosomes are powerful agents to induce changes in cell physiological state very quickly.

4.4.2. hTCEpi-derived exosomes drive higher expression of corneal epithelial markers by HCjE-Gi cells than HCjE-Gi-derived exosomes

The results outlined in this section highlight the role of hTCEpi-derived exosomes for inducing the differentiation of HCjE-Gi cells into the corneal epithelial-like lineage, as assessed by various methods. The internalization studies showed a peak in exosome intake and/or cell membrane docking at 24 hours which may suggest that the major changes in cell behaviour would occur within that time-frame or shortly after. This is shown to be verified mainly for the decreased in the levels of expression of the conjunctival markers that occurs at significant levels within the first 24 hours. On the other hand, the changes in the corneal markers expression are mainly occurring at later time periods. The Reverse Transcriptase qPCR data shows an early peak (6 hours) in expression of epithelial SC markers ΔNp63 and ABCB5, despite being non-significant this increase is likely to indicate an emergence of early epithelial progenitor cells resulting from the de-differentiation of terminally differentiated HCjE-Gi cells. This is followed by a decrease in expression of conjunctival ECs markers KRT7 and KRT13 at 24 and 12 hours, respectively, and a later moderate increase in expression terminally differentiated corneal ECs markers KRT3 and KRT12. Flow cytometry data show even greater differences when the two different exosomes populations are used, noteworthy is the steady decrease in the percentage of KRT3-positive events over time, however at slower rates when hTCEpi-derived exosomes are used. When the two data sets are analysed together some discrepancies are observed, meaning that additional agents are affecting the changes in protein translation. This may be result of miRNAs molecules shown to be present in the exosome cargo that may play a role in increase/decrease the protein abundance without the need of mRNA levels to change. Taken together, these results suggested an early emergence of progenitor ECs, accompanied by a loss of conjunctival-like phenotype and by a differentiation toward a corneal epithelial-like lineage of HCjE-Gi cells in response to hTCEpi-derived exosomes.

4.4.3. HCjE-Gi-derived exosomes drive higher expression of conjunctival epithelial markers by hTCEpi cells than hTCEpi-derived exosomes

This section addresses the role played by HCjE-Gi-derived exosomes on inducing the differentiation of hTCEpi cells into a conjunctival epithelial-like lineage. Similar to the previous section, the internalization studies showed a peak in exosome intake and/or membrane docking after 24 hours. The Reverse Transcriptase qPCR data shows one peak in expression of epithelial SC markers ΔNp63 and ABCB5 at 12 hours (6 hours delayed when compared to previous section) which may indicate the emergence of early epithelial progenitor cells. This is indeed followed by an increase in expression of conjunctival markers KRT7 and KRT13 (the latter at lower magnitude) and a decrease in expression of terminally differentiated corneal ECs markers KRT3 and KRT12. Flow cytometry data show similar results with even greater differences when two different exosomes populations are used, suggesting that the changes observed at transcript levels may then be translated at protein levels. Yet again the role played by the miRNA molecules contained in the exosomes should not be downplayed in its effects on changing the protein abundance without the need in changing the mRNA levels. Based on both data sets, it is suggested that the hTCEpi cells, a corneal cell line, started to show conjunctival epithelial like-characteristics, losing its corneal epithelial-like phenotype in a process that involves an intermediate step of cell de-differentiation.

4.4.4. Exosome cargo characterization shows the presence of mRNA and miRNA molecules

mRNA and miRNA are two families of molecules showed to be part of exosome cargo [571-573] playing important roles in processes as diverse as biomarkers for schizophrenia [574] and cancer progression and metastasis [575]. Others have already shown that mRNA [576, 577] and miRNA molecules [577] can be delivered by exosomes and translated in the presence of the necessary machinery [577].

Exosome cargo was characterized by end-point PCR and Next Generation Sequencing for mRNA and miRNA content, respectively. End-point PCR data shows the presence of mRNA for the markers on interest, exception is made for KRT12 and KRT13 (presence not detected). The presence of these mRNA molecules and the notion that they can be translated [576, 577] aids to understand the rapid cell response in terms of protein turn-over observed.

The information regarding miRNA expression, function and location in the human ocular surface is still very scarce. The most common miRNA molecules, their location within the ocular surface and function, are shown on Table 26.

Table 26 – Most common miRNAs, their location within the ocular surface and function. Adapted from [490, 491, 493, 502, 578-583]. Abbreviations used NA: not assessed, NGS: next generation sequencing, * results obtained from murine studies.

miRNA	Cornea	Limbus	Conjunctiva	Role	NGS results	
					HCjE-Gi	hTCEpi
Up-regulated						
miR-24	NA	NA	NA	Associated with differentiated ECs	++	+++
miR-103	-,-/+	++	NA	Promote epithelial SCs characteristics	NA	NA
miR-107	-,-/+	++	NA	Promote epithelial SCs characteristics	+	+ (++)
miR-125 family	+	++	NA	Maintenance of the adult epidermal SCs	+	-/+
miR-127	+	++	NA	Tumorigenesis	-/+	-
miR-139	+	++	NA	Tumorigenesis	-/+	+
miR-143	+	++	NA	Tumour suppressor, ESC pluripotency	-/+	-/+
miR-145	+	++	NA	Tumour suppressor, ESC pluripotency	+	-
miR-146a	-,-/+	+	NA	Tumour suppressor	++	+
miR-203	NA	NA	NA	Maintenance of the adult epidermal SCs	+++	+
miR-205	+	+	+	Corneal keratinocyte migration (inhibition), highly expressed in mammary progenitor cells	++++	++++
miR-211	+	++	NA	Tumorigenesis	NA	NA
miR-338	+	++	NA	Tumour suppressor	NA	NA
miR-450b-5p	NA	NA	NA	Contribute to the pluripotent state of SCs	-/+	-/+

Down-regulated					NA	NA
miR-184	++	+	-*	Oncogenic, neural stem-cell specific (induces proliferation and inhibits differentiation), cornea-specific	-/+	-
miR-193	++	+	ND	Tumour suppressor	-	-/+

NGS results showed the expression of a total of 1668 different miRNA molecules (precursor and mature), of which 337 showed to be expressed only by HCjE-Gi-derived exosomes, 282 by hTCEpi-derived exosomes, and 1049 to be shared by both exosome populations.

Despite the non-significant differences in the abundance of miR-145, miR-143, miR-205, mir-126, and miR-193 between the two exosomes populations, the higher expression of the first four and the lower expression of the latter observed in HCjE-Gi-derived exosomes suggested a less differentiated state of such cells, as these miRNAs have been found to be involved in corneal epithelial differentiation [502], enriched in limbal regions [490], progenitor cells homeostasis [583], and tumour suppression [582]. Additionally, miR-203 and miR-125b (enriched in the HCjE-Gi-derived exosomes) have been linked with the maintenance of adult epidermal SCs [499-501] and miR-450b-5p to contribute to the pluripotent state of SCs. On the other hand, miR-24 (enriched in the hTCEpi-derived exosomes) functions are mainly related with EC differentiation [494]. NGS results suggested that exosomes released by the HCjE-Gi cells contain miRNAs molecules mainly involved in keeping cells in undifferentiated states while exosomes released by hTCEpi cells contain higher abundances of miRNAs associated with EC differentiation.

From the wide panel of the detected molecules, only 11 showed significant differences in their relative abundance between the two populations, these include miR-598, miR-34c family, miR-146a, miR-155 family, and miR-9 family.

4.4.4.1. miR-598 is downregulated in cancer tissues

The information on miR-598 biology is still very scarce, with no reports yet showing its expression by human ocular ECs. However, Chen et al. have shown that miR-598 is highly downregulated in colorectal cancer tissues and it inhibits metastasis in colorectal cancer by

suppressing JAG1/Notch2 pathways, stimulating epithelial mesenchymal transition (EMT) [584]. These observations suggest that its high expression is involved in cell differentiation.

4.4.4.2. miR-34c is involved in cell differentiation

The miR-34 family consists of three members: miR-34a, miR-34b, and miR-34c. The miR-34 family show the highest induction by p53, a tumour suppressor protein, which prompted the investigation of their role in cancer biology [585]. All members of miR-34 were shown to suppress tumour growth by inhibiting cancer development, metastasis and stemness, a process regulated through the downregulation of their target mRNAs [586, 587]. Others have yet shown an increased expression of miR-34c expression from new-born to sexually mature mouse testes, suggesting its involvement in germ cell differentiation and sperm production, promoting cell differentiation of mouse spermatogonial SCs [578, 588]. Additionally, miR-34c was shown to regulate the differentiation of mouse ESCs into germ cells [578] and all members of the miR-34 family are induced during osteoblast differentiation in bone development [589]. An extensive report on the role played by miR-34 family in modulating EMT has shown that the overexpression of miR-34c attenuated EMT via suppression of Notch/Jag1 pathway [590]. To date no reports have been published showing any role played by this miRNA family in the development of the eye nor epithelial differentiation, however in light of this knowledge it may be deduced that their higher abundance in hTCEpi cells-derived exosomes are an indicative of a more differentiated cell state.

4.4.4.3. miR-146a is involved in the maintenance of LSCs homeostasis

miR-146a overexpression has been associated with delayed wound healing properties in human diabetic corneas, probably due to its putative role in inhibiting cell migration through phosphorylated EGFR and p38 signalling pathways [492]. Winkler et al. have, more recently, shown that miR-146a is overexpressed in limbus versus central cornea suggesting its possible role in LSCs homeostasis [580], therefore playing a role in maintenance and early differentiation state of LSCs. Additionally, its expression in the healthy cornea (central and peripheral) yielded a diffuse and weak expression, whereas the diabetic cornea showed stronger expression, specially at limbal locations [492]. Xu et al. have shown that miR-146a negatively regulated EGFR expression and inhibited tumour growth through the MAPK pathway in a pERK-dependent manner to control migration and proliferation [579]. It has been associated with several diseases, including diabetic nephropathy-associated inflammation [591] and diabetic retinopathy [581]. It also inhibits migration and proliferation of lung cancer cells due to its targeting of EGFR and NF-κB signalling [592]. Putting together,

all these observations, and particularly its higher expression at limbus locations, suggest that its higher abundance in HCjE-Gi-derived exosomes is an indicative of an overall less differentiated cell state.

4.4.4.4. miR-155 represses cell proliferation and differentiation and is highly expressed at limbal locations

TCF4, a target of miR-155, is a crucial transcription factor of Wnt signalling and has been shown to regulate p63/surviving and p57 expression by maintaining the proliferation and migratory properties of human corneal epithelial progenitor cells [593]. Other predicted targets of miR-155 are involved in MAPK, insulin, and mTOR signalling, suggesting potential suppressive effect on cell proliferation, differentiation , and migration [490]. As it has been shown to be enriched in limbal ECs, it antagonizes transcription factors that regulate cell proliferation, differentiation, and apoptosis. Therefore, its higher expression in HCjE-Gi cells-derived exosomes suggest an overall less differentiated cell state.

4.4.4.5. miR-9 is involved in cell differentiation

Very little has been published on the functions of miR-9 on human ocular cell biology. Only two manuscripts have shown an increase in its expression associated with cell apoptosis and differentiation of retinal pigmented ECs [594] and retinal progenitor cells [595]. Other reports pointed in the same direction, with the expression of miR-9 being associated with the differentiation of neural SC [596] and bone marrow mesenchymal SCs into neuronal cells [597].

The significant differences in miRNA content from the two exosomes populations are mainly related with miRNA molecules involved in maintaining and/or promoting an undifferentiated cell state, being their expression higher in exosomes derived from HCjE-Gi cells. The higher abundance of these miRNA molecules in the exosomes released by such cell line suggest three different, but correlated, outcomes. Firstly, it is indicative that HCjE-Gi cells may be in an overall less differentiated state when compared to hTCEpi cells. Secondly, the cargo carried by HCjE-Gi-derived exosomes promoted a delayed intermediate step of cell dedifferentiation as observed by the higher expression of epithelial SC markers ΔNp63 and ABCB5 by hTCEpi cells at later time-points when cultured with HCjE-Gi-derived (12-48 hours, Figure 74 and 36 hours, Figure 75) and compared to the high expression by HCjE-Gi cells when cultured on hTCEpi-derived exosomes at 6-12 hours (Figure 72 and Figure 73). Thirdly, the hTCEpi differentiation toward a conjunctival epithelial-like lineage in response to HCjE-

Gi-derived exosomes appeared to be delayed and more incomplete. Supporting this hypothesis is the relatively constant transcript levels of keratins (KRT3, KRT12, KRT7, and KRT13) up to 48 hours (Figure 74) upon which an up-regulation of epithelial SC markers is seen, suggesting an emergence of progenitor cells. On the other hand, hTCEpi-derived exosomes promoted an early down-regulation in keratin expression on HCjE-Gi cells (24-48 hours for KRT7 and 6-12 hours for KRT13, Figure 72) preceded by an increase in expression of epithelial SC markers ΔNp63 and ABCB5. Taken altogether, these results suggested that HCjE-Gi-derived exosomes have restricted potential for differentiation.

4.4.5. Potential of transdifferentiating human ocular epithelial cells using cell-derived exosomes

The studies outlined in this chapter provide a step towards refinement of protocols to use EVs, and particularly exosomes, for potential therapeutic purposes. However, several improvements to the technique need to be carried out before these potential therapeutic agents can be understood:

i. **Validate the expression** of miRNA molecules by Reverse Transcriptase qPCR, mRNA target assessment, and antagomirs experiments to silence endogenous miRNA to better understand their effects on ECs from human ocular surface. These results should also be verified using primary ECs from the human ocular surface.

ii. **Presence of potential dangerous mRNAs and/or miRNAs.** The presence for undifferentiated cell molecules such as NANOG, OCT4 may be addressed and selectively eradicated to prevent tumour formation upon administration.

iii. **Selectively change their cargo t**o enhance their properties. Remarkably, a study using exosomes extracted from cells genetically modified to express $CD34^{+}$ sonic hedgehog protein, showed infarct size reduction and improvement of cardiac function after 4 weeks, when those exosomes were injected into the infarcted border zone [598].

Chapter 5 – Discussion and Future work

In this chapter, the main results and conclusions obtained in each chapter will be discussed in context with the original aims, the research of others, and the future research work resulting from this thesis. Research related to conjunctival transdifferentiation had its pinnacle in the 1980s and early 1990s with the work of Friedrich Kruse, Scheffer Tseng, and Winston Kao [29, 166-169, 184, 233-242], with very few research articles been published ever since. On the other hand, the field of exosome biogenesis, release, and mechanisms of action, despite being poorly understood, has gained a lot of new insights with the number of publications dramatically increasing over the last decade (over 6200 "exosomes" entries on PubMed on January 2018).

Until recently, tissue-specific SCs were considered to have limited potency, and their derived TACs to be irreversibly committed. This paradigm has been challenged with the recent work of Takahashi and Yamanaka that led to the discovery that mature cells can be reprogrammed to become pluripotent [203]. The idea of adult somatic cell reprogramming has gained new knowledge more recently, with the extracellular environment being one of the triggering agents for such process [599]. One of the best studied models on cell-ECM interactions arises from the skin, where integrin-ECM interactions regulate cell fate [600].

Adult mammalian central corneal cells, which are widely accepted to be differentiated cells, are shown to differentiate into pilosebaceous units when confronted with trichogenic embryonic dermis, or sweat glands when cultured in plantar dermis [601]. The corneal cells lose their high levels of KRT12 expression gaining granular and cornified features, associated with pilosebaceous units, or show the formation of footpads and sweat glands when in plantar dermis [601]. To understand the process of cell reprogramming, the same group of investigators have shown that the first stage of the transformation may be the restoration of a more SC-like phenotype [601]. This is in accordance with the work of Potten and Loeffler, who showed that TACs that left their SC niche are not irreversibly committed to a terminal differentiation pathway but are able to revert to being SCs [64]. Interesting observations have shown that proliferation and differentiation processes are not mutually exclusive, i.e. the expression of a new gene product is not necessarily linked to functional irreversibility [64]. In the same line of studies, Ferraris et al. have induced corneal epithelium from rabbit embryos (23 and 24-day embryos and new-born animals) to form hair follicles when associated with dorsal embryonic dermis. These corneal cells failed to express KRT12 and

then stratified into structures containing hair buds [602]. Many studies have extensively addressed the effect of the external environment stimuli on cell's fate with certain degree of success. These include chondrocyte differentiation and morphogenesis of mammary ECs when cultured in 3D environments [603], and differentiation of dermal cells into neural-like cells when grown on laminin substrates and fed with FGF2-containing medium [604]. Besides ECM physical/mechanical cues, conditioned medium has also been used to differentiate cells toward specific lineages. One study showed that dermal papilla cells cultured with conditioned medium from an endothelial cell line start to express endothelial markers and to exhibit functional activities (formation of capillary-like structures in Matrigel®) [605].

KRT10, an acidic type of keratin filament, is commonly associated with the terminally differentiated suprabasal cells of the stratified epidermis of skin [606]. In rat embryos it also has been shown to be expressed at the limbus of late gestation embryos, persisting after birth and progressively being lost from limbus as the rats age [606]. However, when corneal ECs are cultured under high calcium concentrations they express KRT10 [607], additionally hESCs differentiated into corneal epithelial like cells also express this keratin [178]. These two studies show that corneal ECs when cultured under atypical conditions can express KRT10, suggesting that extracellular cues can promote changes in cell phenotype and possibly reverting them into a more progenitor phenotype, however further investigations are needed to address this point.

Taken together, all these observations suggest that cells cultured in appropriate conditions and given the adequate cues can differentiate towards specific lineages, changing their characteristics to those in accordance to the new environment in which they are placed regardless their differentiation state.

The aim on Chapter 2 was two-fold; firstly, to develop a protocol to promote the alternate differentiation of ECs from the human ocular surface in response to the extracellular protein meshwork, whose morphogenic tissue-specific properties where kept intact. Secondly, to drive the differentiation of hESCs in response to the ECM preparations derived from two different cell lines. The first goal was fulfilled using a derivation of a method firstly established by Gospodarowicz [288] and later utilized by Todorovic et al. to assess the proteins expressed by basal cells using mass spectrometry [289]. The main hurdle faced in these investigations was to efficiently remove all cells and cell debris leaving only ECM proteins on the culture system, as their expression and presence was impossible to detect

until performing the mass spectrometry and immunostaining assays carried out in Chapter 3. However, two main conclusions can be drawn from the studies here outlined: (i) there is a process of EC differentiation in response to the ECM proteins and (ii) this process involves a mechanism of cell dedifferentiation as intermediate step. The first conclusion arises from the higher expression of corneal markers by HCjE-Gi cells upon culture in corneal environment (and vice-versa); and the second conclusion from the higher expression of putative SC markers during the experiments course. Several other studies have shown similar mechanisms of transdifferentiation that involve a first step of cell dedifferentiation that precede the full re-differentiation into the "new" cell type. These include, for example, the transdifferentiation of pancreatic cells to hepatocytes [217] and the vascular endothelium to smooth muscle [218]. In the process of dedifferentiation the cell undergoes reversion from a differentiated gene expression to a progenitor gene expression profile, accompanied by the repression of the development-related gene, and the activation of the genes that keep the cell in the undifferentiated state [608]. The dedifferentiated cells are usually smaller, have fewer organelles, and have higher nucleus/cytoplasm ratio when compared to the more mature cells [608]. At a functional level, the cell eventually regains the ability to proliferate, which means that a differentiated cell can re-enter the cell cycle. A very interesting example of dedifferentiation arises from the work of Pearton et al. who dedifferentiated and reverted mice differentiated corneal ECs into a limbal basal phenotype by triggering them with dermal development signals, a process that involves the activation of Wnt and BMP/Noggin signalling pathways [609, 610].

Further studies must then be performed to firstly, fully characterize the functional potential of the differentiating cells, as some authors have suggested that they may differ from the targeted cell in glycogen metabolism, keratin profiling, and tensile strength [166, 167, 169]. Secondly, the expression of SC markers need to be refined to prevent the risk of formation of tumours upon transplantation. Thirdly, "function-rescue" experiments should also be carried out to confirm if the phenotype of the differentiating cell can be reverted as to the parental cell, because despite being defined as an irreversible switch of one differentiated cell type into another [611], several studies have shown examples of reversible transdifferentiation between cell types, such as the reversible transdifferentiation between two different types of alveolar ECs [612] and blood vascular endothelial cells to a lymphatic-like phenotype [613].

Clinically one of the best-studied examples of metaplasia in response to the extracellular stimuli is the Barrett's oesophagus. This disease is characterized by the replacement of the normal stratified squamous epithelium by simple columnar epithelium with interspaced goblet cells in response to changes in environment acidity due to reflux [614].

The second goal of the Chapter 2 was partially achieved by culturing undifferentiated hESCs in "de-roofed" cultures containing conjunctival or corneal ECM proteins and growth factors trapped within the protein meshwork. While many others investigations have promoted such differentiation using coated surfaces with one single protein [179] and/or using conditioned medium from other cell cultures [178, 314], the studies in this chapter showed that hESCs can be partially differentiated into epithelial-like cells by mimicking the conjunctival and corneal microenvironments. The future potential of this model of hESC differentiation needs, however, to be further improved. Firstly, studies at protein levels (flow cytometry and Western blotting) are essential to evaluate the expression of epithelial markers by the cells undergoing differentiation as great variability is observed on Reverse Transcriptase qPCR results. Secondly, functional studies are required to assess the differences between the functionality of the differentiating cells and the native conjunctival or corneal ECs. Thirdly, the expression of undifferentiated hESC markers needs to be refined and selectively silenced to eliminate the risk of tumour formation upon transplantation. Fourthly, the possible potential of this culture system to provide a novel source for conjunctival cells or LSCs for clinical applications certainly needs to be determined.

Three main achievements were reached in Chapter 3, firstly the reliability of the "de-roofing" method; secondly, the acquaintance of the set of ECM proteins that are responsible for the process of cell differentiation; and thirdly, the intracellular mechanisms that triggered such process. Regarding the first aim, the "de-roofing" method showed to be reliable and, more importantly, replicable. The studies outlined in Chapter 2 and Chapter 3 showed that cells can be driven to differentiate towards a desired lineage in response to the morphogenic properties of the extracellular environment, resultant from the interactions of the different proteins with each other and with other soluble factors [299]. The effect of ECM, and particularly BM, composition on cell behaviour has been extensively addressed elsewhere [178, 179]. However, in most of these studies the morphogenic properties of the extracellular environment are ruled out as simple crude coatings with one single protein are usually performed. Indeed, *in vivo* studies have shown that when conjunctival ECs are cultured on intact corneal BM they express KRT12, suggesting that a more complete

transdifferentiation of these cells can be achieved upon culture with appropriate stimuli (corneal microenvironment mimicry) [175]. Further immunocytochemistry studies should here be carried out not only to visually confirm the presence of more proteins detected by mass spectrometry (in addition to COLXVIIα1, LAMα5, β1, and β2 chains), but also to co-localize some of them. Laminin-integrin co-localization would be of very useful potential to better understand the role of these proteins cross-talk in the process of epithelial differentiation, since integrins in the cell membrane bind to the extracellular laminins to transduce information regarding the ECM to the cell [615].

Regarding the second goal of the Chapter 3, differential cellular response is shown for different laminin isoforms. In addition to protein-dependency, cell response showed also to be concentration and time-dependent. The amount of protein that truly attaches to the cultureware should be determined, as the concentration used in our studies was in accordance with the manufacturer's instructions and others' methods [438]. LAM-511, here used as one of the proteins for substrate functionalization, has extensively been studied due its inhibitory differentiation properties [312, 427, 439], however other laminin isoforms have been tested for the same purpose. Domogatskaya et al. showed that LAM-332 enables ESCs proliferation but not pluripotency, LAM-111 caused ESCs differentiation within 2 weeks, and LAM-411 was not capable of supporting ESC survival [311]. In the same studies, that group have suggested that different integrins chains have different roles in mediating cell adhesion; by blocking β1 integrin they completely inhibited ESCs adhesion to LAM-511 whereas α6 and αv integrin blocking only partially inhibited cell adhesion; α2β1, α3, α4, α5β1, αV, β2, β3, and β4 integrin blocking had no effect on ESCs adhesion [311]. In addition to their potential role in maintaining cells in undifferentiated states, LAM-511 and LAM-521 have been used as substrates to successfully culture corneal endothelial cells, which upon culture in either isoform formed a monolayer with a hexagonal morphology and increased percentage of Ki67-positive cells (proliferative cells). In contrast, the same cell type cultured on LAM-211 functionalized scaffolds showed patchy colonies with fewer cells in proliferative states [427]. Additionally, the levels of phosphorylated (activated) FAK is increased when cells are cultured on LAM-511 when compared to those on LAM-211, suggesting enhanced adhesion to LAM-511 through a mechanism mediated by α3β1 and α6β1 integrin [427]. These studies acknowledge the differential response of cells to laminin isoforms. LAM-511 also functions as a better adhesive substrate for intestinal ECs than LAM-111, LAM-211, and LAM-332 [616], once again showing that different laminin isoforms have differential effects on cells'

behaviour. The ability of corneal ECs to readily adhere, spread, and migrate on preparations of amniotic membrane (mainly composed of LAM-511 and LAM-521) [304, 438, 617-619], may explain its high success in human corneal surface reconstruction. Taken together these observations suggest different cell adhesion affinities to different laminin isoforms [433] and cell type-dependent mechanisms of integrin-laminin interaction [620]. Further studies by Kurpakus-Wheater and colleagues have suggested that human corneal ECs adhere to LAM-511 and LAM-521 mainly through integrin α3β1 and not integrin α6β1 [304, 438]. On the other hand, adhesion to EHS laminin (mainly composed of LAM-111) has been reported to be primarily modulated by integrin α6β1 [621, 622]. Very little is still known about the role of different laminin isoforms in conjunctival EC behaviour. Dowgiert et al. have shown that LAM-211 regulates conjunctival EC adhesion to ECM via α3β1 integrin in a process that activates both Erk1/2 and Akt-1 signalling pathways, enhancing conjunctival EC proliferation [623]. In this regard, our mass spectrometry results showed that integrin α3, α6, β1, and β4 chains are produced by both cell lines, whilst α2, αv, and β6 chains to be produced only by hTCEpi cells. The expression of such variety of integrins suggest that these cells can interact with various laminin isoforms, including with those that are not normally localized on conjunctival or corneal BM. By using function-blocking antibodies to several integrin chains, interesting information would arise from the identification of which integrins mediate conjunctival and corneal EC adhesion to the different laminin isoforms. Amongst the non-integrin receptors, dystroglycan and Lutheran glycoproteins and heparan sulphate glycosaminoglycan have also been shown to mediate the adhesion of conjunctival and corneal ECs to laminins [624-626].

Thirdly, the signalling pathway results enlightened the mechanisms behind the process of cell differentiation. MAPK activation is a downstream event of integrin ligation resulting in the regulation of important cellular processes [387]. Three different subfamilies of the MAPkinases pathway have been described; including the ERK, p38, and JNK/SPK [627]. The phosphorylation levels of the first two were addressed in this study, with no significant differences observed in the residue phosphorylation of the proteins related with p38 pathway, which suggested that the process of epithelial cell differentiation is mainly mediated by the ERK1/2 pathways activated upon Thr202 and Tyr204 phosphorylation. Interesting and useful data would result from experiments in which certain pathways and/or small branches of these pathways were blocked by antibody binding to, therefore, investigate whether the same type of response would be given without the interference of

the extracellular cues. Certainly, the results outlined in Chapter 2 and Chapter 3 together open the door to further studies of cell differentiation with different cell lineages using the hereby developed “de-roofing” method.

Clinically, the advantage of using laminin isoforms to promote the undifferentiated state of ESCs over fibroblast feeder layers arises from the elimination of any animal products that are likely to contaminate cells with pathogens and other immunogenic molecules [628]. Recent observations have reported the utilization of truncated sequences of LAM-511, the so called E8 fragments, in therapeutic applications as they do not present the risk of contamination and, as smaller molecules, they overcame the issues related with the stability and mass production of full laminin isoforms [313]. Additionally, hESCs supportive feeder layers have been shown to produce LAM-511 and express the laminin binding integrins α3β1, α6β1, α7β1 [310], supporting the positive role of such proteins in hESC maintenance.

The aim in Chapter 4 was threefold; firstly, the protocols for exosome extraction and characterization needed to be optimised as, besides the dramatic impact that this field has had recently, little has been done using exosomes derived from cultures of human ocular ECs. In this regard, exosomes were isolated using a method based on differential centrifugation described by Thery et al. [563] with few modifications. The resulting solutions from this isolation/purification method were shown elsewhere to have high purity and to be highly enriched in exosomes [6], consistent with the results herein presented. Secondly, cell response to exogenous exosomes populations was evaluated. Concerning this, only one work has been published to date where exosomes from corneal ECs culture were extracted and used [566]. In the work from Han et al. corneal EC-derived exosomes were shown to mediate communication between corneal ECs and corneal keratocytes and vascular endothelial cells and therefore to be involved in corneal wound healing and neovascularization [566]. On the other hand, countless manuscripts have reported the role played by exosomes extracted from other systems in cell differentiation with high rates of success. These include exosomes derived from lymphoma cell lines to induce the differentiation and proliferation of B cells [629], the differentiation of mesenchymal SC into myofibroblasts using cancer-derived exosomes [630], amongst many others. Thirdly, the characterization of the cargo that would eventually be transferred from the secreting to the recipient cell was assessed. In this regard, an astonishing number of manuscripts have been published, with the majority suggesting an enriched content in mRNA and miRNA molecules. Moreover, exosomal miRNAs have been shown to be involved in many biological processes including cardiovascular protection and

repair [631], differentation and reprogramming [632], neural cells differentiation and glutamate transporter expression [633] and neurite outgrowth [634]. Exosomal cargo has shown considerable differences in the miRNA signature between the limbal and corneal regions, with miRNAs encountered to be enriched at the limbal regions likely to be involved in the maintenance of the undifferentiated cell state. These include miR-145, miR-143, miR-126, miR-338, and miR-10b [490-498, 502]. On the other hand, miR-184, miR-193, miR-149, and miR-575 have been preferentially located in the corneal regions [490-498, 502] and therefore associated with the terminally differentiated phenotype of their constituent cells. Yet again, Han and colleagues have also characterized the cargo carried by corneal epithelial-derived exosomes [566], although regarding its protein content only. Altogether, the studies in this chapter have shown that EVs populations can be extracted from cultures of ECs from the ocular surface. The extracted vesicles showed properties that are in accordance to those of exosome-enriched populations [503], namely CD63 and TSG101-positive content, GRP94 absence, and diameters that range from 80 to 120 nm. Additionally, the exosomal cargo derived from conjunctival and cornea ECs showed to contain various mRNA and miRNA molecules that may be involved in the triggering of events that led to cell differentiation. The cargo characterization showed significant differences in the relative abundance of 11 miRNAs molecules between the two populations. However, as no information is available regarding the effect of such molecules on the cells from the ocular surface, their role was mainly extrapolated from other systems. The significant differences are mainly related to molecules involved in maintaining and/or promoting an undifferentiated cell state, being their expression higher in exosomes derived from HCjE-Gi cells. Further investigations should be then performed in terms of exosomes characterization, namely transmission electron microscope to assess their morphology and Western blotting to evaluate their content in terms of CD63, TSG101, GRP94, and protein cargo assessment. Another exciting set of experiments would be to use miRNA knock-out approaches to investigate which miRNA molecule(s) (detected in Next Generation Sequencing results) is/(are) involved in the process of cell differentiation. Exosome cargo may also be selectively modified not only to eliminate the potential dangerous mRNAs and miRNAs, such as OCT4 and NANOG which would represent a risk of tumour formation, but also to enhance certain properties as has already been shown elsewhere [598, 635, 636]. Finally, “rescue” experiments should also be carried out to confirm if the phenotype of the differentiating cell can be reverted to that of the parental cell in response to endogenous exosomes populations.

When the results from all the previous chapters are interpreted together a few iterations can be made. Firstly, ECs from the ocular surface dedifferentiate prior to fully re-differentiation upon extracellular stimuli. Secondly, differences exist in the differentiation potential between the two cell lines. Regarding this, results in chapter 2 showed that HCjE-Gi ECM has a more accentuated effect on hTCEpi cells differentiation than hTCEpi ECM on HCjE-Gi cells differentiation. Thirdly, primary cells respond similarly to extracellular cues when compared to the immortalized cell lines. Fourthly, Chapter 3 showed that, consistent with the observations made in Chapter 2, hTCEpi cells are more responsive to extracellular stimuli than HCjE-Gi cells upon culture in HCjE-Gi ECM and hTCEpi ECM proteins, respectively. Fifthly, Chapter 4 has shown that the HCjE-Gi and hTCEpi cells-derived exosomes have the potential to trigger the process of EC differentiation. Sixthly, HCjE-Gi cells-derived exosomes contain higher amounts of miRNAs molecules involved in the maintenance of undifferentiated cell states. Taken together these results suggested that the HCjE-Gi cell line is less resilient to differentiation upon external stimuli.

Appendix A – Results analysis

A.1 Reverse Transcriptase qPCR and Melt curves analysis

Housekeeping genes should have stable mRNA expression and the amount of reference gene (given by Ct value) must not vary with the experimental conditions [637]. Amongst a wide library of available house-keeping genes, GAPDH was chosen. One study in human ocular surface epithelium has shown that GAPDH has the second highest stability amongst nine different control genes used [638]. Therefore, GAPDH was chosen as housekeeping genes in this study. Prior utilization, primer-BLAST was conducted using NCBI Primer-BLAST tool.

Melt curve analysis is widely used to evaluate the specificity of the amplified products when intercalating dyes (such as SYBR green) are used. Since many of these dyes bind to any double-stranded DNA products and are not sequence specific, the specificity of amplification is of crucial concern.

The single peak observed in the resulting melt curves is usually interpreted as a pure, single amplicon. In contrast, melt curves that exhibit two or more peaks are indicative of two or more different amplicons.

At the end of the qPCR run, the thermal cycler measures the fluorescence intensity at a certain temperature. The temperature is then increased at a desired rate as the instrument keeps measuring the fluorescence of the sample. At a certain temperature, amplicon-dependent, the double stranded DNA product starts to denature becoming single-stranded, the dye dissociates and the fluorescence decreases. The reduction on fluorescence is measured and plotted as a function of temperature, obtaining the melt curve. Two melting phases can often be observed however, this does not imply the presence of two different amplicons. These two fashion curves may indicate regions of higher stability within the amplicon (such as G/C rich regions) that do not melt immediately. Agarose gel analysis can then be performed to visualize the qPCR products, where the presence of a single band indicates the presence of a single product.

Reverse Transcriptase quantitative PCR using SYBR green as intercalating dye was used in this study to assess the transcript expression. Figure A 1, Figure A 3, Figure A 5 show the resultant melt curve for each amplicon used. All curves exhibit a single peak suggesting a single and pure qPCR product.

Primer efficiency calculated as in Equation 3 and ranging from 80 to 110% is considered acceptable. Figure A 2, Figure A 4, and Figure A 6 show the primer efficiency curves and slopes used for primer efficiency calculation.

$$primer\ efficiency = -1 + 10^{-(\frac{1}{sl})}$$

Equation 3 – Formulae for primer efficiency calculation. For primer efficiency to approach 1 (100%) the value of slope should be -3.334.

Other important information that can be obtained from the efficiency curves is the parallelism of the gene of interest when compared to the housekeeping genes. Ideally, the slope of the line should be -3.334 and the gene of interest and housekeeping gene lines should be parallel, avoiding any line cross-over. This would result not only in perfect primer efficiency but would also avoid any biased results arising from the gene of interest being detected prior its housekeeping gene.

All primers used in these studies exhibit the aforementioned characteristics, exception is made for primers shown in Figure A 4. The primer efficiency for the genes shown in Figure A 4 appear to be out of the acceptable range which may be result of the low level of fit (r^2), and KRT10 transcript was not detected.

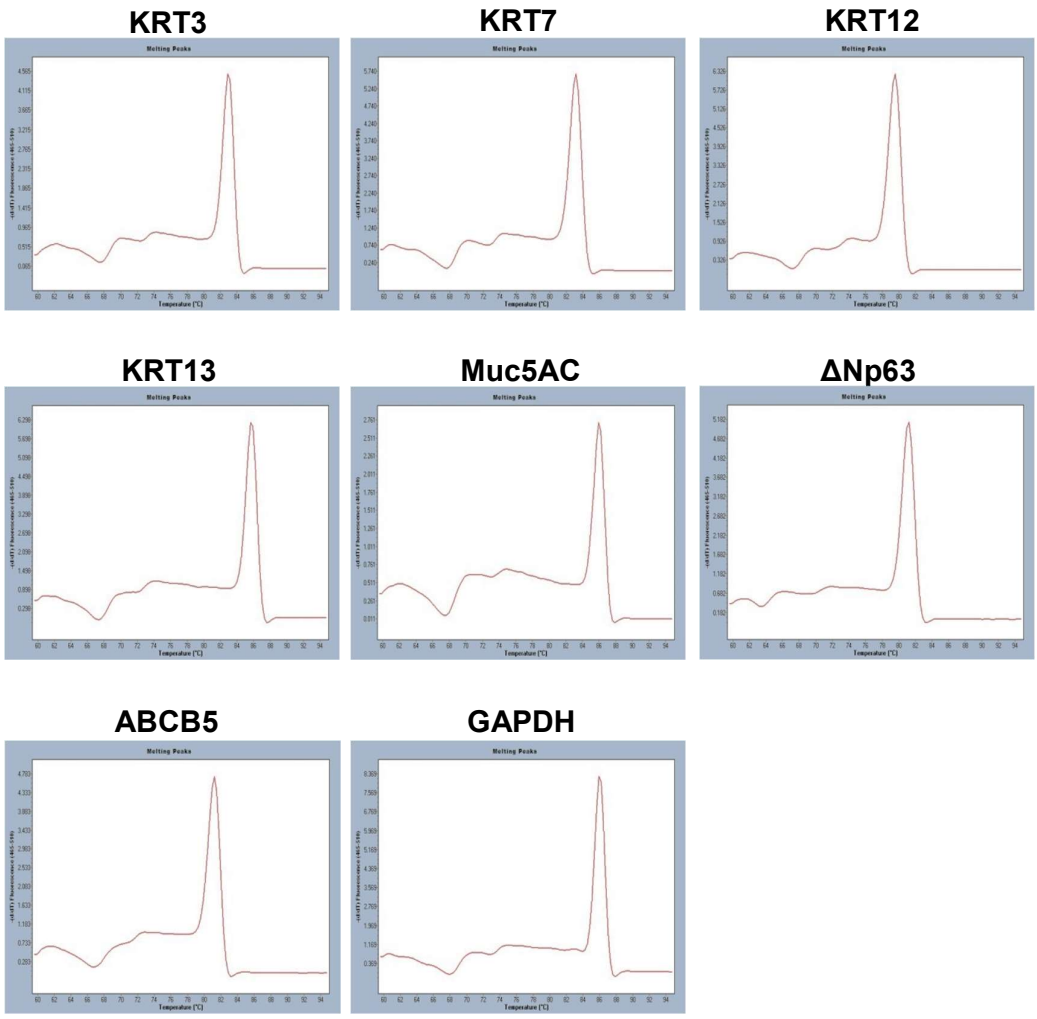

Figure A 1 - Melt curves for each individual amplicon used in chapter 2. All amplicons showed a single peak following melt curve analysis representing a pure and single amplicon. Abbreviations used KRT: Keratin, ABCB5: ATP-binding cassette sub-family B member 5, GAPDH: glyceraldehyde 3-phosphate dehydrogenase.

A

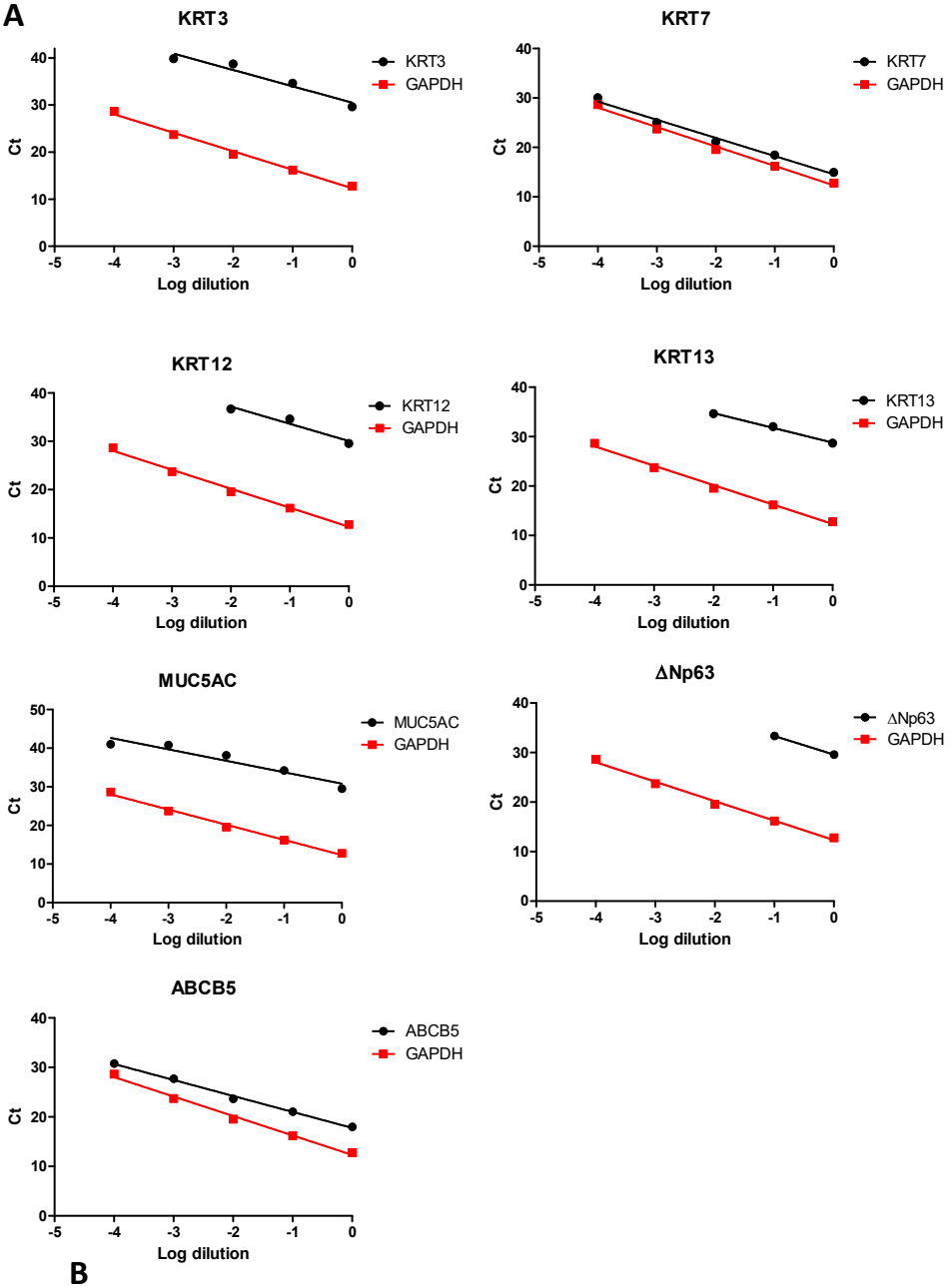

B

	KRT3	KRT7	KRT12	KRT13	MUC5AC	ΔNp63	ABCB5	GAPDH
Slope	-3.472	-3.673	-3.563	-2.985	-2.963	-3.76	-3.228	-3.928
SD	0.63	0.24	0.87	0.20	0.51		0.13	0.20
Efficiency (%)	94.1	87.2	90.8	116.3	1.18	84.5	104.1	79.7
r^2	0.94	0.99	0.94	0.99	0.92		0.99	0.99

Figure A 2 - Primer efficiency analysis for each individual primer used in chapter 2. (A) Graphics showing the efficiency curve. **(B)** Table containing the slopes used for primer efficiency calculation, efficiency, and goodness of fit. Abbreviations used KRT: keratin, MUC: mucin, GAPDH: glyceraldehyde 3-phosphate dehydrogenase, ABCB5: ATP-binding cassette sub-family B member 5.

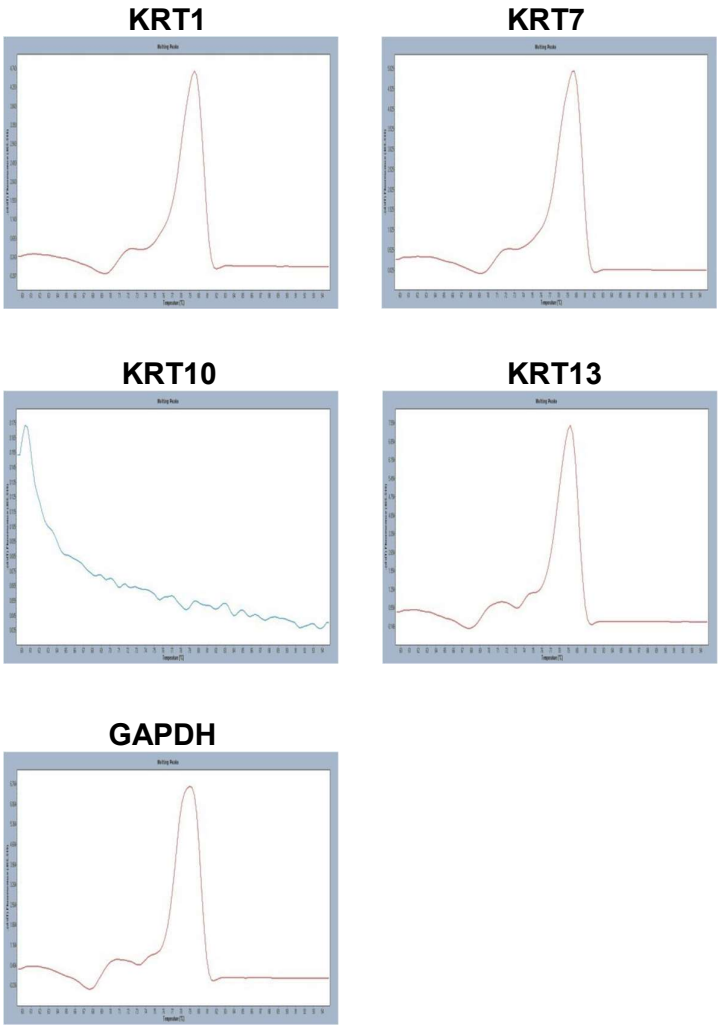

Figure A 3 - Melt curves for each individual amplicon used in chapter 2. All amplicons showed a single peak following melt curve analysis representing a pure and single amplicon. Abbreviations used KRT: keratin, GAPDH: glyceraldehyde 3-phosphate dehydrogenase.

A

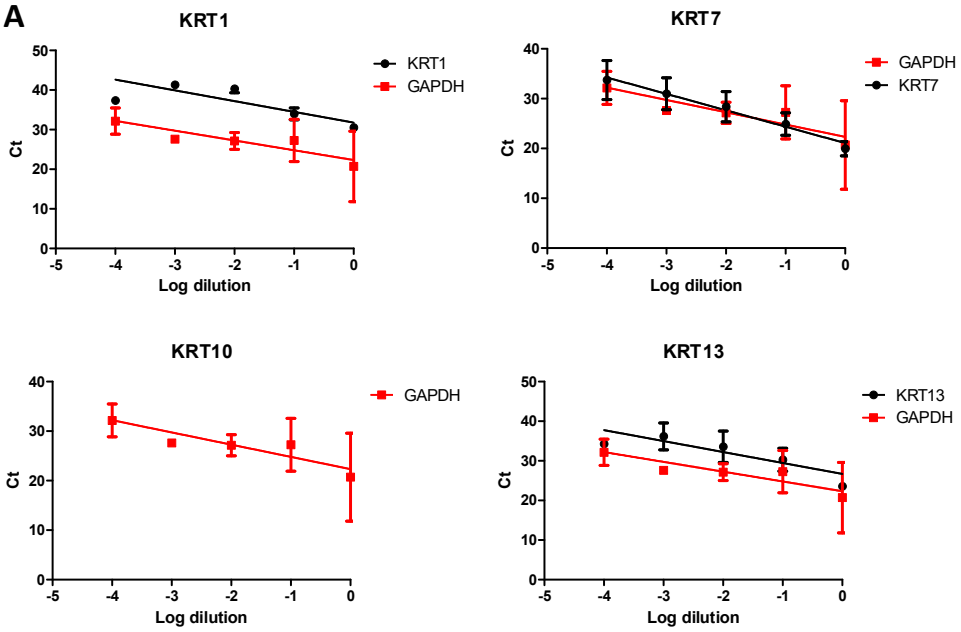

B

	KRT1	KRT7	KRT10	KRT13	GAPDH
Slope	-2.714	-3.293		-2.765	-2.471
SD	0.6921	0.5328		0.9528	1.133
Efficiency (%)	133.5	101.2		129.6	153.9
r^2	0.63	0.76		0.5840	0.34

Figure A 4 - Primer efficiency analysis for each individual primer used in chapter 2. (A) Graphics showing the efficiency curve. **(B)** Table containing the slopes used for primer efficiency calculation, efficiency, and goodness of fit. Abbreviations used KRT: Keratin, GAPDH: glyceraldehyde 3-phosphate dehydrogenase.

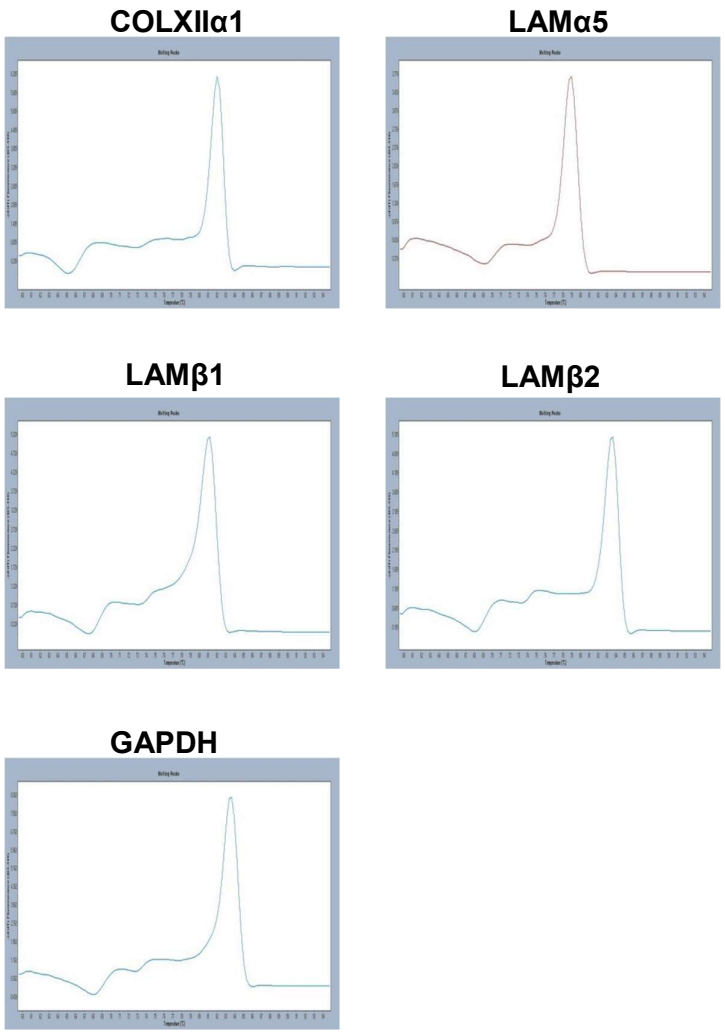

Figure A 5 - Melt curves for each individual amplicon used in chapter 3. All amplicons showed a single peak following melt curve analysis representing a pure, single amplicon. Abbreviations used Abbreviations used COL: collagen, LAM: laminin, GAPDH: glyceraldehyde 3-phosphate dehydrogenase.

A

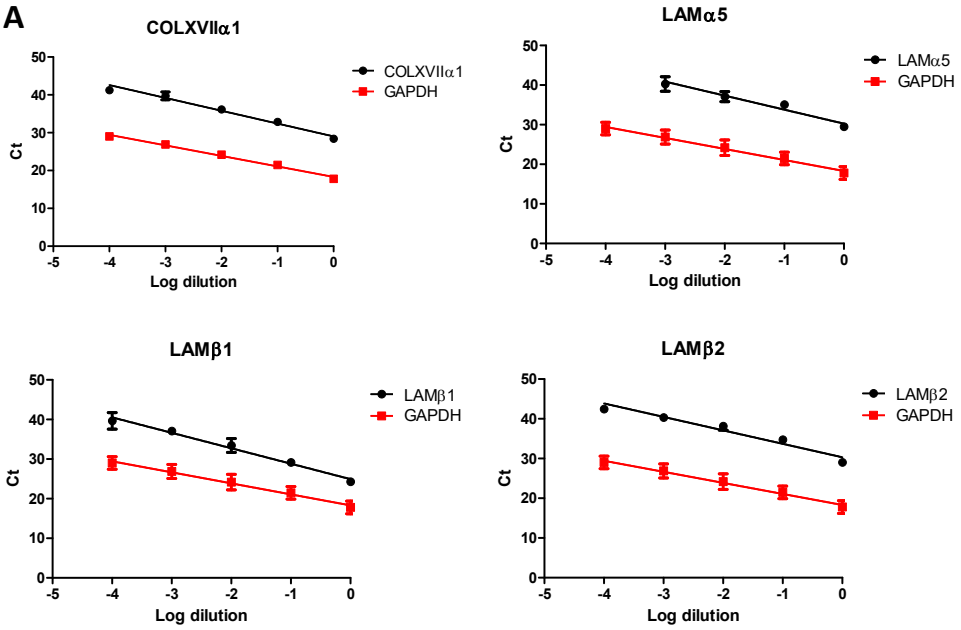

B

	COLXVIIα1	LAMα5	LAMβ1	LAMβ2	GAPDH
Slope	-3.393	-3.539	-3.900	-3.388	-2.785
SD	0.2449	0.2847	0.1812	0.2086	0.2136
Efficiency (%)	97.12	91.68	80.47	97.31	128.59
r^2	0.88	0.90	0.94	0.92	0.86

Figure A 6 - **Primer efficiency analysis for each individual primer used in chapter 3. (A)** Graphics showing the efficiency curve. **(B)** Table containing the slopes used for primer efficiency calculation, efficiency, and goodness of fit. Abbreviations used COL: collagen, GAPDH: glyceraldehyde 3-phosphate dehydrogenase, LAM: laminin.

A.2 Flow cytometry analysis

The percentage of positive events detected by flow cytometry was calculated as shown on Figure A 7. Briefly, the debris and dead cells are discarded by gating out the smallest events detected (R_x). This detection is based on its size distribution given by FSC-A (SSC-A is an indicative of granularity of the event). This results in a new plot where only the true events (cells) will be analysed, Figure A 7. C and F. By overlaying the resultant graphs, a percentage of 'true positive' events can be assessed by subtracting the percentage of positive events on sample (ABCB5 in the example) to the one on isotype control, using as starting point the moment where those two curves cross-over, resulting in the percentage M1, Figure A 7.

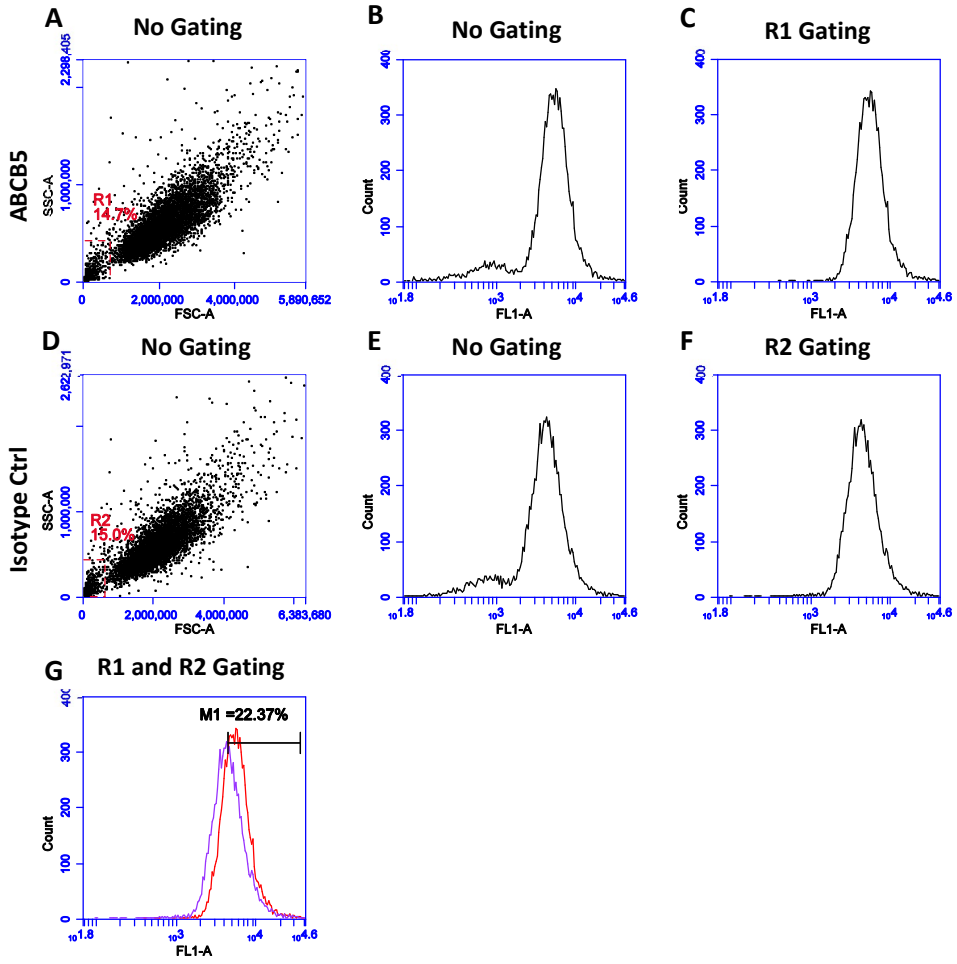

Figure A 7- Flow cytometry example of analysis. Scattered plot A and D show the distribution of size (FSC-A) and granularity (SSC-A) of the non-gated samples. Graphs B and E show the fluorescence distribution (FL1-A) of all events detected of the non-gated samples. Graphs C and F show the fluorescence distribution (FL1-A) of all events detected after gating, excluding the debris and dead cells based on their size distribution (R1 and R2). Graph G shows the resulting difference of true positives between sample (red) and isotype control (purple) (M1) after gating for debris and dead cells. Abbreviations used Ctrl: control, ABCB5: ATP-binding cassette sub-family B, member 5.

Appendix B– human limbal and conjunctival epithelial cultures

B.1 Introduction

To successfully culture primary limbal and conjunctival ECs, a replication of the culture conditions firstly used for skin ECs was used [639]. These conditions included the use of murine feeder layers and supplemented hormonal medium shown to be successful for the culture of limbal and conjunctival ECs.

B.1.1 The murine 3T3 fibroblast feeder layer

Two main reasons have been suggested for the little success on culturing skin and corneal ECs:

i. **Fibroblast contamination.** Due to the proximity of fibroblasts and ECs in both tissues, the isolation of these two types of cell from each other has been shown to be difficult. Another reason that leads to the low success of the culture of primary ECs is the higher proliferative rate of fibroblasts, which may outgrow the ECs, overtaking the culture [640, 641].

ii. **Limited growth.** Successfully established epithelial cultures have been shown to demonstrate a short lifespan with any attempt of sub-culturing being unsuccessful [640, 641].

Until the co-culture of skin ECs with murine 3T3 fibroblasts by Rheinwald and Green, the success rate of epithelial cultures was very limited [639]. 3T3 is a fibroblast cell line established from disaggregated random-bred Swiss mouse embryos [642]. Prior co-culture, the 3T3 fibroblasts are mitotically inactivated by irradiation or upon treatment with mitomycin-C, which is of crucial importance to prevent outgrowth over the primary ECs. Primary ECs have then been reported to grow successfully on a feeder layer of mitotically inactive 3T3 fibroblasts [643]. Moreover, Sun and Green showed that this co-culture model could also be used to sub-culture primary corneal ECs [644]. In the present study, ECs from human cornea and conjunctiva were grown successfully in a 3T3 fibroblasts feeder layer mitotically inactivated with mitomycin-C.

B.1.2 The medium requirements

Primary epithelial cultures grow optimally in humidified atmosphere with 5% CO_2 at 37°C fed with a supplemented hormonal epithelial medium (SHEM) [643, 645]. This media consists of a 3:1 (V/V) ratio of DMEM: Ham F12 supplemented with the following nutritional requirements:

i. **Foetal calf serum (FCS).** FCS is an essential requirement for successful primary EC culture as it contains a mixture of cytokines, growth factors, and hormones (most of them unknown) [646]. In the most recent years, several attempts to eliminate FCS from culture conditions have been tried. These attempts have result in poor maintenance of LSCs with rapid differentiation towards TACs [647].

ii. **Hydrocortisone.** The addition of cortisone is known to improve both the growth and morphology of primary ECs in culture [639]. Others have suggested that hydrocortisone also prevents the deterioration of the 3T3 fibroblasts feeder layer [648].

iii. **Insulin.** The addition of insulin to the medium has been suggested to reduce the requirement of FCS [649, 650]. It stimulates glucose transport into cells and is crucial in the synthesis of glycogen by those cells [649].

iv. **Tri-iodothyronine (T3).** Similar to insulin, the addition of T3 to the culture medium reduces the requirement of FCS [649]. Others have yet suggested that the addition of T3 combined with insulin reduces the requirement of FCS in 50% [643]. T3 is a hormone required in essential cellular metabolic processes, such as growth and development.

v. **Adenine.** Adenine improves the ability of primary ECs to form colonies [651]. As the proliferation of a single primary cell relies upon the formation of colonies of epithelium around this cell, the addition of adenine played a central role on the success of cultured primary ECs.

vi. **Epidermal growth factor (EGF).** EGF promotes the migration of growing ECs preventing the accumulation and subsequent senescence of cells at the centre of the colony. It also prevents the differentiation of progenitor cells promoting a undifferentiated cell stage [652].

B.1.3 Properties of epithelial cells in culture

By studying cultures of limbal and corneal ECs, several authors have suggested the following:

i. **Variations between the limbal regions**. It has been shown that ECs from different areas of the limbus have different ability to generate colonies, with cells from the superior limbus having higher CFE [80]. This finding, alongside with the higher density of palisades of Vogt at this region, which provide higher contact area and protection, suggested these limbal areas as the preferred for LSCs location.

ii. **Variations between the conjunctiva regions.** It has been demonstrated that ECs from different regions of the conjunctiva have similar CFE [80] although slightly higher CFE has been observed in colonies from the superior bulbar and superior fornix of the conjunctiva. Stewart et al. suggested however, an increased CFE at the inferior fornix and medial canthal proposing these areas as the preferred location for the conjunctiva SCs. Higher expression of putative SC markers, ΔNp63α and ABCG2, was also found by Stewart et al. in the inferior forniceal and medial canthal regions of conjunctiva [61]. They suggested that these areas offer higher protection and vascularization, features shared with many others SCs niches [61].

iii. **Ability to sub-culture.** ECs from the limbus, whole bulbar conjunctiva and superior and inferior fornix can be cultured up to 14 passages (ranging from 2 to 3 months) before reaching senescence. Within this period the number of cell doublings range from 80-100 [80].

Appendix C – Publications

References

1. Bartel, D.P., *MicroRNAs: target recognition and regulatory functions.* Cell, 2009. **136**(2): p. 215-33.
2. Bartel, D.P., *MicroRNAs: genomics, biogenesis, mechanism, and function.* Cell, 2004. **116**(2): p. 281-97.
3. Koster, J., et al., *Analysis of the interactions between BP180, BP230, plectin and the integrin α6β4 important for hemidesmosome assembly.* Journal of Cell Science, 2003. **116**(2): p. 387-399.
4. Borradori, L. and A. Sonnenberg, *Structure and Function of Hemidesmosomes: More Than Simple Adhesion Complexes.* Journal of Investigative Dermatology, 1999. **112**(4): p. 411-418.
5. Raposo, G. and W. Stoorvogel, *Extracellular vesicles: Exosomes, microvesicles, and friends.* The Journal of Cell Biology, 2013. **200**(4): p. 373-383.
6. Safdar, A., A. Saleem, and M.A. Tarnopolsky, *The potential of endurance exercise-derived exosomes to treat metabolic diseases.* Nat Rev Endocrinol, 2016. **12**(9): p. 504-17.
7. Jefferson, J.J., C.L. Leung, and R.K. Liem, *Plakins: goliaths that link cell junctions and the cytoskeleton.* Nat Rev Mol Cell Biol, 2004. **5**(7): p. 542-53.
8. Di Girolamo, N., *Stem cells of the human cornea.* Br Med Bull, 2011. **100**: p. 191-207.
9. Dhouailly, D., D.J. Pearton, and F. Michon, *The vertebrate corneal epithelium: from early specification to constant renewal.* Dev Dyn, 2014. **243**(10): p. 1226-41.
10. Schrader, S., et al., *Simulation of an in vitro niche environment that preserves conjunctival progenitor cells.* Regen Med, 2010. **5**(6): p. 877-89.
11. Chandler, J.W. and T.E. Gillette, *Immunologic defense mechanisms of the ocular surface.* Ophthalmology, 1983. **90**(6): p. 585-91.
12. Collins, F.M., *Cellular antimicrobial immunity.* CRC Crit Rev Microbiol, 1978. **7**(1): p. 27-91.
13. Hein, W.R., *Organization of mucosal lymphoid tissue.* Curr Top Microbiol Immunol, 1999. **236**: p. 1-15.
14. Kraehenbuhl, J.P. and M.R. Neutra, *Molecular and cellular basis of immune protection of mucosal surfaces.* Physiol Rev, 1992. **72**(4): p. 853-79.
15. Knop, N. and E. Knop, *Conjunctiva-associated lymphoid tissue in the human eye.* Invest Ophthalmol Vis Sci, 2000. **41**(6): p. 1270-9.
16. Krachmer, J.H., M.J. Mannis, and E.J. Holland, *Cornea E-Book*. 2010: Elsevier Health Sciences.
17. Davson, H. *human eye*. 2017 [cited 2017 Outubro 02, 2017]; Available from: https://www.britannica.com/science/human-eye.
18. Efron, N., M. Al-Dossari, and N. Pritchard, *In vivo confocal microscopy of the bulbar conjunctiva.* Clin Exp Ophthalmol, 2009. **37**(4): p. 335-44.
19. Majumder, P.D., *Anatomy of Conjunctiva*. 2 ed. 2008: eOphtha.
20. Chen, J.J. and S.C. Tseng, *Abnormal corneal epithelial wound healing in partial-thickness removal of limbal epithelium.* Invest Ophthalmol Vis Sci, 1991. **32**(8): p. 2219-33.
21. Ahmad, S., F. Figueiredo, and M. Lako, *Corneal epithelial stem cells: characterization, culture and transplantation.* Regen Med, 2006. **1**(1): p. 29-44.
22. Kolli, S., et al., *Successful Application of Ex Vivo Expanded Human Autologous Oral Mucosal Epithelium for the Treatment of Total Bilateral Limbal Stem Cell Deficiency.* STEM CELLS, 2014. **32**(8): p. 2135-2146.

23. Davis, J.A. and R.R. Reed, *Role of Olf-1 and Pax-6 Transcription Factors in Neurodevelopment.* The Journal of Neuroscience, 1996. **16**(16): p. 5082-5094.
24. Koroma, B.M., J.M. Yang, and O.H. Sundin, *The Pax-6 homeobox gene is expressed throughout the corneal and conjunctival epithelia.* Invest Ophthalmol Vis Sci, 1997. **38**(1): p. 108-20.
25. Sevel, D. and R. Isaacs, *A re-evaluation of corneal development.* Trans Am Ophthalmol Soc, 1988. **86**: p. 178-207.
26. Wolosin, J.M., M.T. Budak, and M.A. Akinci, *Ocular surface epithelial and stem cell development.* Int J Dev Biol, 2004. **48**(8-9): p. 981-91.
27. Mannis, M.J. and E.J. Holland, *Cornea E-Book*. 2016: Elsevier Health Sciences.
28. Huang, J., et al., *FGF-regulated BMP signaling is required for eyelid closure and to specify conjunctival epithelial cell fate.* Development, 2009. **136**(10): p. 1741-50.
29. Kruse, F.E., et al., *Conjunctival transdifferentiation is due to the incomplete removal of limbal basal epithelium.* Invest Ophthalmol Vis Sci, 1990. **31**(9): p. 1903-13.
30. Wei, Z.G., et al., *In vitro growth and differentiation of rabbit bulbar, fornix, and palpebral conjunctival epithelia. Implications on conjunctival epithelial transdifferentiation and stem cells.* Invest Ophthalmol Vis Sci, 1993. **34**(5): p. 1814-28.
31. Wei, Z.G., T.T. Sun, and R.M. Lavker, *Rabbit conjunctival and corneal epithelial cells belong to two separate lineages.* Invest Ophthalmol Vis Sci, 1996. **37**(4): p. 523-33.
32. Thomson, J.A., et al., *Embryonic stem cell lines derived from human blastocysts.* Science, 1998. **282**(5391): p. 1145-7.
33. Thomson, J.A., et al., *Embryonic Stem Cell Lines Derived from Human Blastocysts.* Science, 1998. **282**(5391): p. 1145-1147.
34. Becker, K.A., et al., *Self-renewal of human embryonic stem cells is supported by a shortened G1 cell cycle phase.* J Cell Physiol, 2006. **209**(3): p. 883-93.
35. White, J. and S. Dalton, *Cell cycle control of embryonic stem cells.* Stem Cell Rev, 2005. **1**(2): p. 131-8.
36. Stead, E., et al., *Pluripotent cell division cycles are driven by ectopic Cdk2, cyclin A/E and E2F activities.* Oncogene, 2002. **21**(54): p. 8320-33.
37. Bickenbach, J.R., *Identification and behavior of label-retaining cells in oral mucosa and skin.* J Dent Res, 1981. **60 Spec No C**: p. 1611-20.
38. deFazio, A., et al., *Immunohistochemical detection of proliferating cells in vivo.* J Histochem Cytochem, 1987. **35**(5): p. 571-7.
39. Morris, R.J., S.M. Fischer, and T.J. Slaga, *Evidence that the centrally and peripherally located cells in the murine epidermal proliferative unit are two distinct cell populations.* J Invest Dermatol, 1985. **84**(4): p. 277-81.
40. Kruse, F.E. and S.C. Tseng, *Proliferative and differentiative response of corneal and limbal epithelium to extracellular calcium in serum-free clonal cultures.* J Cell Physiol, 1992. **151**(2): p. 347-60.
41. Cotsarelis, G., et al., *Existence of slow-cycling limbal epithelial basal cells that can be preferentially stimulated to proliferate: implications on epithelial stem cells.* Cell, 1989. **57**(2): p. 201-9.
42. Kitazawa, T., et al., *The mechanism of accelerated corneal epithelial healing by human epidermal growth factor.* Invest Ophthalmol Vis Sci, 1990. **31**(9): p. 1773-8.
43. Schofield, R., *The stem cell system.* Biomed Pharmacother, 1983. **37**(8): p. 375-80.
44. Schofield, R., *The relationship between the spleen colony-forming cell and the haemopoietic stem cell.* Blood Cells, 1978. **4**(1-2): p. 7-25.
45. Watt, F.M. and B.L. Hogan, *Out of Eden: stem cells and their niches.* Science, 2000. **287**(5457): p. 1427-30.

46. Schlotzer-Schrehardt, U., et al., *Characterization of extracellular matrix components in the limbal epithelial stem cell compartment.* Exp Eye Res, 2007. **85**(6): p. 845-60.
47. Spradling, A., D. Drummond-Barbosa, and T. Kai, *Stem cells find their niche.* Nature, 2001. **414**(6859): p. 98-104.
48. Davanger, M. and A. Evensen, *Role of the Pericorneal Papillary Structure in Renewal of Corneal Epithelium.* Nature, 1971. **229**(5286): p. 560-561.
49. Townsend, W.M., *The limbal palisades of Vogt.* Transactions of the American Ophthalmological Society, 1991. **89**: p. 721-756.
50. Kulkarni, B., et al., *Comparative transcriptional profiling of the limbal epithelial crypt demonstrates its putative stem cell niche characteristics.* BMC Genomics, 2010. **11**(1): p. 526.
51. Dua, H.S., et al., *Limbal epithelial crypts: a novel anatomical structure and a putative limbal stem cell niche.* Br J Ophthalmol, 2005. **89**(5): p. 529-32.
52. Gipson, I.K., *The epithelial basement membrane zone of the limbus.* Eye (Lond), 1989. **3 (Pt 2)**: p. 132-40.
53. Keene, D.R., et al., *Type VII collagen forms an extended network of anchoring fibrils.* J Cell Biol, 1987. **104**(3): p. 611-21.
54. Chen, Z., et al., *Characterization of putative stem cell phenotype in human limbal epithelia.* Stem Cells, 2004. **22**(3): p. 355-66.
55. Higa, K., et al., *Melanocytes in the corneal limbus interact with K19-positive basal epithelial cells.* Exp Eye Res, 2005. **81**(2): p. 218-23.
56. Schlotzer-Schrehardt, U. and F.E. Kruse, *Identification and characterization of limbal stem cells.* Exp Eye Res, 2005. **81**(3): p. 247-64.
57. West-Mays, J.A. and D.J. Dwivedi, *The keratocyte: Corneal stromal cell with variable repair phenotypes.* The International Journal of Biochemistry & Cell Biology, 2006. **38**(10): p. 1625-1631.
58. Li, D.Q. and S.C. Tseng, *Differential regulation of keratinocyte growth factor and hepatocyte growth factor/scatter factor by different cytokines in human corneal and limbal fibroblasts.* J Cell Physiol, 1997. **172**(3): p. 361-72.
59. Li, D.Q. and S.C. Tseng, *Differential regulation of cytokine and receptor transcript expression in human corneal and limbal fibroblasts by epidermal growth factor, transforming growth factor-alpha, platelet-derived growth factor B, and interleukin-1 beta.* Invest Ophthalmol Vis Sci, 1996. **37**(10): p. 2068-80.
60. Sotozono, C., et al., *Paracrine role of keratinocyte growth factor in rabbit corneal epithelial cell growth.* Exp Eye Res, 1994. **59**(4): p. 385-91.
61. Stewart, R.M., et al., *Human Conjunctival Stem Cells are Predominantly Located in the Medial Canthal and Inferior Forniceal Areas.* Invest Ophthalmol Vis Sci, 2015. **56**(3): p. 2021-30.
62. Solari, H.P., et al., *Histopathological study of lesions of the caruncle: a 15-year single center review.* Diagn Pathol, 2009. **4**: p. 29.
63. Hall, P.A. and F.M. Watt, *Stem cells: the generation and maintenance of cellular diversity.* Development, 1989. **106**(4): p. 619-33.
64. Potten, C.S. and M. Loeffler, *Stem cells: attributes, cycles, spirals, pitfalls and uncertainties. Lessons for and from the crypt.* Development, 1990. **110**(4): p. 1001-20.
65. Lehrer, M.S., T.T. Sun, and R.M. Lavker, *Strategies of epithelial repair: modulation of stem cell and transit amplifying cell proliferation.* J Cell Sci, 1998. **111 (Pt 19)**: p. 2867-75.
66. Matsuda, M., J.L. Ubels, and H.F. Edelhauser, *A larger corneal epithelial wound closes at a faster rate.* Invest Ophthalmol Vis Sci, 1985. **26**(6): p. 897-900.

67. Ebato, B., J. Friend, and R.A. Thoft, *Comparison of central and peripheral human corneal epithelium in tissue culture.* Invest Ophthalmol Vis Sci, 1987. **28**(9): p. 1450-6.
68. Lavker, R.M., et al., *Relative proliferative rates of limbal and corneal epithelia. Implications of corneal epithelial migration, circadian rhythm, and suprabasally located DNA-synthesizing keratinocytes.* Invest Ophthalmol Vis Sci, 1991. **32**(6): p. 1864-75.
69. Thoft, R.A. and J. Friend, *The X, Y, Z hypothesis of corneal epithelial maintenance.* Invest Ophthalmol Vis Sci, 1983. **24**(10): p. 1442-3.
70. Hanna, C. and J.E. O'Brien, *CEll production and migration in the epithelial layer of the cornea.* Archives of Ophthalmology, 1960. **64**(4): p. 536-539.
71. Kaye, D.B., *Epithelial response in penetrating keratoplasty.* Am J Ophthalmol, 1980. **89**(3): p. 381-7.
72. Kinoshita, S., J. Friend, and R.A. Thoft, *Sex chromatin of donor corneal epithelium in rabbits.* Invest Ophthalmol Vis Sci, 1981. **21**(3): p. 434-41.
73. Ren, H. and G. Wilson, *Apoptosis in the corneal epithelium.* Invest Ophthalmol Vis Sci, 1996. **37**(6): p. 1017-25.
74. Lemp, M.A. and W.D. Mathers, *Corneal epithelial cell movement in humans.* Eye (Lond), 1989. **3 (Pt 4)**: p. 438-45.
75. Ebrahimi, M., E. Taghi-Abadi, and H. Baharvand, *Limbal Stem Cells in Review.* J Ophthalmic Vis Res, 2009. **4**(1): p. 40-58.
76. Secker, G. and J. Daniels, *Limbal epithelial stem cells of the cornea*. 2009.
77. Majo, F., et al., *Oligopotent stem cells are distributed throughout the mammalian ocular surface.* Nature, 2008. **456**(7219): p. 250-254.
78. West, J.D., N.J. Dorà, and J.M. Collinson, *Evaluating alternative stem cell hypotheses for adult corneal epithelial maintenance.* World Journal of Stem Cells, 2015. **7**(2): p. 281-299.
79. Dua, H.S., et al., *The role of limbal stem cells in corneal epithelial maintenance: testing the dogma.* Ophthalmology, 2009. **116**(5): p. 856-63.
80. Pellegrini, G., et al., *Location and clonal analysis of stem cells and their differentiated progeny in the human ocular surface.* J Cell Biol, 1999. **145**(4): p. 769-82.
81. Vascotto, S.G. and M. Griffith, *Localization of candidate stem and progenitor cell markers within the human cornea, limbus, and bulbar conjunctiva in vivo and in cell culture.* Anat Rec A Discov Mol Cell Evol Biol, 2006. **288**(8): p. 921-31.
82. Tsubota, K., et al., *Clinical application of living-related conjunctival-limbal allograft.* Am J Ophthalmol, 2002. **133**(1): p. 134-5.
83. Wei, Z.G., et al., *Label-retaining cells are preferentially located in fornical epithelium: implications on conjunctival epithelial homeostasis.* Invest Ophthalmol Vis Sci, 1995. **36**(1): p. 236-46.
84. Budak, M.T., et al., *Ocular surface epithelia contain ABCG2-dependent side population cells exhibiting features associated with stem cells.* J Cell Sci, 2005. **118**(Pt 8): p. 1715-24.
85. Nagasaki, T. and J. Zhao, *Uniform distribution of epithelial stem cells in the bulbar conjunctiva.* Invest Ophthalmol Vis Sci, 2005. **46**(1): p. 126-32.
86. Wei, Z.G., et al., *Clonal analysis of the in vivo differentiation potential of keratinocytes.* Invest Ophthalmol Vis Sci, 1997. **38**(3): p. 753-61.
87. Lemp, M., *The Dry Eye: A Comprehensive Guide*. 1992, Heidelberg, Germany: Springer Verlag.
88. Ebato, B., J. Friend, and R.A. Thoft, *Comparison of limbal and peripheral human corneal epithelium in tissue culture.* Invest Ophthalmol Vis Sci, 1988. **29**(10): p. 1533-7.

89. Kenyon, K.R. and S.C. Tseng, *Limbal autograft transplantation for ocular surface disorders.* Ophthalmology, 1989. **96**(5): p. 709-22; discussion 722-3.
90. Huang, A.J. and S.C. Tseng, *Corneal epithelial wound healing in the absence of limbal epithelium.* Invest Ophthalmol Vis Sci, 1991. **32**(1): p. 96-105.
91. Waring, G.O., 3rd, A.M. Roth, and M.B. Ekins, *Clinical and pathologic description of 17 cases of corneal intraepithelial neoplasia.* Am J Ophthalmol, 1984. **97**(5): p. 547-59.
92. Reya, T., et al., *Stem cells, cancer, and cancer stem cells.* Nature, 2001. **414**(6859): p. 105-11.
93. Goldberg, M.F. and A.J. Bron, *Limbal palisades of Vogt.* Transactions of the American Ophthalmological Society, 1982. **80**: p. 155-171.
94. Wiley, L., et al., *Regional heterogeneity in human corneal and limbal epithelia: an immunohistochemical evaluation.* Invest Ophthalmol Vis Sci, 1991. **32**(3): p. 594-602.
95. Yoon, J.J., S. Ismail, and T. Sherwin, *Limbal stem cells: Central concepts of corneal epithelial homeostasis.* World J Stem Cells, 2014. **6**(4): p. 391-403.
96. Majo, F., et al., *Oligopotent stem cells are distributed throughout the mammalian ocular surface.* Nature, 2008. **456**(7219): p. 250-4.
97. Amitai-Lange, A., et al., *Lineage tracing of stem and progenitor cells of the murine corneal epithelium.* Stem Cells, 2015. **33**(1): p. 230-9.
98. Kameishi, S., et al., *Remodeling of epithelial cells and basement membranes in a corneal deficiency model with long-term follow-up.* Lab Invest, 2015. **95**(2): p. 168-79.
99. Collinson, J.M., et al., *Clonal analysis of patterns of growth, stem cell activity, and cell movement during the development and maintenance of the murine corneal epithelium.* Dev Dyn, 2002. **224**(4): p. 432-40.
100. Wolosin, J.M., *Cell markers and the side population phenotype in ocular surface epithelial stem cell characterization and isolation.* Ocul Surf, 2006. **4**(1): p. 10-23.
101. Pellegrini, G., et al., *p63 identifies keratinocyte stem cells.* Proc Natl Acad Sci U S A, 2001. **98**(6): p. 3156-61.
102. Di Iorio, E., et al., *Isoforms of DeltaNp63 and the migration of ocular limbal cells in human corneal regeneration.* Proc Natl Acad Sci U S A, 2005. **102**(27): p. 9523-8.
103. Di Iorio, E., et al., *Q-FIHC: quantification of fluorescence immunohistochemistry to analyse p63 isoforms and cell cycle phases in human limbal stem cells.* Microsc Res Tech, 2006. **69**(12): p. 983-91.
104. de Paiva, C.S., et al., *ABCG2 transporter identifies a population of clonogenic human limbal epithelial cells.* Stem Cells, 2005. **23**(1): p. 63-73.
105. Watanabe, K., et al., *Human limbal epithelium contains side population cells expressing the ATP-binding cassette transporter ABCG2.* FEBS Lett, 2004. **565**(1-3): p. 6-10.
106. Ramirez-Miranda, A., et al., *Keratin 13 is a more specific marker of conjunctival epithelium than keratin 19.* Mol Vis, 2011. **17**: p. 1652-61.
107. Schermer, A., S. Galvin, and T.T. Sun, *Differentiation-related expression of a major 64K corneal keratin in vivo and in culture suggests limbal location of corneal epithelial stem cells.* J Cell Biol, 1986. **103**(1): p. 49-62.
108. Merjava, S., et al., *The spectrum of cytokeratins expressed in the adult human cornea, limbus and perilimbal conjunctiva.* Histol Histopathol, 2011. **26**(3): p. 323-31.
109. Benard, J., S. Douc-Rasy, and J.C. Ahomadegbe, *TP53 family members and human cancers.* Hum Mutat, 2003. **21**(3): p. 182-91.
110. Du, Y., et al., *Functional reconstruction of rabbit corneal epithelium by human limbal cells cultured on amniotic membrane.* Molecular vision, 2003. **9**: p. 635-643.

111. Espana, E.M., et al., *Characterization of corneal pannus removed from patients with total limbal stem cell deficiency.* Invest Ophthalmol Vis Sci, 2004. **45**(9): p. 2961-6.
112. Harkin, D.G., et al., *Analysis of p63 and cytokeratin expression in a cultivated limbal autograft used in the treatment of limbal stem cell deficiency.* British Journal of Ophthalmology, 2004. **88**(9): p. 1154-1158.
113. Rees, D.C., E. Johnson, and O. Lewinson, *ABC transporters: the power to change.* Nat Rev Mol Cell Biol, 2009. **10**(3): p. 218-27.
114. Bunting, K.D., *ABC transporters as phenotypic markers and functional regulators of stem cells.* Stem Cells, 2002. **20**(1): p. 11-20.
115. Chen, W., et al., *Existence of small slow-cycling Langerhans cells in the limbal basal epithelium that express ABCG2.* Exp Eye Res, 2007. **84**(4): p. 626-34.
116. Ksander, B.R., et al., *ABCB5 is a limbal stem cell gene required for corneal development and repair.* Nature, 2014. **advance online publication**.
117. Belkin, A.M. and M.A. Stepp, *Integrins as receptors for laminins.* Microsc Res Tech, 2000. **51**(3): p. 280-301.
118. Stepp, M.A., et al., *Localized distribution of alpha 9 integrin in the cornea and changes in expression during corneal epithelial cell differentiation.* J Histochem Cytochem, 1995. **43**(4): p. 353-62.
119. Maseruka, H., R. Bonshek, and A. Tullo, *Tenascin-C expression in normal, inflamed, and scarred human corneas.* Br J Ophthalmol, 1997. **81**(8): p. 677-82.
120. Stepp, M.A. and L. Zhu, *Upregulation of alpha 9 integrin and tenascin during epithelial regeneration after debridement in the cornea.* J Histochem Cytochem, 1997. **45**(2): p. 189-201.
121. Hayashi, R., et al., *N-Cadherin is expressed by putative stem/progenitor cells and melanocytes in the human limbal epithelial stem cell niche.* Stem Cells, 2007. **25**(2): p. 289-96.
122. Barbaro, V., et al., *C/EBPdelta regulates cell cycle and self-renewal of human limbal stem cells.* J Cell Biol, 2007. **177**(6): p. 1037-49.
123. Mayer, M.P. and B. Bukau, *Hsp70 chaperones: Cellular functions and molecular mechanism.* Cellular and Molecular Life Sciences, 2005. **62**(6): p. 670-684.
124. Bellmann, K., et al., *Heat shock protein hsp70 overexpression confers resistance against nitric oxide.* FEBS Lett, 1996. **391**(1-2): p. 185-8.
125. Mosser, D.D., et al., *Role of the human heat shock protein hsp70 in protection against stress-induced apoptosis.* Mol Cell Biol, 1997. **17**(9): p. 5317-27.
126. Beere, H.M., et al., *Heat-shock protein 70 inhibits apoptosis by preventing recruitment of procaspase-9 to the Apaf-1 apoptosome.* Nat Cell Biol, 2000. **2**(8): p. 469-75.
127. Fan, G.C., *Role of Heat Shock Proteins in Stem Cell Behavior.* Prog Mol Biol Transl Sci, 2012. **111**: p. 305-22.
128. Lyle, S., et al., *The C8/144B monoclonal antibody recognizes cytokeratin 15 and defines the location of human hair follicle stem cells.* J Cell Sci, 1998. **111 (Pt 21)**: p. 3179-88.
129. Yoshida, S., et al., *Cytokeratin 15 can be used to identify the limbal phenotype in normal and diseased ocular surfaces.* Invest Ophthalmol Vis Sci, 2006. **47**(11): p. 4780-6.
130. Moll, R., M. Divo, and L. Langbein, *The human keratins: biology and pathology.* Histochem Cell Biol, 2008. **129**(6): p. 705-33.
131. Revoltella, R.P., et al., *Epithelial stem cells of the eye surface.* Cell Prolif, 2007. **40**(4): p. 445-61.
132. Gipson, I.K. and T. Inatomi, *Mucin genes expressed by the ocular surface Epithelium.* Progress in Retinal and Eye Research, 1997. **16**(1): p. 81-98.

133. Perez-Vilar, J. and R. Hill, *Mucin Family of Glycoproteins*, in *Encyclopedia of Biological Chemistry*, E. Lennarz & Lane, Editor. 2004, Oxford: Academic Press/Elsevier. p. 758–764.
134. Gipson, I.K. and P. Argueso, *Role of mucins in the function of the corneal and conjunctival epithelia.* Int Rev Cytol, 2003. **231**: p. 1-49.
135. Argüeso, P. and I.K. Gipson, *Epithelial Mucins of the Ocular Surface: Structure, Biosynthesis and Function.* Experimental Eye Research, 2001. **73**(3): p. 281-289.
136. Birchenough, G.M., et al., *New developments in goblet cell mucus secretion and function.* Mucosal Immunol, 2015. **8**(4): p. 712-9.
137. Irvine, A.D., et al., *Mutations in cornea-specific keratin K3 or K12 genes cause Meesmann's corneal dystrophy.* Nat Genet, 1997. **16**(2): p. 184-7.
138. McLean, W.H. and C.B. Moore, *Keratin disorders: from gene to therapy.* Hum Mol Genet, 2011. **20**(R2): p. R189-97.
139. Allen, E.H.A., et al., *Keratin 12 missense mutation induces the unfolded protein response and apoptosis in Meesmann epithelial corneal dystrophy.* Hum Mol Genet, 2016. **25**(6): p. 1176-91.
140. Chen, Z., et al., *Gap junction protein connexin 43 serves as a negative marker for a stem cell-containing population of human limbal epithelial cells.* Stem Cells, 2006. **24**(5): p. 1265-73.
141. Donisi, P.M., et al., *Analysis of limbal stem cell deficiency by corneal impression cytology.* Cornea, 2003. **22**(6): p. 533-8.
142. Kasper, M., et al., *Patterns of cytokeratin and vimentin expression in the human eye.* Histochemistry, 1988. **89**(4): p. 369-77.
143. Barbaro, V., et al., *Evaluation of ocular surface disorders: a new diagnostic tool based on impression cytology and confocal laser scanning microscopy.* Br J Ophthalmol, 2010. **94**(7): p. 926-32.
144. Schrader, S., et al., *Tissue engineering for conjunctival reconstruction: established methods and future outlooks.* Curr Eye Res, 2009. **34**(11): p. 913-24.
145. Kurpakus, M.A., M.T. Maniaci, and M. Esco, *Expression of keratins K12, K4 and K14 during development of ocular surface epithelium.* Curr Eye Res, 1994. **13**(11): p. 805-14.
146. Meller, D. and S.C. Tseng, *Conjunctival epithelial cell differentiation on amniotic membrane.* Invest Ophthalmol Vis Sci, 1999. **40**(5): p. 878-86.
147. Ramaekers, F., et al., *Tissue distribution of keratin 7 as monitored by a monoclonal antibody.* Experimental Cell Research, 1987. **170**(1): p. 235-249.
148. Moll, R., et al., *The catalog of human cytokeratins: patterns of expression in normal epithelia, tumors and cultured cells.* Cell, 1982. **31**(1): p. 11-24.
149. Krenzer, K.L. and T.F. Freddo, *Cytokeratin expression in normal human bulbar conjunctiva obtained by impression cytology.* Invest Ophthalmol Vis Sci, 1997. **38**(1): p. 142-52.
150. Poli, M., et al., *Immunocytochemical Diagnosis of Limbal Stem Cell Deficiency: Comparative Analysis of Current Corneal and Conjunctival Biomarkers.* Cornea, 2015. **34**(7): p. 817-23.
151. Inatomi, T., et al., *Expression of secretory mucin genes by human conjunctival epithelia.* Invest Ophthalmol Vis Sci, 1996. **37**(8): p. 1684-92.
152. Gipson, I.K., et al., *Mucin gene expression in immortalized human corneal-limbal and conjunctival epithelial cell lines.* Invest Ophthalmol Vis Sci, 2003. **44**(6): p. 2496-506.
153. Garcia, I., et al., *Comparative Study of Limbal Stem Cell Deficiency Diagnosis Methods: Detection of MUC5AC mRNA and Goblet Cells in Corneal Epithelium.* Ophthalmology, 2012. **119**(5): p. 923-929.

154. Ahmad, S., et al., *Stem cell therapies for ocular surface disease.* Drug Discov Today, 2010. **15**(7-8): p. 306-13.
155. Dua, H.S. and A. Azuara-Blanco, *Limbal stem cells of the corneal epithelium.* Surv Ophthalmol, 2000. **44**(5): p. 415-25.
156. Casaroli-Marano, R.P., et al., *Potential Role of Induced Pluripotent Stem Cells (IPSCs) for Cell-Based Therapy of the Ocular Surface.* Journal of Clinical Medicine, 2015. **4**(2): p. 318-342.
157. Utheim, T.P., *Limbal epithelial cell therapy: past, present, and future.* Methods Mol Biol, 2013. **1014**: p. 3-43.
158. Dua, H.S. and J.V. Forrester, *The corneoscleral limbus in human corneal epithelial wound healing.* Am J Ophthalmol, 1990. **110**(6): p. 646-56.
159. Dua, H.S., J.A. Gomes, and A. Singh, *Corneal epithelial wound healing.* Br J Ophthalmol, 1994. **78**(5): p. 401-8.
160. Egbert, P.R., S. Lauber, and D.M. Maurice, *A simple conjunctival biopsy.* Am J Ophthalmol, 1977. **84**(6): p. 798-801.
161. Puangsricharern, V. and S.C. Tseng, *Cytologic evidence of corneal diseases with limbal stem cell deficiency.* Ophthalmology, 1995. **102**(10): p. 1476-85.
162. Burman, S. and V. Sangwan, *Cultivated limbal stem cell transplantation for ocular surface reconstruction.* Clinical ophthalmology (Auckland, N.Z.), 2008. **2**(3): p. 489-502.
163. Mann, I. and B.D. Pullinger, *A Study of Mustard Gas Lesions of the Eyes of Rabbits and Men: (Section of Ophthalmology).* Proc R Soc Med, 1942. **35**(3): p. 229-244.7.
164. Friedenwald, J.S., W. Buschke, and R.O. Scholz, *Effects of mustard and nitrogen mustard on mitotic and wound healing activities of the corneal epithelium.* Bull Johns Hopkins Hosp, 1948. **82**(2): p. 148-60.
165. Friedenwald, J.S., *Growth pressure and metaplasia of conjunctival and corneal epithelium.* Documenta Ophthalmologica, 1951. **5**(1): p. 184-192.
166. Thoft, R.A. and J. Friend, *Biochemical transformation of regenerating ocular surface epithelium.* Invest Ophthalmol Vis Sci, 1977. **16**(1): p. 14-20.
167. Kinoshita, S., J. Friend, and R.A. Thoft, *Biphasic cell proliferation in transdifferentiation of conjunctival to corneal epithelium in rabbits.* Invest Ophthalmol Vis Sci, 1983. **24**(8): p. 1008-14.
168. Harris, T.M., et al., *Biochemical transformation of bulbar conjunctiva into corneal epithelium: an electrophoretic analysis.* Exp Eye Res, 1985. **41**(5): p. 597-605.
169. Friend, J. and R.A. Thoft, *Functional competence of regenerating ocular surface epithelium.* Invest Ophthalmol Vis Sci, 1978. **17**(2): p. 134-9.
170. Kurpakus, M.A., E.L. Stock, and J.C. Jones, *The role of the basement membrane in differential expression of keratin proteins in epithelial cells.* Dev Biol, 1992. **150**(2): p. 243-55.
171. Xu, Y.G., et al., *Development of a rabbit corneal equivalent using an acellular corneal matrix of a porcine substrate.* Mol Vis, 2008. **14**: p. 2180-9.
172. Yang, S.P., X.Z. Yang, and G.P. Cao, *Conjunctiva reconstruction by induced differentiation of human amniotic epithelial cells.* Genet Mol Res, 2015. **14**(4): p. 13823-34.
173. Terranova, V.P. and R.M. Lyall, *Chemotaxis of human gingival epithelial cells to laminin. A mechanism for epithelial cell apical migration.* J Periodontol, 1986. **57**(5): p. 311-7.
174. Guo, M. and F. Grinnell, *Basement membrane and human epidermal differentiation in vitro.* J Invest Dermatol, 1989. **93**(3): p. 372-8.

175. Kurpakus, M.A., E.L. Stock, and J.C.R. Jones, *The role of the basement membrane in differential expression of keratin proteins in epithelial cells.* Developmental Biology, 1992. **150**(2): p. 243-255.
176. Tinois, E., et al., *Growth and differentiation of human keratinocytes on extracellular matrix.* Arch Dermatol Res, 1987. **279**(4): p. 241-6.
177. Birkenfeld, A., et al., *Indication of selective growth of human endometrial epithelial cells on extracellular matrix.* In Vitro Cell Dev Biol, 1988. **24**(12): p. 1188-92.
178. Ahmad, S., et al., *Differentiation of human embryonic stem cells into corneal epithelial-like cells by in vitro replication of the corneal epithelial stem cell niche.* Stem Cells, 2007. **25**(5): p. 1145-55.
179. Blazejewska, E.A., et al., *Corneal limbal microenvironment can induce transdifferentiation of hair follicle stem cells into corneal epithelial-like cells.* Stem Cells, 2009. **27**(3): p. 642-52.
180. Baylis, O., et al., *13 years of cultured limbal epithelial cell therapy: a review of the outcomes.* J Cell Biochem, 2011. **112**(4): p. 993-1002.
181. Jeng, B.H., et al., *Management of focal limbal stem cell deficiency associated with soft contact lens wear.* Cornea, 2011. **30**(1): p. 18-23.
182. Poon, A.C., et al., *Autologous serum eyedrops for dry eyes and epithelial defects: clinical and in vitro toxicity studies.* Br J Ophthalmol, 2001. **85**(10): p. 1188-97.
183. Tsubota, K., et al., *Reconstruction of the corneal epithelium by limbal allograft transplantation for severe ocular surface disorders.* Ophthalmology, 1995. **102**(10): p. 1486-96.
184. Chen, J.J. and S.C. Tseng, *Corneal epithelial wound healing in partial limbal deficiency.* Invest Ophthalmol Vis Sci, 1990. **31**(7): p. 1301-14.
185. Pellegrini, G., et al., *Long-term restoration of damaged corneal surfaces with autologous cultivated corneal epithelium.* Lancet, 1997. **349**(9057): p. 990-3.
186. Shortt, A.J., et al., *Transplantation of ex vivo cultured limbal epithelial stem cells: a review of techniques and clinical results.* Surv Ophthalmol, 2007. **52**(5): p. 483-502.
187. Sangwan, V.S., et al., *Clinical outcomes of xeno-free autologous cultivated limbal epithelial transplantation: a 10-year study.* Br J Ophthalmol, 2011. **95**(11): p. 1525-9.
188. Sangwan, V.S., et al., *Simple limbal epithelial transplantation (SLET): a novel surgical technique for the treatment of unilateral limbal stem cell deficiency.* Br J Ophthalmol, 2012. **96**(7): p. 931-4.
189. Grueterich, M., E.M. Espana, and S.C. Tseng, *Ex vivo expansion of limbal epithelial stem cells: amniotic membrane serving as a stem cell niche.* Surv Ophthalmol, 2003. **48**(6): p. 631-46.
190. Tsai, R.J., L.M. Li, and J.K. Chen, *Reconstruction of damaged corneas by transplantation of autologous limbal epithelial cells.* N Engl J Med, 2000. **343**(2): p. 86-93.
191. Koizumi, N., et al., *Cultivated corneal epithelial stem cell transplantation in ocular surface disorders.* Ophthalmology, 2001. **108**(9): p. 1569-74.
192. Nishida, K., et al., *Corneal Reconstruction with Tissue-Engineered Cell Sheets Composed of Autologous Oral Mucosal Epithelium.* New England Journal of Medicine, 2004. **351**(12): p. 1187-1196.
193. Homma, R., et al., *Induction of epithelial progenitors in vitro from mouse embryonic stem cells and application for reconstruction of damaged cornea in mice.* Invest Ophthalmol Vis Sci, 2004. **45**(12): p. 4320-6.
194. Ma, Y., et al., *Reconstruction of chemically burned rat corneal surface by bone marrow-derived human mesenchymal stem cells.* Stem Cells, 2006. **24**(2): p. 315-21.
195. Reza, H.M., et al., *Umbilical cord lining stem cells as a novel and promising source for ocular surface regeneration.* Stem Cell Rev, 2011. **7**(4): p. 935-47.

196. Sangwan, V.S., et al., *Use of autologous cultured limbal and conjunctival epithelium in a patient with severe bilateral ocular surface disease induced by acid injury: a case report of unique application.* Cornea, 2003. **22**(5): p. 478-81.
197. Di Girolamo, N., et al., *A contact lens-based technique for expansion and transplantation of autologous epithelial progenitors for ocular surface reconstruction.* Transplantation, 2009. **87**(10): p. 1571-8.
198. Sangwan, V.S., et al., *Successful reconstruction of damaged ocular outer surface in humans using limbal and conjuctival stem cell culture methods.* Biosci Rep, 2003. **23**(4): p. 169-74.
199. Dua, H.S., et al., *The amniotic membrane in ophthalmology.* Surv Ophthalmol, 2004. **49**(1): p. 51-77.
200. Burr, H.S., *Embryonic Development and Induction*. Yale J Biol Med. 1938 Oct;11(1):95-6.
201. Gurdon, J.B., T.R. Elsdale, and M. Fischberg, *Sexually Mature Individuals of Xenopus laevis from the Transplantation of Single Somatic Nuclei.* Nature, 1958. **182**(4627): p. 64-65.
202. Chin, M.T., *Reprogramming cell fate: a changing story.* Front Cell Dev Biol, 2014. **2**: p. 46.
203. Takahashi, K. and S. Yamanaka, *Induction of pluripotent stem cells from mouse embryonic and adult fibroblast cultures by defined factors.* Cell, 2006. **126**(4): p. 663-76.
204. Kragl, M., et al., *Cells keep a memory of their tissue origin during axolotl limb regeneration.* Nature, 2009. **460**(7251): p. 60-5.
205. Di Tullio, A., et al., *CCAAT/enhancer binding protein α (C/EBPα)-induced transdifferentiation of pre-B cells into macrophages involves no overt retrodifferentiation.* Proceedings of the National Academy of Sciences of the United States of America, 2011. **108**(41): p. 17016-17021.
206. Jayawardena, T.M., et al., *MicroRNA-mediated in vitro and in vivo direct reprogramming of cardiac fibroblasts to cardiomyocytes.* Circulation Research, 2012. **110**(11): p. 1465-1473.
207. Eguchi, G. and T.S. Okada, *Differentiation of Lens Tissue from the Progeny of Chick Retinal Pigment Cells Cultured In Vitro: A Demonstration of a Switch of Cell Types in Clonal Cell Culture.* Proceedings of the National Academy of Sciences of the United States of America, 1973. **70**(5): p. 1495-1499.
208. Selman, K. and F.C. Kafatos, *Transdifferentiation in the labial gland of silk moths: is DNA required for cellular metamorphosis?* Cell Differentiation, 1974. **3**(2): p. 81-94.
209. Wolff, G., *Entwicklungsphyiologische Studien. I. Die Regeneration der Urodelenlinse.* . Wilhelm Roux Arch. Entw.-Mech. Org., 1895. **1**: p. 380-390.
210. Taylor, S.M. and P.A. Jones, *Multiple new phenotypes induced in 10T1/2 and 3T3 cells treated with 5-azacytidine.* Cell, 1979. **17**(4): p. 771-9.
211. Lassar, A.B., B.M. Paterson, and H. Weintraub, *Transfection of a DNA locus that mediates the conversion of 10T1/2 fibroblasts to myoblasts.* Cell, 1986. **47**(5): p. 649-56.
212. Beresford, W.A., *Direct transdifferentiation: can cells change their phenotype without dividing?* Cell Differ Dev, 1990. **29**(2): p. 81-93.
213. Zhou, Q., et al., *In vivo reprogramming of adult pancreatic exocrine cells to [bgr]-cells.* Nature, 2008. **455**(7213): p. 627-632.
214. Song, K., et al., *Heart repair by reprogramming non-myocytes with cardiac transcription factors.* Nature, 2012. **485**(7400): p. 599-604.

215. Torper, O., et al., *Generation of induced neurons via direct conversion in vivo.* Proceedings of the National Academy of Sciences of the United States of America, 2013. **110**(17): p. 7038-7043.
216. Qian, L., et al., *In vivo reprogramming of murine cardiac fibroblasts into induced cardiomyocytes.* Nature, 2012. **485**(7400): p. 593-598.
217. Shen, C.N., et al., *Transdifferentiation of pancreas to liver.* Mech Dev, 2003. **120**(1): p. 107-16.
218. Frid, M.G., V.A. Kale, and K.R. Stenmark, *Mature vascular endothelium can give rise to smooth muscle cells via endothelial-mesenchymal transdifferentiation: in vitro analysis.* Circ Res, 2002. **90**(11): p. 1189-96.
219. Huang, P., et al., *Induction of functional hepatocyte-like cells from mouse fibroblasts by defined factors.* Nature, 2011. **475**(7356): p. 386-389.
220. Vierbuchen, T., et al., *Direct conversion of fibroblasts to functional neurons by defined factors.* Nature, 2010. **463**(7284): p. 1035-41.
221. Ginsberg, M., et al., *Efficient direct reprogramming of mature amniotic cells into endothelial cells by ETS factors and TGFbeta suppression.* Cell, 2012. **151**(3): p. 559-75.
222. Karamariti, E., et al., *Smooth muscle cells differentiated from reprogrammed embryonic lung fibroblasts through DKK3 signaling are potent for tissue engineering of vascular grafts.* Circ Res, 2013. **112**(11): p. 1433-43.
223. Addis, R.C., et al., *Optimization of direct fibroblast reprogramming to cardiomyocytes using calcium activity as a functional measure of success.* J Mol Cell Cardiol, 2013. **60**: p. 97-106.
224. Kim, K., et al., *Epigenetic memory in induced pluripotent stem cells.* Nature, 2010. **467**(7313): p. 285-90.
225. Kim, K., et al., *Donor cell type can influence the epigenome and differentiation potential of human induced pluripotent stem cells.* Nat Biotechnol, 2011. **29**(12): p. 1117-9.
226. Feng, R., et al., *PU.1 and C/EBPalpha/beta convert fibroblasts into macrophage-like cells.* Proc Natl Acad Sci U S A, 2008. **105**(16): p. 6057-62.
227. Marro, S., et al., *Direct lineage conversion of terminally differentiated hepatocytes to functional neurons.* Cell Stem Cell, 2011. **9**(4): p. 374-82.
228. Shen, C.-N., Z.D. Burke, and D. Tosh, *Transdifferentiation, Metaplasia and Tissue Regeneration.* Organogenesis, 2004. **1**(2): p. 36-44.
229. Slack, J.M., *Epithelial metaplasia and the second anatomy.* Lancet, 1986. **2**(8501): p. 268-71.
230. Slack, J.M. and D. Tosh, *Transdifferentiation and metaplasia--switching cell types.* Curr Opin Genet Dev, 2001. **11**(5): p. 581-6.
231. Pomerantz, J. and H.M. Blau, *Nuclear reprogramming: a key to stem cell function in regenerative medicine.* Nat Cell Biol, 2004. **6**(9): p. 810-6.
232. Echeverri, K. and E.M. Tanaka, *Ectoderm to mesoderm lineage switching during axolotl tail regeneration.* Science, 2002. **298**(5600): p. 1993-6.
233. Shapiro, M.S., J. Friend, and R.A. Thoft, *Corneal re-epithelialization from the conjunctiva.* Invest Ophthalmol Vis Sci, 1981. **21**(1 Pt 1): p. 135-42.
234. Tseng, S.C., *Concept and application of limbal stem cells.* Eye (Lond), 1989. **3 (Pt 2)**: p. 141-57.
235. Thoft, R.A., *Conjunctival transplantation.* Arch Ophthalmol, 1977. **95**(8): p. 1425-7.
236. Clinch, T.E., K.M. Goins, and L.M. Cobo, *Treatment of contact lens-related ocular surface disorders with autologous conjunctival transplantation.* Ophthalmology, 1992. **99**(4): p. 634-8.

237. Sangwan, V.S., *Limbal stem cells in health and disease.* Biosci Rep, 2001. **21**(4): p. 385-405.
238. Friedenwald, J., *Growth pressure and metaplasia of conjunctival and corneal epithelium.* Documenta Ophthalmologica, 1951. **5-6**(1): p. 184-192.
239. Tseng, S.C., et al., *Goblet cell density and vascularization during conjunctival transdifferentiation.* Invest Ophthalmol Vis Sci, 1984. **25**(10): p. 1168-76.
240. Thoft, R.A., J. Friend, and H.S. Murphy, *Ocular surface epithelium and corneal vascularization in rabbits. I. The role of wounding.* Invest Ophthalmol Vis Sci, 1979. **18**(1): p. 85-92.
241. Tseng, S.C., M. Farazdaghi, and A.A. Rider, *Conjunctival transdifferentiation induced by systemic vitamin A deficiency in vascularized rabbit corneas.* Invest Ophthalmol Vis Sci, 1987. **28**(9): p. 1497-504.
242. Aitken, D., et al., *An ultrastructural study of rabbit ocular surface transdifferentiation.* Investigative Ophthalmology & Visual Science, 1988. **29**(2): p. 224-231.
243. Dua, H., *The conjunctiva in corneal epithelial wound healing.* Br J Ophthalmol, 1998. **82**(12): p. 1407-11.
244. Logan, W.S., *VItamin a and keratinization.* Archives of Dermatology, 1972. **105**(5): p. 748-753.
245. Tseng, S.C., et al., *Inhibition of conjunctival transdifferentiation by topical retinoids.* Invest Ophthalmol Vis Sci, 1987. **28**(3): p. 538-42.
246. Rask, L., et al., *Vitamin A supply of the cornea.* Exp Eye Res, 1980. **31**(2): p. 201-11.
247. Raviola, G., *Conjunctival and episcleral blood vessels are permeable to blood-borne horseradish peroxidase.* Invest Ophthalmol Vis Sci, 1983. **24**(6): p. 725-36.
248. Ubels, J.L. and S.M. MacRae, *Vitamin A is present as retinol in the tears of humans and rabbits.* Curr Eye Res, 1984. **3**(6): p. 815-22.
249. Ubels, J.L., K.M. Foley, and V. Rismondo, *Retinol secretion by the lacrimal gland.* Invest Ophthalmol Vis Sci, 1986. **27**(8): p. 1261-8.
250. Elias, P.M. and M.L. Williams, *Retinoids, cancer, and the skin.* Arch Dermatol, 1981. **117**(3): p. 160-8.
251. Moyer, P.D., et al., *Conjunctival epithelial cells can resurface denuded cornea, but do not transdifferentiate to express cornea-specific keratin 12 following removal of limbal epithelium in mouse.* Differentiation, 1996. **60**(1): p. 31-8.
252. Rozario, T. and D.W. DeSimone, *The Extracellular Matrix In Development and Morphogenesis: A Dynamic View.* Dev Biol, 2010. **341**(1): p. 126-40.
253. Zhang, J., et al., *Comparison of beneficial factors for corneal wound-healing of rat mesenchymal stem cells and corneal limbal stem cells on the xenogeneic acellular corneal matrix in vitro.* Mol Vis, 2012. **18**: p. 161-73.
254. Ang, L.P., et al., *Cultivated human conjunctival epithelial transplantation for total limbal stem cell deficiency.* Invest Ophthalmol Vis Sci, 2010. **51**(2): p. 758-64.
255. Hayashi, Y., et al., *Integrins regulate mouse embryonic stem cell self-renewal.* Stem Cells, 2007. **25**(12): p. 3005-15.
256. Cheng, P., et al., *Fibronectin mediates mesendodermal cell fate decisions.* Development, 2013. **140**(12): p. 2587-96.
257. Nakayama, K.H., L. Hou, and N.F. Huang, *Role of Extracellular Matrix Signaling Cues in Modulating Cell Fate Commitment for Cardiovascular Tissue Engineering.* Advanced Healthcare Materials, 2014. **3**(5): p. 628-641.
258. Chambers, I., et al., *Functional expression cloning of Nanog, a pluripotency sustaining factor in embryonic stem cells.* Cell, 2003. **113**(5): p. 643-55.
259. Mitsui, K., et al., *The homeoprotein Nanog is required for maintenance of pluripotency in mouse epiblast and ES cells.* Cell, 2003. **113**(5): p. 631-42.

260. Nichols, J., et al., *Formation of pluripotent stem cells in the mammalian embryo depends on the POU transcription factor Oct4.* Cell, 1998. **95**(3): p. 379-91.
261. Henderson, J.K., et al., *Preimplantation human embryos and embryonic stem cells show comparable expression of stage-specific embryonic antigens.* Stem Cells, 2002. **20**(4): p. 329-37.
262. Draper, J.S., et al., *Surface antigens of human embryonic stem cells: changes upon differentiation in culture.* Journal of Anatomy, 2002. **200**(3): p. 249-258.
263. Stojkovic, M., et al., *Derivation of human embryonic stem cells from day-8 blastocysts recovered after three-step in vitro culture.* Stem Cells, 2004. **22**(5): p. 790-7.
264. Przyborski, S.A., *Differentiation of human embryonic stem cells after transplantation in immune-deficient mice.* Stem Cells, 2005. **23**(9): p. 1242-50.
265. Dalton, S., *Signaling networks in human pluripotent stem cells.* Curr Opin Cell Biol, 2013. **25**(2): p. 241-6.
266. Palmieri, S.L., et al., *Oct-4 transcription factor is differentially expressed in the mouse embryo during establishment of the first two extraembryonic cell lineages involved in implantation.* Dev Biol, 1994. **166**(1): p. 259-67.
267. Pesce, M., et al., *Differential expression of the Oct-4 transcription factor during mouse germ cell differentiation.* Mechanisms of Development, 1998. **71**(1–2): p. 89-98.
268. Li, M., et al., *Generation of purified neural precursors from embryonic stem cells by lineage selection.* Curr Biol, 1998. **8**(17): p. 971-4.
269. Lin, T., et al., *p53 induces differentiation of mouse embryonic stem cells by suppressing Nanog expression.* Nat Cell Biol, 2005. **7**(2): p. 165-71.
270. Ying, Q.L., et al., *BMP induction of Id proteins suppresses differentiation and sustains embryonic stem cell self-renewal in collaboration with STAT3.* Cell, 2003. **115**(3): p. 281-92.
271. Beattie, G.M., et al., *Activin A maintains pluripotency of human embryonic stem cells in the absence of feeder layers.* Stem Cells, 2005. **23**(4): p. 489-95.
272. Heldin, C.H., K. Miyazono, and P. ten Dijke, *TGF-beta signalling from cell membrane to nucleus through SMAD proteins.* Nature, 1997. **390**(6659): p. 465-71.
273. Attisano, L. and J.L. Wrana, *Mads and Smads in TGF beta signalling.* Curr Opin Cell Biol, 1998. **10**(2): p. 188-94.
274. Okita, K. and S. Yamanaka, *Intracellular signaling pathways regulating pluripotency of embryonic stem cells.* Curr Stem Cell Res Ther, 2006. **1**(1): p. 103-11.
275. Liu, J., et al., *Notch Signaling in the Regulation of Stem Cell Self-Renewal and Differentiation.* Current Topics in Developmental Biology, 2010. **92**: p. 367-409.
276. Coraux, C., et al., *Reconstituted skin from murine embryonic stem cells.* Curr Biol, 2003. **13**(10): p. 849-53.
277. Kurosawa, H., *Methods for inducing embryoid body formation: in vitro differentiation system of embryonic stem cells.* Journal of Bioscience and Bioengineering, 2007. **103**(5): p. 389-398.
278. Itskovitz-Eldor, J., et al., *Differentiation of human embryonic stem cells into embryoid bodies compromising the three embryonic germ layers.* Molecular Medicine, 2000. **6**(2): p. 88-95.
279. Pan, G.J., et al., *Stem cell pluripotency and transcription factor Oct4.* Cell Res, 2002. **12**(5-6): p. 321-9.
280. Yuan, H., et al., *Developmental-specific activity of the FGF-4 enhancer requires the synergistic action of Sox2 and Oct-3.* Genes Dev, 1995. **9**(21): p. 2635-45.
281. Scholer, H.R., T. Ciesiolka, and P. Gruss, *A nexus between Oct-4 and E1A: implications for gene regulation in embryonic stem cells.* Cell, 1991. **66**(2): p. 291-304.

282. Niwa, H., J.-i. Miyazaki, and A.G. Smith, *Quantitative expression of Oct-3/4 defines differentiation, dedifferentiation or self-renewal of ES cells.* Nat Genet, 2000. **24**(4): p. 372-376.
283. Avilion, A.A., et al., *Multipotent cell lineages in early mouse development depend on SOX2 function.* Genes & Development, 2003. **17**(1): p. 126-140.
284. Rheinwald, J.G., et al., *A Two-Stage, p16INK4A- and p53-Dependent Keratinocyte Senescence Mechanism That Limits Replicative Potential Independent of Telomere Status.* Molecular and Cellular Biology, 2002. **22**(14): p. 5157-5172.
285. Robertson, D.M., et al., *Characterization of Growth and Differentiation in a Telomerase-Immortalized Human Corneal Epithelial Cell Line.* Investigative Ophthalmology & Visual Science, 2005. **46**(2): p. 470-478.
286. Todaro, G.J. and H. Green, *QUANTITATIVE STUDIES OF THE GROWTH OF MOUSE EMBRYO CELLS IN CULTURE AND THEIR DEVELOPMENT INTO ESTABLISHED LINES.* The Journal of Cell Biology, 1963. **17**(2): p. 299-313.
287. Baxter, M.A., et al., *Analysis of the distinct functions of growth factors and tissue culture substrates necessary for the long-term self-renewal of human embryonic stem cell lines.* Stem Cell Research, 2009. **3**(1): p. 28-38.
288. Gospodarowicz, D., *Preparation of extracellular matrices produced by cultured bovine corneal endothelial cells and PF-HR-9 endodermal cells: their use in cell culture.* Methods for Preparation of Media, Supplements and Substrata for Serum Free Animal Cell Culture, 1984: p. 275-293.
289. Todorovic, V., et al., *Detection of differentially expressed basal cell proteins by mass spectrometry.* Mol Cell Proteomics, 2010. **9**(2): p. 351-61.
290. Livak, K.J. and T.D. Schmittgen, *Analysis of relative gene expression data using real-time quantitative PCR and the 2(-Delta Delta C(T)) Method.* Methods, 2001. **25**(4): p. 402-8.
291. Boukamp, P., et al., *Normal keratinization in a spontaneously immortalized aneuploid human keratinocyte cell line.* The Journal of Cell Biology, 1988. **106**(3): p. 761-771.
292. Kawasaki, S., et al., *Clusters of corneal epithelial cells reside ectopically in human conjunctival epithelium.* Invest Ophthalmol Vis Sci, 2006. **47**(4): p. 1359-67.
293. Franke, W.W., et al., *Change of cytokeratin filament organization during the cell cycle: selective masking of an immunologic determinant in interphase PtK2 cells.* J Cell Biol, 1983. **97**(4): p. 1255-60.
294. Mackay, A.M., R.P. Tracy, and J.E. Craighead, *Cytokeratin expression in rat mesothelial cells in vitro is controlled by the extracellular matrix.* J Cell Sci, 1990. **95 (Pt 1)**: p. 97-107.
295. Kurpakus, M.A., E.L. Stock, and J.C. Jones, *Analysis of wound healing in an in vitro model: early appearance of laminin and a 125 × 10(3) Mr polypeptide during adhesion complex formation.* Journal of Cell Science, 1990. **96**(4): p. 651-660.
296. Chen, W.Y., et al., *Conjunctival epithelial cells do not transdifferentiate in organotypic cultures: expression of K12 keratin is restricted to corneal epithelium.* Curr Eye Res, 1994. **13**(10): p. 765-78.
297. Tata, P.R., et al., *Dedifferentiation of committed epithelial cells into stem cells in vivo.* Nature, 2013. **503**(7475): p. 218-223.
298. García-Arrarás, J.E., et al., *Cell dedifferentiation and epithelial to mesenchymal transitions during intestinal regeneration in H. glaberrima.* BMC Developmental Biology, 2011. **11**(1): p. 61.
299. Adams, J.C. and F.M. Watt, *Regulation of development and differentiation by the extracellular matrix.* Development, 1993. **117**(4): p. 1183-98.

300. Lin, C.Q. and M.J. Bissell, *Multi-faceted regulation of cell differentiation by extracellular matrix.* Faseb j, 1993. **7**(9): p. 737-43.
301. Juliano, R.L. and S. Haskill, *Signal transduction from the extracellular matrix.* J Cell Biol, 1993. **120**(3): p. 577-85.
302. Clark, E.A. and J.S. Brugge, *Integrins and signal transduction pathways: the road taken.* Science, 1995. **268**(5208): p. 233-9.
303. Jones, J.C., et al., *A function for the integrin alpha 6 beta 4 in the hemidesmosome.* Cell Regulation, 1991. **2**(6): p. 427-438.
304. Lin, L., C. Daneshvar, and M. Kurpakus-Wheater, *Evidence for differential signaling in human conjunctival epithelial cells adherent to laminin isoforms.* Exp Eye Res, 2000. **70**(4): p. 537-46.
305. Naganuma, K., et al., *Epigenetic alterations of the keratin 13 gene in oral squamous cell carcinoma.* BMC Cancer, 2014. **14**.
306. Roh, C., et al., *Multi-potentiality of a new immortalized epithelial stem cell line derived from human hair follicles.* In Vitro Cell Dev Biol Anim, 2008. **44**(7): p. 236-44.
307. Wild, G.A. and D. Mischke, *Variation and frequency of cytokeratin polypeptide patterns in human squamous non-keratinizing epithelium.* Exp Cell Res, 1986. **162**(1): p. 114-26.
308. Guilak, F., et al., *Control of stem cell fate by physical interactions with the extracellular matrix.* Cell Stem Cell, 2009. **5**(1): p. 17-26.
309. Wang, H., X. Luo, and J. Leighton, *Extracellular Matrix and Integrins in Embryonic Stem Cell Differentiation.* Biochem Insights, 2015. **8**(Suppl 2): p. 15-21.
310. Hongisto, H., et al., *Laminin-511 expression is associated with the functionality of feeder cells in human embryonic stem cell culture.* Stem Cell Research, 2012. **8**(1): p. 97-108.
311. Domogatskaya, A., et al., *Laminin-511 but Not -332, -111, or -411 Enables Mouse Embryonic Stem Cell Self-Renewal In Vitro.* STEM CELLS, 2008. **26**(11): p. 2800-2809.
312. Rodin, S., et al., *Long-term self-renewal of human pluripotent stem cells on human recombinant laminin-511.* Nat Biotechnol, 2010. **28**(6): p. 611-5.
313. Miyazaki, T., et al., *Laminin E8 fragments support efficient adhesion and expansion of dissociated human pluripotent stem cells.* Nat Commun, 2012. **3**: p. 1236.
314. Huang, D., et al., *[The study on induced differentiation of embryonic stem cells into conjunctival epithelial-like cells].* Yan Ke Xue Bao, 2003. **19**(2): p. 117-21.
315. Drukker, M., et al., *Characterization of the expression of MHC proteins in human embryonic stem cells.* Proc Natl Acad Sci U S A, 2002. **99**(15): p. 9864-9.
316. Yang, X., et al., *Cell Movement Patterns during Gastrulation in the Chick Are Controlled by Positive and Negative Chemotaxis Mediated by FGF4 and FGF8.* Developmental Cell, 2002. **3**(3): p. 425-437.
317. Shellard, A. and R. Mayor, *Chemotaxis during neural crest migration.* Seminars in Cell & Developmental Biology, 2016. **55**: p. 111-118.
318. Jin, T., *Gradient sensing during chemotaxis.* Current Opinion in Cell Biology, 2013. **25**(5): p. 532-537.
319. Roussos, E.T., J.S. Condeelis, and A. Patsialou, *Chemotaxis in cancer.* Nat Rev Cancer, 2011. **11**(8): p. 573-587.
320. Zabel, B.A., A. Rott, and E.C. Butcher, *Leukocyte Chemoattractant Receptors in Human Disease Pathogenesis.* Annual Review of Pathology: Mechanisms of Disease, 2015. **10**(1): p. 51-81.
321. Blanco-Mezquita, J.T., A.E.K. Hutcheon, and J.D. Zieske, *Role of Thrombospondin-1 in Repair of Penetrating Corneal WoundsRepair of Penetrating Corneal Wounds.* Investigative Ophthalmology & Visual Science, 2013. **54**(9): p. 6262-6268.

322. Weber, M., et al., *Interstitial Dendritic Cell Guidance by Haptotactic Chemokine Gradients.* Science, 2013. **339**(6117): p. 328-332.
323. Li, S., et al., *The role of the dynamics of focal adhesion kinase in the mechanotaxis of endothelial cells.* Proceedings of the National Academy of Sciences, 2002. **99**(6): p. 3546-3551.
324. Gao, Y., et al., *The ECM-Cell Interaction of Cartilage Extracellular Matrix on Chondrocytes.* BioMed Research International, 2014. **2014**: p. 648459.
325. Rosso, F., et al., *From cell-ECM interactions to tissue engineering.* J Cell Physiol, 2004. **199**(2): p. 174-80.
326. Yoneda, A. and J.R. Couchman, *Regulation of cytoskeletal organization by syndecan transmembrane proteoglycans.* Matrix Biol, 2003. **22**(1): p. 25-33.
327. Lodish H, B.A., Zipursky SL, et al., *Molecular Cell Biology*. 4th ed. 2000: New York: W. H. Freeman.
328. Schlaepfer, D.D., et al., *Integrin-mediated signal transduction linked to Ras pathway by GRB2 binding to focal adhesion kinase.* Nature, 1994. **372**(6508): p. 786-91.
329. Rundhaug, J.E., *Matrix metalloproteinases and angiogenesis.* J Cell Mol Med, 2005. **9**(2): p. 267-85.
330. Davis, G.E. and D.R. Senger, *Endothelial extracellular matrix: biosynthesis, remodeling, and functions during vascular morphogenesis and neovessel stabilization.* Circ Res, 2005. **97**(11): p. 1093-107.
331. Ferrara, N., *Binding to the Extracellular Matrix and Proteolytic Processing: Two Key Mechanisms Regulating Vascular Endothelial Growth Factor Action.* Molecular Biology of the Cell, 2010. **21**(5): p. 687-690.
332. Ortiz, A., et al., *Fibronectin (FN) decreases glomerular lesions and synthesis of tumour necrosis factor-alpha (TNF-alpha), platelet-activating factor (PAF) and FN in proliferative glomerulonephritis.* Clin Exp Immunol, 1995. **101**(2): p. 334-40.
333. Gordon, M.Y., *Extracellular matrix of the marrow microenvironment.* Br J Haematol, 1988. **70**(1): p. 1-4.
334. Rachfal, A.W. and D.R. Brigstock, *Connective tissue growth factor (CTGF/CCN2) in hepatic fibrosis.* Hepatol Res, 2003. **26**(1): p. 1-9.
335. Huhtala, M.T., O.T. Pentikainen, and M.S. Johnson, *A dimeric ternary complex of FGFR [correction of FGFR1], heparin and FGF-1 leads to an 'electrostatic sandwich' model for heparin binding.* Structure, 1999. **7**(6): p. 699-709.
336. de Pereda, J.M., et al., *Advances and perspectives of the architecture of hemidesmosomes: lessons from structural biology.* Cell Adh Migr, 2009. **3**(4): p. 361-4.
337. Uematsu, J., et al., *Demonstration of type II hemidesmosomes in a mammary gland epithelial cell line, BMGE-H.* J Biochem, 1994. **115**(3): p. 469-76.
338. Green, K.J. and J.C. Jones, *Desmosomes and hemidesmosomes: structure and function of molecular components.* The FASEB Journal, 1996. **10**(8): p. 871-81.
339. Laurila, P. and I. Leivo, *Basement membrane and interstitial matrix components form separate matrices in heterokaryons of PYS-2 cells and fibroblasts.* J Cell Sci, 1993. **104 (Pt 1)**: p. 59-68.
340. Timpl, R., *Structure and biological activity of basement membrane proteins.* Eur J Biochem, 1989. **180**(3): p. 487-502.
341. Voss, B., et al., *Immunocytochemical investigation on the distribution of small chondroitin sulfate-dermatan sulfate proteoglycan in the human.* J Histochem Cytochem, 1986. **34**(8): p. 1013-9.
342. Yamada, K.M., *Fibronectin and Other Cell Interactive Glycoproteins*, in *Cell Biology of Extracellular Matrix: Second Edition*, E.D. Hay, Editor. 1991, Springer US: Boston, MA. p. 111-146.

343. Sanes, J.R., et al., *Molecular heterogeneity of basal laminae: isoforms of laminin and collagen IV at the neuromuscular junction and elsewhere.* J Cell Biol, 1990. **111**(4): p. 1685-99.
344. Qin, P., et al., *Localization of basement membrane-associated protein isoforms during development of the ocular surface of mouse eye.* Dev Dyn, 1997. **209**(4): p. 367-76.
345. Timpl, R., et al., *A network model for the organization of type IV collagen molecules in basement membranes.* Eur J Biochem, 1981. **120**(2): p. 203-11.
346. Kato, M., et al., *Basement membrane proteoglycan in various tissues: characterization using monoclonal antibodies to the Engelbreth-Holm-Swarm mouse tumor low density heparan sulfate proteoglycan.* J Cell Biol, 1988. **106**(6): p. 2203-10.
347. Yurchenco, P.D., *Basement membranes: cell scaffoldings and signaling platforms.* Cold Spring Harb Perspect Biol, 2011. **3**(2).
348. Sarrazin, S., W.C. Lamanna, and J.D. Esko, *Heparan sulfate proteoglycans.* Cold Spring Harb Perspect Biol, 2011. **3**(7).
349. Hynes, R.O. and A. Naba, *Overview of the Matrisome—An Inventory of Extracellular Matrix Constituents and Functions.* Cold Spring Harb Perspect Biol, 2012. **4**(1).
350. Muiznieks, L.D. and F.W. Keeley, *Molecular assembly and mechanical properties of the extracellular matrix: A fibrous protein perspective.* Biochimica et Biophysica Acta (BBA) - Molecular Basis of Disease, 2013. **1832**(7): p. 866-875.
351. Fukuda, K., et al., *Differential distribution of subchains of the basement membrane components type IV collagen and laminin among the amniotic membrane, cornea, and conjunctiva.* Cornea, 1999. **18**(1): p. 73-9.
352. Tuori, A., et al., *The immunohistochemical composition of the human corneal basement membrane.* Cornea, 1996. **15**(3): p. 286-94.
353. Aumailley, M., et al., *A simplified laminin nomenclature.* Matrix Biol, 2005. **24**(5): p. 326-32.
354. Schneider, H., C. Mühle, and F. Pacho, *Biological function of laminin-5 and pathogenic impact of its deficiency.* European Journal of Cell Biology, 2007. **86**(11-12): p. 701-717.
355. Tzu, J. and M.P. Marinkovich, *Bridging structure with function: Structural, regulatory, and developmental role of laminins.* International Journal of Biochemistry and Cell Biology, 2008. **40**(2): p. 199-214.
356. Goldfinger, L.E., M.S. Stack, and J.C.R. Jones, *Processing of Laminin-5 and Its Functional Consequences: Role of Plasmin and Tissue-type Plasminogen Activator.* The Journal of Cell Biology, 1998. **141**(1): p. 255-265.
357. Talts, J.F., et al., *Structural and Functional Analysis of the Recombinant G Domain of the Laminin α4 Chain and Its Proteolytic Processing in Tissues.* Journal of Biological Chemistry, 2000. **275**(45): p. 35192-35199.
358. Yamada, M. and K. Sekiguchi, *Chapter Six - Molecular Basis of Laminin–Integrin Interactions*, in *Current Topics in Membranes*, J.H. Miner, Editor. 2015, Academic Press. p. 197-229.
359. Taniguchi, Y., et al., *The C-terminal Region of Laminin β Chains Modulates the Integrin Binding Affinities of Laminins.* Journal of Biological Chemistry, 2009. **284**(12): p. 7820-7831.
360. Yamada, M. and K. Sekiguchi, *Molecular Basis of Laminin–Integrin Interactions.* Current Topics in Membranes, 2015. **76**: p. 197-229.
361. Miner, J.H., et al., *The Laminin α Chains: Expression, Developmental Transitions, and Chromosomal Locations of α1-5, Identification of Heterotrimeric Laminins 8–11, and Cloning of a Novel α3 Isoform.* The Journal of Cell Biology, 1997. **137**(3): p. 685-701.

362. Burgeson, R.E., et al., *A new nomenclature for the laminins.* Matrix Biol, 1994. **14**(3): p. 209-11.
363. Durbeej, M., *Laminins.* Cell and Tissue Research, 2009. **339**(1): p. 259.
364. Miner, J.H. and P.D. Yurchenco, *Laminin functions in tissue morphogenesis.* Annu Rev Cell Dev Biol, 2004. **20**: p. 255-84.
365. Iorio, V., L.D. Troughton, and K.J. Hamill, *Laminins: Roles and Utility in Wound Repair.* Advances in Wound Care, 2015. **4**(4): p. 250-263.
366. Ljubimov, A.V., et al., *Human corneal epithelial basement membrane and integrin alterations in diabetes and diabetic retinopathy.* J Histochem Cytochem, 1998. **46**(9): p. 1033-41.
367. Klaffky, E., et al., *Trophoblast-specific expression and function of the integrin alpha 7 subunit in the peri-implantation mouse embryo.* Dev Biol, 2001. **239**(1): p. 161-75.
368. Miner, J.H., *Laminins and their roles in mammals.* Microsc Res Tech, 2008. **71**(5): p. 349-56.
369. Ekblom, P., P. Lonai, and J.F. Talts, *Expression and biological role of laminin-1.* Matrix Biol, 2003. **22**(1): p. 35-47.
370. Hallmann, R., et al., *Expression and function of laminins in the embryonic and mature vasculature.* Physiol Rev, 2005. **85**(3): p. 979-1000.
371. Suzuki, N., F. Yokoyama, and M. Nomizu, *Functional sites in the laminin alpha chains.* Connect Tissue Res, 2005. **46**(3): p. 142-52.
372. Scheele, S., et al., *Laminin isoforms in development and disease.* J Mol Med (Berl), 2007. **85**(8): p. 825-36.
373. Ido, H., et al., *Laminin Isoforms Containing the γ3 Chain Are Unable to Bind to Integrins due to the Absence of the Glutamic Acid Residue Conserved in the C-terminal Regions of the γ1 and γ2 Chains.* Journal of Biological Chemistry, 2008. **283**(42): p. 28149-28157.
374. Taniguchi, Y., et al., *The C-terminal region of laminin beta chains modulates the integrin binding affinities of laminins.* J Biol Chem, 2009. **284**(12): p. 7820-31.
375. Li, S., et al., *The Role of Laminin in Embryonic Cell Polarization and Tissue Organization.* Developmental Cell, 2003. **4**(5): p. 613-624.
376. Hamill, K.J., A.S. Paller, and J.C.R. Jones, *Adhesion and Migration, the Diverse Functions of the Laminin α3 Subunit.* Dermatol Clin, 2010. **28**(1): p. 79.
377. Cohen, M.W., et al., *Laminin-induced Clustering of Dystroglycan on Embryonic Muscle Cells: Comparison with Agrin-induced Clustering.* The Journal of Cell Biology, 1997. **136**(5): p. 1047-1058.
378. Colognato, H. and P.D. Yurchenco, *The laminin alpha2 expressed by dystrophic dy(2J) mice is defective in its ability to form polymers.* Curr Biol, 1999. **9**(22): p. 1327-30.
379. Humphries, M.J., *Integrin Structure.* Biochemical Society Transactions, 2000. **28**(4): p. 311-340.
380. Alberts B, J.A., Lewis J, et al. , *Molecular Biology of the Cell*. 4th ed. 2002: New York: Garland Science.
381. Geiger, B., et al., *Transmembrane crosstalk between the extracellular matrix and the cytoskeleton.* Nat Rev Mol Cell Biol, 2001. **2**(11): p. 793-805.
382. Zaidel-Bar, R., et al., *Early molecular events in the assembly of matrix adhesions at the leading edge of migrating cells.* Journal of Cell Science, 2003. **116**(22): p. 4605-4613.
383. Humphries, J.D., A. Byron, and M.J. Humphries, *INTEGRIN LIGANDS.* J Cell Sci, 2006. **119**(Pt 19): p. 3901-3.
384. Dowling, J., Q.C. Yu, and E. Fuchs, *Beta4 integrin is required for hemidesmosome formation, cell adhesion and cell survival.* J Cell Biol, 1996. **134**(2): p. 559-72.

385. Edelman, A.M., D.K. Blumenthal, and E.G. Krebs, *Protein serine/threonine kinases.* Annu Rev Biochem, 1987. **56**: p. 567-613.
386. Ballou, L.M., P. Jeno, and G. Thomas, *Protein phosphatase 2A inactivates the mitogen-stimulated S6 kinase from Swiss mouse 3T3 cells.* J Biol Chem, 1988. **263**(3): p. 1188-94.
387. Kornberg, L.J., et al., *Signal transduction by integrins: increased protein tyrosine phosphorylation caused by clustering of beta 1 integrins.* Proceedings of the National Academy of Sciences, 1991. **88**(19): p. 8392-8396.
388. Ono, K. and J. Han, *The p38 signal transduction pathway Activation and function.* Cellular Signalling, 2000. **12**(1): p. 1-13.
389. Rubinfeld, H. and R. Seger, *The ERK cascade: a prototype of MAPK signaling.* Mol Biotechnol, 2005. **31**(2): p. 151-74.
390. Roux, P.P. and J. Blenis, *ERK and p38 MAPK-activated protein kinases: a family of protein kinases with diverse biological functions.* Microbiol Mol Biol Rev, 2004. **68**(2): p. 320-44.
391. Boulton, T.G., et al., *ERKs: a family of protein-serine/threonine kinases that are activated and tyrosine phosphorylated in response to insulin and NGF.* Cell, 1991. **65**(4): p. 663-75.
392. Jaaro, H., et al., *Nuclear translocation of mitogen-activated protein kinase kinase (MEK1) in response to mitogenic stimulation.* Proc Natl Acad Sci U S A, 1997. **94**(8): p. 3742-7.
393. Marshall, C.J., *Specificity of receptor tyrosine kinase signaling: transient versus sustained extracellular signal-regulated kinase activation.* Cell, 1995. **80**(2): p. 179-85.
394. Demoulin, J.B., et al., *Distinct roles for STAT1, STAT3, and STAT5 in differentiation gene induction and apoptosis inhibition by interleukin-9.* J Biol Chem, 1999. **274**(36): p. 25855-61.
395. Ho, H.H. and L.B. Ivashkiv, *Role of STAT3 in Type I Interferon Responses: NEGATIVE REGULATION OF STAT1-DEPENDENT INFLAMMATORY GENE ACTIVATION.* Journal of Biological Chemistry, 2006. **281**(20): p. 14111-14118.
396. Meissl, K., et al., *The good and the bad faces of STAT1 in solid tumours.* Cytokine, 2017. **89**: p. 12-20.
397. Battle, T.E., R.A. Lynch, and D.A. Frank, *Signal transducer and activator of transcription 1 activation in endothelial cells is a negative regulator of angiogenesis.* Cancer Res, 2006. **66**(7): p. 3649-57.
398. Yang, X.O., et al., *STAT3 Regulates Cytokine-mediated Generation of Inflammatory Helper T Cells.* Journal of Biological Chemistry, 2007. **282**(13): p. 9358-9363.
399. Kameyama, H., et al., *Significance of Stat3 Signaling in Epithelial Cell Differentiation of Fetal Mouse Lungs.* Acta Histochem Cytochem, 2017. **50**(1): p. 1-9.
400. Heron-Milhavet, L., et al., *Akt1 and Akt2: differentiating the aktion.* Histol Histopathol, 2011. **26**(5): p. 651-62.
401. Bouchard, V., et al., *Fak/Src signaling in human intestinal epithelial cell survival and anoikis: differentiation state-specific uncoupling with the PI3-K/Akt-1 and MEK/Erk pathways.* J Cell Physiol, 2007. **212**(3): p. 717-28.
402. Brunet, A., et al., *Akt promotes cell survival by phosphorylating and inhibiting a Forkhead transcription factor.* Cell, 1999. **96**(6): p. 857-68.
403. Frame, S. and P. Cohen, *GSK3 takes centre stage more than 20 years after its discovery.* Biochem J, 2001. **359**(Pt 1): p. 1-16.
404. Scholle, F., K.M. Bendt, and N. Raab-Traub, *Epstein-Barr virus LMP2A transforms epithelial cells, inhibits cell differentiation, and activates Akt.* J Virol, 2000. **74**(22): p. 10681-9.

405. Kuo, S.Z., et al., *Salinomycin induces cell death and differentiation in head and neck squamous cell carcinoma stem cells despite activation of epithelial-mesenchymal transition and Akt.* BMC Cancer, 2012. **12**: p. 556.
406. Moschetta, M., et al., *Therapeutic targeting of the mTOR-signalling pathway in cancer: benefits and limitations.* Br J Pharmacol, 2014. **171**(16): p. 3801-13.
407. Zhao, C., et al., *mTOR-mediated dedifferentiation of the retinal pigment epithelium initiates photoreceptor degeneration in mice.* J Clin Invest, 2011. **121**(1): p. 369-83.
408. Sun, X., et al., *AMPK improves gut epithelial differentiation and barrier function via regulating Cdx2 expression.* Cell Death Differ, 2017. **24**(5): p. 819-831.
409. Vu, N.D. and P. Zelenka, *Phosphorylation of ribosomal protein S6 during lens cell differentiation: Correlation with translational efficiency.* Current Eye Research, 1987. **6**(5): p. 703-708.
410. Eckert, R.L., et al., *p38 Mitogen-activated protein kinases on the body surface--a function for p38 delta.* J Invest Dermatol, 2003. **120**(5): p. 823-8.
411. Ullmann, U., et al., *GSK-3-specific inhibitor-supplemented hESC medium prevents the epithelial–mesenchymal transition process and the up-regulation of matrix metalloproteinases in hESCs cultured in feeder-free conditions.* MHR: Basic science of reproductive medicine, 2008. **14**(3): p. 169-179.
412. Rho, O., et al., *Impact of mTORC1 Inhibition on Keratinocyte Proliferation During Skin Tumor Promotion in Wild-Type and BK5.Akt(WT) Mice.* Mol Carcinog, 2014. **53**(11): p. 871-82.
413. Yurchenco, P.D., et al., *The alpha chain of laminin-1 is independently secreted and drives secretion of its beta- and gamma-chain partners.* Proc Natl Acad Sci U S A, 1997. **94**(19): p. 10189-94.
414. Doi, M., et al., *Recombinant human laminin-10 (alpha5beta1gamma1). Production, purification, and migration-promoting activity on vascular endothelial cells.* J Biol Chem, 2002. **277**(15): p. 12741-8.
415. Kortesmaa, J., P. Yurchenco, and K. Tryggvason, *Recombinant laminin-8 (alpha(4)beta(1)gamma(1)). Production, purification,and interactions with integrins.* J Biol Chem, 2000. **275**(20): p. 14853-9.
416. Pathan, M., et al., *FunRich: An open access standalone functional enrichment and interaction network analysis tool.* PROTEOMICS, 2015. **15**(15): p. 2597-2601.
417. Lin, L.I.N., C. Daneshvar, and M. Kurpakus-Wheater, *Evidence for Differential Signaling in Human Conjunctival Epithelial Cells Adherent to Laminin Isoforms.* Experimental Eye Research, 2000. **70**(4): p. 537-546.
418. Ricard-Blum, S., *The Collagen Family.* Cold Spring Harb Perspect Biol, 2011. **3**(1).
419. Nykvist, P., et al., *The Cell Adhesion Domain of Type XVII Collagen Promotes Integrin-mediated Cell Spreading by a Novel Mechanism.* Journal of Biological Chemistry, 2001. **276**(42): p. 38673-38679.
420. Hirako, Y., et al., *Demonstration of the Molecular Shape of BP180, a 180-kDa Bullous Pemphigoid Antigen and Its Potential for Trimer Formation.* Journal of Biological Chemistry, 1996. **271**(23): p. 13739-13745.
421. Schäcke, H., et al., *Two Forms of Collagen XVII in Keratinocytes: A FULL-LENGTH TRANSMEMBRANE PROTEIN AND A SOLUBLE ECTODOMAIN.* Journal of Biological Chemistry, 1998. **273**(40): p. 25937-25943.
422. Jonsson, F., et al., *Mutations in Collagen, Type XVII, Alpha 1 (COL17A1) Cause Epithelial Recurrent Erosion Dystrophy (ERED).* Human Mutation, 2015. **36**(4): p. 463-473.
423. Fine, J.D., et al., *Eye involvement in inherited epidermolysis bullosa: experience of the National Epidermolysis Bullosa Registry.* Am J Ophthalmol, 2004. **138**(2): p. 254-62.

424. Colognato, H. and P.D. Yurchenco, *Form and function: the laminin family of heterotrimers.* Dev Dyn, 2000. **218**(2): p. 213-34.
425. Kurpakus, M.A.M. and L.L. Lin, *The lack of extracellular laminin ß2 chain deposition correlates to the loss of conjunctival epithelial keratin K4 localization in culture.* Current Eye Research, 1999. **18**(1): p. 28-38.
426. Vuoristo, S., et al., *Laminin isoforms in human embryonic stem cells: synthesis, receptor usage and growth support.* J Cell Mol Med, 2009. **13**(8b): p. 2622-33.
427. Okumura, N., et al., *Laminin-511 and -521 Enable Efficient In Vitro Expansion of Human Corneal Endothelial CellsLaminin-511 and -521 Enable Expansion of HCECs.* Investigative Ophthalmology & Visual Science, 2015. **56**(5): p. 2933-2942.
428. Raeder, S. and T.P. Utheim, *Transplant storage*. 2008, Google Patents.
429. Gipson, I.K., *The epithelial basement membrane zone of the limbus.* Eye, 1989. **3**(2): p. 132-140.
430. Gordon, M.K., et al., *Type XVII collagen (BP 180) in the developing avian cornea.* Invest Ophthalmol Vis Sci, 1997. **38**(1): p. 153-66.
431. Torricelli, A.A.M., *The Corneal Epithelial Basement Membrane: Structure, Function, and Disease.* 2013. **54**(9): p. 6390-400.
432. Tryggvason, K., *The laminin family.* Current Opinion in Cell Biology, 1993. **5**(5): p. 877-882.
433. Nishiuchi, R., et al., *Ligand-binding specificities of laminin-binding integrins: a comprehensive survey of laminin-integrin interactions using recombinant alpha3beta1, alpha6beta1, alpha7beta1 and alpha6beta4 integrins.* Matrix Biol, 2006. **25**(3): p. 189-97.
434. Smyth, N., et al., *Absence of basement membranes after targeting the LAMC1 gene results in embryonic lethality due to failure of endoderm differentiation.* J Cell Biol, 1999. **144**(1): p. 151-60.
435. Durbeej, M., *Laminins.* Cell Tissue Res, 2010. **339**(1): p. 259-68.
436. Chen, Z.-L. and S. Strickland, *Laminin γ1 is critical for Schwann cell differentiation, axon myelination, and regeneration in the peripheral nerve.* The Journal of Cell Biology, 2003. **163**(4): p. 889-899.
437. Ljubimov, A.V., et al., *Human corneal basement membrane heterogeneity: topographical differences in the expression of type IV collagen and laminin isoforms.* Lab Invest, 1995. **72**(4): p. 461-73.
438. Kurpakus, M.A., et al., *Human corneal epithelial cell adhesion to laminins.* Curr Eye Res, 1999. **19**(2): p. 106-14.
439. Polisetti, N., et al., *Laminin-511 and -521-based matrices for efficient ex vivo-expansion of human limbal epithelial progenitor cells.* Sci Rep, 2017. **7**.
440. Bissell, M.J. and M.H. Barcellos-Hoff, *The influence of extracellular matrix on gene expression: is structure the message?* J Cell Sci Suppl, 1987. **8**: p. 327-43.
441. *Kalinin is more efficient than laminin in promoting adhesion of primary keratinocytes and some other epithelial cells and has a different requirement for integrin receptors.* J Cell Biol, 1994. **125**(1): p. 205-14.
442. Carter, W.G., et al., *The role of integrins alpha 2 beta 1 and alpha 3 beta 1 in cell-cell and cell-substrate adhesion of human epidermal cells.* The Journal of Cell Biology, 1990. **110**(4): p. 1387-1404.
443. Ido, H., et al., *Molecular dissection of the alpha-dystroglycan- and integrin-binding sites within the globular domain of human laminin-10.* J Biol Chem, 2004. **279**(12): p. 10946-54.
444. Burdon, T., et al., *Suppression of SHP-2 and ERK signalling promotes self-renewal of mouse embryonic stem cells.* Dev Biol, 1999. **210**(1): p. 30-43.

445. Ihara, S., et al., *Dual control of neurite outgrowth by STAT3 and MAP kinase in PC12 cells stimulated with interleukin-6.* Embo j, 1997. **16**(17): p. 5345-52.
446. Manning, B.D. and L.C. Cantley, *AKT/PKB Signaling: Navigating Downstream.* Cell, 2007. **129**(7): p. 1261-1274.
447. Hermanson, O., K. Jepsen, and M.G. Rosenfeld, *N-CoR controls differentiation of neural stem cells into astrocytes.* Nature, 2002. **419**(6910): p. 934-9.
448. Sato, N., et al., *Maintenance of pluripotency in human and mouse embryonic stem cells through activation of Wnt signaling by a pharmacological GSK-3-specific inhibitor.* Nat Med, 2004. **10**(1): p. 55-63.
449. Castro-Muñozledo, F., *The Mammalian Limbal Stem Cell Niche: A Complex Interaction Between Cells, Growth Factors and Extracellular Matrix*, in *Biology in Stem Cell Niche*, K. Turksen, Editor. 2015, Springer International Publishing: Cham. p. 23-56.
450. Fujita, M., et al., *Heat shock protein27 expression and cell differentiation in ameloblastomas.* Int J Med Sci, 2013. **10**(10): p. 1271-7.
451. de Thonel, A., et al., *HSP27 controls GATA-1 protein level during erythroid cell differentiation.* Blood, 2010. **116**(1): p. 85-96.
452. Jubin, T., et al., *Poly ADP-ribose polymerase-1: Beyond transcription and towards differentiation.* Seminars in Cell & Developmental Biology, 2017. **63**: p. 167-179.
453. Moldovan, L., et al., *Analyzing the Circulating MicroRNAs in Exosomes/Extracellular Vesicles from Serum or Plasma by qRT-PCR*, in *Circulating MicroRNAs*, N. Kosaka, Editor. 2013, Humana Press. p. 129-145.
454. Trams, E.G., et al., *Exfoliation of membrane ecto-enzymes in the form of micro-vesicles.* Biochim Biophys Acta, 1981. **645**(1): p. 63-70.
455. Caby, M.-P., et al., *Exosomal-like vesicles are present in human blood plasma.* International Immunology, 2005. **17**(7): p. 879-887.
456. Ogawa, Y., et al., *Proteomic Analysis of Two Types of Exosomes in Human Whole Saliva.* Biological and Pharmaceutical Bulletin, 2011. **34**(1): p. 13-23.
457. Sahlen, G.E., et al., *Ultrastructure of the secretion of prostasomes from benign and malignant epithelial cells in the prostate.* Prostate, 2002. **53**(3): p. 192-9.
458. Grigor'eva, A.E., et al., *[Characteristics of exosomes andmicroparticles discovered in human tears].* Biomed Khim, 2016. **62**(1): p. 99-106.
459. Simons, M. and G. Raposo, *Exosomes – vesicular carriers for intercellular communication.* Current Opinion in Cell Biology, 2009. **21**(4): p. 575-581.
460. Thery, C., M. Ostrowski, and E. Segura, *Membrane vesicles as conveyors of immune responses.* Nat Rev Immunol, 2009. **9**(8): p. 581-593.
461. Cocucci, E., G. Racchetti, and J. Meldolesi, *Shedding microvesicles: artefacts no more.* Trends Cell Biol, 2009. **19**(2): p. 43-51.
462. Thery, C., M. Ostrowski, and E. Segura, *Membrane vesicles as conveyors of immune responses.* Nat Rev Immunol, 2009. **9**(8): p. 581-93.
463. Pan, B.T., et al., *Electron microscopic evidence for externalization of the transferrin receptor in vesicular form in sheep reticulocytes.* J Cell Biol, 1985. **101**(3): p. 942-8.
464. Conde-Vancells, J., et al., *Characterization and comprehensive proteome profiling of exosomes secreted by hepatocytes.* J Proteome Res, 2008. **7**(12): p. 5157-66.
465. Yanez-Mo, M., et al., *Tetraspanin-enriched microdomains: a functional unit in cell plasma membranes.* Trends Cell Biol, 2009. **19**(9): p. 434-46.
466. Escola, J.M., et al., *Selective enrichment of tetraspan proteins on the internal vesicles of multivesicular endosomes and on exosomes secreted by human B-lymphocytes.* J Biol Chem, 1998. **273**(32): p. 20121-7.

467. Lötvall, J., et al., *Minimal experimental requirements for definition of extracellular vesicles and their functions: a position statement from the International Society for Extracellular Vesicles.* 2014, 2014.
468. Pols, M.S. and J. Klumperman, *Trafficking and function of the tetraspanin CD63.* Experimental Cell Research, 2009. **315**(9): p. 1584-1592.
469. van Niel, G., et al., *The tetraspanin CD63 regulates ESCRT-independent and -dependent endosomal sorting during melanogenesis.* Dev Cell, 2011. **21**(4): p. 708-21.
470. Stefani, F., et al., *UBAP1 is a component of an endosome-specific ESCRT-I complex that is essential for MVB sorting.* Curr Biol, 2011. **21**(14): p. 1245-50.
471. Baietti, M.F., et al., *Syndecan-syntenin-ALIX regulates the biogenesis of exosomes.* Nat Cell Biol, 2012. **14**(7): p. 677-85.
472. Christianson, J.C., et al., *OS-9 and GRP94 deliver mutant alpha1-antitrypsin to the Hrd1-SEL1L ubiquitin ligase complex for ERAD.* Nat Cell Biol, 2008. **10**(3): p. 272-82.
473. Thery, C., L. Zitvogel, and S. Amigorena, *Exosomes: composition, biogenesis and function.* Nat Rev Immunol, 2002. **2**(8): p. 569-579.
474. Subra, C., et al., *Exosome lipidomics unravels lipid sorting at the level of multivesicular bodies.* Biochimie, 2007. **89**(2): p. 205-212.
475. Brouwers, J.F., et al., *Distinct lipid compositions of two types of human prostasomes.* PROTEOMICS, 2013. **13**(10-11): p. 1660-1666.
476. Laulagnier, K., et al., *Characterization of exosome subpopulations from RBL-2H3 cells using fluorescent lipids.* Blood Cells, Molecules, and Diseases, 2005. **35**(2): p. 116-121.
477. *Single exosome study reveals subpopulations distributed among cell lines with variability related to membrane content.* Journal of Extracellular Vesicles, 2015. **4**(1): p. 28533.
478. Bellingham, S.A., B.M. Coleman, and A.F. Hill, *Small RNA deep sequencing reveals a distinct miRNA signature released in exosomes from prion-infected neuronal cells.* Nucleic Acids Research, 2012. **40**(21): p. 10937-10949.
479. Nolte-'t Hoen, E.N.M., et al., *Deep sequencing of RNA from immune cell-derived vesicles uncovers the selective incorporation of small non-coding RNA biotypes with potential regulatory functions.* Nucleic Acids Research, 2012. **40**(18): p. 9272-9285.
480. Valadi, H., et al., *Exosome-mediated transfer of mRNAs and microRNAs is a novel mechanism of genetic exchange between cells.* Nat Cell Biol, 2007. **9**(6): p. 654-659.
481. Goldie, B.J., et al., *Activity-associated miRNA are packaged in Map1b-enriched exosomes released from depolarized neurons.* Nucleic Acids Research, 2014. **42**(14): p. 9195-9208.
482. Batagov, A.O., V.A. Kuznetsov, and I.V. Kurochkin, *Identification of nucleotide patterns enriched in secreted RNAs as putative cis-acting elements targeting them to exosome nano-vesicles.* BMC Genomics, 2011. **12 Suppl 3**: p. S18.
483. Villarroya-Beltri, C., et al., *Sumoylated hnRNPA2B1 controls the sorting of miRNAs into exosomes through binding to specific motifs.* Nat Commun, 2013. **4**: p. 2980.
484. Kosaka, N., et al., *Neutral Sphingomyelinase 2 (nSMase2)-dependent Exosomal Transfer of Angiogenic MicroRNAs Regulate Cancer Cell Metastasis.* Journal of Biological Chemistry, 2013. **288**(15): p. 10849-10859.
485. Bobrie, A., et al., *Exosome secretion: molecular mechanisms and roles in immune responses.* Traffic, 2011. **12**(12): p. 1659-68.
486. Taylor, D.D. and C. Gercel-Taylor, *MicroRNA signatures of tumor-derived exosomes as diagnostic biomarkers of ovarian cancer.* Gynecologic Oncology, 2008. **110**(1): p. 13-21.

487. Tay, Y., et al., *MicroRNAs to Nanog, Oct4 and Sox2 coding regions modulate embryonic stem cell differentiation.* Nature, 2008. **455**(7216): p. 1124-8.
488. Vasudevan, S., Y. Tong, and J.A. Steitz, *Switching from repression to activation: microRNAs can up-regulate translation.* Science, 2007. **318**(5858): p. 1931-4.
489. Kozomara, A. and S. Griffiths-Jones, *miRBase: integrating microRNA annotation and deep-sequencing data.* Nucleic Acids Res, 2011. **39**(Database issue): p. D152-7.
490. Teng, Y., et al., *Signature microRNAs in human cornea limbal epithelium.* Funct Integr Genomics, 2015. **15**(3): p. 277-94.
491. Raghunath, A. and E. Perumal, *Micro-RNAs and their roles in eye disorders.* Ophthalmic Res, 2015. **53**(4): p. 169-86.
492. Funari, V.A., et al., *Differentially Expressed Wound Healing-Related microRNAs in the Human Diabetic Cornea.* PLoS ONE, 2013. **8**(12): p. e84425.
493. Ryan, D.G., M. Oliveira-Fernandes, and R.M. Lavker, *MicroRNAs of the mammalian eye display distinct and overlapping tissue specificity.* Mol Vis, 2006. **12**: p. 1175-84.
494. Shalom-Feuerstein, R., et al., *Pluripotent stem cell model reveals essential roles for miR-450b-5p and miR-184 in embryonic corneal lineage specification.* Stem Cells, 2012. **30**(5): p. 898-909.
495. Peng, H., et al., *microRNA-103/107 Family Regulates Multiple Epithelial Stem Cell Characteristics.* Stem Cells, 2015. **33**(5): p. 1642-56.
496. Derrick, T., et al., *Conjunctival MicroRNA expression in inflammatory trachomatous scarring.* PLoS Negl Trop Dis, 2013. **7**(3): p. e2117.
497. Derrick, T., et al., *Inverse relationship between microRNA-155 and -184 expression with increasing conjunctival inflammation during ocular Chlamydia trachomatis infection.* BMC Infectious Diseases, 2016. **16**(1): p. 60.
498. Xu, S., *microRNA expression in the eyes and their significance in relation to functions.* Progress in Retinal and Eye Research, 2009. **28**(2): p. 87-116.
499. Yi, R., et al., *A skin microRNA promotes differentiation by repressing 'stemness'.* Nature, 2008. **452**(7184): p. 225-9.
500. Lena, A.M., et al., *miR-203 represses 'stemness' by repressing DeltaNp63.* Cell Death Differ, 2008. **15**(7): p. 1187-95.
501. Zhang, L., et al., *Specific microRNAs are preferentially expressed by skin stem cells to balance self-renewal and early lineage commitment.* Cell Stem Cell, 2011. **8**(3): p. 294-308.
502. Lee, S.K., et al., *MicroRNA-145 regulates human corneal epithelial differentiation.* PLoS One, 2011. **6**(6): p. e21249.
503. Lotvall, J., et al., *Minimal experimental requirements for definition of extracellular vesicles and their functions: a position statement from the International Society for Extracellular Vesicles.* J Extracell Vesicles, 2014. **3**: p. 26913.
504. Raposo, G., et al., *Accumulation of Major Histocompatibility Complex Class II Molecules in Mast Cell Secretory Granules and Their Release upon Degranulation.* Molecular Biology of the Cell, 1997. **8**(12): p. 2631-2645.
505. Wolfers, J., et al., *Tumor-derived exosomes are a source of shared tumor rejection antigens for CTL cross-priming.* Nat Med, 2001. **7**(3): p. 297-303.
506. Théry, C., et al., *Proteomic Analysis of Dendritic Cell-Derived Exosomes: A Secreted Subcellular Compartment Distinct from Apoptotic Vesicles.* The Journal of Immunology, 2001. **166**(12): p. 7309-7318.
507. Rabesandratana, H., et al., *Decay-accelerating factor (CD55) and membrane inhibitor of reactive lysis (CD59) are released within exosomes during In vitro maturation of reticulocytes.* Blood, 1998. **91**(7): p. 2573-80.

508. Clayton, A., et al., *Analysis of antigen presenting cell derived exosomes, based on immuno-magnetic isolation and flow cytometry.* J Immunol Methods, 2001. **247**(1-2): p. 163-74.
509. Katzmann, D.J., M. Babst, and S.D. Emr, *Ubiquitin-Dependent Sorting into the Multivesicular Body Pathway Requires the Function of a Conserved Endosomal Protein Sorting Complex, ESCRT-I.* Cell. **106**(2): p. 145-155.
510. Hicke, L., *A new ticket for entry into budding vesicles-ubiquitin.* Cell, 2001. **106**(5): p. 527-30.
511. Reggiori, F. and H.R.B. Pelham, *Sorting of proteins into multivesicular bodies: ubiquitin-dependent and -independent targeting.* The EMBO Journal, 2001. **20**(18): p. 5176-5186.
512. Andreu, Z. and M. Yáñez-Mó, *Tetraspanins in Extracellular Vesicle Formation and Function.* Front Immunol, 2014. **5**.
513. Buschow, S.I., et al., *MHC class II-associated proteins in B-cell exosomes and potential functional implications for exosome biogenesis.* Immunol Cell Biol, 2010. **88**(8): p. 851-6.
514. Blanchard, N., et al., *TCR activation of human T cells induces the production of exosomes bearing the TCR/CD3/zeta complex.* J Immunol, 2002. **168**(7): p. 3235-41.
515. Raposo, G., et al., *B lymphocytes secrete antigen-presenting vesicles.* J Exp Med, 1996. **183**(3): p. 1161-72.
516. Gruenberg, J. and F.R. Maxfield, *Membrane transport in the endocytic pathway.* Curr Opin Cell Biol, 1995. **7**(4): p. 552-63.
517. Möbius, W., et al., *Immunoelectron Microscopic Localization of Cholesterol Using Biotinylated and Non-cytolytic Perfringolysin O.* Journal of Histochemistry & Cytochemistry, 2002. **50**(1): p. 43-55.
518. Henne, W.M., N.J. Buchkovich, and S.D. Emr, *The ESCRT pathway.* Dev Cell, 2011. **21**(1): p. 77-91.
519. Tamai, K., et al., *Exosome secretion of dendritic cells is regulated by Hrs, an ESCRT-0 protein.* Biochem Biophys Res Commun, 2010. **399**(3): p. 384-90.
520. Hurley, J.H. and P.I. Hanson, *Membrane budding and scission by the ESCRT machinery: it's all in the neck.* Nat Rev Mol Cell Biol, 2010. **11**(8): p. 556-66.
521. Wollert, T., et al., *Membrane scission by the ESCRT-III complex.* Nature, 2009. **458**(7235): p. 172-7.
522. Colombo, M., et al., *Analysis of ESCRT functions in exosome biogenesis, composition and secretion highlights the heterogeneity of extracellular vesicles.* Journal of Cell Science, 2013. **126**(24): p. 5553-5565.
523. Trajkovic, K., et al., *Ceramide Triggers Budding of Exosome Vesicles into Multivesicular Endosomes.* Science, 2008. **319**(5867): p. 1244-1247.
524. Theos, A.C., et al., *A lumenal domain-dependent pathway for sorting to intralumenal vesicles of multivesicular endosomes involved in organelle morphogenesis.* Dev Cell, 2006. **10**(3): p. 343-54.
525. Chairoungdua, A., et al., *Exosome release of beta-catenin: a novel mechanism that antagonizes Wnt signaling.* J Cell Biol, 2010. **190**(6): p. 1079-91.
526. Tejera, E., et al., *CD81 regulates cell migration through its association with Rac GTPase.* Mol Biol Cell, 2013. **24**(3): p. 261-73.
527. Cai, H., K. Reinisch, and S. Ferro-Novick, *Coats, Tethers, Rabs, and SNAREs Work Together to Mediate the Intracellular Destination of a Transport Vesicle.* Developmental Cell. **12**(5): p. 671-682.
528. Zerial, M. and H. McBride, *Rab proteins as membrane organizers.* Nat Rev Mol Cell Biol, 2001. **2**(2): p. 107-17.

529. Ostrowski, M., et al., *Rab27a and Rab27b control different steps of the exosome secretion pathway.* Nat Cell Biol, 2010. **12**(1): p. 19-30.
530. Hsu, C., et al., *Regulation of exosome secretion by Rab35 and its GTPase-activating proteins TBC1D10A–C.* The Journal of Cell Biology, 2010. **189**(2): p. 223-232.
531. Savina, A., et al., *Rab11 Promotes Docking and Fusion of Multivesicular Bodies in a Calcium-Dependent Manner.* Traffic, 2005. **6**(2): p. 131-143.
532. Rao, S.K., et al., *Identification of SNAREs Involved in Synaptotagmin VII-regulated Lysosomal Exocytosis.* Journal of Biological Chemistry, 2004. **279**(19): p. 20471-20479.
533. Fader, C.M., et al., *TI-VAMP/VAMP7 and VAMP3/cellubrevin: two v-SNARE proteins involved in specific steps of the autophagy/multivesicular body pathways.* Biochimica et Biophysica Acta (BBA) - Molecular Cell Research, 2009. **1793**(12): p. 1901-1916.
534. Proux-Gillardeaux, V., et al., *Expression of the Longin domain of TI-VAMP impairs lysosomal secretion and epithelial cell migration.* Biology of the Cell, 2007. **99**(5): p. 261-271.
535. Heijnen, H.F.G., et al., *Activated Platelets Release Two Types of Membrane Vesicles: Microvesicles by Surface Shedding and Exosomes Derived From Exocytosis of Multivesicular Bodies and ・-Granules.* Blood, 1999. **94**(11): p. 3791-3799.
536. Obregon, C., et al., *Exovesicles from Human Activated Dendritic Cells Fuse with Resting Dendritic Cells, Allowing Them to Present Alloantigens.* The American Journal of Pathology. **169**(6): p. 2127-2136.
537. Johnstone, R.M., et al., *Vesicle formation during reticulocyte maturation. Association of plasma membrane activities with released vesicles (exosomes).* J Biol Chem, 1987. **262**(19): p. 9412-20.
538. Harding, C., J. Heuser, and P. Stahl, *Receptor-mediated endocytosis of transferrin and recycling of the transferrin receptor in rat reticulocytes.* J Cell Biol, 1983. **97**(2): p. 329-39.
539. Parolini, I., et al., *Microenvironmental pH Is a Key Factor for Exosome Traffic in Tumor Cells.* Journal of Biological Chemistry, 2009. **284**(49): p. 34211-34222.
540. Denzer, K., et al., *Follicular Dendritic Cells Carry MHC Class II-Expressing Microvesicles at Their Surface.* The Journal of Immunology, 2000. **165**(3): p. 1259-1265.
541. Mallegol, J., et al., *T84-intestinal epithelial exosomes bear MHC class II/peptide complexes potentiating antigen presentation by dendritic cells.* Gastroenterology, 2007. **132**(5): p. 1866-76.
542. Vidal, M., P. Mangeat, and D. Hoekstra, *Aggregation reroutes molecules from a recycling to a vesicle-mediated secretion pathway during reticulocyte maturation.* Journal of Cell Science, 1997. **110**(16): p. 1867-1877.
543. Harding, C. and P. Stahl, *Transferrin recycling in reticulocytes: pH and iron are important determinants of ligand binding and processing.* Biochem Biophys Res Commun, 1983. **113**(2): p. 650-8.
544. Rak, J., *Microparticles in Cancer.* Semin Thromb Hemost, 2010. **36**(08): p. 888-906.
545. Hood, J.L., R.S. San, and S.A. Wickline, *Exosomes Released by Melanoma Cells Prepare Sentinel Lymph Nodes for Tumor Metastasis.* Cancer Research, 2011. **71**(11): p. 3792-3801.
546. Van Niel, G., et al., *Intestinal epithelial cells secrete exosome–like vesicles.* Gastroenterology. **121**(2): p. 337-349.
547. Mack, M., et al., *Transfer of the chemokine receptor CCR5 between cells by membrane-derived microparticles: a mechanism for cellular human immunodeficiency virus 1 infection.* Nat Med, 2000. **6**(7): p. 769-75.

548. Escudier, B., et al., *Vaccination of metastatic melanoma patients with autologous dendritic cell (DC) derived-exosomes: results of thefirst phase I clinical trial.* Journal of Translational Medicine, 2005. **3**: p. 10-10.
549. Chaput, N., et al., *The potential of exosomes in immunotherapy.* Expert Opin Biol Ther, 2005. **5**(6): p. 737-47.
550. Viaud, S., et al., *Dendritic cell-derived exosomes for cancer immunotherapy: what's next?* Cancer Res, 2010. **70**(4): p. 1281-5.
551. Pitt, J.M., et al., *Dendritic cell-derived exosomes for cancer therapy.* J Clin Invest, 2016. **126**(4): p. 1224-32.
552. Besse, B., et al., *Dendritic cell-derived exosomes as maintenance immunotherapy after first line chemotherapy in NSCLC.* OncoImmunology, 2016. **5**(4): p. e1071008.
553. Escudier, B., et al., *Vaccination of metastatic melanoma patients with autologous dendritic cell (DC) derived-exosomes: results of thefirst phase I clinical trial.* J Transl Med, 2005. **3**(1): p. 10.
554. Morse, M.A., et al., *A phase I study of dexosome immunotherapy in patients with advanced non-small cell lung cancer.* J Transl Med, 2005. **3**(1): p. 9.
555. Dai, S., et al., *Phase I clinical trial of autologous ascites-derived exosomes combined with GM-CSF for colorectal cancer.* Mol Ther, 2008. **16**(4): p. 782-90.
556. Viaud, S., et al., *Dendritic cell-derived exosomes promote natural killer cell activation and proliferation: a role for NKG2D ligands and IL-15Ralpha.* PLoS One, 2009. **4**(3): p. e4942.
557. Bruno, S., et al., *Renal regenerative potential of different extra-cellular vesicle populations derived from bone marrow mesenchymal stromal cells.* Tissue Eng Part A, 2017.
558. Aliotta, J.M., et al., *Exosomes induce and reverse monocrotaline-induced pulmonary hypertension in mice.* Cardiovasc Res, 2016. **110**(3): p. 319-30.
559. Burger, D., et al., *Human endothelial colony-forming cells protect against acute kidney injury: role of exosomes.* Am J Pathol, 2015. **185**(8): p. 2309-23.
560. Xu, R., et al., *Highly-purified exosomes and shed microvesicles isolated from the human colon cancer cell line LIM1863 by sequential centrifugal ultrafiltration are biochemically and functionally distinct.* Methods, 2015. **87**: p. 11-25.
561. Wen, S., et al., *Mesenchymal stromal cell-derived extracellular vesicles rescue radiation damage to murine marrow hematopoietic cells.* Leukemia, 2016. **30**(11): p. 2221-2231.
562. Robertson, D.M., et al., *Characterization of growth and differentiation in a telomerase-immortalized human corneal epithelial cell line.* Invest Ophthalmol Vis Sci, 2005. **46**(2): p. 470-8.
563. Thery, C., et al., *Isolation and characterization of exosomes from cell culture supernatants and biological fluids.* Curr Protoc Cell Biol, 2006. **Chapter 3**: p. Unit 3.22.
564. Franzen, C.A., et al., *Characterization of Uptake and Internalization of Exosomes by Bladder Cancer Cells.* BioMed Research International, 2014. **2014**: p. 11.
565. Taraboletti, G., et al., *Bioavailability of VEGF in tumor-shed vesicles depends on vesicle burst induced by acidic pH.* Neoplasia, 2006. **8**(2): p. 96-103.
566. Han, K.Y., et al., *Potential role of corneal epithelial cell-derived exosomes in corneal wound healing and neovascularization.* Sci Rep, 2017. **7**: p. 40548.
567. Henderson, M.C. and D.O. Azorsa, *The genomic and proteomic content of cancer cell-derived exosomes.* Front Oncol, 2012. **2**: p. 38.
568. Muralidharan-Chari, V., et al., *Microvesicles: mediators of extracellular communication during cancer progression.* J Cell Sci, 2010. **123**(Pt 10): p. 1603-11.

569. Evans-Osses, I., L.H. Reichembach, and M.I. Ramirez, *Exosomes or microvesicles? Two kinds of extracellular vesicles with different routes to modify protozoan-host cell interaction.* Parasitol Res, 2015. **114**(10): p. 3567-75.
570. Feng, D., et al., *Cellular internalization of exosomes occurs through phagocytosis.* Traffic, 2010. **11**(5): p. 675-87.
571. Moldovan, L., et al., *Analyzing the circulating microRNAs in exosomes/extracellular vesicles from serum or plasma by qRT-PCR.* Methods Mol Biol, 2013. **1024**: p. 129-45.
572. Bellingham, S.A., B.M. Coleman, and A.F. Hill, *Small RNA deep sequencing reveals a distinct miRNA signature released in exosomes from prion-infected neuronal cells.* Nucleic Acids Res, 2012. **40**(21): p. 10937-49.
573. Nolte-'t Hoen, E.N.M., et al., *Deep sequencing of RNA from immune cell-derived vesicles uncovers the selective incorporation of small non-coding RNA biotypes with potential regulatory functions.* Nucleic Acids Res, 2012. **40**(18): p. 9272-85.
574. Raghavan, V., et al., *Hypothesis: Exosomal microRNAs as potential biomarkers for schizophrenia.* Med Hypotheses, 2017. **103**: p. 21-25.
575. Kahlert, C. and R. Kalluri, *Exosomes in tumor microenvironment influence cancer progression and metastasis.* J Mol Med (Berl), 2013. **91**(4): p. 431-7.
576. Skog, J., et al., *Glioblastoma microvesicles transport RNA and proteins that promote tumour growth and provide diagnostic biomarkers.* Nat Cell Biol, 2008. **10**(12): p. 1470-1476.
577. Valadi, H., et al., *Exosome-mediated transfer of mRNAs and microRNAs is a novel mechanism of genetic exchange between cells.* Nat Cell Biol, 2007. **9**(6): p. 654-9.
578. Zhang, S., et al., *MIR-34c regulates mouse embryonic stem cells differentiation into male germ-like cells through RARg.* Cell Biochem Funct, 2012. **30**(8): p. 623-32.
579. Xu, B., et al., *MiR-146a suppresses tumor growth and progression by targeting EGFR pathway and in a p-ERK-dependent manner in castration-resistant prostate cancer.* Prostate, 2012. **72**(11): p. 1171-8.
580. Winkler, M.A., et al., *Targeting miR-146a to treat delayed wound healing in human diabetic organ-cultured corneas.* PLoS One, 2014. **9**(12): p. e114692.
581. Wang, Q., et al., *Regulation of retinal inflammation by rhythmic expression of MiR-146a in diabetic retina.* Invest Ophthalmol Vis Sci, 2014. **55**(6): p. 3986-94.
582. Williams, M., et al., *miR-193a-3p is a potential tumor suppressor in malignant pleural mesothelioma.* Oncotarget, 2015. **6**(27): p. 23480-95.
583. Chao, C.H., et al., *MicroRNA-205 signaling regulates mammary stem cell fate and tumorigenesis.* J Clin Invest, 2014. **124**(7): p. 3093-106.
584. Chen, J., et al., *miR-598 inhibits metastasis in colorectal cancer by suppressing JAG1/Notch2 pathway stimulating EMT.* Experimental Cell Research, 2017. **352**(1): p. 104-112.
585. Rokavec, M., et al., *The p53/miR-34 axis in development and disease.* J Mol Cell Biol, 2014. **6**(3): p. 214-30.
586. Hermeking, H., *The miR-34 family in cancer and apoptosis.* Cell Death Differ, 2010. **17**(2): p. 193-9.
587. Li, L., et al., *MiR-34a inhibits proliferation and migration of breast cancer through down-regulation of Bcl-2 and SIRT1.* Clin Exp Med, 2013. **13**(2): p. 109-17.
588. Bouhallier, F., et al., *Role of miR-34c microRNA in the late steps of spermatogenesis.* Rna, 2010. **16**(4): p. 720-31.
589. Bae, Y., et al., *miRNA-34c regulates Notch signaling during bone development.* Hum Mol Genet, 2012. **21**(13): p. 2991-3000.
590. Morizane, R., et al., *miR-34c attenuates epithelial-mesenchymal transition and kidney fibrosis with ureteral obstruction.* Scientific Reports, 2014. **4**: p. 4578.

591. Huang, Y., et al., *Involvement of inflammation-related miR-155 and miR-146a in diabetic nephropathy: implications for glomerular endothelial injury.* BMC Nephrology, 2014. **15**: p. 142-142.
592. Chen, G., et al., *miR-146a inhibits cell growth, cell migration and induces apoptosis in non-small cell lung cancer cells.* PLoS One, 2013. **8**(3): p. e60317.
593. Lu, R., et al., *Transcription factor TCF4 maintains the properties of human corneal epithelial stem cells.* Stem Cells, 2012. **30**(4): p. 753-61.
594. Kutty, R.K., et al., *MicroRNA expression in human retinal pigment epithelial (ARPE-19) cells: Increased expression of microRNA-9 by N-(4-Hydroxyphenyl)retinamide.* Mol Vis, 2010. **16**: p. 1475-86.
595. Hu, Y., et al., *Reciprocal actions of microRNA-9 and TLX in the proliferation and differentiation of retinal progenitor cells.* Stem Cells Dev, 2014. **23**(22): p. 2771-81.
596. Zhao, C., et al., *A feedback regulatory loop involving microRNA-9 and nuclear receptor TLX in neural stem cell fate determination.* Nat Struct Mol Biol, 2009. **16**(4): p. 365-71.
597. Han, R., et al., *MiR-9 promotes the neural differentiation of mouse bone marrow mesenchymal stem cells via targeting zinc finger protein 521.* Neurosci Lett, 2012. **515**(2): p. 147-52.
598. Mackie, A.R., et al., *Sonic hedgehog-modified human CD34+ cells preserve cardiac function after acute myocardial infarction.* Circ Res, 2012. **111**(3): p. 312-21.
599. Hay, E.D., *Extracellular matrix alters epithelial differentiation.* Curr Opin Cell Biol, 1993. **5**(6): p. 1029-35.
600. Watt, F.M. and H. Fujiwara, *Cell-Extracellular Matrix Interactions in Normal and Diseased Skin.* Cold Spring Harb Perspect Biol, 2011. **3**(4).
601. Ferraris, C., et al., *Adult corneal epithelium basal cells possess the capacity to activate epidermal, pilosebaceous and sweat gland genetic programs in response to embryonic dermal stimuli.* Development, 2000. **127**(24): p. 5487-95.
602. Ferraris, C., C. Chaloin-Dufau, and D. Dhouailly, *Transdifferentiation of embryonic and postnatal rabbit corneal epithelial cells.* Differentiation, 1994. **57**(2): p. 89-96.
603. Baker, B.M. and C.S. Chen, *Deconstructing the third dimension – how 3D culture microenvironments alter cellular cues.* Journal of Cell Science, 2012. **125**(13): p. 3015-3024.
604. Richardson, G.D., et al., *Plasticity of Rodent and Human Hair Follicle Dermal Cells:Implications for Cell Therapy and Tissue Engineering.* Journal of Investigative Dermatology Symposium Proceedings, 2005. **10**(3): p. 180-183.
605. Bell, E., et al., *Dermal stem cells can differentiate down an endothelial lineage.* Stem Cells Dev, 2012. **21**(16): p. 3019-30.
606. Waters, J.M., G.D. Richardson, and C.A.B. Jahoda, *Keratin 10 (K10) is expressed suprabasally throughout the limbus of embryonic and neonatal rat corneas, with interrupted expression in the adult limbus.* Experimental Eye Research, 2009. **89**(3): p. 435-438.
607. Kawakita, T., et al., *Calcium-induced abnormal epidermal-like differentiation in cultures of mouse corneal-limbal epithelial cells.* Invest Ophthalmol Vis Sci, 2004. **45**(10): p. 3507-12.
608. Cai, S., X. Fu, and Z. Sheng, *Dedifferentiation: A New Approach in Stem Cell Research.* BioScience, 2007. **57**(8): p. 655-662.
609. Pearton, D.J., Y. Yang, and D. Dhouailly, *Transdifferentiation of corneal epithelium into epidermis occurs by means of a multistep process triggered by dermal developmental signals.* Proceedings of the National Academy of Sciences of the United States of America, 2005. **102**(10): p. 3714-3719.

610. Pearton, D.J., C. Ferraris, and D. Dhouailly, *Transdifferentiation of corneal epithelium: evidence for a linkage between the segregation of epidermal stem cells and the induction of hair follicles during embryogenesis.* Int J Dev Biol, 2004. **48**(2-3): p. 197-201.
611. Tosh, D. and J.M. Slack, *How cells change their phenotype.* Nat Rev Mol Cell Biol, 2002. **3**(3): p. 187-94.
612. Danto, S.I., et al., *Reversible transdifferentiation of alveolar epithelial cells.* American Journal of Respiratory Cell and Molecular Biology, 1995. **12**(5): p. 497-502.
613. Cooley, L.S., et al., *Reversible transdifferentiation of blood vascular endothelial cells to a lymphatic-like phenotype in vitro.* Journal of Cell Science, 2010. **123**(21): p. 3808-3816.
614. Stein, H.J. and J.R. Siewert, *Barrett's esophagus: pathogenesis, epidemiology, functional abnormalities, malignant degeneration, and surgical management.* Dysphagia, 1993. **8**(3): p. 276-88.
615. Giancotti, F.G. and E. Ruoslahti, *Integrin signaling.* Science, 1999. **285**(5430): p. 1028-32.
616. Turck, N., et al., *Laminin isoforms: biological roles and effects on the intracellular distribution of nuclear proteins in intestinal epithelial cells.* Experimental Cell Research, 2005. **303**(2): p. 494-503.
617. Kikkawa, Y., N. Sanzen, and K. Sekiguchi, *Isolation and characterization of laminin-10/11 secreted by human lung carcinoma cells. laminin-10/11 mediates cell adhesion through integrin alpha3 beta1.* J Biol Chem, 1998. **273**(25): p. 15854-9.
618. Kikkawa, Y., et al., *Integrin binding specificity of laminin-10/11: laminin-10/11 are recognized by alpha 3 beta 1, alpha 6 beta 1 and alpha 6 beta 4 integrins.* J Cell Sci, 2000. **113 (Pt 5)**: p. 869-76.
619. Sasaki, T. and R. Timpl, *Domain IVa of laminin alpha5 chain is cell-adhesive and binds beta1 and alphaVbeta3 integrins through Arg-Gly-Asp.* FEBS Lett, 2001. **509**(2): p. 181-5.
620. Tani, T., V.P. Lehto, and I. Virtanen, *Expression of laminins 1 and 10 in carcinoma cells and comparison of their roles in cell adhesion.* Exp Cell Res, 1999. **248**(1): p. 115-21.
621. Rousselle, P., et al., *Kalinin: an epithelium-specific basement membrane adhesion molecule that is a component of anchoring filaments.* J Cell Biol, 1991. **114**(3): p. 567-76.
622. Sonnenberg, A., et al., *Integrin recognition of different cell-binding fragments of laminin (P1, E3, E8) and evidence that alpha 6 beta 1 but not alpha 6 beta 4 functions as a major receptor for fragment E8.* J Cell Biol, 1990. **110**(6): p. 2145-55.
623. Dowgiert, J., G. Sosne, and M. Kurpakus-Wheater, *Laminin-2 stimulates the proliferation of epithelial cells in a conjunctival epithelial cell line.* Cell Prolif, 2004. **37**(2): p. 161-75.
624. Hasenson, S., et al., *The immortalized human corneal epithelial cells adhere to laminin-10 by using Lutheran glycoproteins and integrin α3β1.* Experimental Eye Research, 2005. **81**(4): p. 415-421.
625. Yu, H. and J.F. Talts, *Beta1 integrin and alpha-dystroglycan binding sites are localized to different laminin-G-domain-like (LG) modules within the laminin alpha5 chain G domain.* Biochem J, 2003. **371**(Pt 2): p. 289-99.
626. Lin, L. and M. Kurpakus-Wheater, *Laminin alpha5 chain adhesion and signaling in conjunctival epithelial cells.* Invest Ophthalmol Vis Sci, 2002. **43**(8): p. 2615-21.
627. Ono, K. and J. Han, *The p38 signal transduction pathway: activation and function.* Cell Signal, 2000. **12**(1): p. 1-13.

628. Heiskanen, A., et al., *N-glycolylneuraminic acid xenoantigen contamination of human embryonic and mesenchymal stem cells is substantially reversible.* Stem Cells, 2007. **25**(1): p. 197-202.
629. Gutzeit, C., et al., *Exosomes derived from Burkitt's lymphoma cell lines induce proliferation, differentiation, and class-switch recombination in B cells.* J Immunol, 2014. **192**(12): p. 5852-62.
630. Chowdhury, R., et al., *Cancer exosomes trigger mesenchymal stem cell differentiation into pro-angiogenic and pro-invasive myofibroblasts.* Oncotarget, 2015. **6**(2): p. 715-31.
631. Emanueli, C., et al., *Exosomes and exosomal miRNAs in cardiovascular protection and repair.* Vascul Pharmacol, 2015. **71**: p. 24-30.
632. Quesenberry, P.J., et al., *Role of extracellular RNA-carrying vesicles in cell differentiation and reprogramming.* Stem Cell Res Ther, 2015. **6**: p. 153.
633. Lee, H.K., et al., *Mesenchymal stem cells deliver exogenous miRNAs to neural cells and induce their differentiation and glutamate transporter expression.* Stem Cells Dev, 2014. **23**(23): p. 2851-61.
634. Xin, H., et al., *Exosome-mediated transfer of miR-133b from multipotent mesenchymal stromal cells to neural cells contributes to neurite outgrowth.* Stem Cells, 2012. **30**(7): p. 1556-64.
635. Trivedi, M., et al., *Modification of tumor cell exosome content by transfection with wt-p53 and microRNA-125b expressing plasmid DNA and its effect on macrophage polarization.* Oncogenesis, 2016. **5**(8): p. e250-.
636. Luan, X., et al., *Engineering exosomes as refined biological nanoplatforms for drug delivery.* Acta Pharmacol Sin, 2017. **38**(6): p. 754-63.
637. Eisenberg, E. and E.Y. Levanon, *Human housekeeping genes, revisited.* Trends in Genetics, 2013. **29**(10): p. 569-574.
638. Kulkarni, B., et al., *Validation of endogenous control genes for gene expression studies on human ocular surface epithelium.* PLoS One, 2011. **6**(8): p. e22301.
639. Rheinwald, J.G. and H. Green, *Serial cultivation of strains of human epidermal keratinocytes: the formation of keratinizing colonies from single cells.* Cell, 1975. **6**(3): p. 331-43.
640. Flaxman, B.A., M.A. Lutzner, and E.J. Van Scott, *Cell Maturation and Tissue Organization in Epithelial Outgrowths from Skin and Buccal Mucosa In Vitro1.* The Journal of Investigative Dermatology, 1967. **49**(3): p. 322-332.
641. Newsome, D.A., et al., *Human corneal cells in vitro: morphology and histocompatibility (HL-A) antigens of pure cell populations.* Invest Ophthalmol, 1974. **13**(1): p. 23-32.
642. Todaro, G.J. and H. Green, *Quantitative studies of the growth of mouse embryo cells in culture and their development into established lines.* J Cell Biol, 1963. **17**: p. 299-313.
643. Freshney, R.I., *Other Epithelial Cells*, in *Culture of Epithelial Cells*. 2002, John Wiley & Sons, Inc. p. 401-436.
644. Sun, T.T. and H. Green, *Cultured epithelial cells of cornea, conjunctiva and skin: absence of marked intrinsic divergence of their differentiated states.* Nature, 1977. **269**(5628): p. 489-93.
645. Rheinwald, J.G., *Serial cultivation of normal human epidermal keratinocytes.* Methods Cell Biol, 1980. **21A**: p. 229-54.
646. Allman, M.I., et al., *Rabbit corneal epithelial cells grown in vitro without serum.* Invest Ophthalmol, 1976. **15**(8): p. 666-8.
647. Kruse, F.E. and S.C. Tseng, *A serum-free clonal growth assay for limbal, peripheral, and central corneal epithelium.* Invest Ophthalmol Vis Sci, 1991. **32**(7): p. 2086-95.

648. Pera, M.F. and P.A. Gorman, *In vitro analysis of multistage epidermal carcinogenesis: development of indefinite renewal capacity and reduced growth factor requirements in colony forming keratinocytes precedes malignant transformation.* Carcinogenesis, 1984. **5**(5): p. 671-82.
649. Hayashi, I., J. Larner, and G. Sato, *Hormonal growth control of cells in culture.* In Vitro, 1978. **14**(1): p. 23-30.
650. Maciag, T., et al., *An endocrine approach to the control of epidermal growth: serum-free cultivation of human keratinocytes.* Science, 1981. **211**(4489): p. 1452-4.
651. Allen-Hoffmann, B.L. and J.G. Rheinwald, *Polycyclic aromatic hydrocarbon mutagenesis of human epidermal keratinocytes in culture.* Proc Natl Acad Sci U S A, 1984. **81**(24): p. 7802-6.
652. Rheinwald, J.G. and H. Green, *Epidermal growth factor and the multiplication of cultured human epidermal keratinocytes.* Nature, 1977. **265**(5593): p. 421-424.